Summary of the Bulletin of the International Seismological Centre

2015

July – December

Volume 52 Issue II

www.isc.ac.uk

isc-mirror.iris.washington.edu

ISSN 2309-236X

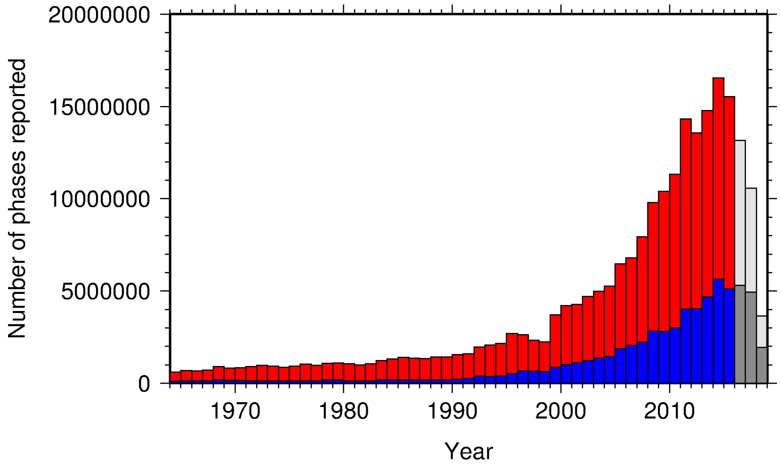

The number of phases (red) and number of amplitudes (blue) collected by the ISC for events each year since 1964. The data in grey covers the current period where data are still being collected before the ISC review takes place and are accurate at the time of publication. See Section 8.3.

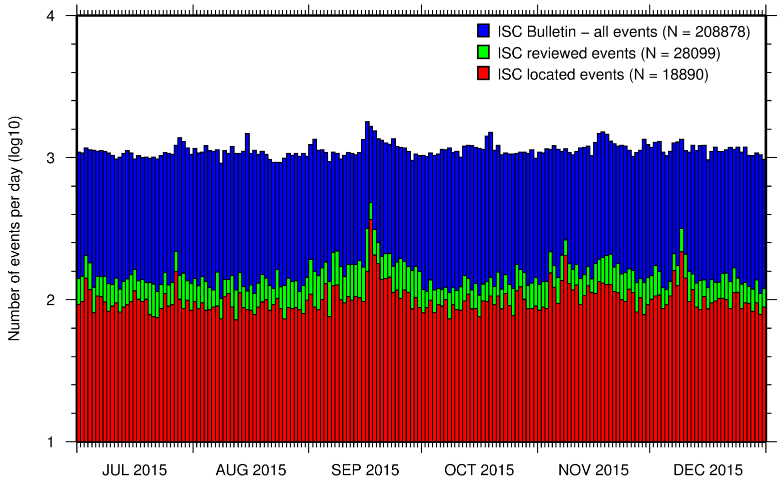

The number of events within the Bulletin for the current summary period. The vertical scale is logarithmic. See Section 9.1.

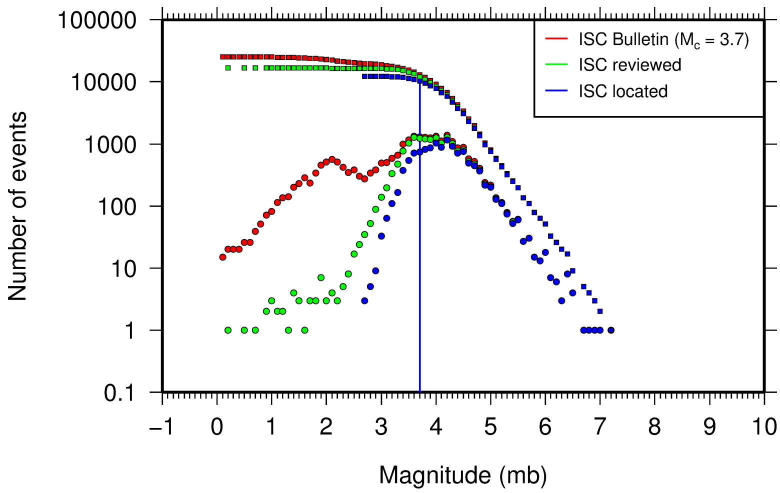

Frequency and cumulative frequency magnitude distribution for all events in the ISC Bulletin, ISC reviewed events and events located by the ISC. The magnitude of completeness (M_C) is shown for the ISC Bulletin. Note: only events with values of m_b are represented in the figure. See Section 9.4.

Summary of the Bulletin of the International Seismological Centre

2015

July - December

Volume 52 Issue II

Produced and edited by:
Kathrin Lieser, James Harris and Dmitry Storchak

Published by
International Seismological Centre

ISC Data Products
http://www.isc.ac.uk/products/

ISC Bulletin:
    http://www.isc.ac.uk/iscbulletin/search

ISC Bulletin and Catalogue monthly files, to the last reviewed month in FFB or ISF1 format:
    ftp://www.isc.ac.uk/pub/[isf|ffb]/bulletin/*yyyy*/*yyyymm*.gz
    ftp://www.isc.ac.uk/pub/[isf|ffb]/catalogue/*yyyy*/*yyyymm*.gz Datafiles for the ISC data before the rebuild:
    ftp://www.isc.ac.uk/pub/prerebuild/[isf|ffb]/bulletin/*yyyy*/*yyyymm*.gz
    ftp://www.isc.ac.uk/pub/prerebuild/[isf|ffb]/catalogue/*yyyy*/*yyyymm*.gz

ISC-EHB Bulletin:
    http://www.isc.ac.uk/isc-ehb/search/

IASPEI Reference Event List (GT bulletin):
    http://www.isc.ac.uk/gtevents/search/

ISC-GEM Global Instrumental Earthquake Catalogue:
    http://http://www.isc.ac.uk/iscgem/download.php

ISC Event Bibliography:
    http://www.isc.ac.uk/event_bibliography/bibsearch.php

International Seismograph Station Registry:
    http://www.isc.ac.uk/registries/search/

Seismological Contacts:
    http://www.isc.ac.uk/projects/seismocontacts/

International Seismological Centre
Pipers Lane
Thatcham
RG19 4NS
United Kingdom
www.isc.ac.uk

ISSN 2309-236X

Printed and bound in Wales by Cambrian Printers.

Contents

1

Preface

Dear Colleague,

This is the second and concluding 2015 issue of the Summary of the ISC Bulletin that remains the most fundamental reason for continued operations at the ISC. This issue covers seismic events that occurred during the period from July to December 2015.

This publication contains a description of the ISC data available on the included DVD-ROM and from the ISC website. It contains information on the ISC, its Members, Sponsors and Data Providers. It offers analysis of the data contributed to the ISC by many seismological agencies worldwide as well as analysis of the data in the ISC Bulletin itself. This somewhat smaller issue misses some of the standard information on routine procedures usually published in the first issue of each year.

We continue publishing invited articles describing the history, current status and operational procedures at those networks that contribute seismic bulletin data to the ISC. This time it is the turn for the central seismological observatory at the Federal Institute for Geosciences and Natural Resources (BGR) in Hanover, Germany. The second invited article covers parameters of macroseismic recordings of a rare natural earthquake that occurred in Central Ural Mountain region in Russia.

We hope that you find this relatively new publication useful in your work. If your home-institution or company is unable, for one reason or another, to support the long-term international operations of the ISC in full by becoming a Member, then, please, consider subscribing to this publication by contacting us at admin@isc.ac.uk.

With kind regards to our Data Contributors, Members, Sponsors and users,

Dr Dmitry A. Storchak
Director
International Seismological Centre (ISC)

2

The International Seismological Centre

2.1 The ISC Mandate

The International Seismological Centre (ISC) was set up in 1964 with the assistance of UNESCO as a successor to the International Seismological Summary (ISS) to carry forward the pioneering work of Prof. John Milne, Sir Harold Jeffreys and other British scientists in collecting, archiving and processing seismic station and network bulletins and preparing and distributing the definitive summary of world seismicity.

Under the umbrella of the International Association of Seismology and Physics of the Earth Interior (IASPEI/IUGG), the ISC has played an important role in setting international standards such as the International Seismic Bulletin Format (ISF), the IASPEI Standard Seismic Phase List (SSPL) and both the old and New IASPEI Manual of the Seismological Observatory Practice (NMSOP-2) (www.iaspei.org/projects/NMSOP.html).

The ISC has contributed to scientific research and prominent scientists such as John Hodgson, Eugine Herrin, Hal Thirlaway, Jack Oliver, Anton Hales, Ola Dahlman, Shigeji Suehiro, Nadia Kondorskaya, Vit Karnik, Stephan Müller, David Denham, Bob Engdahl, Adam Dziewonski, John Woodhouse and Guy Masters all considered it an important duty to serve on the ISC Executive Committee and the Governing Council.

The current mission of the ISC is to maintain:

- the ISC **Bulletin** – the longest continuous definitive summary of World seismicity (collaborating with 130 seismic networks and data centres around the world). (www.isc.ac.uk/iscbulletin/)
- the International Seismographic Station Registry (**IR**, jointly with the World Data Center for Seismology, Denver). (www.isc.ac.uk/registries/)
- the IASPEI Reference Event List (Ground Truth, **GT**, jointly with IASPEI). (www.isc.ac.uk/gtevents/)

These are fundamentally important tasks. Bulletin data produced, archived and distributed by the ISC for almost 50 years are the definitive source of such information and are used by thousands of seismologists worldwide for seismic hazard estimation, for tectonic studies and for regional and global imaging of the Earth's structure. Key information in global tomographic imaging is derived from the analysis of ISC data. The ISC Bulletin served as a major source of data for such well known products as the ak135 global 1-D velocity model and the EHB (*Engdahl et al.*, 1998) and Centennial (*Engdahl and Villaseñor*, 2002) catalogues. It presents an important quality-control benchmark for the Comprehensive Nuclear-Test-Ban Treaty Organization (CTBTO). Hypocentre parameters from the ISC Bulletin are used by the Data Management Center of the Incorporated Research Institutions for Seismology (IRIS DMC) to serve event-oriented user-requests for waveform data. The ISC-GEM Bulletin is a cornerstone of the ISC-GEM Global Instrumental Reference Earthquake Catalogue for Global Earthquake risk Model (GEM).

The ISC Bulletin contains over 6 million seismic events: earthquakes, chemical and nuclear explosions, mine blasts and mining induced events. At least 1.7 million of them are regional and teleseismically recorded events that have been reviewed by the ISC analysts. The ISC Bulletin contains approximately 200 million individual seismic station readings of arrival times, amplitudes, periods, SNR, slowness and azimuth, reported by approximately 17,000 seismic stations currently registered in the IR. Over 6,000 stations have contributed to the ISC Bulletin in recent years. This number includes the numerous sites of the USArray. The IASPEI GT List currently contains 8816 events for which latitude, longitude and depth of origin are known with high confidence (to 5 km or better) and seismic signals were recorded at regional and/or teleseismic distances.

2.2 Brief History of the ISC

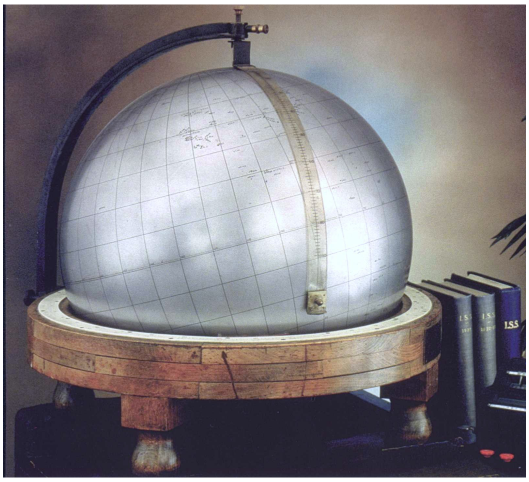

Figure 2.1: *The steel globe bearing positions of early seismic stations was used for locating positions of earthquakes for the International Seismological Summaries.*

Earthquake effects have been noted and documented from the earliest times, but it is only since the development of earthquake recording instruments in the latter half of the 19th century that a proper study of their occurrence has been possible. After the first teleseismic observation of an earthquake in 1889, the need for international exchange of readings was recognised in 1895 by Prof. John Milne and by Ernst von Rebeur Paschwitz together with Georg Gerland, resulting in the publication of the first international seismic bulletins. Milne's "Shide Circulars" were issued under the auspices of the Seismological Committee of the British Association for the Advancement of Science (BAAS), while co-workers of Gerland at the Central Bureau of the International Association of Seismology worked independently in Strasbourg (BCIS).

Following Milne's death in 1913, Seismological Bulletins of the BAAS were continued under Prof. H.H. Turner, later based at Oxford University. Upon formal post-war dissolution of the International Association of Seismology in 1922 the newly founded Seismological Section of the International Union of Geodesy and Geophysics (IUGG) set up the International Seismological Summary (ISS) to continue at Oxford under Turner, to produce the definitive global catalogues from the 1918 data-year onwards, under the auspices of IUGG and with the support of the BAAS.

ISS production, led by several professors at Oxford University, and Sir Harold Jeffreys at Cambridge

University, continued until it was superseded by the ISC Bulletin, after the ISC was formed in Edinburgh in 1964 with Dr P.L. Willmore as its first director.

During the period 1964 to 1970, with the help of UNESCO and other international scientific bodies, the ISC was reconstituted as an international non-governmental body, funded by interested institutions from various countries. Initially there were supporting members from seven countries, now there are almost 60, and member institutions include national academies, research foundations, government departments and research institutes, national observatories and universities. Each member, contributing a minimum unit of subscription or more, appoints a representative to the ISC's Governing Council, which meets every two years to decide the ISC's policy and operational programme. Representatives from the International Association of Seismology and Physics of the Earth's Interior also attend these meetings. The Governing Council appoints the Director and a small Executive Committee to oversee the ISC's operations.

Figure 2.2: *ISC building in Thatcham, Berkshire, UK.*

In 1975, the ISC moved to Newbury in southern England to make use of better computing facilities there. The ISC subsequently acquired its own computer and in 1986 moved to its own building at Pipers Lane, Thatcham, near Newbury. The internal layout of the new premises was designed for the ISC and includes not only office space but provision for the storage of extensive stocks of ISS and ISC publications and a library of seismological observatory bulletins, journals and books collected over many tens of years.

In 1997 the first set of the ISC Bulletin CD-ROMs was produced (not counting an earlier effort at USGS). The first ISC website appeared in 1998 and the first ISC database was put in day-to-day operations from 2001.

Throughout 2009-2011 a major internal reconstruction of the ISC building was undertaken to allow for more members of staff working in mainstream ISC operations as well as major development projects such as the CTBTO Link, ISC-GEM Catalogue and the ISC Bulletin Rebuild.

2.3 Former Directors of the ISC and its U.K. Predecessors

John Milne
Publisher of the Shide Circular Reports on Earthquakes
1899-1913

Herbert Hall Turner

Seismological Bulletins of the BAAS

1913-1922
Director of the ISS
1922-1930

Harry Hemley Plaskett
Director of the ISS
1931-1946

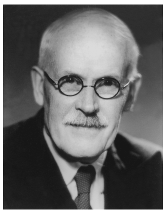

Harold Jeffreys
Director of the ISS
1946-1957

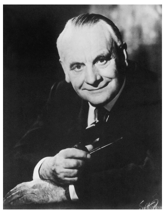

Robert Stoneley
Director of the ISS
1957-1963

P.L. (Pat) Willmore
Director of the ISS
1963-1970
Director of the ISC
1964-1970

Edouard P. Arnold
Director of the ISC
1970-1977

Anthony A. Hughes
Director of the ISC
1977-1997

Raymond J. Willemann
Director of the ISC
1998-2003

Avi Shapira
Director of the ISC
2004-2007

2.4 Member Institutions of the ISC

Article IV(a-b) of the ISC Working Statutes stipulates that any national academy, agency, scientific institution or other non-profit organisation may become a Member of the ISC on payment to the ISC of a sum equal to at least one unit of subscription and the nomination of a voting representative to serve on the ISC's governing body. Membership shall be effective for one year from the date of receipt at the ISC of the annual contribution of the Member and is thereafter renewable for periods of one year.

The ISC is currently supported with funding from its 62 Member Institutions and a four-year Grant Award EAR-1417970 from the US National Science Foundation.

Figures 2.3 and 2.4 show major sectors to which the ISC Member Institutions belong and proportional financial contributions that each of these sectors make towards the ISC's annual budget.

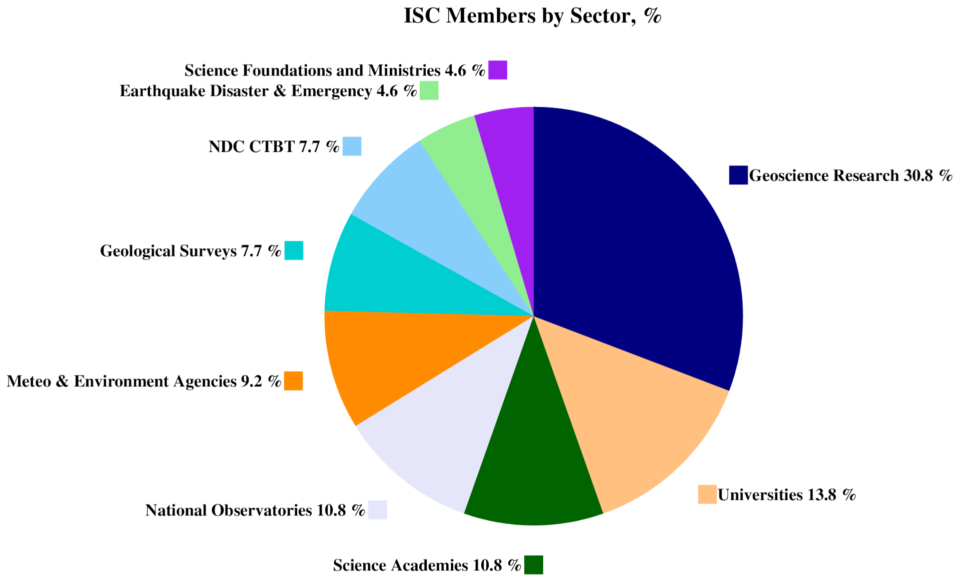

Figure 2.3: *Distribution of the ISC Member Institutions by sector in year 2013 as a percentage of total number of Members.*

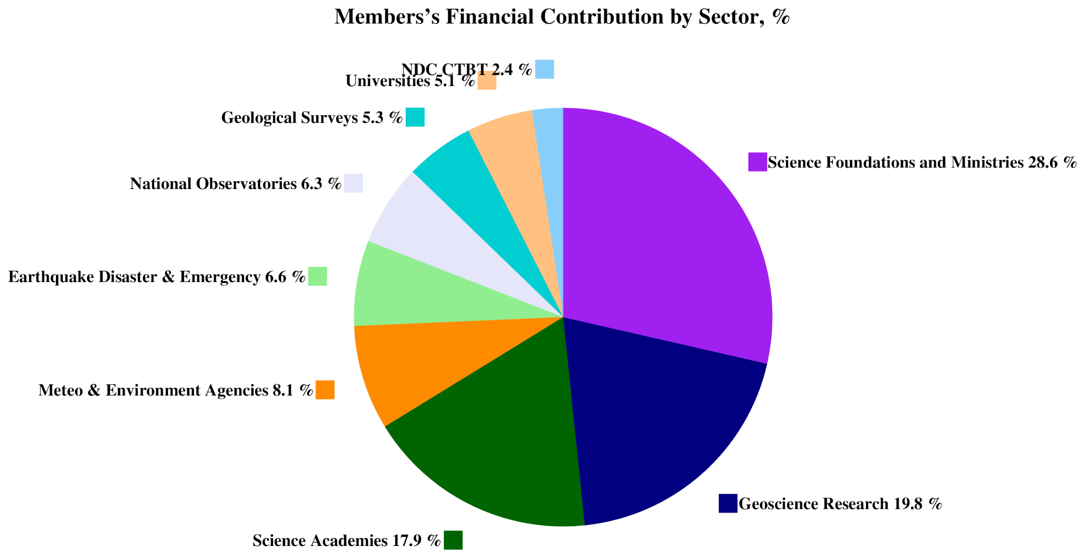

Figure 2.4: *Distribution of Member's financial contributions to the ISC by sector in year 2013 as a percentage of total annual Member contributions.*

There follows a list of all current Member Institutions with a category (1 through 9) assigned according to the ISC Working Statutes. Each category relates to the number of membership units contributed.

Centre de Recherche en Astronomie, Astrophysique et Géophysique (CRAAG) Algeria www.craag.dz Category: 1	Instituto Nacional de Prevención Sísmica (INPRES) Argentina www.inpres.gov.ar Category: 1	Geoscience Australia Australia www.ga.gov.au Category: 4

Bundesministerium für Wissenschaft, Forschung und Wirtschaft (BMWFW)
Austria
www.bmbwk.gv.at
Category: 2

Centre of Geophysical Monitoring (CGM) of the National Academy of Sciences of Belarus
Belarus
www.cgm.org.by
Category: 1

Belgian Science Policy Office (BELSPO)
Belgium

Category: 1

Universidade de São Paulo, Centro de Sismologia
Brazil
www.sismo.iag.usp.br
Category: 1

Seismological Observatory, Institute of Geosciences, University of Brasilia
Brazil
www.obsis.unb.br
Category: 1

The Geological Survey of Canada
Canada
gsc.nrcan.gc.ca
Category: 4

Centro Sismologico Nacional, Universidad de Chile
Chile
ingenieria.uchile.cl
Category: 1

China Earthquake Administration
China
www.cea.gov.cn
Category: 4

Institute of Earth Sciences, Academia Sinica
Chinese Taipei
www.earth.sinica.edu.tw
Category: 1

Geological Survey Department
Cyprus
www.moa.gov.cy
Category: 1

Insitute of Geophysics, Academy of Sciences of the Czech Republic
Czech Republic
www.avcr.cz
Category: 1

Geological Survey of Denmark and Greenland (GEUS)
Denmark
www.geus.dk
Category: 2

National Research Institute for Astronomy and Geophysics (NRIAG), Cairo
Egypt
www.nriag.sci.eg
Category: 1

The University of Helsinki
Finland
www.helsinki.fi
Category: 2

Laboratoire de Détection et de Géophysique/CEA
France
www-dase.cea.fr
Category: 2

Institute National des Sciences de l'Univers
France
www.insu.cnrs.fr
Category: 4

GeoForschungsZentrum Potsdam
Germany
www.gfz-potsdam.de
Category: 2

Bundesanstalt für Geowissenschaften und Rohstoffe
Germany
www.bgr.bund.de
Category: 4

The Seismological Institute, National Observatory of Athens
Greece
www.noa.gr
Category: 1

The Hungarian Academy of Sciences
Hungary
www.mta.hu
Category: 1

The Icelandic Meteorological Office
Iceland
www.vedur.is
Category: 1

National Centre for Seismology, Ministry of Earth Sciences of India
India
www.moes.gov.in
Category: 4

Iraqi Meteorological Organization and Seismology
Iraq
www.imos-tm.com
Category: 1

The Geophysical Institute of Israel
Israel
www.gii.co.il
Category: 1

Soreq Nuclear Research Centre (SNRC)
Israel
www.soreq.gov.il
Category: 1

Istituto Nazionale di Geofisica e Vulcanologia
Italy
www.ingv.it
Category: 3

Istituto Nazionale di Oceanografia e di Geofisica Sperimentale
Italy
www.ogs.trieste.it
Category: 1

University of the West Indies at Mona
Jamaica
www.mona.uwi.edu
Category: 1

Japan Agency for Marine-Earth Science and Technology (JAMSTEC)
Japan
www.jamstec.go.jp
Category: 2

Earthquake Research Institute, University of Tokyo
Japan
www.eri.u-tokyo.ac.jp
Category: 3

The Japan Meteorological Agency (JMA)
Japan
www.jma.go.jp
Category: 5

National Institute of Polar Research (NIPR)
Japan
www.nipr.ac.jp
Category: 1

Royal Scientific Society
Jordan
www.rss.jo
Category: 1

Centro de Investigación Científica y de Educación Superior de Ensenada (CICESE)
Mexico
resnom.cicese.mx
Category: 1

Institute of Geophysics, National University of Mexico
Mexico
www.igeofcu.unam.mx
Category: 1

The Royal Netherlands Meteorological Institute (KNMI)
Netherlands
www.knmi.nl
Category: 2

GNS Science
New Zealand
www.gns.cri.nz
Category: 3

The University of Bergen
Norway
www.uib.no
Category: 2

Stiftelsen NORSAR
Norway
www.norsar.no
Category: 2

Institute of Geophysics, Polish Academy of Sciences
Poland
www.igf.edu.pl
Category: 1

Instituto Português do Mar e da Atmosfera
Portugal
www.ipma.pt
Category: 2

Red Sísmica de Puerto Rico
Puerto Rico
redsismica.uprm.edu
Category: 1

Korean Meterological Administration
Republic of Korea
www.kma.go.kr
Category: 1

National Institute for Earth Physics
Romania
www.infp.ro
Category: 1

Russian Academy of Sciences
Russia
www.ras.ru
Category: 5

Earth Observatory of Singapore (EOS), an autonomous Institute of Nanyang Technological University
Singapore
www.earthobservatory.sg
Category: 1

Environmental Agency of Slovenia
Slovenia
www.arso.gov.si
Category: 1

Council for Geoscience
South Africa
www.geoscience.org.za
Category: 1

Institut Cartogràfic i Geològic de Catalunya (ICGC)
Spain
www.icgc.cat
Category: 1

Institute of Earth Sciences Jaume Almera
Spain
www.ictja.csic.es
Category: 1

Uppsala Universitet
Sweden
www.uu.se
Category: 2

National Defence Research Establishment (FOI)
Sweden
www.foi.se
Category: 1

The Swiss Academy of Sciences
Switzerland
www.scnat.ch
Category: 2

The Seismic Research Centre, University of the West Indies at St. Augustine
Trinidad and Tobago
www.uwiseismic.com
Category: 1

Kandilli Observatory and Earthquake Research Institute
Turkey
www.koeri.boun.edu.tr
Category: 1

Disaster and Emergency Management Authority (AFAD)
Turkey
www.deprem.gov.tr
Category: 2

AWE Blacknest
United Kingdom
www.blacknest.gov.uk
Category: 1

The Royal Society
United Kingdom
www.royalsociety.org
Category: 6

British Geological Survey
United Kingdom
www.bgs.ac.uk
Category: 2

Incorporated Research Institutions for Seismology
U.S.A.
www.iris.edu
Category: 1

National Earthquake Information Center, U.S. Geological Survey
U.S.A.
www.neic.usgs.gov
Category: 1

The National Science Foundation of the United States. (Grant No. EAR-1417970)
U.S.A.
www.nsf.gov
Category: 9

In addition the ISC is currently in receipt of grants from the International Data Centre (IDC) of the Preparatory Commission of the Comprehensive Nuclear-Test-Ban Treaty Organization (CTBTO), FM Global, Lighthill risk Network, OYO, USGS (Award G15AC00202) and BGR.

2.5 Sponsoring Organisations

Article IV(c) of the ISC Working Statutes stipulates any commercial organisation with an interest in the objectives and/or output of the ISC may become an Associate Member of the ISC on payment of an Associate membership fee, but without entitlement to representation with a vote on the ISC's governing body.

www.reftek.com

REF TEK designs and manufactures application specific, high-performance, battery-operated, field-portable geophysical data acquisition devices for the global market. With over 35 years of experience, REF TEK provides customers with complete turnkey solutions that include high resolution recorders, broadband sensors, state-of-the-art communications (V-SAT, GPRS, etc), installation, training, and continued customer support. Over 7,000 REF TEK instruments are currently being used globally for multiple applications. From portable earthquake monitoring to telemetry earthquake monitoring, earthquake aftershock recording to structural monitoring and more, REF TEK equipment is suitable for a wide variety of application needs.

http://www.geosig.com/

GeoSIG provides earthquake, seismic, structural, dynamic and static monitoring and measuring solutions As an ISO Certified company, GeoSIG is a world leader in design and manufacture of a diverse range of high quality, precision instruments for vibration and earthquake monitoring. GeoSIG instruments are at work today in more than 100 countries around the world with well-known projects such as the NetQuakes installation with USGS and Oresund Bridge in Denmark. GeoSIG offers off-the-shelf solutions as well as highly customised solutions to fulfil the challenging requirements in many vertical markets including the following:

- Earthquake Early Warning and Rapid Response (EEWRR)
- Seismic and Earthquake Monitoring and Measuring
- Industrial Facility Seismic Monitoring and Shutdown
- Structural Analysis and Ambient Vibration Testing
- Induced Vibration Monitoring
- Research and Scientific Applications

http://www.guralp.com/

Güralp has been developing revolutionary force-feedback broadband seismic instrumentation for more than thirty years. Our sensors record seismic signals of all kinds, from teleseismic events occurring on the other side of the planet, to microseisms induced by unconventional hydrocarbon extraction. Our sophisticated digitisers record these signals with the highest resolution and accurate timing.

We supply individual instruments or complete seismic systems. Our services include field support such as installation and maintenance, to complete network and data management.

We design our instruments to meet increasingly complex requirements for deployment in the most challenging circumstances. As a result, you will find Güralp instruments gathering seismic data in the harshest of environments, from the Antarctic ice sheet; to boreholes 100s of metres deep; to the world's most active volcanoes and deepest ocean trenches.

http://src.com.au/

The Seismology Research Centre is an Australian earthquake observatory that began developing their own seismic recorders and data processing software in the late 1970s when digital recorders were uncommon. The Gecko is the SRC's 7th generation of seismic recorder, now available with a variety of integrated sensors to meet every monitoring requirement, including:

- Strong Motion Accelerographs
- 2Hz and 4.5Hz Blast Vibration Monitors
- Short Period 1Hz Seismographs
- Broadband 200s-1500Hz Optical Seismographs

Visit src.com.au/downloads/waves to grab a free copy of the SRC's MiniSEED waveform viewing and analysis software application, Waves.

2.6 Data Contributing Agencies

In addition to its Members and Sponsors, the ISC owes its existence and successful long-term operations to its 150 seismic bulletin data contributors. These include government agencies responsible for national seismic networks, geoscience research institutions, geological surveys, meteorological agencies, universities, national data centres for monitoring the CTBT and individual observatories. There would be no ISC Bulletin available without the regular stream of data that are unselfishly and generously contributed to the ISC on a free basis.

East African Network
EAF

The Institute of Seismology, Academy of Sciences of Albania
Albania
TIR

Centre de Recherche en Astronomie, Astrophysique et Géophysique
Algeria
CRAAG

Instituto Nacional de Prevención Sísmica
Argentina
SJA

Universidad Nacional de La Plata
Argentina
LPA

National Survey of Seismic Protection
Armenia
NSSP

Curtin University
Australia
CUPWA

Geoscience Australia
Australia
AUST

International Data Centre, CTBTO
Austria
IDC

Zentralanstalt für Meteorologie und Geodynamik (ZAMG)
Austria
VIE

Republic Center of Seismic Survey
Azerbaijan
AZER

Royal Observatory of Belgium
Belgium
UCC

Observatorio San Calixto
Bolivia
SCB

Republic Hydrometeorological Service, Seismological Observatory, Banja Luka
Bosnia and Herzegovina
RHSSO

Instituto Astronomico e Geofísico
Brazil
VAO

Geophysical Institute, Bulgarian Academy of Sciences
Bulgaria
SOF

Seismological Observatory of Mount Cameroon
Cameroon
SOMC

Canadian Hazards Information Service, Natural Resources Canada
Canada
OTT

Centro Sismológico Nacional, Universidad de Chile
Chile
GUC

China Earthquake Networks Center
China
BJI

Institute of Earth Sciences, Academia Sinica
Chinese Taipei
ASIES

CWB
Chinese Taipei
TAP

Red Sismológica Nacional de Colombia
Colombia
RSNC

Sección de Sismología, Vulcanología y Exploración Geofísica
Costa Rica
UCR

Seismological Survey of the Republic of Croatia
Croatia
ZAG

Servicio Sismológico Nacional Cubano
Cuba
SSNC

Cyprus Geological Survey Department
Cyprus
NIC

West Bohemia Seismic Network
Czech Republic
WBNET

The Institute of Physics of the Earth (IPEC)
Czech Republic
IPEC

Geophysical Institute, Academy of Sciences of the Czech Republic
Czech Republic
PRU

Geological Survey of Denmark and Greenland
Denmark
DNK

Observatorio Sismologico Politecnico Loyola
Dominican Republic
OSPL

Servicio Nacional de Sismología y Vulcanología
Ecuador
IGQ

National Research Institute of Astronomy and Geophysics
Egypt
HLW

Servicio Nacional de Estudios Territoriales
El Salvador
SNET

University of Addis Ababa
Ethiopia
AAE

Seismological Observatory Skopje
FYR Macedonia
SKO

Institute of Seismology, University of Helsinki
Finland
HEL

Laboratoire de Détection et de Géophysique/CEA
France
LDG

EOST / RéNaSS
France
STR

Laboratoire de Géophysique/CEA
French Polynesia
PPT

Institute of Earth Sciences/ National Seismic Monitoring Center
Georgia
TIF

Alfred Wegener Institute for Polar and Marine Research
Germany
AWI

Bundesanstalt für Geowissenschaften und Rohstoffe
Germany
BGR

Geophysikalisches Observatorium Collm
Germany
CLL

Seismological Observatory Berggießhübel, TU Bergakademie Freiberg
Germany
BRG

National Observatory of Athens
Greece
ATH

Department of Geophysics, Aristotle University of Thessaloniki
Greece
THE

University of Patras, Department of Geology
Greece
UPSL

INSIVUMEH
Guatemala
GCG

Hong Kong Observatory
Hong Kong
HKC

Geodetic and Geophysical Reasearch Institute, Hungarian Academy of Sciences
Hungary
KRSZO

Geodetic and Geophysical Research Institute
Hungary
BUD

Icelandic Meteorological Office
Iceland
REY

National Geophysical Research Institute
India
HYB

National Centre for Seismology of the Ministry of Earth Sciences of India
India
NDI

Badan Meteorologi, Klimatologi dan Geofisika
Indonesia
DJA

International Institute of Earthquake Engineering and Seismology (IIEES)
Iran
THR

Tehran University
Iran
TEH

Iraqi Meteorological and Seismology Organisation
Iraq
ISN

The Geophysical Institute of Israel
Israel
GII

Laboratory of Research on Experimental and Computational Seimology
Italy
RISSC

Dipartimento per lo Studio del Territorio e delle sue Risorse (RSNI)
Italy
GEN

Istituto Nazionale di Geofisica e Vulcanologia
Italy
ROM

Istituto Nazionale di Oceanografia e di Geofisica Sperimentale (OGS)
Italy
TRI

MedNet Regional Centroid - Moment Tensors
Italy
MED_RCMT

Station Géophysique de Lamto
Ivory Coast
LIC

Jamaica Seismic Network
Jamaica
JSN

National Institute of Polar Research
Japan
SYO

The Matsushiro Seismological Observatory
Japan
MAT

National Research Institute for Earth Science and Disaster Prevention
Japan
NIED

Japan Meteorological Agency
Japan
JMA

Jordan Seismological Observatory
Jordan
JSO

Seismological Experimental Methodological Expedition
Kazakhstan
SOME

National Nuclear Center
Kazakhstan
NNC

Kuwait Institute for Scientific Research
Kuwait
KISR

Institute of Seismology, Academy of Sciences of Kyrgyz Republic
Kyrgyzstan
KRNET

Kyrgyz Seismic Network
Kyrgyzstan
KNET

Latvian Seismic Network
Latvia
LVSN

National Council for Scientific Research
Lebanon
GRAL

Geological Survey of Lithuania
Lithuania
LIT

European Center for Geodynamics and Seismology
Luxembourg
ECGS

Macao Meteorological and Geophysical Bureau
Macao, China
MCO

Antananarivo
Madagascar
TAN

Geological Survey Department Malawi
Malawi
GSDM

Malaysian Meteorological Service
Malaysia
KLM

Instituto de Geofísica de la UNAM
Mexico
MEX

Centro de Investigación Científica y de Educación Superior de Ensenada
Mexico
ECX

Institute of Geophysics and Geology
Moldova
MOLD

Seismological Institute of Montenegro
Montenegro
PDG

Centre National de Recherche
Morocco
CNRM

The Geological Survey of Namibia
Namibia
NAM

National Seismological Centre, Nepal
Nepal
DMN

IRD Centre de Nouméa
New Caledonia
NOU

Institute of Geological and Nuclear Sciences
New Zealand
WEL

Instituto Nicaraguense de Estudios Territoriales - INETER
Nicaragua
INET

University of Bergen
Norway
BER

Stiftelsen NORSAR
Norway
NAO

Sultan Qaboos University
Oman
OMAN

Micro Seismic Studies Programme, PINSTECH
Pakistan
MSSP

Universidad de Panama
Panama
UPA

Philippine Institute of Volcanology and Seismology
Philippines
MAN

Institute of Geophysics, Polish Academy of Sciences
Poland
WAR

Instituto Português do Mar e da Atmosfera, I.P.
Portugal
INMG

Sistema de Vigilância Sismológica dos Açores
Portugal
SVSA

Instituto Geofisico do Infante Dom Luiz
Portugal
IGIL

Centre of Geophysical Monitoring of the National Academy of Sciences of Belarus
Republic of Belarus
BELR

Inst. of Seismology and Geodynamics, V.I. Vernadsky Crimean Federal University
Republic of Crimea
CFUSG

Korea Meteorological Administration
Republic of Korea
KMA

National Institute for Earth Physics
Romania
BUC

Institute of Environmental Problems of the North, Russian Academy of Sciences
Russia
IEPN

Yakutiya Regional Seismological Center, GS SB RAS
Russia
YARS

Kamchatkan Experimental and Methodical Seismological Department, GS RAS
Russia
KRSC

North Eastern Regional Seismological Centre, GS RAS
Russia
NERS

Kola Regional Seismic Centre, GS RAS
Russia
KOLA

Sakhalin Experimental and Methodological Seismological Expedition, GS RAS
Russia
SKHL

Baykal Regional Seismological Centre, GS SB RAS
Russia
BYKL

Geophysical Survey of Russian Academy of Sciences
Russia
MOS

Mining Institute of the Ural Branch of the Russian Academy of Sciences
Russia
MIRAS

Altai-Sayan Seismological Centre, GS SB RAS
Russia
ASRS

Saudi Geological Survey
Saudi Arabia
SGS

Seismological Survey of Serbia
Serbia
BEO

Geophysical Institute, Slovak Academy of Sciences
Slovakia
BRA

Slovenian Environment Agency
Slovenia
LJU

Ministry of Mines, Energy and Rural Electrification
Solomon Islands
HNR

Council for Geoscience
South Africa
PRE

Real Instituto y Observatorio de la Armada
Spain
SFS

Institut Cartogràfic i Geològic de Catalunya
Spain
MRB

Instituto Geográfico Nacional
Spain
MDD

Sudan Seismic Network
Sudan
SSN

UPPSALA UNIVERSITET

University of Uppsala
Sweden
UPP

Swiss Seismological Service (SED)
Switzerland
ZUR

Thai Meteorological Department
Thailand
BKK

The Seismic Research Centre
Trinidad and Tobago
TRN

Institut National de la Météorologie
Tunisia
TUN

Kandilli Observatory and Research Institute
Turkey
ISK

Disaster and Emergency Management Presidency
Turkey
DDA

National Earthquake Information Center
U.S.A.
NEIC

The Global CMT Project
U.S.A.
GCMT

Red Sísmica de Puerto Rico
U.S.A.
RSPR

IRIS Data Management Center
U.S.A.
IRIS

Pacific Northwest Seismic Network
U.S.A.
PNSN

Subbotin Institute of Geophysics, National Academy of Sciences
Ukraine
SIGU

Dubai Seismic Network
United Arab Emirates
DSN

British Geological Survey
United Kingdom
BGS

Institute of Seismology, Academy of Sciences, Republic of Uzbekistan
Uzbekistan
ISU

Fundación Venezolana de Investigaciones Sismológicas
Venezuela
FUNV

National Center for Scientific Research
Vietnam
PLV

Geological Survey Department of Zambia
Zambia
LSZ

Goetz Observatory
Zimbabwe
BUL

2.7 ISC Staff

Listed below are the staff (and their country of origin) who were employed at the ISC at the time of this ISC Bulletin Summary.

- Dmitry Storchak
- Director
- Russia/United Kingdom

- Lynn Elms
- Administration Officer
- United Kingdom

- James Harris
- Senior System and Database Administrator
- United Kingdom

- Alfie James Barber
- System Administrator
- United Kingdom

- Gergely Csontos
- Web Developer
- Hungary

- John Eve
- Data Collection Officer
- United Kingdom

- Edith Korger
- Data Collection Seismologist
- Austria

- Domenico Di Giacomo
- Seismologist
- Italy

- Konstantinos Lentas
- Seismologist/Developer
- Greece

- Rosemary Hulin (née Wylie)
- Analyst/Administrator
- United Kingdom

- Blessing Shumba
- Seismologist/Analyst
- Zimbabwe

- Rebecca Verney
- Analyst
- United Kingdom

- Elizabeth Ayres (née Ball)
- Analyst/Historical Data Entry Officer
- United Kingdom

- Kathrin Lieser
- Seismologist/Analyst
- Germany

- Lonn Brown
- Seismologist/Analyst
- Canada

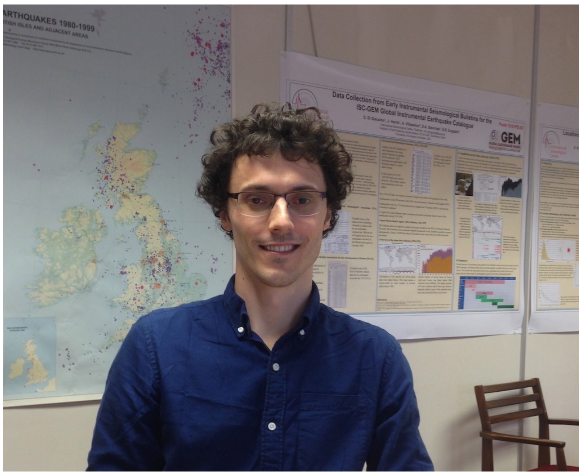

- Charikleia Gkarlaouni
- Seismologist/Analyst
- Greece

- Peter Franek
- Seismologist/Analyst
- Slovakia

- Angeliki Adamaki
- Seismologist/Analyst
- Greece

- Burak Sakarya
- Seismologist/Analyst
- Turkey

- Daniela Olaru
- Historical Data Entry Officer
- Romania

3

Availability of the ISC Bulletin

The ISC Bulletin is available from the following sources:

- Web searches
  The entire ISC Bulletin is available directly from the ISC website via tailored searches.
  (www.isc.ac.uk/iscbulletin/search)
  (isc-mirror.iris.washington.edu/iscbulletin/search)
  - Bulletin search - provides the most verbose output of the ISC Bulletin in ISF or QuakeML.
  - Event catalogue - only outputs the prime hypocentre for each event, producing a simple list of events, locations and magnitudes.
  - Arrivals - search for arrivals in the ISC Bulletin. Users can search for specific phases for selected stations and events.
- CD-ROMs/DVD-ROMs

  CDs/DVDs can be ordered from the ISC for any published volume (one per year), or for all back issues of the Bulletin (not including the latest volume). The data discs contain the Bulletin as a PDF, in IASPEI Seismic Format (ISF), and in Fixed Format Bulletin (FFB) format. An event catalogue is also included, together with the International Registry of seismic station codes.
- FTP site

  The ISC Bulletin is also available to download from the ISC ftp site, which contains the Bulletin in PDF, ISF and FFB formats. (ftp://www.isc.ac.uk)
  (ftp://isc-mirror.iris.washington.edu)

Mirror service

A mirror of the ISC database, website and ftp site is available at IRIS DMC (isc-mirror.iris.washington.edu), which benefits from their high-speed internet connection, providing an alternative method of accessing the ISC Bulletin.

4

Citing the International Seismological Centre

Data from the ISC should always be cited. This includes use by academic or commercial organisations, as well as individuals. A citation should show how the data were retrieved and may be in one of these suggested forms:

Data retrieved from the ISC web site:

- International Seismological Centre, On-line Bulletin, http://www.isc.ac.uk, Internatl. Seismol. Cent., Thatcham, United Kingdom, 2018.

Data transcribed from the IASPEI reference event bulletin:

- International Seismological Centre, Reference Event Bulletin, http://www.isc.ac.uk, Internatl. Seismol. Cent., Thatcham, United Kingdom, 2018.

Data transcribed from the EHB bulletin:

- International Seismological Centre, EHB Bulletin, http://www.isc.ac.uk, Internatl. Seismol. Cent., Thatcham, United Kingdom, 2018.

Data copied from ISC CD-ROMs/DVD-ROMs:

- International Seismological Centre, Bulletin Disks 1-26 [CD-ROM], Internatl. Seismol. Cent., Thatcham, United Kingdom, 2018.

Data transcribed from the printed Bulletin:

- International Seismological Centre, Bull. Internatl. Seismol. Cent., 46(9-12), Thatcham, United Kingdom, 2009.

Data transcribed from the printed Summary of the Bulletin:

- International Seismological Centre, Summ. Bull. Internatl. Seismol. Cent., July - December 2018, 52(II), Thatcham, United Kingdom, 2018.

The ISC is named as a valid data centre for citations within American Geophysical Union (AGU) publications. As such, please follow the AGU guidelines when referencing ISC data in one of their journals. The ISC may be cited as both the institutional author of the Bulletin and the source from which the data were retrieved.

BibTex entry example:

```
@manual{ISCcitation2018,
author = "International Seismological Centre",
title = "On-line Bulletin",
organization = "Internatl. Seismol. Cent.",
note = "http://www.isc.ac.uk",
address = "Thatcham, United Kingdom",
year = "2018"
}
```

5

Operational Procedures of Contributing Agencies

5.1 Seismological Central Observatory (SZO) of BGR, Germany

Gernot Hartmann, Thomas Plenefisch and Klaus Stammler
Federal Institute for Geosciences and Natural Resources (BGR), Hanover, Germany

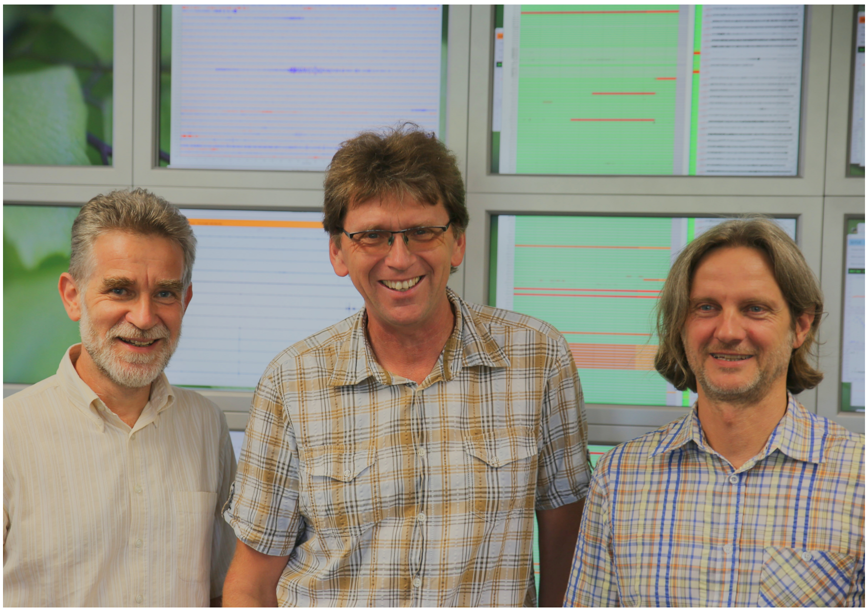

Gernot Hartmann, Thomas Plenefisch and Klaus Stammler

5.1.1 Introduction

The Seismological Central Observatory (SZO) is a department of the Federal Institute for Geosciences and Natural Resources (BGR) in Hanover (Germany). The three main tasks of the SZO are to observe and analyse earthquakes mainly focused on Germany and adjacent regions, to consult the government and national industry in the field of induced seismicity and to fulfill the German commitments for the verification of the Comprehensive Nuclear-Test-Ban Treaty (CTBT). In order to meet these requirements the SZO runs a considerable amount of seismic stations and hosts the date centre for seismological broadband data in Germany. It also supports the open data policy in seismology and therefore all waveform data are available to the public.

5.1.2 Station Network and Data Management

Station Network

The GRSN (German Regional Seismic Network) currently consists of 45 stations (Figure 5.1). They are all equipped with broadband sensors, mostly Streckeisen STS-2 and STS-2.5. The data are recorded continuously and transmitted via DSL connections or cellphone networks (GPRS, LTE) into the data centre of the Federal Institute for Geosciences and Natural Resources (BGR) in Hanover. The core of the GRSN, consisting of eight stations, was installed in 1991 in addition to the previously existing Gräfenberg array (see next paragraph). The number of stations was increased stepwise since then until today's configuration was reached. The available sample rates are usually 100 Hz and 20 Hz, at some stations also 1 Hz. The station sites have been carefully selected in order to approximate an even distribution over the area of Germany and to obtain optimum locations concerning noise conditions. The network serves as a backbone for the German seismological community and is used for the observation and analysis of local, regional and teleseismic events.

A unique subset of these stations is formed by the Gräfenberg array (GRF) situated in the Franconian Jura region in the South-East of Germany (see Fig. 5.1). The 13 stations of the array were installed between 1975 and 1980 and since then we record continuous digital broadband data from all stations. The stations are located in an area of about 50 x 100 km. The main purpose of this array has been, and still is, the observation and analysis of teleseismic signals. In the beginning the stations were equipped with the first generation of Streckeisen STS-1 instruments with a bandwidth of 20 s to 5 Hz at a sampling rate of 20 Hz. At ten sites there existed vertical channels only and at three sites three component systems were installed. As digitisers we used our own developments, since no suitable devices for high resolution seismic records were available at that time. These instruments were replaced by STS-2 seismometers and Reftek 130 digitisers in 2006 resulting in three component recordings and 20 and 100 Hz sampling rates at each station site. This GRF data set contains the longest history of digital broadband array data worldwide.

In addition to the backbone network GRSN, denser and mostly short-period networks are operated by a number of state agencies, but only a fraction of them is publicly accessible and technically compatible with the GRSN. The data of a large part of these open and technically compatible stations is also collected by the BGR and hosted by its data centre. The stations are provided mainly by universities, state agencies and some long-term monitoring projects. Due to their main task of monitoring specific areas, some of them are installed at locations with limited recording capabilities and only a small number of these stations is equipped with broadband instruments, the others have mid- or short-period seismometers.

A third group of dedicated stations is operated by the BGR within the frame of the Comprehensive Nuclear-Test-Ban Treaty (CTBT), consisting of a 25 element short-period seismic array with an aperture of 4 km (GERES) and two infrasound arrays in the Bavarian Forest (IS26, 8 elements) and Antarctica (IS27, 9 elements) as well as some additional infrasound training stations in Germany (see Section 5.1.4).

All three station groups together (GRSN, local networks and CTBT stations) total about 180 seismic stations from within Germany plus about 20 infrasound stations that are currently transmitted to the data centre in Hanover.

Data Archive

The seismic and infrasound data archive of the BGR consists of permanently archived continuous data of the stations described in the section above. As already mentioned, the oldest data in this archive are GRF array data from 1975 (only a few data segments of one station, the continuous operation started in 1976). In 1991 the GRSN was installed and started operation at eight sites and was extended many times up to the current number of stations. At the beginning, in 1975, the archive media was 800 bpi (bytes per inch) reel tapes written in a self-designed data format. After several time consuming recopy operations using 1600 bpi tapes, WORM disks and CDs the complete data set of the archive is now stored on RAID systems using miniSEED as storage format. The total size is about 30 TB. Currently it is growing by about 10 GB a day. All data are openly available through various interfaces, the most common interface currently is via FDSN webservices (see Section 5.1.2).

Data Flow

All stations described above are connected to the data centre in Hanover via the seedlink protocol (`https://www.seiscomp3.org/doc/applications/seedlink.html`). Their continuous data arrive in the data centre a few seconds after they have been recorded. There the data are collected, quality checked and processed by event detectors (Figure 5.2). After some weeks at temporary disk locations the data are permanently archived and several backup copies are created. The storage media used are RAID systems, for the backups a redundant RAID system, a tape robot system and removable hard disks are used. The tape robot handles three copies automatically, together with the two redundant RAID systems and two copies on external disks our data reside on seven physically different media in order to minimise the probability of data loss due to media failure. Time segmented subsets of the data get checksums and are regularly checked for integrity including all backup copies.

Quality Checks

Automatic processes (own Python software) are running to analyse the data streams for quality issues. The routines check for data gaps, timing problems (using correlation and array features) and irregular amplitude deviations in comparison to the mean of all other traces. Additionally the log channels of the digitizers are scanned for state-of-health (SOH) parameters reported. The parameters are extracted and statistically analysed, unusual deviations produce warning or error messages. All information gathered (i.e. status messages) is collected in a database connected to an automatic alarm system to activate station operators on duty to fix hardware and software issues in the data centre or at the station site as soon as possible.

Integration in EIDA

The BGR is part of the virtual European data centre EIDA (European Integrated Data Center, `https://www.orfeus-eu.org/data/eida`). There, under the umbrella of ORFEUS, a number of European data

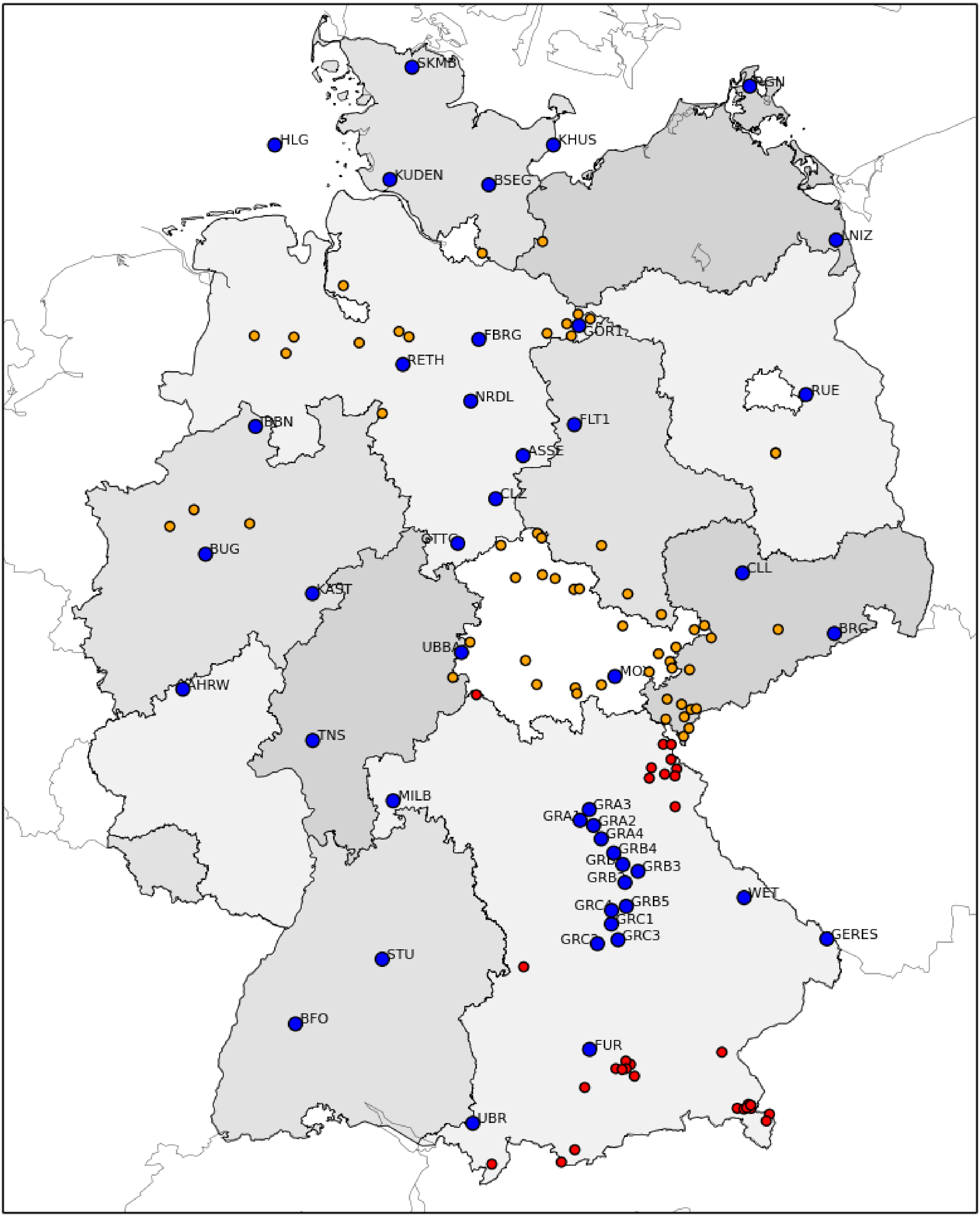

__Figure 5.1:__ Map of open stations in Germany. The labeled, blue circles show the locations of the GRSN stations, the unlabeled, orange circles indicate local networks and long-term project stations hosted by the BGR and the red circles show the Bavarian network hosted at a separate server. All stations are available through EIDA (see Section 5.1.2). The gray shaded areas indicate the federal states within Germany.

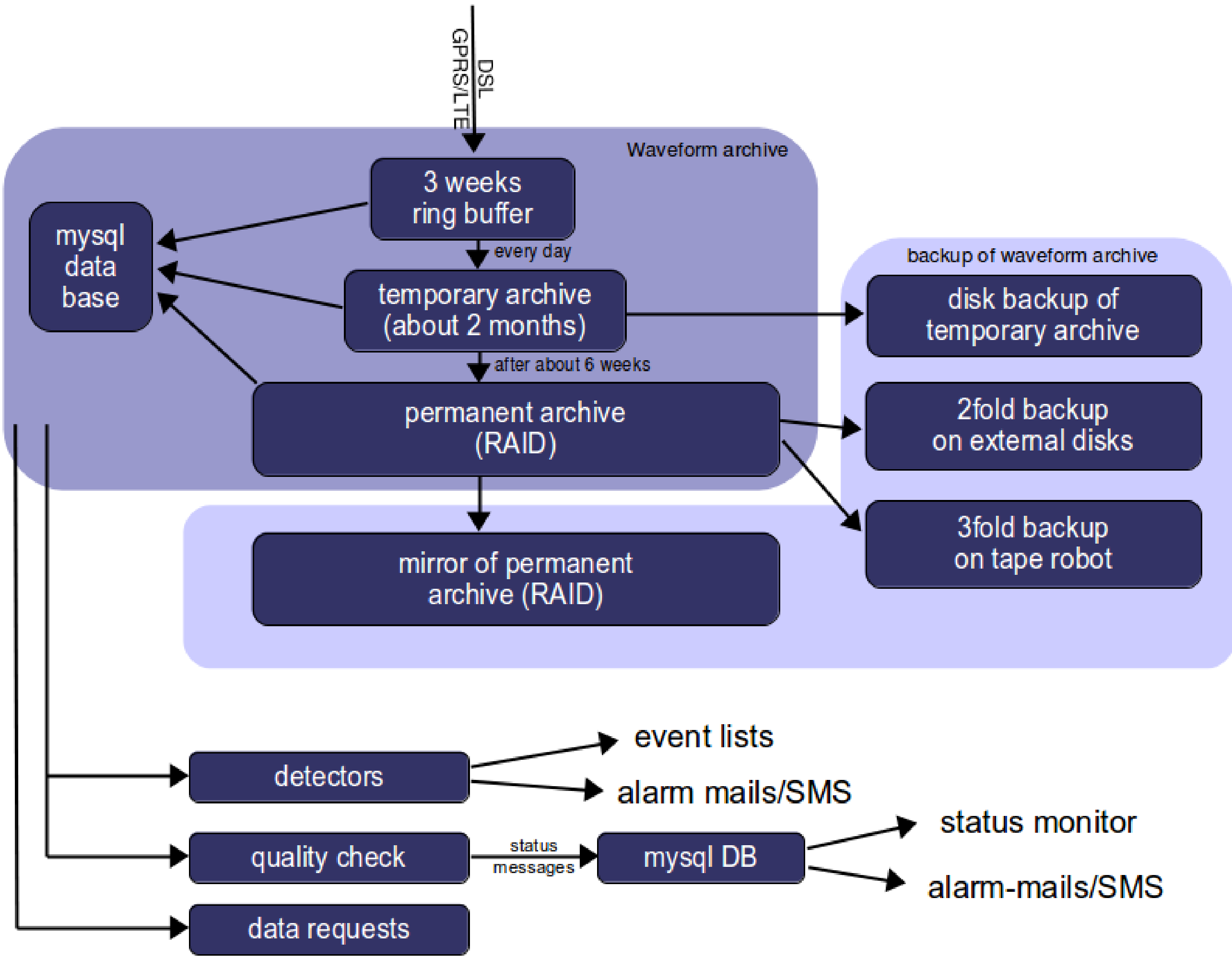

Figure 5.2: *Schematic data flow inside the data centre. The data flow in online and are stored in ring buffers on seedlink servers. Full day files are copied into a temporary archive. After about 6 weeks the data are permanently archived on large RAID systems. For all storage systems backups exist, the permanent archive has in total 6 backup copies on different media. All data access is managed by a database, feeding data into detectors, data requests and quality check routines. A second database handles status messages connected to a viewing interface and alarm triggers.*

centres agreed to standardise their data format, the access to their waveform data as well as procedures for quality checks. A common platform enables the user to access waveforms of thousands of stations in Europe with a few clicks or to integrate EIDA waveforms in their data processing algorithms using standard retrieval software, currently arclink (about to be retired) and FDSN webservices (as offered by IRIS).

5.1.3 Routine Data Analysis

After the GRSN went in operation in 1991 and a continuous online transmission of the waveform data to the BGR was settled, a processing pipeline for regular analysis of seismic events in Germany and adjacent areas was developed. The analysis procedures evolved since that time as well as the number of stations were steadily increased. Nowadays, the seismological analysis makes use of more than 200 stations in and around Germany. The near real time digital waveform data as well as data from the past are permanently available in the seismic waveform data archive of BGR (see Section 5.1.2).

Automated Detection Process and Manual Event Review

We employ a number of detection algorithms to scan the continuous data streams for seismic events. We implemented simple STA/LTA detectors, an FK-array detector, run Seiscomp3 (`https://www.seiscomp3.org`) on the data traces and developed a self-made grid search detector analyzing summation signals along phase travel time curves. The results of all detectors are grouped and combined into a detection list with preliminary locations. Relevant events trigger an alarm to the analyst on duty. The interface to the detection list is implemented as an internal web site offering preview waveform figures and resolution diagrams.

In a daily routine the analyst on duty reviews this list of detection manually and verifies or rejects the events. The analysis is performed with the Seismic Handler software package (*Stammler*, 1993). We focus on seismic events in Germany as well as on regional and teleseismic events, for which signals were recorded at German stations. For detection and analysis of events close to the national borders we receive online waveform data of about 50 stations from Germany's neighbouring countries to complement our data set. In case of strong earthquakes, a quick epicenter determination can be provided some minutes after the alert of the near real time detector.

Analysis of Local Seismic Events

In general, seismic events in Germany with magnitude 2 and above are located, the magnitudes are estimated and the source is classified as tectonic, induced or man-made. Furthermore, events in neighboring countries with magnitudes larger than 3 are analyzed, if clear phases on GRSN stations are observed. The results are stored in an event data base and are retrievable from the BGR website. A simplified velocity model for Germany is used if a large number of stations in a wide distance range are incorporated. This model is based on mean travel time curves derived from phase readings at GRSN stations for the past 25 years. For specific regions we make use of locally defined velocity models, e.g. in Vogtland or Northern Germany (see Section 5.1.5). The epicenter parameter and the phase readings are sent to the European-Mediterranean Seismological Centre (EMSC) after finishing the daily routine analysis.

Earthquake Catalogue for Germany

The event database at BGR contains all estimated parameters of the manually reviewed local seismic events. Besides the event determination of BGR, the results of seismological agencies of the federal states of Germany and universities are collected and associated in this data base. These agencies operate small-scale local station networks and can provide precise location results for events within their monitoring area. They are marked as preferred solutions. Additionally, epicenter data from earthquake catalogues of neighboring countries will be included and associated to events in the data base, when such publications becomes available. Customized compilations of bulletins are provided regularly or on request. The main product is the "Data Catalogue of Earthquakes in Germany and Adjacent Areas". Since the beginning of regular earthquake analysis with GRSN at the BGR, the catalogue is published monthly.

The information is given in the international standardized format ISF/IMS1.0 (`http://www.isc.ac.uk/standards/isf`). The catalogue is made available at the BGR website (`http://www.bgr.bund.de/erdbebenkatalog-deutschland`). Furthermore, the catalogue is sent to a number of recipients, e.g. to the ISC for their integration in the final ISC Bulletin.

Since 1974 the German earthquake catalogue was published yearly, until 1997 as printed matter, more recently electronically only. The monograph "Erdbebenkatalog für Deutschland" by *Leydecker* (2011), contains historical earthquakes before that time, wherein the first entry dates back to the year 813. The German earthquake catalogue has a magnitude of completeness of 2. It mainly contains tectonic earthquakes. However, since increasing mining activities triggered a higher rate of seismic stress release, more so-called mining induced events were detected and included in the event data base. Last but not least, explosions mainly in quarries and opencast mines are seismically recorded. Some of them are larger than magnitude 2, and therefore they are analyzed and included in the event data base as well.

Figure 5.3 shows the seismicity in Germany in the past 20 years. On average about 500 seismic events with magnitude above 2 are analysed every year. Of these 30% are tectonic earthquakes, 14% induced events, and 56% quarry blasts and explosions. However, no blast exceeded a magnitude of 3. Whereas, one earthquake per year on average is larger than magnitude 4. The tectonic active regions are the Lower Rhine area, the Upper Rhine Graben, Lake Constance area, Swabian Jura, the Alps area, and the Vogtland region. The occurrence of swarm quakes in the Vogtland is of special interest (see Section 5.1.5). The mining induced events are concentrated in the different mining areas: Coal mining caused the events in the Ruhr coal mining district and the Saar mining district. After abandoning mining in the Saar district in 2008 and the closing of all mines but one in the Ruhr district, the seismic activity was almost completely eliminated. Induced events by potash mining are registered in the Werra potash mining district and the South Harz mining district. Natural gas production caused an increasing number of seismic events in Northern Germany in the past 10 years (see Section 5.1.5). The utilization of geothermal energy is also accompanied by the risk of occurrence of seismic events as seen near Landau and Munich.

Analysis of Teleseismic Events

Besides investigations of local seismic events there is also a routine analysis of regional and teleseismic events at the SZO. Following the definition in the New Manual of Seismological Observatory Practice (NMSOP) (*Bormann*, 2012) we define as regional seismic events those occurring in the distance range up to 15 degrees (dominated by crustal and uppermost mantle phases) while events above 15 degrees distance are regarded as teleseismic. At the SZO teleseismic events are solely located with stations in Germany and in some cases supplemented by stations from neighbouring countries. The procedure is based on a detection list automatically created by several distinct trigger algorithms. Since only stations in Germany and surrounding countries are involved - which are far away from the seismic events - we apply array methods to identify distinct seismic phases and to locate the events. Either by f-k analysis of the data of the densely spaced Gräfenberg array sites or by coherent phase picking at waveforms of the large aperture GRSN stations we retrieve slowness and azimuth values for teleseismic phases. This direction information is used for backtracking the raypaths to estimate the epicenter. For events in the distance range below 100 degrees the first arriving P-phase is used for location. Figure 5.4 shows an example of the f-k analysis for a magnitude 8 event offshore Mexico (08.09.2017, 04:49:21 UTC, Ms 8.3)

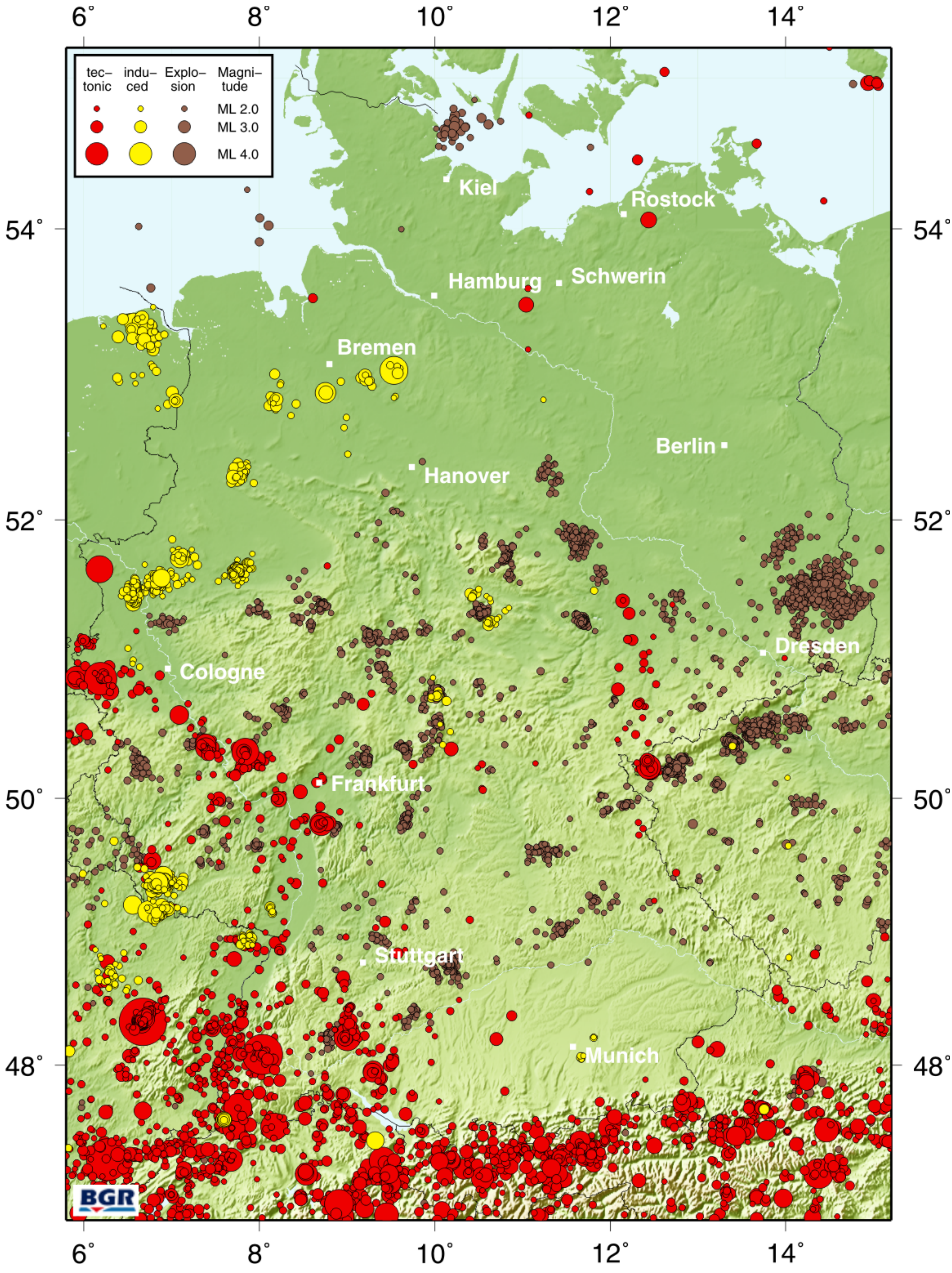

Figure 5.3: *Seismic events with magnitude 2.0 and above in Germany and adjacent regions in the recent 20 years (1998-2017). The tectonic events, induced events, and explosions are colour coded. The different magnitudes of the events correspond to the size of the circles.*

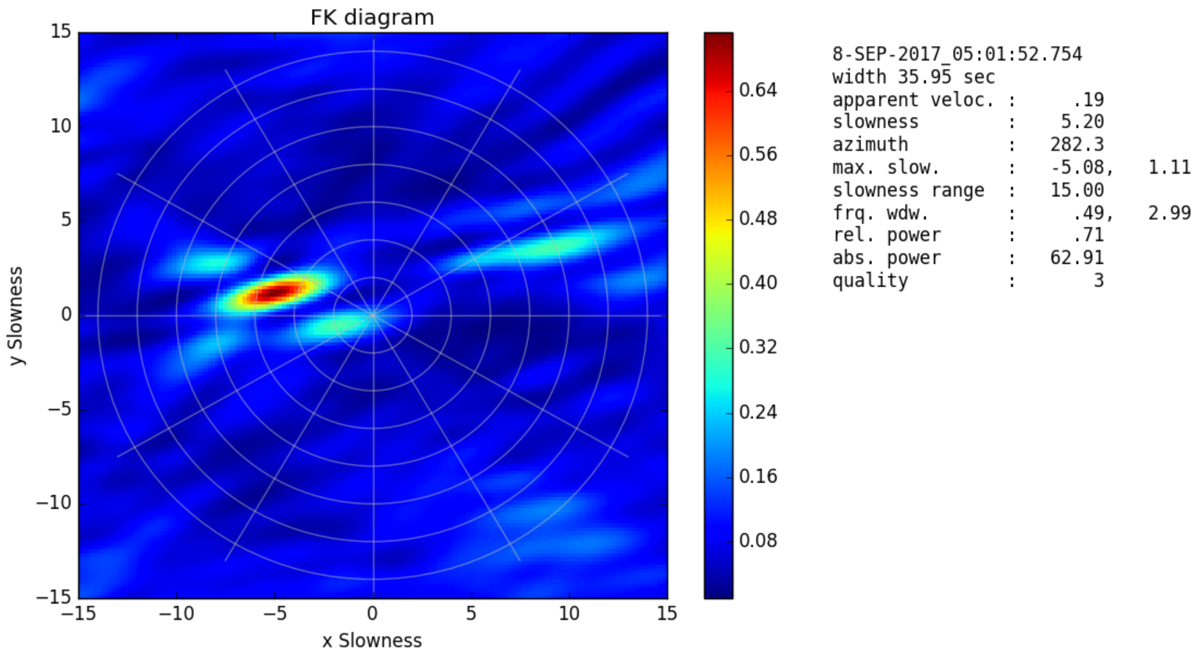

Figure 5.4: *Result of the f-k analysis for the P wavetrain of an event offshore Mexico (08.09.2017, 04:49:21 UTC, Ms 8.3) recorded at the Gräfenberg array. The inferred slowness and azimuth can be used to backtrack the ray and determine the epicenter.*

recorded at the Gräfenberg array. The inferred slowness is 5.20 and the azimuth 282 degrees.

For all P phases the body wave magnitudes are calculated and for events with a source depth shallower than 50 km the surface magnitude Ms is determined at stations GRA1 and MOX. Beside such common parameters as hypocenters, magnitudes, onset times and phase amplitudes, slowness and azimuths, which are important for teleseismic events, are also stored in a teleseismic database. As for the local events the data are transmitted to the EMSC immediately after manual analysis and monthly bulletins are sent to the ISC. Figure 5.5 shows all teleseismic events of 2017 that had been analyzed by the SZO with stations in Germany. Altogether, these are 1089 events. 837 events were located with our own algorithms. For the other 252 events we provide phase picks but no reasonably precise locations were found. In these cases locations from other agencies, mostly from NEIC or EMSC, were associated.

Depth Phases, Secondary Phases and Core Phases

In the routine analysis a special emphasis is also given to later phases. On one hand this is related to the detection and analysis of depth phases like pP or sP which appear after the P phase. Such a depth phase is comparably easy to identify as its slowness is identical or at least very similar to its related direct phase. Only when a prominent depth phase is visible, is the depth of the event determined, otherwise a fixed depth (e.g. 10 or 33 km) is chosen and assigned to the event. On the other hand, later phases like S, PcP, PP, SS, SKS etc. are also picked in the case of a stronger event, mostly for events above magnitude 6. We use so-called "phase maps" in order to identify later phases which may be worthwhile for further analysis. For a set of phases it shows a comparison between the theoretical values of travel time and slowness and a possibly corresponding occurrence of signal energy derived

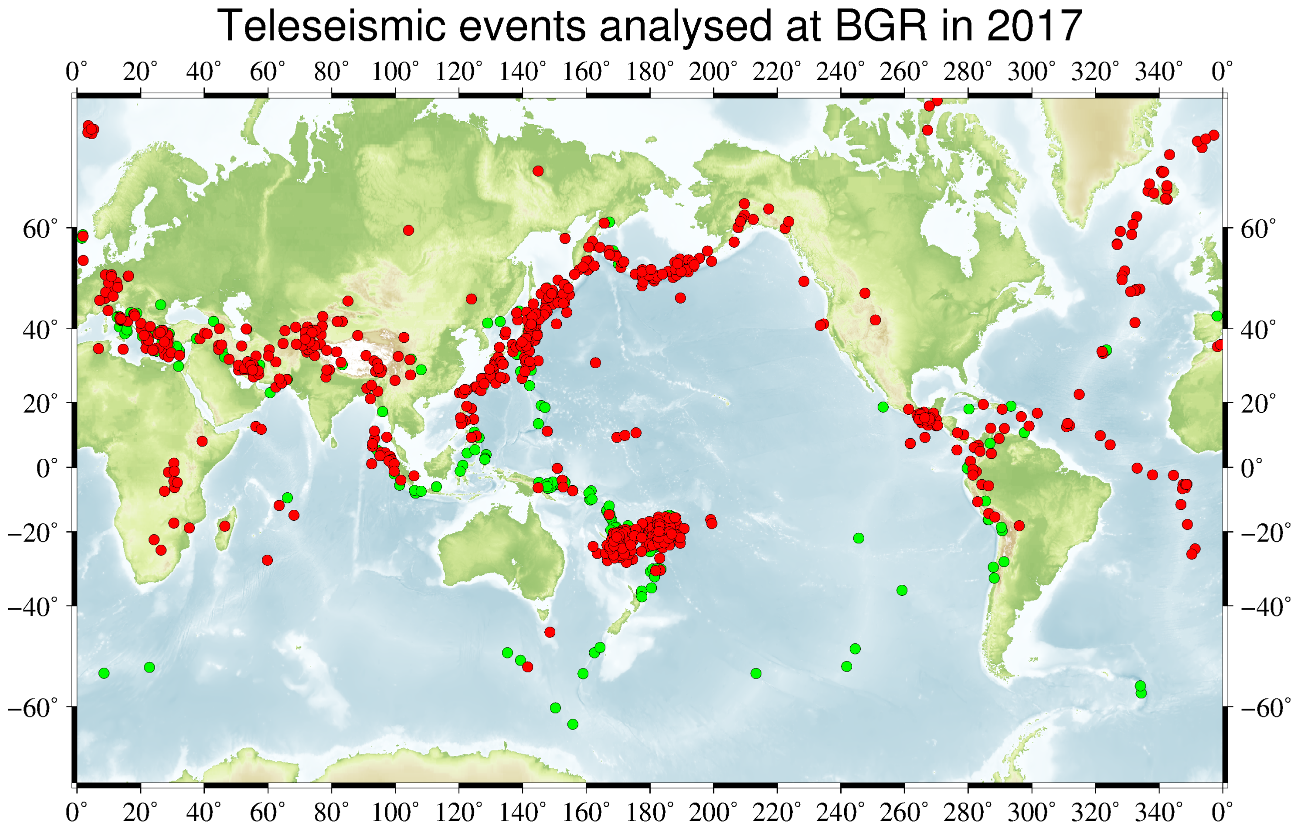

Figure 5.5: *World map showing epicenters of all teleseismic events that had been analyzed at the Central Seismological Observatory (SZO) of BGR for the year 2017. Red circles depict the events with epicenter location of BGR, green circles those for which only phase readings at German stations are associated to epicenter locations from other agencies.*

from array data of GRF and GRSN. Thereby, the plot helps the analyst to find those secondary phases which may be analysable. An example of this procedure is given in Figure 5.6 for the Mexico event of 08.09.2017 mentioned above. Figure 5.7 shows the three-component seismograms of the offshore Mexico event recorded at GRA1 comprising body and surface waves as well as the identified and picked direct phase (P) and later phases (S, SS, L).

Nearly 40% of our located events contain core phases generated at sources in the distance range greater than 140 degrees. These events are mostly located within the subduction zone at Fiji and Tonga, one of the most seismically active regions in the world. Since the epicentral distance between Fiji/Tonga and stations in Germany ranges between 142 degrees and 150 degrees, our stations are in most cases in or close to the caustic of the PKP branches in about 144 degrees. At the caustic the PKP phases (PKPdf, PKPbc and PKPab) are of comparably strong amplitude and can be easily identified by traveltime and slowness on short period filtered records. Especially, the PKPbc is dominant from 146 degrees to about 153 degrees. Due to the strong variation of the PKPbc slowness with distance, the phase is very suitable to locate the events. Therefore, and with respect to the caustic, we are sometimes able to locate events down to a magnitude of 4. Depending on the hypocenter and the radiation it is sometimes possible to identify and pick all three PKP branches and moreover in some cases also the corresponding depth phases. For deep Fiji events we are able in numerous cases to locate them and their depths in comparable accuracy to NEIC, GFZ and EMSC.

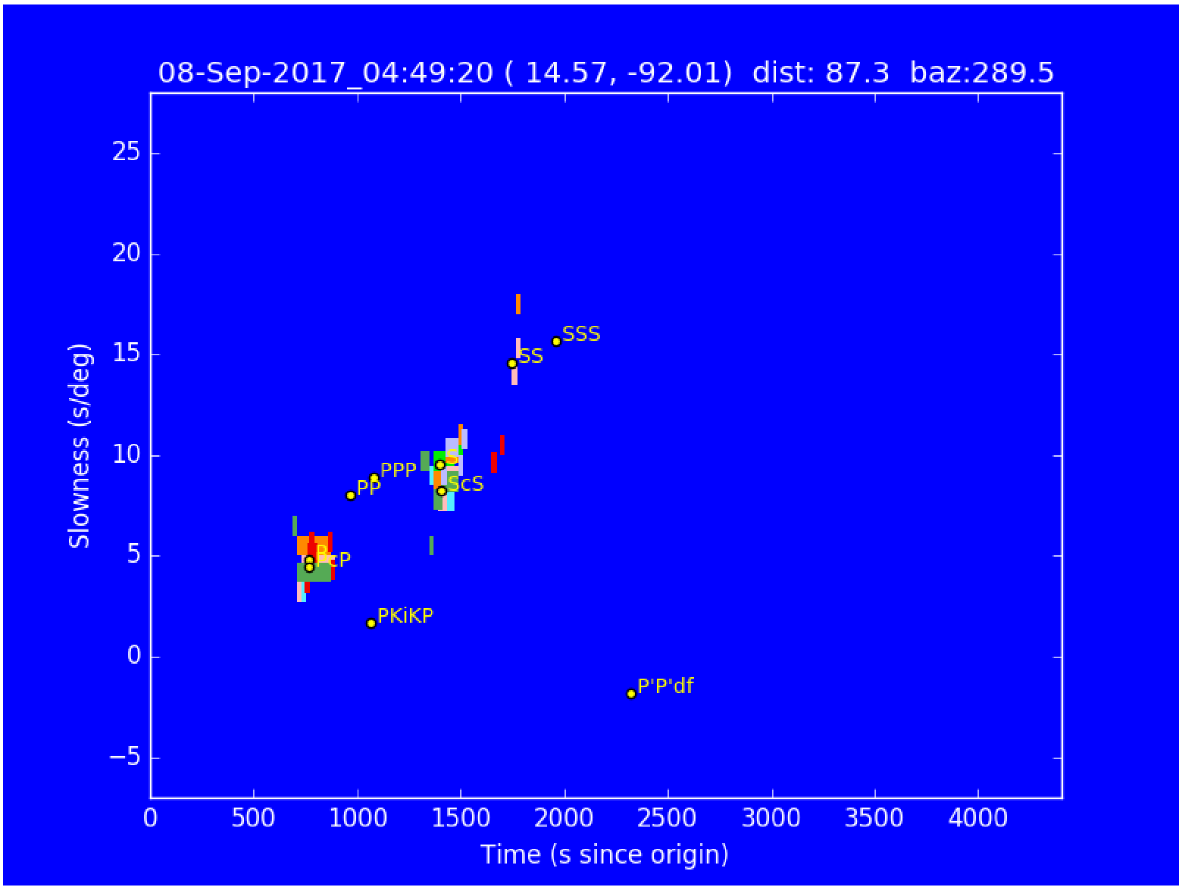

Figure 5.6: Phase map calculated for the magnitude 8 event offshore Mexico (08.09.2017, 04:49:21 UTC, Ms 8.3). The theoretical onset times and slowness of distinct phases are given by labeled circles. Coloured bars denote times for which coherent energy is found in the "real" seismograms either for the Gräfenberg array or for the GRSN (different colors are related to different filters, components or arrays not explained here). In case theoretical values coincide with a coloured bar an analysis of the phase may be worthwhile.

Table 5.1: Quantity of particular picked phases in 2017. PKP are PKP phases which could not be unequivocally assigned to one of the three PKP branches.*

Direct Phases	Quantity
P	10844
pP	1139
sP	61
Pdif	280
sPdif	26

PKP Phases	Quantity
PKPdf	1237
PKPbc	5655
PKPab	733
pPKPdf	82
pPKPbc	685
pPKPab	11

Later P Phases	Quantity
PP	341
PcP	18
PKP*	117
PKiKP	72

S + L Phases	Quantity
S	217
SS	27
ScS	1
SKPdf	11
SKPab	1
L	1437

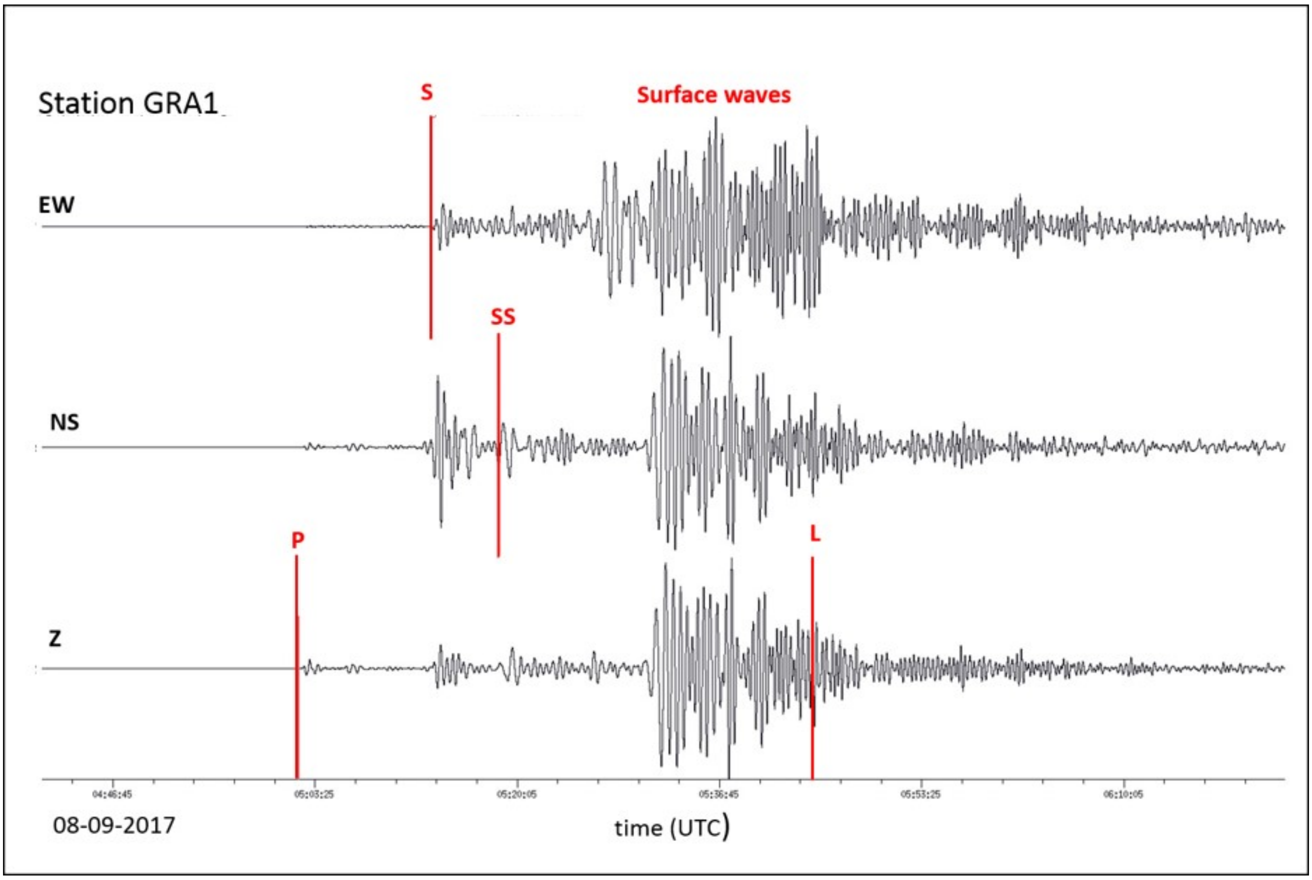

Figure 5.7: Three component seismogram of the magnitude 8 event offshore Mexico (08.09.2017, 04:49:21 UTC, Ms 8.3) recorded at station GRA1 of the Gräfenberg array. The SRO-LP filtered seismograms show the body and surface waves as well as identified and picked phases.

In summary, altogether 10844 P phases, 306 Pdif phases, 1888 later phases and 8403 PKP phases including depth phases have been determined in the year 2017 and incorporated in our database (Table 5.1). In case of a strong and/or important earthquake, like the Tohoku earthquake 2011, the Amatrice earthquake 2016 or the recent Lombok event 2018 we create special websites, give information and interviews to the media and respond to questions from the public.

5.1.4 Operating the German National Data Center for the Verification of the CTBT

The development of nuclear weapons is attended by the necessity for nuclear tests, most of them are conducted beneath the surface. Seismological stations are predestined for the monitoring of underground explosions. Consequently, the BGR with its Central Seismological Observatory was requested to host the German national data center (NDC) for the verification of the CTBT. After the Partial Test Ban Treaty was signed in 1963, the initial Gräfenberg array (GRF) was installed by the Advanced Research Projects Agency (ARPA) of the United States of America in order to register nuclear explosions mainly in the former Soviet Union. In the 1970s the array was reconfigured and modernized and became the world's first broad band digital seismic array (see Section 5.1.2). Thus, the data archive at BGR provides seismic GRF recordings for nearly all nuclear tests at the different test sites for more than 40 years.

Small aperture arrays for better detection capability of nuclear tests in regional distances were installed in the 1980s in Norway, Finland, and Germany. The GERES array is part of those stations. The geological conditions and distance from urban areas made it a highly sensitive station, which became one of 50 primary seismic stations (PS19) in the International Monitoring System (IMS) of the CTBT. The BGR assumed the responsibility as station operator in 1997. The array was upgraded to fulfill the requirements of the IMS.

Since the CTBT prohibits not only underground nuclear tests but also explosions in the ocean and in the atmosphere, hydroacoustic and infrasound techniques are necessary for the verification of the treaty. In this regard, the BGR established the infrasound array IS26, which is co-located to the seismic PS19 array. In 2001, it became the first certified infrasound station of the IMS. Another infrasound station (IS27) at the instigation of BGR was installed at the German Antarctic research station Neumayer. Finally, BGR equipped the seismic station SNAA at the South African Antarctic research base SANAE in co-operation with the Council for Geosciences in South Africa. This is a three component station and acts as an auxiliary seismic IMS station (AS035).

Ensuring the reliable operation of the German IMS stations is one task of the German NDC for the verification of the CTBT. Main criteria are a data availability of at least 98 % per annum with a maximum transmission latency of 5 minutes to the international data center (IDC). The second important NDC task is to provide the German government with the scientific expertise in monitoring nuclear explosions. Moreover, the NDC is located at the interface between CTBTO and the German verification community and supports research activities on verification-related issues. The German NDC benefits very much from the integration with the Central Seismological Observatory (SZO) at BGR. For the analysis of suspicious events, the NDC makes use of all IMS data complemented by data of international seismic networks, which are freely available through international data centres (e.g. IRIS). This allows independent processing, aimed at improving detection capability, localization and source identification. For example, the set of six nuclear explosions in North Korea within the recent 12 years allows a comprehensive assessment with precise results of relative location and source mechanism. Figure 5.8 shows the recordings of the six North Korean nuclear explosions at the German IMS station PS19 (GERES).

5.1.5 Analysis of Special Seismic Events

Induced Seismicity at the Natural Gas Fields in Northern Germany

The Northern German basin is a tectonic region of relatively low seismic activity with only singular and weak tectonic events. However, during recent decades seismicity rose in the vicinity of natural gas fields in that area with continuous gas gathering. Due to the spatial vicinity of the earthquakes to the operated gas fields and their occurrence starting after the beginning of extraction they are ranked as induced seismic events. The area of epicenters of these events extend 50 km NS and 400 km EW from the border to the Netherlands in the West to Altmark region in the East (Figure 5.9).

Altogether, more than 80 events with ML 0.5 to 4.5 were detected and analyzed between 1977 and 2017. Many of them were felt by some of the inhabitants up to 15 km from the epicenter whereas the strongest one, the magnitude 4.5 event close to the village of Rotenburg on 20th October 2004, was felt in Hamburg as far as 65 km from the epicenter. Whereas epicenters could be determined precisely, other

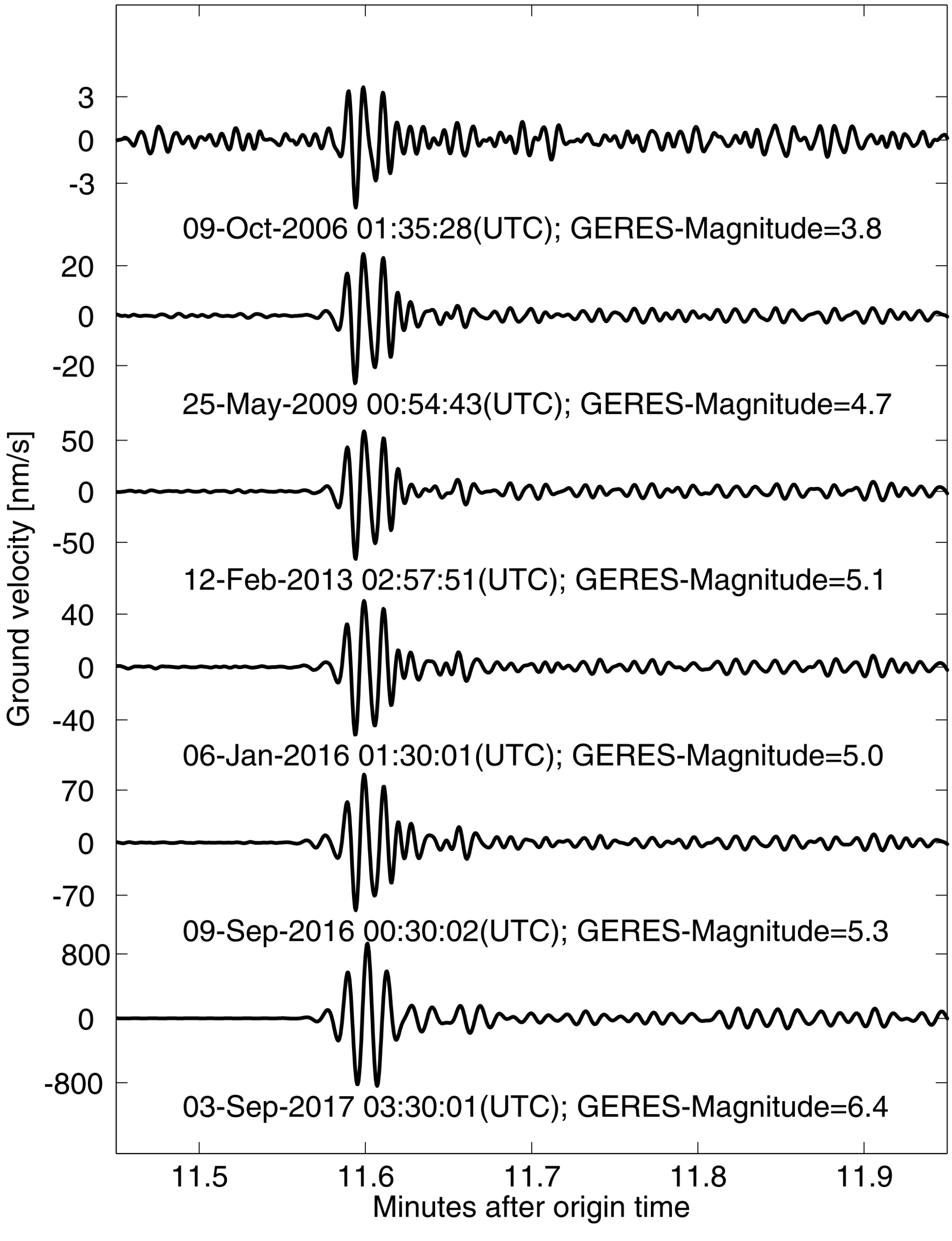

Figure 5.8: *Recording of nuclear explosions: The six North Korean nuclear explosions were recorded at the German IMS station PS19 (GERES) about 11.58 minutes after origin time. The seismic beams are displayed, which are estimated from the filtered traces (Bandpass 1.2-2.8 Hz) of the 25 array elements. The signals of the P wave are highly correlated due to the similar source conditions of the individual nuclear explosions. They differ mainly in the amplitudes, from which the GERES magnitude is calculated.*

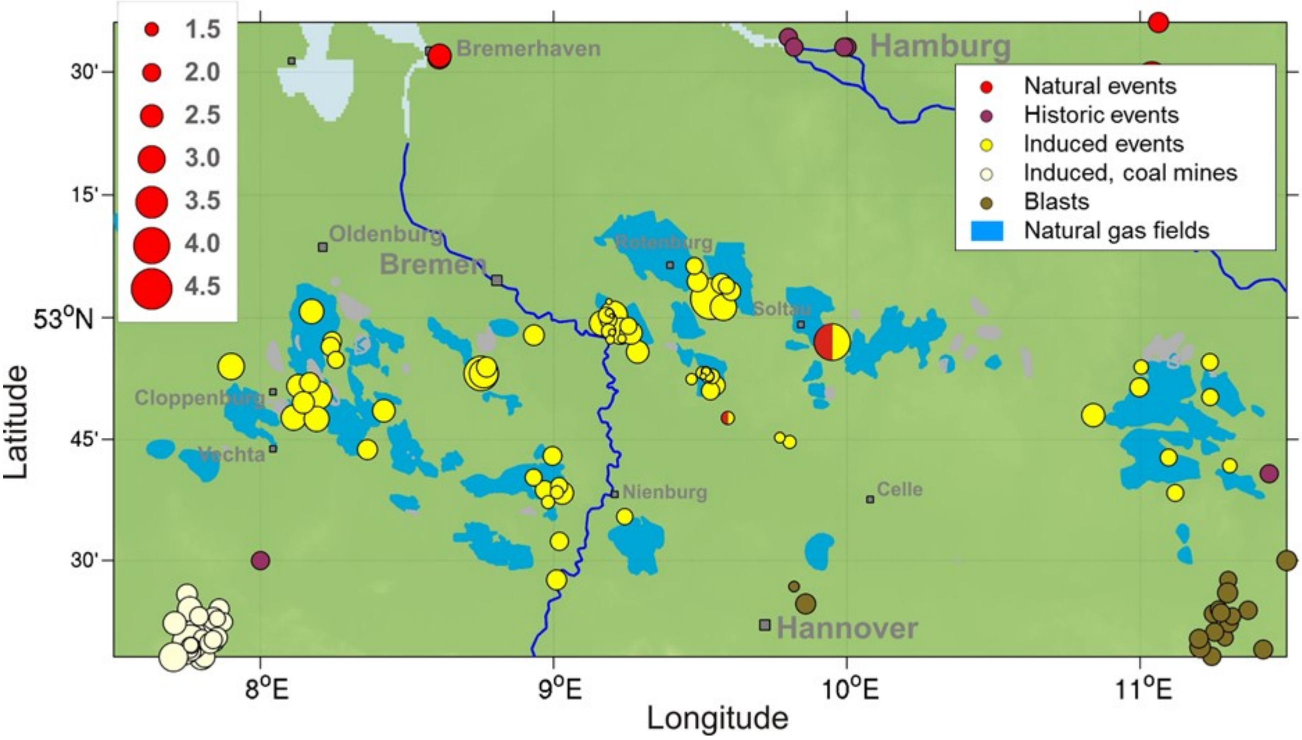

Figure 5.9: *Seismicity in the vicinity of the natural gas fields (blue) in Northern Germany of the years 1977 to 2016. Events are divided into induced events (yellow), natural events (red), blasts (brown) or historical events (purple). The bicolored event is the Soltau earthquake of 1977 for which it is still not clear if it is induced or natural. (Source: Nicolai Gestermann)*

source parameters, such as focal depths and focal mechanisms, were of lower accuracy. This was mainly caused by the sparse station coverage in the area, at least until 2010, and unfavourable signal-to-noise conditions as a result of thick sedimentary layers. The situation changed when the SZO installed some permanent and temporary stations in the area from 2010 onwards and the gas production companies also started to renew and extend their monitoring networks. On the basis of the enlarged networks focal depths are now more precisely determined for the recent events. It became apparent that most of the events have focal depths close to the reservoir horizon, a further indication for their classification as induced events.

The process of earthquake generation is still not well understood. Trigger mechanisms have not systematically been investigated. However, it is commonly accepted that there is a pressure reduction in the reservoir as a consequence of the gas extraction which leads to heterogeneous compaction within the reservoir and variations in the local stress field. The majority of the focal mechanisms calculated so far represents normal faulting and orientations of nodal planes being in quite good agreement with the strike direction of tectonic faults limiting the natural gas fields.

Knowledge and competence in the field of induced seismicity is of great importance for the SZO as division of BGR. As a subordinated agency of the federal government BGR has a duty to inform and advise the government as well as the public in any issues of energy supply as well as of protection of the civil population. In this context the expertise of BGR in the field of induced seismicity and its aftermath is steadily demanded during recent years.

Swarm Earthquakes in Vogtland/NW-Bohemia

An interesting area exhibiting natural seismicity in Germany is the Vogtland/NW-Bohemia area at the border between Germany and the Czech Republic. It is known as one of the most famous earthquake swarm regions in Europe. The special type of seismicity - called swarms - is expressed by the accumulation of a huge number of events of similar magnitude and their episodic reoccurrence. During a swarm hundreds or thousands of earthquakes without a distinct main shock occur spatially and temporally clustered.

The most recent swarm in Vogtland/NW-Bohemia occurred between the 10th of May and the beginning of August 2018. With more than 1000 detectable events and magnitudes up to 3.9 it is one of the most prominent swarms in last decades succeeding the big swarms of 2011, 2008, 2000 and 1985/86. The swarm is located close to the small village of Novy Kostel on Czech territory close to the border with Germany. The events were felt by a huge number of inhabitants on the Czech and German side and numerous requests were posed to the SZO. The SZO launched a press release and several interviews were given to the media. During the routine analysis at the SZO more than 100 events with magnitude above 2 were located and incorporated in our database as well as in the German earthquake catalogue where our analysis supplements the analysis of the universities, in this case the analysis of Collm Geophysical Observatory of the Leipzig University (for more information on Collm observatory and their analysis of events in Vogtland region see article in Summary of the Bulletin of the ISC by *Wendt and Buchholz* (2017)) and the TSN (seismic network of Thuringia) of the Jena University. The epicentres of the new swarm as well as those of the preceding swarms are given in Figure 5.10. The new swarm is located in the more northern part of the NNW-SSE oriented cloud of epicentres formed by preceding swarms. Primarily, all epicentres follow the strike of the Marianske Lazne fault zone and parallel striking fault systems and are located close to the crossing with the Eger rift.

The detailed analysis of the distinct swarm events is not only of statistical interest and to hold a complete catalogue. The analysed Vogtland events are also a basis for scientific investigations with respect to the physical and tectonic reasons and processes of the swarms, which are still under debate. There are many indications for some kind of volcanic phenomena as reasons for the swarms and some recent scientists have formulated the hypothesis that the swarms may be a kind of precursor for the formation of a volcano.

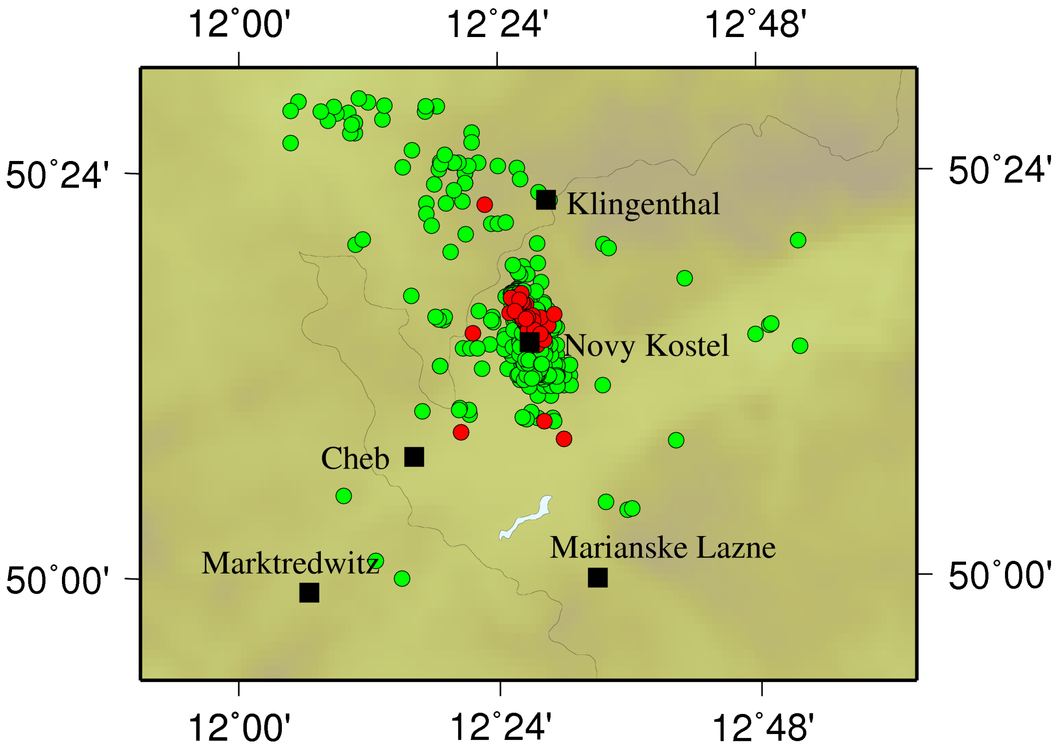

Figure 5.10: *Epicenters of earthquakes recorded and analysed at the SZO for the broader region of Vogtland/NW-Bohemia. Green circles denote the events since 1990, red circles the events of the recent swarm in 2018.*

5.1.6 References

Bormann, P. (Ed.) (2012), New Manual of Seismological Observatory Practice (NMSOP-2), IASPEI, GFZ German Research Centre for Geosciences, Potsdam, `http://doi.org/10.2312/GFZ.NMSOP-2`.

Leydecker, G. (2011), Erdbebenkatalog für Deutschland mit Randgebieten für die Jahre 800 bis 2008. (Earthquake catalogue for Germany and adjacent areas for the years 800 to 2008). *Geologisches Jahrbuch*, *E59*, BGR Hanover.

Stammler, K. (1993), Seismic Handler – Programmable multichannel data handler for interactive and automatic processing of seismological analyses, *Computers & Geosciences*, *19*(2), 135–140, `http://www.seismic-handler.org`, `http://doi.org/10.1016/0098-3004(93)90110-Q`.

Wendt, S. and P. Buchholz (2017), Collm Geophysical Observatory, *Summ. Bull. Internatl. Seismol. Cent.*, January – June 2014, *51*(I), pp. 32–44, `http://doi.org/10.5281/zenodo.996043`.

6

Summary of Seismicity, July - December 2015

The largest event in this Summary's time period was the M_W 8.3 Illapel earthquake near the coast of central Chile (16/09/2015 22:54:30.59 UTC, 31.6407°S, 71.6892°W, 12 km, 2352 stations (ISC)). With 80 entries to date in the Event Bibliography (*Di Giacomo et al.*, 2014; *International Seismological Centre*, 2018) it was also the event that most interested the scientific community for this time period. The megathrust event ruptured an about 200 km long stretch along the Central Chilean subduction zone where the Nazca Plate subducts beneath the South American Plate (*Ye et al.*, 2017). Previous larger earthquakes occured in this region in 1943 and 1880 (e.g. *Satake and Heidarzadeh*, 2017; *Ye et al.*, 2017). The Chilean subduction zone is prone to large megathrust events with the Illapel event being the third tsunamigenic earthquake with a magnitude greater than 8 in Northern and Central Chile in this decade (first event was the 2010 Mw 8.8 Maule event, second was the 2014 Mw 8.1 Iquique event). The largest slip (between 5 and 16 m) is located about 70 km to the NW of the epicentre and with the shallow part of the slip seeming to extend to the trench axis (*Satake and Heidarzadeh*, 2017). The main shock triggered various aftershocks (1388 events in the ISC Bulletin between 33°S to 29°S and 73°W to 71°W in the two weeks following the main shock). The aftershocks in the northern part of the rupture area show an upper and lower cluster along dip. This was also observed for the Maule event, suggesting that this might be a pattern for the Central Chilean margin (*Lange et al.*, 2016).

Moving about 20 degrees further north along the South American margin, on 24 November the second and third largest earthquakes during this Summary's time period occured at about 600 km depth. These two events are only separated by about 5 minutes and show similar magnitudes: M_W 7.6 for the earlier event and M_W 7.7 for the later event (2015/11/24 22:45:38.34 UTC, 10.6182°S, 70.9438°W, 609 km, 2770 Stations (ISC); 2015/11/24 22:50:53.30 (UTC), 10.1097°S, 71.0971°W, 621 km, 2202 Stations (ISC)). Those types of events, a pair of similarly sized earthquakes which occur very close in time and location, are often referred to as "doublets" (*Hayes et al.*, 2017). Both normal faulting events nucleated within the the subducted Nazca Plate on the same fault (*Ruiz et al.*, 2017; *Ye et al.*, 2016; *Zahradník et al.*, 2017). *Ruiz et al.* (2017) show in their study, using teleseismic and regional data, that the overall resemblance between the two events (similarity in geometry, rupture velocity, stress drop and radiated energy) suggest that they share a similar brittle rupture process and nucleated under very similar conditions. *Ye et al.* (2016) on the other hand conclude in their study, using teleseismic data, that the first event was a brittle rupture while the second one was a more dissipative rupture because of a much larger seismic moment, smaller rupture area and lower rupture speed for the second event compared to the first one.

The period between July and December 2015 produced 12 earthquakes with $M_W \geq 7$; these are listed in Table 6.2.

Figure 6.1 shows the number of moderate and large earthquakes in the second half of 2015. The distribution of the number of earthquakes should follow the Gutenberg-Richter law.

Table 6.1: Summary of events by type between July and December 2015.

felt earthquake	112
known earthquake	164941
known chemical explosion	7592
known induced event	3251
known mine explosion	975
known rockburst	381
known experimental explosion	49
suspected collapse	1
suspected earthquake	25504
suspected chemical explosion	942
suspected induced event	2
suspected mine explosion	5193
suspected rockburst	195
unknown	1
total	209139

Table 6.2: Summary of the earthquakes of magnitude Mw ≥ 7 between July and December 2015.

Date	lat	lon	depth	Mw	Flinn-Engdahl Region
2015-09-16 22:54:30	-31.64	-71.69	12	8.3	Near coast of central Chile
2015-11-24 22:50:53	-10.11	-71.10	621	7.7	Peru-Brazil border region
2015-11-24 22:45:38	-10.62	-70.94	609	7.6	Peru-Brazil border region
2015-10-26 09:09:39	36.50	70.53	204	7.5	Hindu Kush region
2015-12-07 07:50:04	38.13	72.88	14	7.3	Tajikistan
2015-10-20 21:52:02	-14.84	167.36	142	7.1	Vanuatu Islands
2015-09-16 23:18:41	-31.52	-71.53	29	7.1	Near coast of central Chile
2015-12-04 22:24:57	-47.68	85.31	25	7.1	Southeast Indian Ridge
2015-07-18 02:27:32	-10.46	165.10	11	7.0	Santa Cruz Islands
2015-11-11 01:54:37	-29.48	-71.94	3	7.0	Near coast of central Chile
2015-07-27 21:41:20	-2.71	138.54	47	7.0	Irian Jaya
2015-11-11 02:46:19	-29.52	-72.05	7	7.0	Off coast of central Chile

Figures 6.2 to 6.6 show the geographical distribution of moderate and large earthquakes in various magnitude ranges.

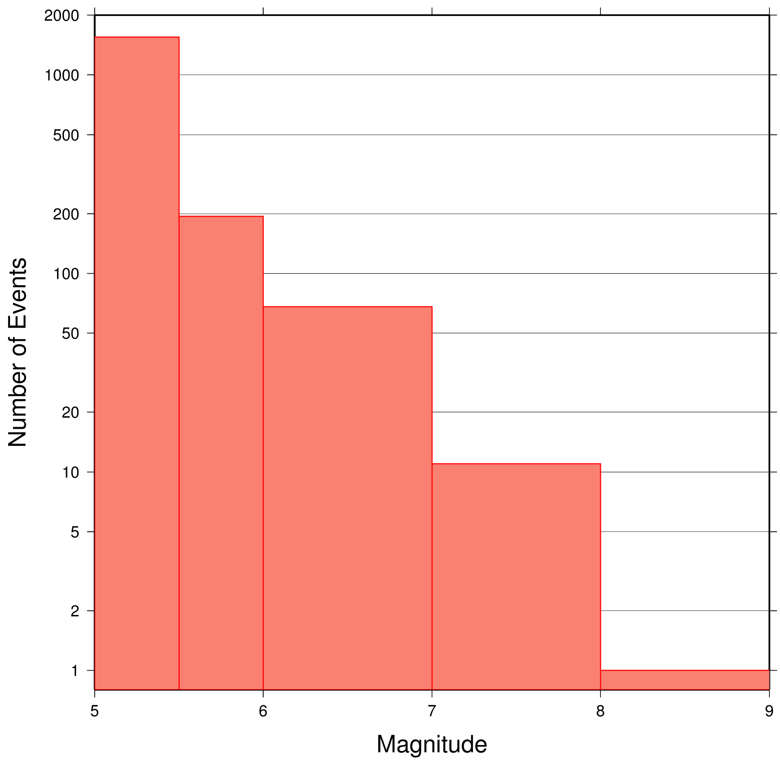

Figure 6.1: *Number of moderate and large earthquakes between July and December 2015. The non-uniform magnitude bias here correspond with the magnitude intervals used in Figures 6.2 to 6.6.*

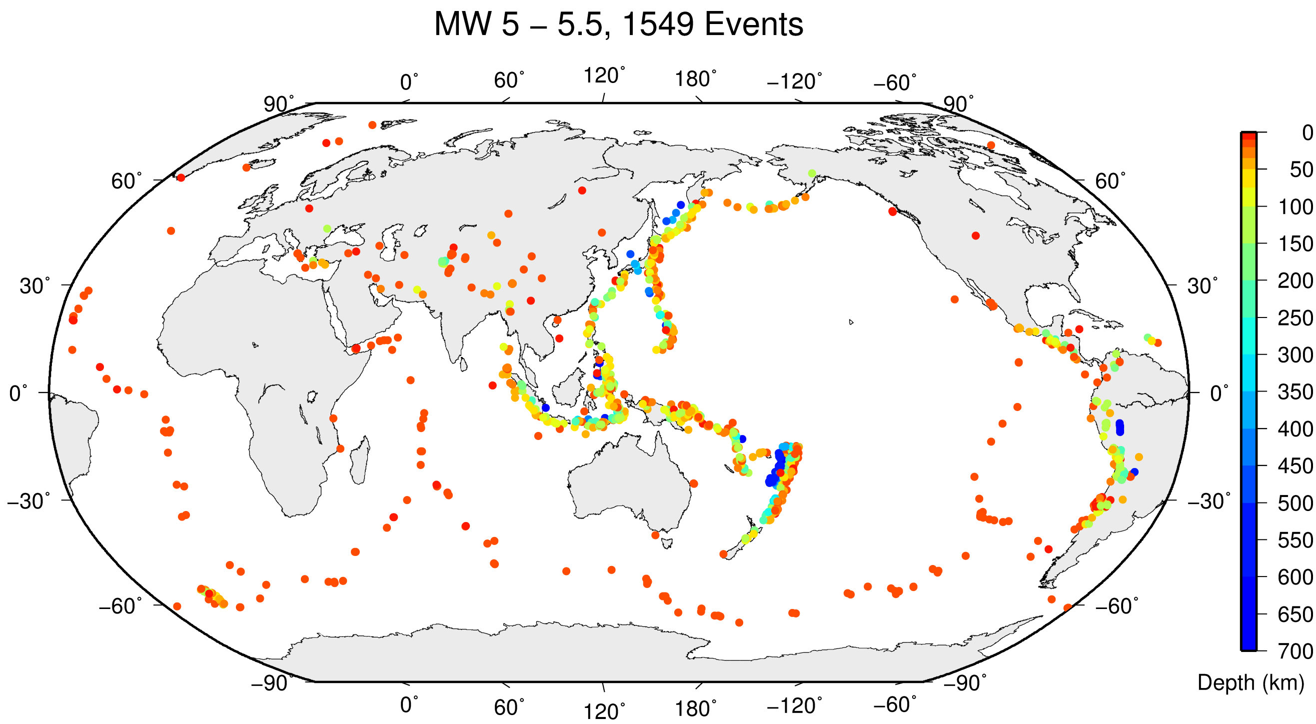

Figure 6.2: *Geographic distribution of magnitude 5-5.5 earthquakes between July and December 2015.*

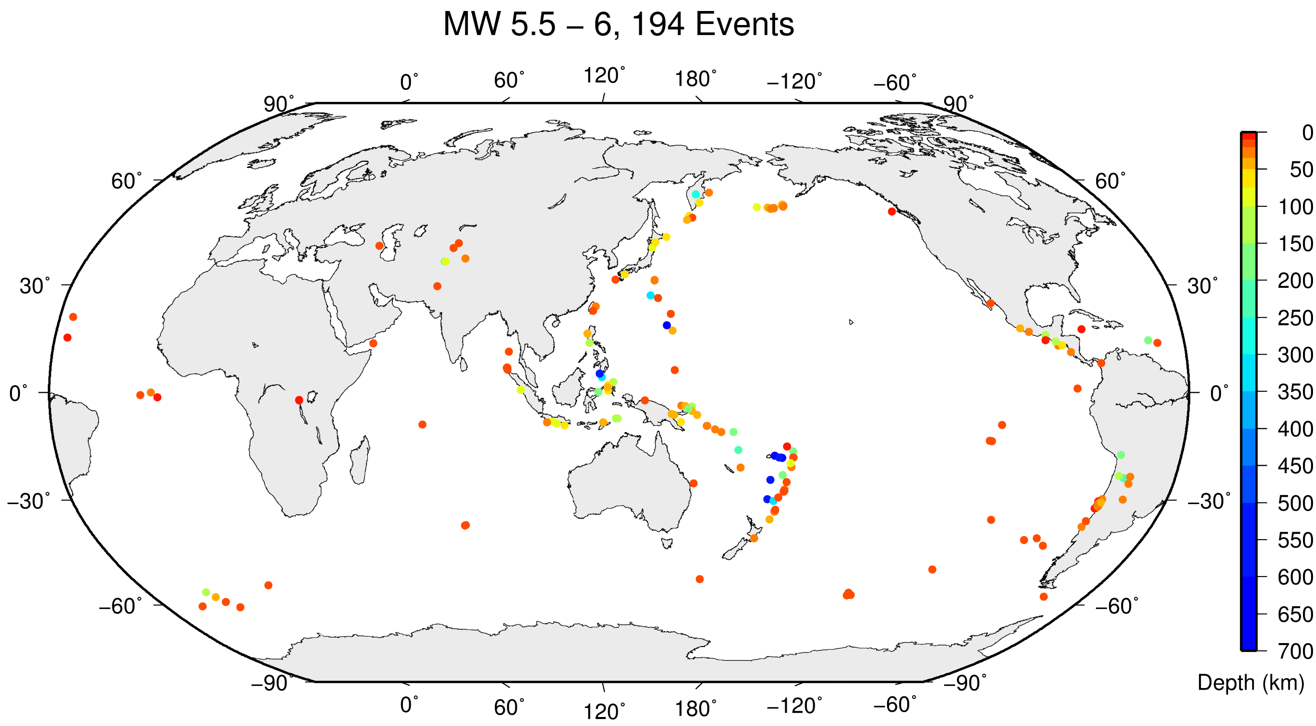

__Figure 6.3:__ Geographic distribution of magnitude 5.5-6 earthquakes between July and December 2015.

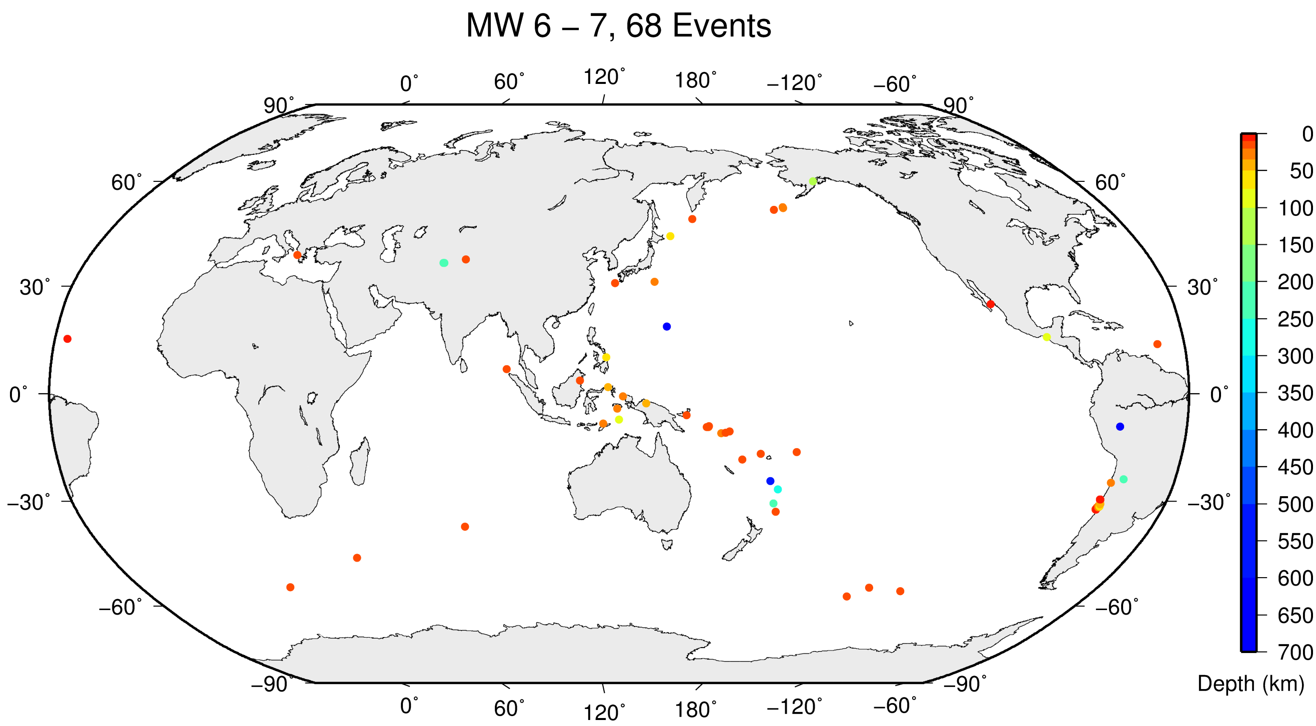

__Figure 6.4:__ Geographic distribution of magnitude 6-7 earthquakes between July and December 2015.

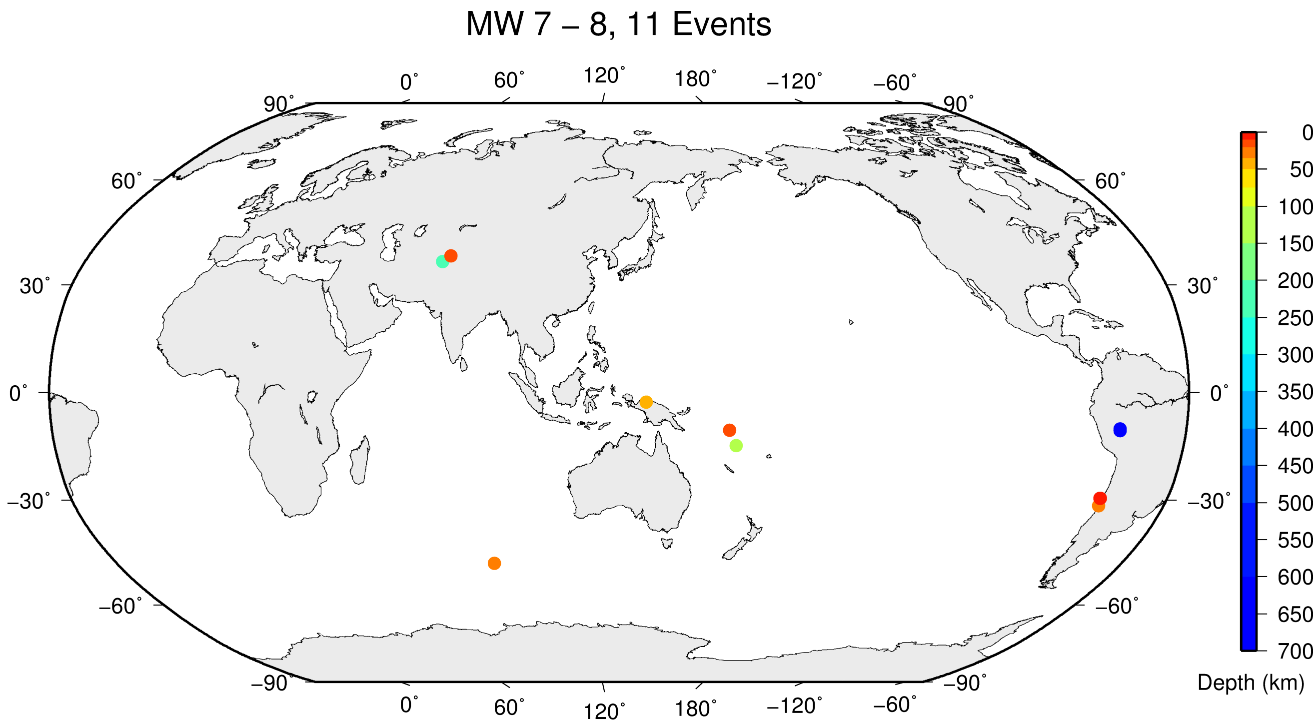

Figure 6.5: *Geographic distribution of magnitude 7-8 earthquakes between July and December 2015.*

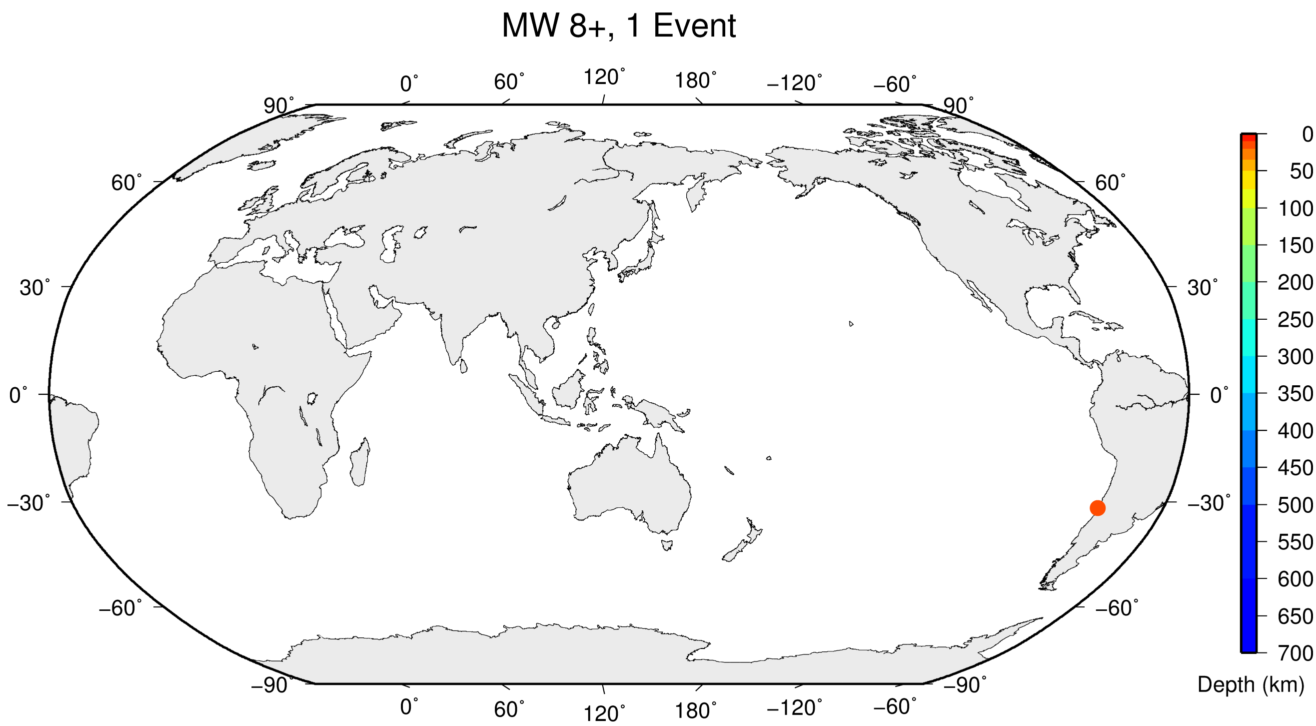

Figure 6.6: *Geographic distribution of magnitude 8+ earthquakes between July and December 2015.*

References

Di Giacomo, D., D.A. Storchak, N. Safronova, P. Ozgo, J. Harris, R. Verney and I. Bondár (2014), A New ISC Service: The Bibliography of Seismic Events, *Seismol. Res. Lett.*, *85*(2), 354–360, https://doi.org/10.1785/0220130143.

Hayes, G.P., E.K. Myers, J.W. Dewey, R.W. Briggs, P.S. Earle, H.M. Benz, G.M. Smoczyk, H.E. Flamme, W.D. Barnhart, R.D. Gold, and K.P Furlong (2017), Tectonic summaries of magnitude 7 and greater earthquakes from 2000 to 2015, *U.S. Geological Survey Open-File Report 2016–1192*, https://doi.org/10.3133/ofr20161192.

International Seismological Centre, On-line Event Bibliography, www.isc.ac.uk/event_bibliography, Internatl. Seis. Cent., Thatcham, United Kingdom, 2018.

Lange, D., J. Geersen, S. Barrientos, M. Moreno, I. Grevemeyer, E. Contreras-Reyes and H. Kopp (2016) Aftershock seismicity and tectonic setting of the 2015 September 16 Mw 8.3 Illapel earthquake, Central Chile, *Geophys. J. Int*, *206*(2), 1424–1430, https://doi.org/10.1093/gji/ggw218.

Ruiz, S., H. Tavera, P. Poli, C. Herrera, C. Flores, E. Rivera and R. Madariaga (2017), The deep Peru 2015 doublet earthquakes, *Earth Planet. Sci. Lett.*, *478*, 102–109, https://doi.org/10.1016/j.epsl.2017.08.036.

Satake K. and M. Heidarzadeh (2017), A Review of Source Models of the 2015 Illapel, Chile Earthquake and Insights from Tsunami Data. *In:* Braitenberg C., Rabinovich A. (eds) The Chile-2015 (Illapel) Earthquake and Tsunami, 1–9, Birkhäuser, Cham, https://doi.org/10.1007/978-3-319-57822-4_1.

Ye, L., T. Lay, H. Kanamori, Z. Zhan, and Z. Duputel (2016), Diverse rupture processes in the 2015 Peru deep earthquake doublet, *Sci. Adv.*, *2*(6), e1600581, https://doi.org/10.1126/sciadv.1600581.

Ye, L., T. Lay, H. Kanamori, and K.D. Koper (2017), Rapidly estimated seismic source parameters for the 16 September 2015 Illapel, Chile Mw 8.3 earthquake, *In:* Braitenberg C., Rabinovich A. (eds) The Chile-2015 (Illapel) Earthquake and Tsunami, 11–22, Birkhäuser, Cham, https://doi.org/10.1007/978-3-319-57822-4_2.

Zahradník, J., H. Čížková, C.R. Bina, E. Sokos, J. Janský, H. Tavera, and J. Carvalho (2017), A recent deep earthquake doublet in light of long-term evolution of Nazca subduction, *Sci. Rep.*, *7*, 45153, https://doi.org/10.1038/srep45153.

7

Notable Events

7.1 Macroseismic Field Anisotropy of the M_L 4.7 Earthquake of 18 October 2015 in Central Urals, Russia

Ruslan A. Dyagilev[1], Natalia S. Guseva[2], Filipp G. Verkholantsev[1]

[1] Geophysical Survey of Russian Academy of Sciences (GS RAS), Obninsk, Russia
[2] Mining Institute of Ural Branch of Russian Academy of Sciences (MI UB RAS), Perm, Russia


Ruslan A. Dyagilev


Natalia S. Guseva


Filipp G. Verkholantsev

This publication is an English adaption of an article that was first published in Russian in the Russian Geophysics Journal (2016, Vol. 5, pp. 42–46).

7.1.1 Introduction

On 18 October 2015 at 21:44:55 (GMT) a unique event happened in the Central Urals – a tectonic earthquake with magnitude M_L 4.7 that was felt over a very large area in the Sverdlovsk region and Perm Krai. An event of this magnitude is quite rare for this region. It may be noted that this was the strongest earthquake in the last 100 years. Events with large magnitudes have only happened in the Central Urals twice before. According to the historical records, the first one took place in 1798 in the vicinity of Perm, the second in 1914 near Pervouralsk (Bilimbay). The Bilimbay earthquake was also recorded instrumentally.

The earthquake was registered by 10 stations of the Ural seismological network run by GS RAS and MI UB RAS and the instrumental data obtained allowed the determination of the source parameters for the event (Tab. 7.1, Fig. 7.1). Information on the macroseismic impact was collected as well. In this article we analyse the macroseismic field and obtain coefficients of the Intensity(I)-Magnitude(M)-Distance(R)-relation. In the 1970's the I-M-R relation was determined for a wider area including most of the European part of Russia, the Urals and Western Siberia. To obtain the coefficients only for the

Urals region was not possible because of low seismicity in the area and, thus, a lack of data. The M_L 4.7 event in October 2015 changed this situation substantially. Now, we can determine the I-M-R-relation for the Urals region which contributes to seismic hazard assessment in the area.

Table 7.1: *Source parameters of the earthquake on 18 October, 2015 in the Central Urals.*

Time UTC	Lat degrees	Long degrees	Depth km	M	Notes
21:44:55	57.12 ±0.04	59.05 ±0.11	12	M_L 4.7 ±0.2	MI UB RAS solution according to the records of the stations ARU, SVE, PR0R, PR1R, PR3R, PR4R, PR7R, KAUR, SVUR, BA1R.
21:44:53.84	57.08	59.03	14	mb 4.4	ISC solution (168 Stations, *International Seismological Centre*, 2018)

7.1.2 Macroseismic Data

To describe the effects of the earthquake on the Earth's surface, the experts at MI UB RAS and GS RAS collected macroseismic data in the epicentral area during the first few days after the earthquake. Answers to the main part of the questionnaires were obtained by a personal survey of local residents near the epicenter. Data on the macroseismic effects was also received via the website "Seismological monitoring at the territory of the Western Urals" (`http://pts.mi-perm.ru/region/index.html`, in Russian), where the residents of other settlements are able to answer the same questions in absentia. In addition, a survey questionnaire was sent to the local administration of the 50 settlements located on the periphery of the shaking zone.

The survey was aimed at identifying the nature of several macroseismic indicators: sensations felt by the people during the earthquake, shaking of household items, damage to buildings and structures, changes in the environment. To simplify the task of data collection, the questionnaire, with a total of 38 questions, was set up as a form with multiple descriptions of possible manifestations of the earthquake that may be marked or not by the respondent. The combination of marked manifestations is a base for calculating the earthquake's intensity at one point on the surface. A set of questionnaires collected from a group of randomly selected respondents in a local area is used to obtain a more reliable estimation of seismic intensity for this area or settlement. Statistically, the more respondents there are, the smaller the error in estimated intensity, which should be computed with an accuracy of 0.1 point. In some settlements the number of respondents was small due to low population density. In the end, more than 200 questionnaires from 85 localities were collected. The collected data became the basis for the assessment of seismic intensity in terms of the MSK-64 scale (*Medvedev*, 1968).

The results of the survey show that people were feeling the event quite clearly not only in the nearby localities but also at distances more than 100 km away from the epicenter. Within a radius of 10-20 km from the instrumental epicentre strong shocks were reported, as well as clattering of dishes, vibration of windows, swaying of light objects and shaking of major appliances. Many witnesses woke up and ran outside. The passage of seismic waves was accompanied by sound effects. People described their

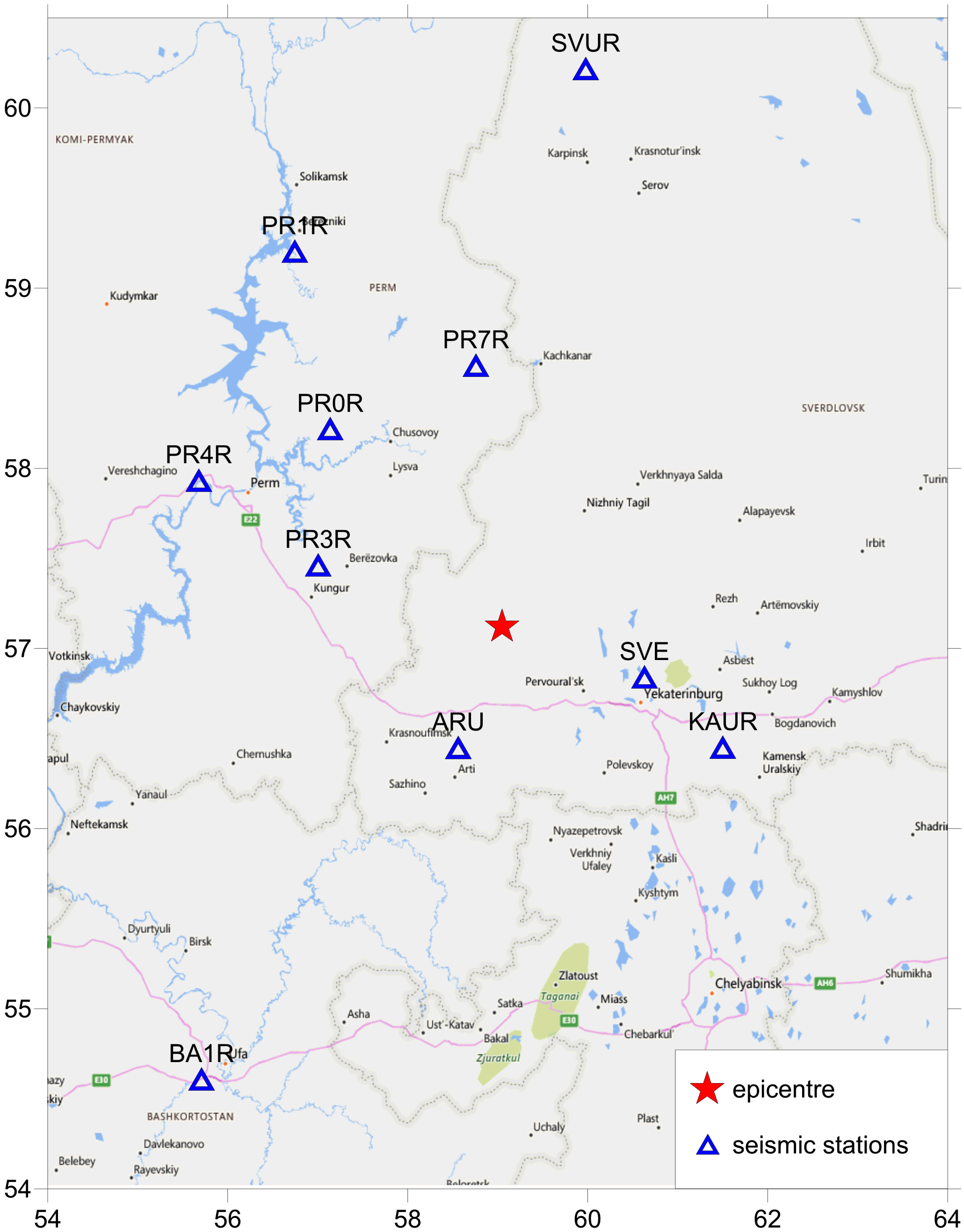

Figure 7.1: *Map showing the epicenter of the earthquake and stations that provided data to calculate source parameters.*

impressions as "shock, vibration, as if snow had fallen from the roof", "rumble, as if a truck had rammed into the corner of the house". At distances up to 100 km tremors, vibrations and shaking lasting up to 5 s were reported, as well as trembling of windows and glassware and a rumble "like a train passing by or a plane flying". The boundary of the shaking zone is located at a distance of about 130 km from the epicenter, where tremors were weak, barely perceptible or not sensed at all. It should be noted that ground motions were spreading considerably further to the NW of the epicentre than to other directions. For example, in Perm at a distance of 190 km on the upper floors of buildings distinctive shaking and tremors were felt. According to the collected surveys damage to buildings and constructions was not identified in any of the surveyed localities. However, on the internet there were some reports of cracked windows in the kindergarden no. 30 in the town of Novoutkinsk and concrete slabs being moved at the dam of Kamensky reservoir.

According to the questionnaires the intensity in every locality was defined based on the observations of the witnesses. Where several questionnaires were received, the average intensity I and its standard deviation σ were determined according to the following equations (*Federal Agency for Technical Regulation and Metrology*, 2017):

$$I = \frac{\sum n_i I_i}{\sum n_i},$$
$$\sigma = \pm\sqrt{\frac{\sum n_i I_i^2 - I_i^2 \sum n_i}{\sum n_i \sum (n_i - 1)}},$$

where I_i is the estimated intensity for the i^{th} macroseismic indicator and n_i the number of respondents presenting the i_{th} macroseismic indicator. A summary of intensities for the different localities is provided in Table 7.2.

Table 7.2: *Summary of intensities in terms of the MSK-64 scale.*

Localities	**Intesity points**
Sabik, Sarga, Chusovoye	5
Staroutkinsk, Pervomaiskiy, Starobukharovo, Kuzino, Sylva, Ilim, Novoutkinsk, Progress, Shalya, Pervouralsk	4-5
Bisert', Krylosovo, Pervomaiskoye, Taraskovo, Kalinovo, Bilimbay, Yekaterinburg	4
Novouralsk, Visim, Pochinok, Afanasievskoye, Russkiy Potam, Bol'shoy Ut, Arti, Verkhniaya Pyshma, Kungur	3-4
Shamary, Molebka, Nizhniy Tagil, Ust'-Kishert', Sysert', Bol'shoye Zaozerie	3
Achit, Kyn, Manchazh, Krasnoufimsk, Polevskoy, Sarana, Oktyabrskiy, Sars, Lys'va, Verkhniaya Salda, Kyshtym, Chernushka, Perm, Polazna, Chusovoy, Tyoplaya Gora, Gornozavodsk, Suksun, Kamensk-Uralskiy	2-3

7.1.3 Isoseismal Maps

An isoseismal map was built by interpolating the raw data using the software package Surfer 12 where the Kriging gridding method gave the best results (Fig. 7.2). The macroseismic field of the earthquake shows a prominent spatial anisotropy. Such behavior is common for many macroseismic fields of other

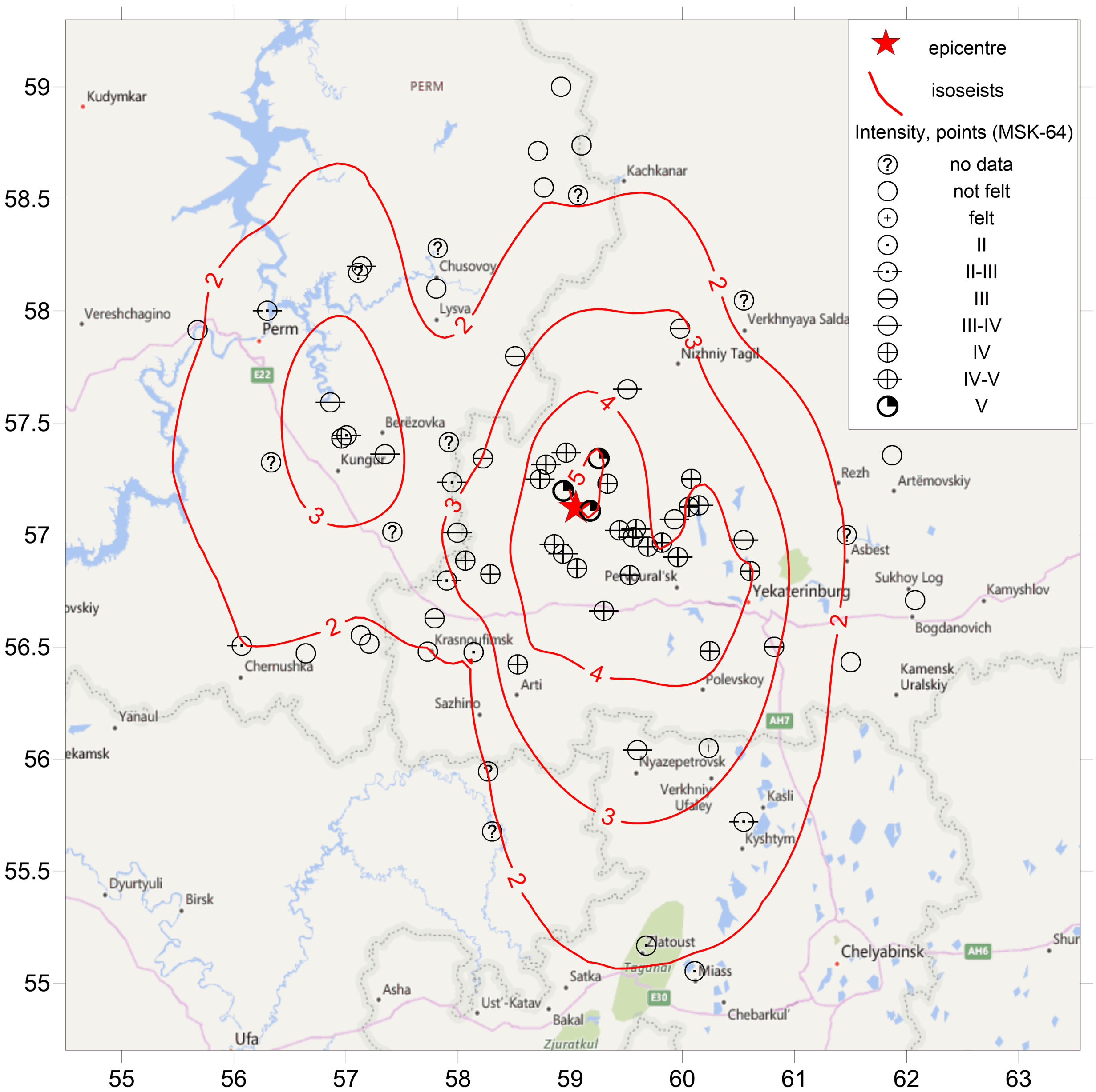

Figure 7.2: *Isoseismal map obtained by interpolation with Kriging gridding method.*

earthquakes (*Dzhanuzakov*, 2013). Further, the macroseismic fields shows two maxima of intensity: one maximum (5 points) at the epicenter and a second, slightly lower, maximum (3-4 points) to the West and North-West from the epicenter in the territory of Perm Krai. This distribution of macroseismic intensities in this area could also be observed for the Bilimbay event hundred years ago (*Veis-Ksenofontova*, 1940).

For modelling the macroseismic field there are a variety of methods in the literature. The earliest classic models, such as the model of Blake-Shebalin or Covesligeti-Shebalin (*Shebalin*, 2003; *Blake*, 1941), assume that the source is a point, and the seismic effect is distributed in a homogeneous environment, meaning that it is not direction-dependent. The simplicity of the classic models makes them appropriate to apply in more complicated cases. For example, in the work of *Dzhanuzakov* (2013) the effect along and across the structures of the Northern Tien Shan is described by two different equations. The similar approach can be found in other seismic areas (*Solomatin*, 2013) for earthquakes with different magnitudes. More modern approaches to describe the macroseismic effect distribution, such as the model of *Gusev and*

Shumilina (1999), consider a spreading source, due to which the intensity depends on the orientation of the fault plane and the location of the observation point relative to this plane. In the study of *Kulchitsky* (2014) the method of approximation is shown. It allows to correctly describe the macroseismic effect of earthquakes where only a limited amount of macroseismic data can be collected due to the location of the epicentre (e.g. in the sea or on the border to another country). Despite the point notion of the source, this approach still allows for indirectly taking into account spreading sources and regional patterns of seismic waves propagation, including the anisotropic component of the macroseismic field.

Since the Ural earthquakes are relatively small (maximum magnitude according to *Shebalin et al.* (2000) does not exceed 5.5) with an average depth of 15 km they can be considered as seismic point sources. Structures elongated from the North to the South in the basement and the sedimentary cover create conditions for anisotropic propagation of the seismic waves. The study area does not provide favourable geographical conditions for a representative collection of macroseismic data, despite the fact that it is located inside the continent and belongs to one state, because of an irregular arrangement of settlements and the existence of vast uninhabited areas. This makes the approach proposed by *Kulchitsky* (2014) appropriate, which will be discussed in more detail in the following paragraph.

According to *Kulchitsky* (2014), the basis for the description of the macroseismic field is the Intensity(I)-Magnitude(M)-Distance(R)-relation of Shebalin-Blake:

$$I(r) = 1.5\ M_{LH} - b\ \lg(r) + c, \tag{7.1}$$

where M_{LH} is another expression for M_S, r is the hypocentral distance in km, b and c are empirical coefficients. In this work the value of magnitude M_{LH} was calculated from M_L with the relationship: $0.8\ M_L - 0.6\ M_S = 1.04$ (*Ambraseys*, 1990). In Equation 7.1 the azimuthal-dependent heterogeneity for b can be defined, as follows:

$$b = b_0 + \sum_{k=1}^{n} (B_{sk} \sin(\alpha k) + B_{ck} \cos(\alpha k)), \tag{7.2}$$

where n is the order of the trigonometric polynomial responsible for the complexity of the spatial asymmetry in the calculated field and B_{sk}, B_{ck} are polynomial coefficients responsible for the shape and intensity of asymmetry. To find the unknown components c, b_0, B_{sk}, B_{ck} the method of least squares is used.

In the case of an isotropic field (coefficients B_{sk}, B_{ck} are neglected) the components are $b_0 = 3.18$ and $c = 2.48$, which slightly differs from the average values adopted previously for this region ($b_0 = 3.5$, $c = 3.0$) (*Medvedev*, 1968). However, the analysis of field residuals obtained with the new coefficients reveals that their distribution is dependent on intensity I. Red circles in Figure 7.3 show the residuals where the red dashed line is a linear approximation of the residuals. The residuals for $I < 3.1$ are slightly less than observed while for $I > 3.1$ they are slightly larger. After an iterative correction of coefficients b_0 and c we found the values $b_0 = 3.84$, $c = 3.76$ which make the residuals not dependent on intensity (blue circles and blue solid line in Figure 7.3). The standard deviation of residuals before correction is 0.2 points. After correction it increases to 0.3 points.

To calculate the anisotropic component of the macroseismic field, *Kulchitsky* (2014) recommends n to be $n = 5$ in Equation 7.1 for many and well distributed collected macroseismic data points. For a lower

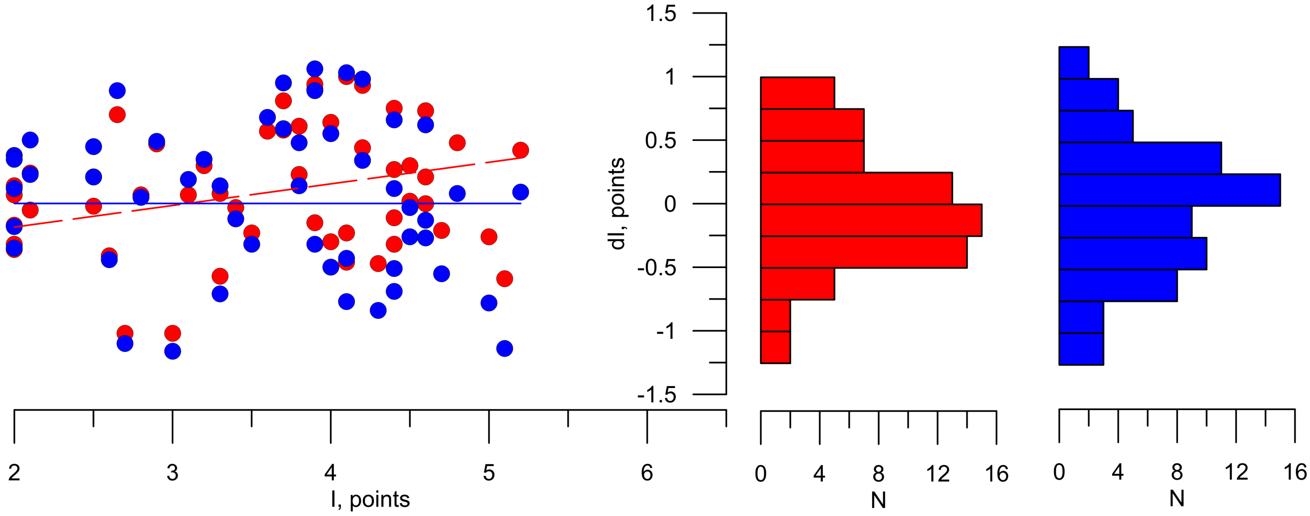

Figure 7.3: *Intensity residuals against intensity (left) and histogram of intensity residuals (right). Data without correction are shown with red circles and bars, adjusted data are shown with blue circles and bars.*

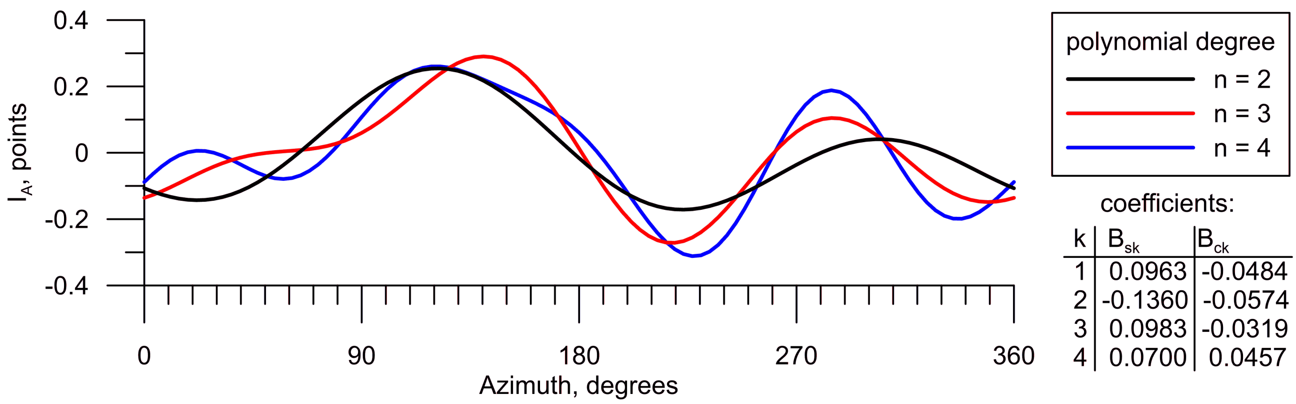

Figure 7.4: *The anisotropic component of the macroseismic field I_A for different polynomial degrees.*

amount of data with a poorer distribution n should be less than 5. The anisotropic component I_A of the macroseismic field for $n = 2, 3, 4$ dependent on azimuth is shown in Figure 7.4. A basic characteristic can be observed for all polynomial degrees described above with the largest deviations at azimuths about 120 degrees, 220 degrees and 280 degrees.

The results of constructing the macroseismic field for $n = 2, 3, 4$ are shown in Figure 7.5. The isoseismal map for $n = 2$ reflects a generalised understanding of the anisotropy and attenuation of seismic waves, for which the elliptical shape indicates a strong azimuthal deviation from a uniform propagation of the wave field. The axis of dominant propagation has an azimuth of 126 degrees (Fig. 7.4). For $n = 3$ the largest anisotropic component shows a similar azimuth (140 degrees) but the isoseismals do not follow a strict elliptical shape anymore and an additional component with an azimuth of about 40 degrees can be observed (Fig. 7.5). For $n = 4$ this second component is even stronger and the isoseismals are almost cross-shaped with azimuths of the axes of prevailing propagation of the seismic field at about 22 degrees and 284 degrees.

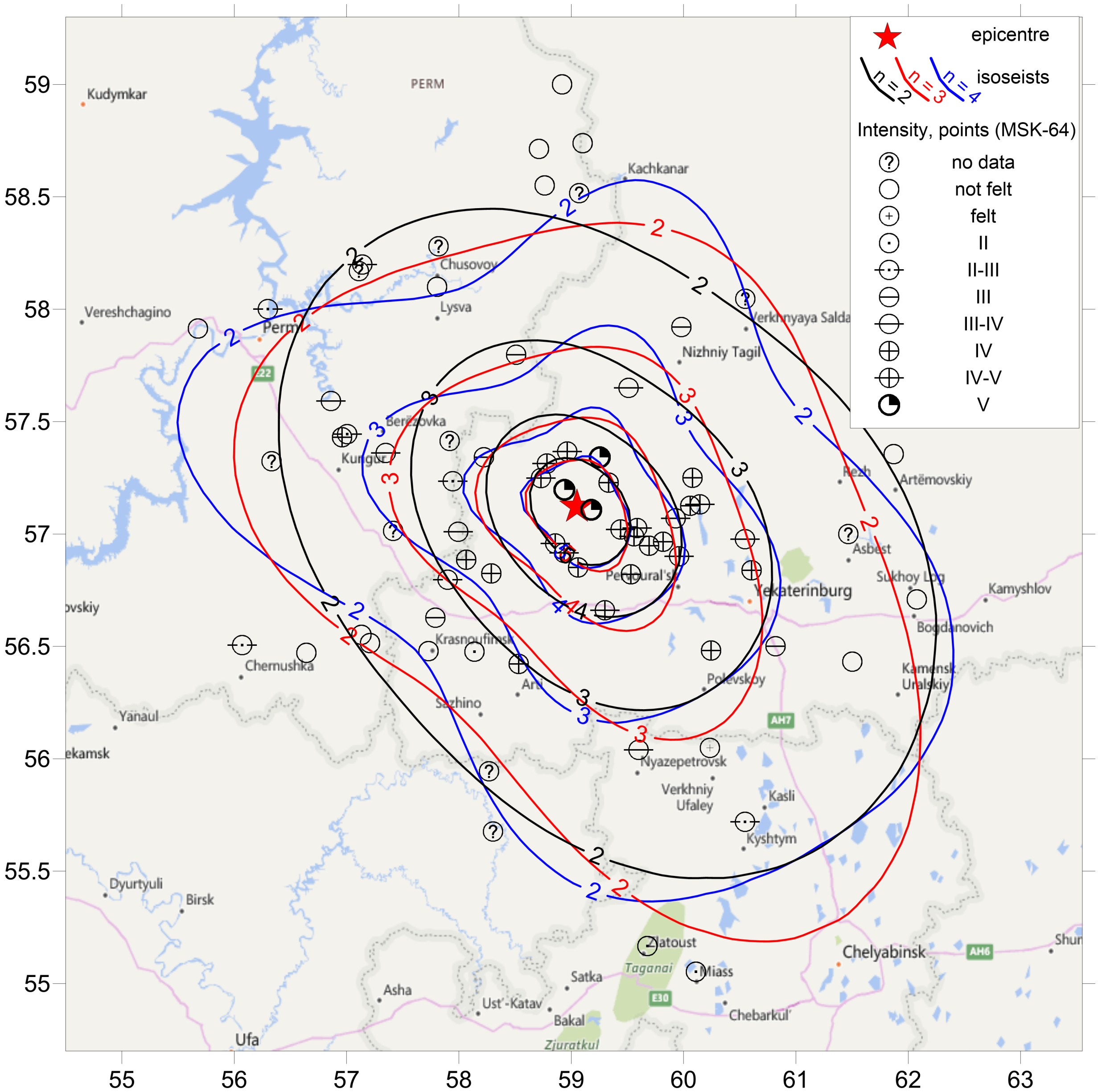

Figure 7.5: *Isoseismal map obtained by approximation method for* $n = 2, 3, 4$.

7.1.4 Discussion and Conclusions

By interpolating the results of the questionnaires and by modeling the macroseismic field by using the approximation method we constructed isoseismal maps of the M_L 4.7 event of 18 October 2015 in the Central Urals. An anisotropic distribution could be observed in each of the methods. The anisotropic component with an azimuth of about 22 degrees observed for $n = 3, 4$ can be explained by the orientation of the principal tectonic structures, folds and faults zones, of the Urals along which seismic attenuation is weaker. On the other hand, the component with a NW-SW direction which is observed in all isoseismal maps cannot be explained by geological features in the area. One of the possible reasons for such local enhancement of shaking in the Perm region could be soil features. However, as a rule ground amplifications are more patchy and the influence on the soil requires a separate research.

Modeling the macroseismic field by the approximation method with trigonometric polynomials allows a more accurate estimation of intensity of future strong earthquakes for a wide area of the Central Urals. We obtained two sets of coefficients with different sensitivity to intensity. Both sets provide acceptable levels of variance (0.2-0.3 points), therefore the intensity independent set of coefficients is preferable. The new macroseismic coefficients with an isotropic component ($b_0 = 3.84$, $c = 3.76$) are in line with values found in other regions. They also allow a direct estimation of the intensity at the epicenter (I_0) where there are no observation points. Substituting the coefficients in Equations 7.1 and 7.2 gives an intensity of $I_0 = 5.8$ points, with a possible error of $\pm$ 0.6 points. This is very close to the values reported by the settlements closest to the epicentre (Sabik, Sarga and Chusovoye).

The earthquake on 18 October 2015 gave for the first time in many years the opportunity to study the distribution of macroseismic effects on a wide area covering almost the entire Central Urals for a wide range of intensity values (from 2 to 5 points). None of the previously recorded instrumentally tectonic earthquakes in the Urals gave such a significant amount of primary data. All known major events with magnitude 5.0 or more, occurred in the period from the late 18th to the early 20th century when definitions of shaking intensities and instrumental observations were not as advanced as they are today.

The overall result of our study provides a basis for more accurate calculations of the seismic intensity for future earthquakes and allows a better assessment of the seismic hazard in the Central Urals.

7.1.5 References

Ambraseys, N.N. (1990), Uniform magnitude re-evaluation of European earthquakes associated with strong-motion records, *Earthquake Engng. Struct. Dyn.*, *19*(1), pp. 1–20, `https://doi.org/doi:10.1002/eqe.4290190103`.

Blake, A. (1941), On the estimation of the focal depth from macroseismic data, *Bulletin of Seismological Society of America*, *31*(3), pp. 225–231.

Dzhanuzakov, K. Dzh. (2013), Regional features of an attenuation of strong earthquakes intensity in Kyrgyzstan and its adjacent regions, *Bulletin of the Institute of Seismology of the National Academy of Science of the Kyrgyz Republic*, *2*(2), pp. 13–18 (in Russian).

Federal Agency for Technical Regulation and Metrology (2017), Earthquakes. Seismic intensity scale, *National standard of Russian Federation GOST R 57546-2017*, Moscow, 32 p. (in Russian).

Gusev, A. A. and L.S. Shumilina (1999), Modeling the Intensity-Magnitude-Distance Relation Based on the Concept of an Incoherent Extended Earthquake Source, *Volcanology and Seismology*, *4–5*, pp. 29–40 (in Russian). English version: (2000), *Volcanology and Seismology*, *21*, pp. 443–463.

International Seismological Centre, On-line Bulletin, `http://www.isc.ac.uk`, Internatl. Seismol. Cent., Thatcham, United Kingdom, 2018.

Kulchitsky, V. E. (2014), Estimation of decay parameters for the intensity of anisotropic macroseismic fields, *Geophysical Journal*, *36*(2), pp. 138–149 (in Russian).

Medvedev, S.V. (Ed.) (1968), Seismic zoning in the USSR, *Nauka*, Moscow, 476 p. (in Russian).

Shebalin, N. V., V.G. Trifonov, A.I. Kozhurin, V.I. Ulomov, R.E Tatevossian and A.I. Ioffe (2000), A Unified Seismotectonic Zonation of Northern Eurasia, *Journal of Earthquake Prediction Research*, *8*, pp. 8–31.

Shebalin, N. V. (2003), Problems of macroseismic studies, *Computational seismology*, *34*, GEOS, Moscow, pp. 55–285 (in Russian).

Solomatin, A.V. (2013), Construction of refined model equations of the macroseismic fields for the earthquakes of the Kuril-Kamchatka region. Interpolation and regression approaches, *Vestnik KRAUNTS Phys.-Math. Sciences.*, *1*(6), pp. 30–42 (in Russian).

Veis-Ksenofontova, Z. G. and V.V. Popov (1940), On the issue of the seismic characteristic of the Urals, *Proceedings of the Seismological Institute of the USSR Academy of Sciences*, *104*, USSR Academy of Sciences Publishing House, Moscow (in Russian).

8

Statistics of Collected Data

8.1 Introduction

The ISC Bulletin is based on the parametric data reports received from seismological agencies around the world. With rare exceptions, these reports include the results of waveform review done by analysts at network data centres and observatories. These reports include combinations of various bulletin elements such as event hypocentre estimates, moment tensors, magnitudes, event type and felt and damaging data as well as observations of the various seismic waves recorded at seismic stations.

Data reports are received in different formats that are often agency specific. Once an authorship is recognised, the data are automatically parsed into the ISC database and the original reports filed away to be accessed when necessary. Any reports not recognised or processed automatically are manually checked, corrected and re-processed. This chapter describes the data that are received at the ISC before the production of the reviewed Bulletin.

Notably, the ISC integrates all newly received data reports into the automatic ISC Bulletin (available on-line) soon after these reports are made available to ISC, provided it is done before the submission deadline that currently stands at 12 months following an event occurrence.

With data constantly being reported to the ISC, even after the ISC has published its review, the total data shown as collected, in this chapter, is limited to two years after the time of the associated reading or event, i.e. any hypocentre data collected two years after the event are not reflected in the figures below.

8.2 Summary of Agency Reports to the ISC

A total of 150 agencies have reported data for July 2015 to December 2015. The parsing of these reports into the ISC database is summarised in Table 8.1.

Table 8.1: *Summary of the parsing of reports received by the ISC from a total of 150 agencies, containing data for this summary period.*

	Number of reports
Total collected	4031
Automatically parsed	3101
Manually parsed	930

Data collected by the ISC consists of multiple data types. These are typically one of:

- Bulletin, hypocentres with associated phase arrival observations.

- Catalogue, hypocentres only.
- Unassociated phase arrival observations.

In Table 8.2, the number of different data types reported to the ISC by each agency is listed. The number of each data type reported by each agency is also listed. Agencies reporting indirectly have their data type additionally listed for the agency that reported it. The agencies reporting indirectly may also have 'hypocentres with associated phases' but with no associated phases listed - this is because the association is being made by the agency reporting directly to the ISC. Summary maps of the agencies and the types of data reported are shown in Figure 8.1 and Figure 8.2.

Table 8.2: *Agencies reporting to the ISC for this summary period. Entries in bold are for new or renewed reporting by agencies since the previous six-month period.*

Agency	Country	Directly or indirectly reporting (D/I)	Hypocentres with associated phases	Hypocentres without associated phases	Associated phases	Unassociated phases	Amplitudes
TIR	Albania	D	287	5	3971	19	806
CRAAG	Algeria	D	326	0	1533	131	0
LPA	Argentina	D	0	0	0	1235	0
SJA	Argentina	D	663	94	26933	0	4498
NSSP	Armenia	D	60	1	700	0	0
AUST	Australia	D	725	12	16714	0	0
CUPWA	Australia	D	32	0	411	0	0
IDC	Austria	D	18157	1	398038	0	326794
VIE	Austria	D	4042	61	37363	794	37395
AZER	Azerbaijan	D	46	0	2383	0	0
UCC	Belgium	D	647	0	6546	70	1226
SCB	Bolivia	D	35	0	1025	0	201
RHSSO	Bosnia and Herzegovina	D	714	0	12448	7041	0
BDF	**Brazil**	**I NEIC**	**1**	**15**	**0**	**0**	**0**
VAO	Brazil	D	1259	12	47869	0	0
SOF	Bulgaria	D	236	0	1383	0	0
SOMC	Cameroon	D	0	0	0	8	0
OTT	Canada	D	2030	38	49323	0	3011
PGC	Canada	I OTT	1581	0	38327	0	0
GUC	Chile	D	4658	908	133649	3117	38018
BJI	China	D	1529	56	83146	28042	57168
ASIES	Chinese Taipei	D	0	51	0	0	0
TAP	Chinese Taipei	D	24230	58	977548	0	0
RSNC	Colombia	D	5588	4	159243	33794	50965
ICE	Costa Rica	I UCR	0	2	0	0	0
UCR	Costa Rica	D	391	13	11609	0	1029
ZAG	Croatia	D	1	1	0	53306	0
SSNC	Cuba	D	179	0	3134	0	1293
NIC	Cyprus	D	694	5	16998	0	8691
IPEC	Czech Republic	D	425	0	2855	23216	1351
PRU	Czech Republic	D	5162	0	46225	244	12624
WBNET	**Czech Republic**	**D**	**35**	**0**	**659**	**0**	**0**
DNK	Denmark	D	1584	1106	19877	29446	10537
OSPL	Dominican Republic	D	587	2	5499	0	1895
IGQ	Ecuador	D	0	68	2836	0	0
HLW	Egypt	D	203	1	2384	0	0
SNET	El Salvador	D	1281	41	24784	5	4650
SSS	El Salvador	I UCR	0	1	0	0	0
EST	Estonia	I HEL	273	2	0	0	0
AAE	Ethiopia	D	24	0	442	245	4
SKO	FYR Macedonia	D	1010	3	11797	3709	2055
FIA0	Finland	I HEL	3	0	0	0	0

Table 8.2: *(continued)*

Agency	Country	Directly or indirectly reporting (D/I)	Hypocentres with associated phases	Hypocentres without associated phases	Associated phases	Unassociated phases	Amplitudes
HEL	Finland	D	7169	4401	149580	0	22273
CSEM	France	I BGR	2341	1074	0	0	0
LDG	France	D	2375	87	48329	16	19780
STR	France	D	1720	0	26369	2	0
PPT	French Polynesia	D	1293	0	9061	977	9962
TIF	Georgia	D	0	227	0	4738	0
AWI	Germany	D	3301	0	13228	787	0
BGR	Germany	D	726	211	18910	0	7062
BNS	Germany	I BGR	1	24	0	0	0
BRG	Germany	D	0	0	0	7982	4103
BUG	Germany	I BGR	11	3	0	0	0
CLL	Germany	D	4	0	102	8665	2832
GDNRW	Germany	I BGR	1	13	0	0	0
GFZ	Germany	I SJA	28	1	0	0	0
HLUG	Germany	I BGR	2	1	0	0	0
LEDBW	Germany	I BGR	6	5	0	0	0
LER	**Germany**	**I BGR**	**1**	**1**	**0**	**0**	**0**
ATH	Greece	D	11003	32	276981	0	86064
THE	Greece	D	4649	67	96811	5432	29050
UPSL	Greece	D	0	14	0	0	0
GCG	Guatemala	D	305	0	1583	0	0
HKC	Hong Kong	D	0	0	0	31	0
BUD	Hungary	D	0	0	0	3919	0
KRSZO	Hungary	D	299	0	3929	0	1551
REY	Iceland	D	34	0	1108	0	0
HYB	India	D	821	287	1327	0	109
MERI	India	I NDI	5	0	0	0	0
NDI	India	D	564	505	9766	1794	2871
DJA	Indonesia	D	3844	92	67005	0	83293
TEH	Iran	D	534	27	22056	0	4405
THR	Iran	D	373	1	4154	0	1240
ISN	Iraq	D	253	0	1656	0	606
GII	Israel	D	289	0	4497	0	0
GEN	Italy	D	565	2	6181	566	0
MED_RCMT	Italy	D	0	138	0	0	0
RISSC	Italy	D	8	0	135	0	0
ROM	Italy	D	7373	106	490611	195261	325690
TRI	Italy	D	0	0	0	7920	0
LIC	Ivory Coast	D	992	0	2976	0	1979
JSN	Jamaica	D	113	0	548	14	0
JMA	Japan	D	57498	0	460752	941	0
MAT	Japan	D	0	0	0	8244	0
NIED	Japan	D	0	750	0	0	0
SYO	Japan	D	0	0	0	1925	0
JSO	Jordan	D	8	2	87	0	101
NNC	Kazakhstan	D	8571	1	101353	0	94792
SOME	Kazakhstan	D	5012	176	71143	0	63769
KISR	Kuwait	D	482	24	2866	111	458
KNET	Kyrgyzstan	D	1401	0	11394	0	2759
KRNET	Kyrgyzstan	D	5407	0	88436	0	0
LVSN	Latvia	D	250	0	3469	0	2023
GRAL	Lebanon	D	307	0	1957	338	0
LIT	Lithuania	D	411	423	3453	1854	202
ECGS	Luxembourg	D	260	0	2448	0	0
MCO	Macao, China	D	0	0	0	38	0
TAN	Madagascar	D	0	0	0	146	0
GSDM	Malawi	D	0	0	0	332	0
KLM	Malaysia	D	524	0	2133	0	0
ECX	Mexico	D	468	2	9106	0	1186
MEX	Mexico	D	5581	219	59797	19	0
MOLD	Moldova	D	0	0	0	913	516
PDG	Montenegro	D	287	0	6761	0	3272
CNRM	Morocco	D	2386	121	24899	183	0

Table 8.2: *(continued)*

Agency	Country	Directly or indirectly reporting (D/I)	Hypocentres with associated phases	Hypocentres without associated phases	Associated phases	Unassociated phases	Amplitudes
NAM	Namibia	D	16	0	61	19	0
DMN	Nepal	D	1251	1	13332	0	9574
NOU	New Caledonia	D	2315	959	25727	0	4764
WEL	New Zealand	D	5973	53	222378	126	223688
INET	Nicaragua	D	8	1501	0	0	0
BER	Norway	D	2859	2285	58184	3288	12451
NAO	Norway	D	2531	1248	7201	0	2102
OMAN	Oman	D	466	0	14852	0	0
MSSP	Pakistan	D	0	0	0	1134	0
UPA	Panama	D	530	0	10358	0	74
ARE	Peru	I NEIC	12	53	0	0	0
LIM	Peru	I HYB	0	7	0	0	0
MAN	Philippines	D	1	1703	0	18995	5745
WAR	Poland	D	0	0	0	8900	322
IGIL	Portugal	D	685	0	3272	0	1090
INMG	Portugal	D	1528	0	39250	1351	13174
SVSA	Portugal	D	569	0	11436	3427	5578
BELR	Republic of Belarus	D	0	0	0	27127	7849
CFUSG	Republic of Crimea	D	9	51	270	662	545
KMA	Republic of Korea	D	1513	0	19729	0	0
BUC	Romania	D	957	15	17598	55206	6218
ASRS	Russia	D	119	1	2548	10	314
BYKL	Russia	D	131	0	14462	0	4904
DRS	Russia	I MOS	131	119	0	0	0
IEPN	Russia	D	75	0	707	4579	1600
KOLA	Russia	D	187	0	796	0	0
KRSC	Russia	D	594	0	19731	0	0
MIRAS	Russia	D	133	0	958	0	475
MOS	Russia	D	1924	253	307800	0	108680
NERS	Russia	D	29	0	759	0	347
NORS	Russia	I MOS	42	134	0	0	0
SKHL	Russia	D	523	517	16391	0	7775
YARS	Russia	D	498	0	7122	0	4813
SGS	Saudi Arabia	D	17	0	230	0	0
BEO	Serbia	D	1490	0	24653	1499	0
BRA	Slovakia	D	0	0	0	21086	0
LJU	Slovenia	D	1410	168	19207	3390	6584
HNR	Solomon Islands	D	0	0	0	1605	0
PRE	South Africa	D	565	0	9497	384	3236
MDD	Spain	D	2377	2	73073	0	55739
MRB	Spain	D	535	0	12647	0	5088
SFS	Spain	D	546	0	3674	353	0
SSN	Sudan	D	40	0	201	0	14
UPP	Sweden	D	1354	2973	14763	0	0
ZUR	Switzerland	D	460	0	12220	0	6299
BKK	Thailand	D	4218	864	50974	0	58838
TRN	Trinidad and Tobago	D	0	1978	0	56795	0
TUN	Tunisia	D	0	47	0	0	0
DDA	Turkey	D	9857	2	211420	0	68559
ISK	Turkey	D	10952	20	154634	3159	90484
AEIC	U.S.A.	I NEIC	1666	592	67564	0	0
ANF	U.S.A.	I IRIS	130	1550	0	0	0
BUT	U.S.A.	I NEIC	39	15	435	0	0
GCMT	U.S.A.	D	0	2182	0	0	0
HVO	U.S.A.	I NEIC	138	3	44	0	0
IRIS	U.S.A.	D	2865	1550	204928	0	0
LDO	U.S.A.	I NEIC	12	4	105	0	0
NCEDC	U.S.A.	I NEIC	202	3	3083	0	0
NEIC	U.S.A.	D	17411	10934	1459952	183	657325

Table 8.2: *(continued)*

Agency	Country	Directly or indirectly reporting (D/I)	Hypocentres with associated phases	Hypocentres without associated phases	Associated phases	Unassociated phases	Amplitudes
PAS	U.S.A.	I NEIC	41	11	853	0	0
PNSN	U.S.A.	D	0	106	0	0	0
REN	U.S.A.	I NEIC	457	13	945	0	0
RSPR	U.S.A.	D	3720	9	46062	0	0
SCEDC	U.S.A.	I IRIS	68	0	0	0	0
SEA	U.S.A.	I NEIC	50	92	5314	0	0
SLM	U.S.A.	I NEIC	50	2	1488	0	0
TUL	U.S.A.	I NEIC	1295	3	0	0	0
UUSS	U.S.A.	I NEIC	21	0	400	0	0
WES	U.S.A.	I IRIS	5	0	0	0	0
SIGU	Ukraine	D	118	0	3566	0	2128
DSN	United Arab Emirates	D	432	0	5857	0	0
BGS	United Kingdom	D	357	18	9329	48	3533
EAF	Unknown	D	1455	22	8062	11177	36
ISU	Uzbekistan	D	168	0	1741	0	0
CAR	Venezuela	I NEIC	2	28	0	0	0
FUNV	Venezuela	D	345	0	6751	0	0
PLV	Vietnam	D	12	0	144	0	74
LSZ	Zambia	D	36	0	201	37	34
BUL	Zimbabwe	D	438	0	3495	477	3

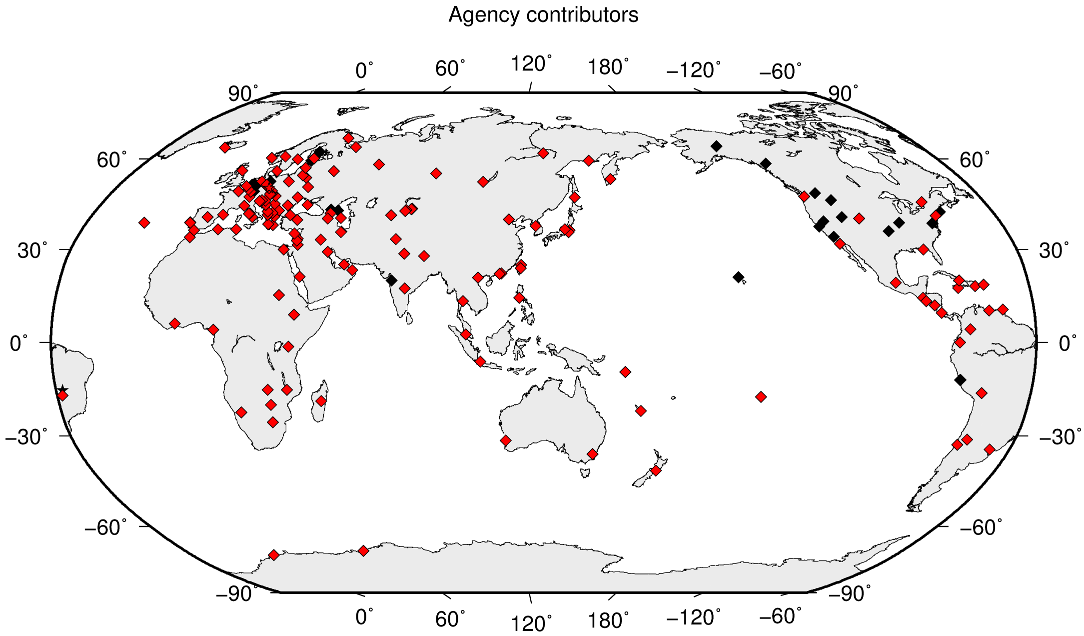

Figure 8.1: *Map of agencies that have contributed data to the ISC for this summary period. Agencies that have reported directly to the ISC are shown in red. Those that have reported indirectly (via another agency) are shown in black. Any new or renewed agencies, since the last six-month period, are shown by a star. Each agency is listed in Table 8.2.*

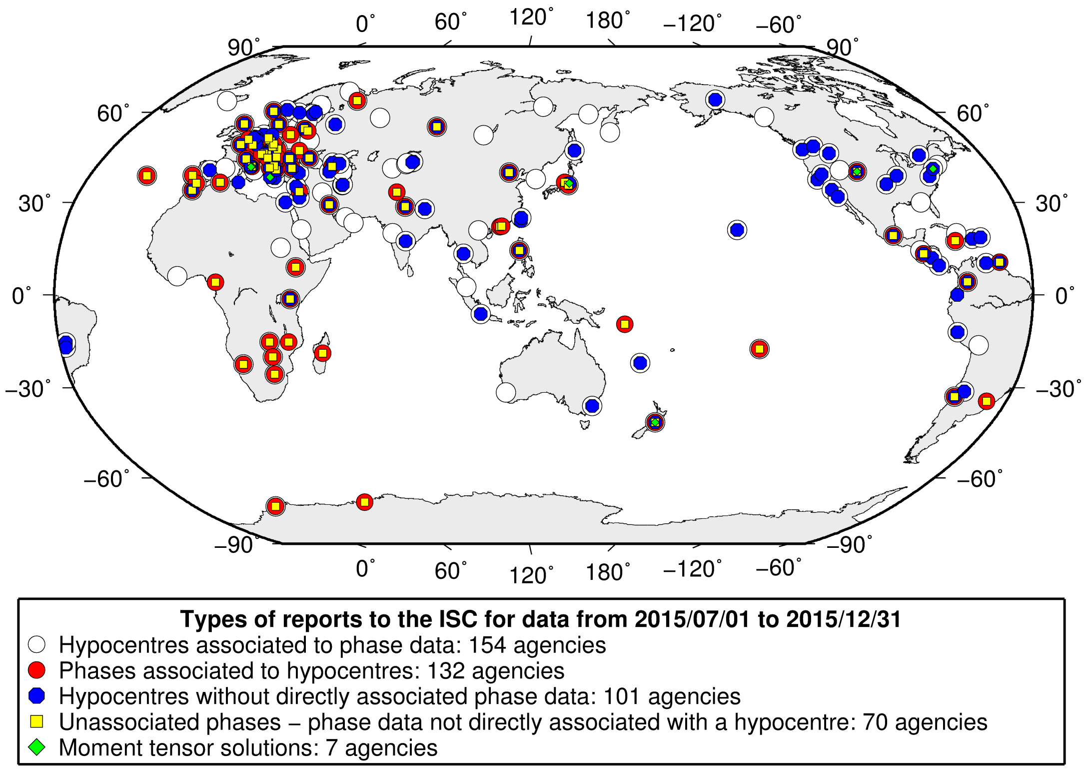

Figure 8.2: *Map of the different data types reported by agencies to the ISC. A full list of the data types reported by each agency is shown in Table 8.2.*

8.3 Arrival Observations

The collection of phase arrival observations at the ISC has increased dramatically with time. The increase in reported phase arrival observations is shown in Figure 8.3.

The reports with phase data are summarised in Table 8.3. This table is split into three sections, providing information on the reports themselves, the phase data, and the stations reporting the phase data. A map of the stations contributing these phase data is shown in Figure 8.4.

The ISC encourages the reporting of phase arrival times together with amplitude and period measurements whenever feasible. Figure 8.5 shows the percentage of events for which phase arrival times from each station are accompanied with amplitude and period measurements.

Figure 8.6 indicates the number of amplitude and period measurement for each station.

Together with the increase in the number of phases (Figure 8.3), there has been an increase in the number of stations reported to the ISC. The increase in the number of stations is shown in Figure 8.7. This increase can also be seen on the maps for stations reported each decade in Figure 8.8.

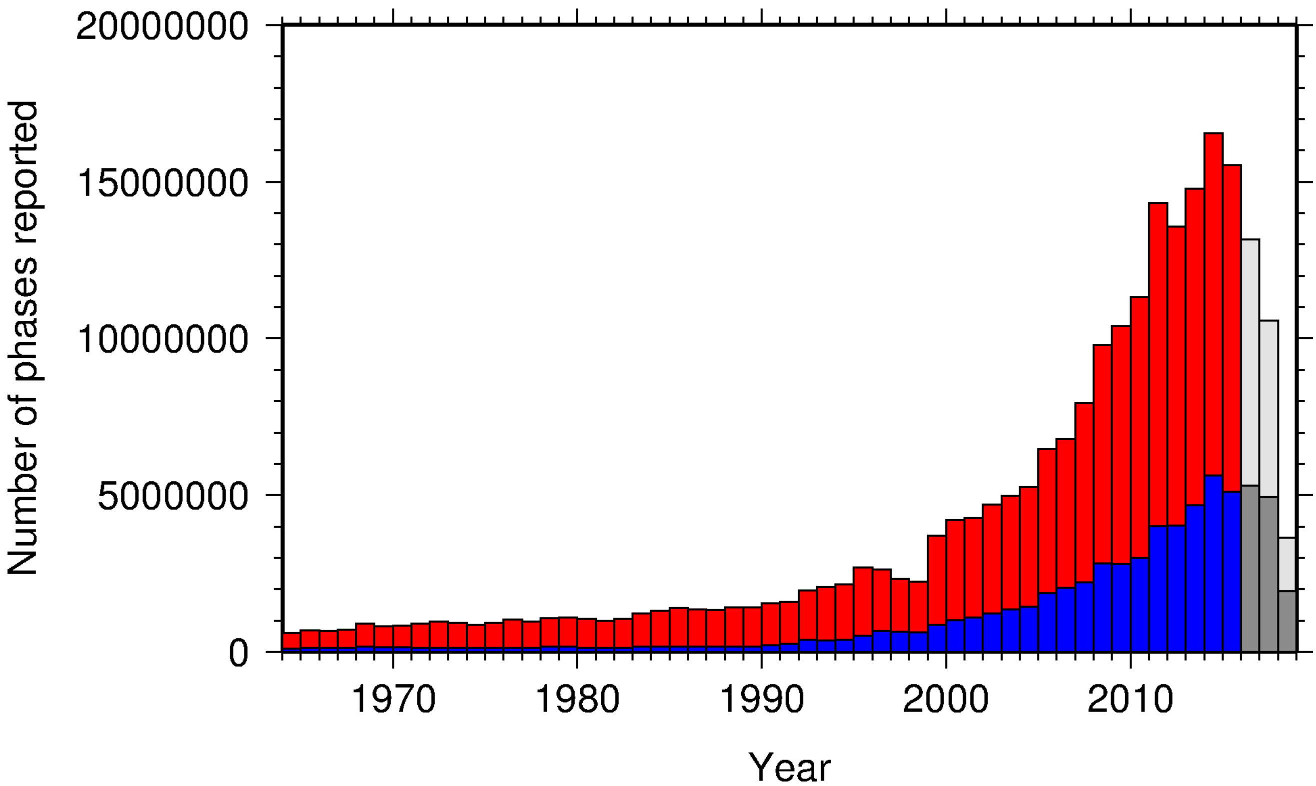

Figure 8.3: *Histogram showing the number of phases (red) and number of amplitudes (blue) collected by the ISC for events each year since 1964. The data in grey covers the current period where data are still being collected before the ISC review takes place and is accurate at the time of publication.*

Table 8.3: *Summary of reports containing phase arrival observations.*

Reports with phase arrivals	3895
Reports with phase arrivals including amplitudes	1179
Reports with only phase arrivals (no hypocentres reported)	229
Total phase arrivals received	7902634
Total phase arrival-times received	7439547
Number of duplicate phase arrival-times	594203 (8.0%)
Number of amplitudes received	2694515
Stations reporting phase arrivals	7712
Stations reporting phase arrivals with amplitude data	4451
Max number of stations per report	1884

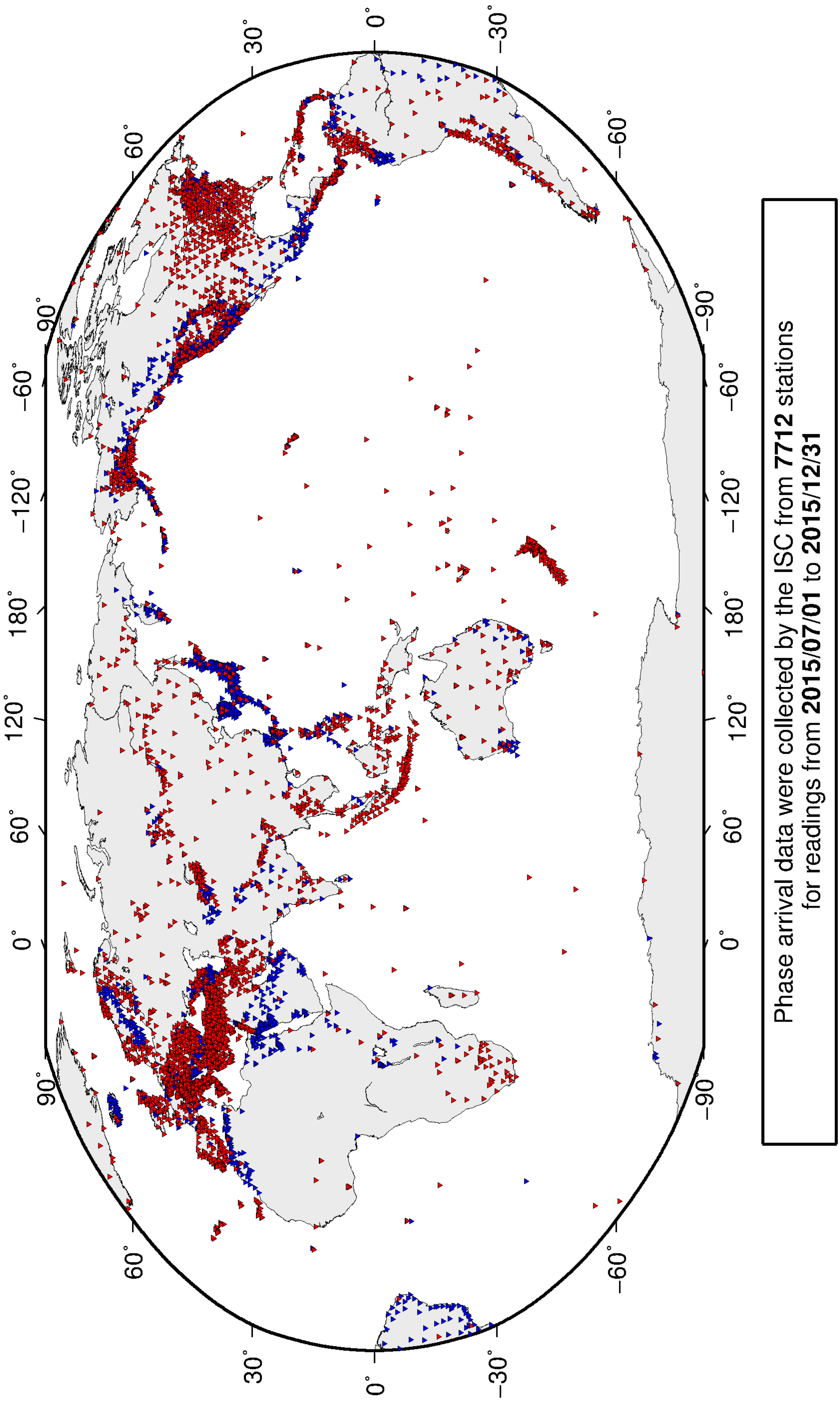

Figure 8.4: *Stations contributing phase data to the ISC for readings from July 2015 to the end of December 2015. Stations in blue provided phase arrival times only; stations in red provided both phase arrival times and amplitude data.*

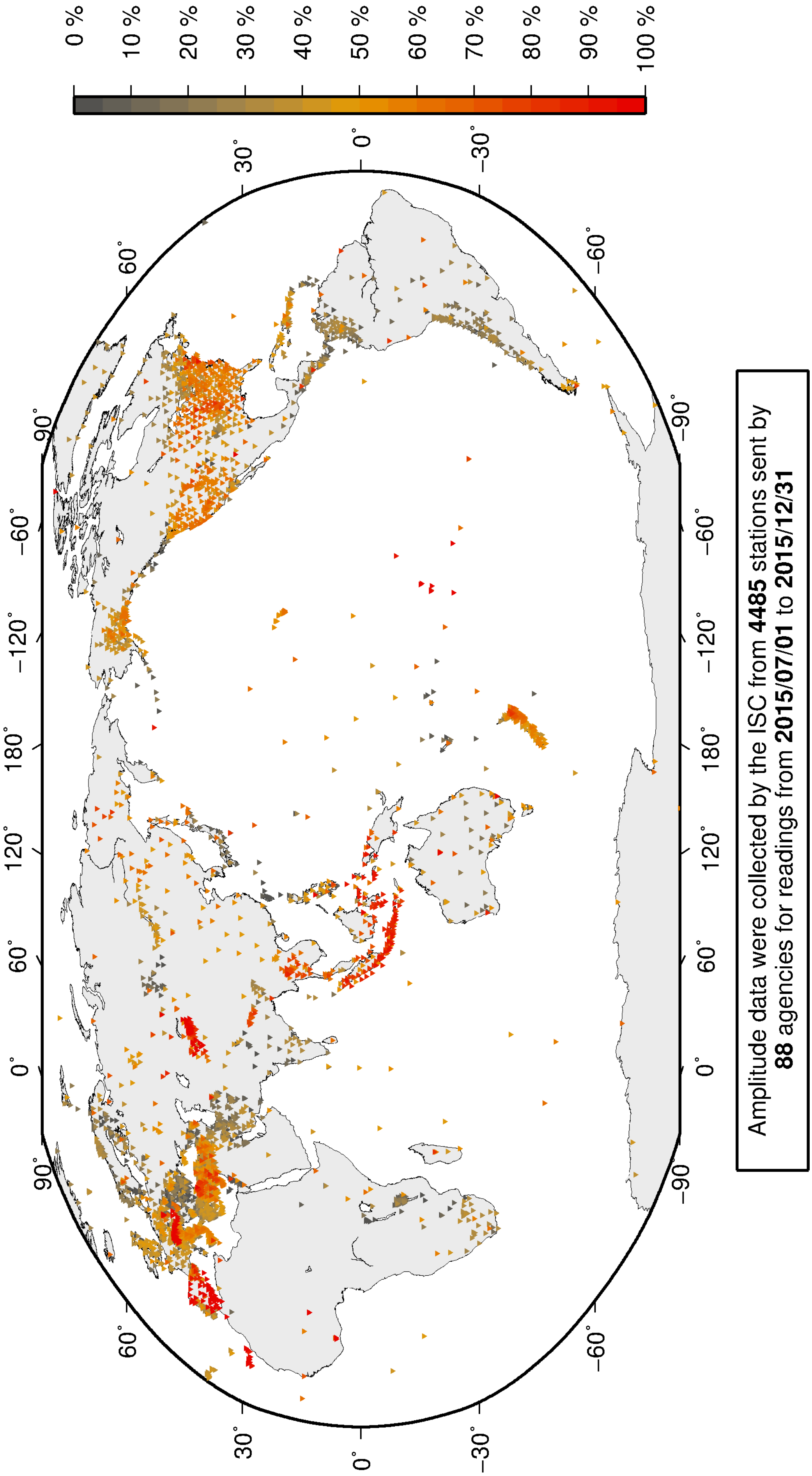

Figure 8.5: *Percentage of events for which phase arrival times from each station are accompanied with amplitude and period measurements.*

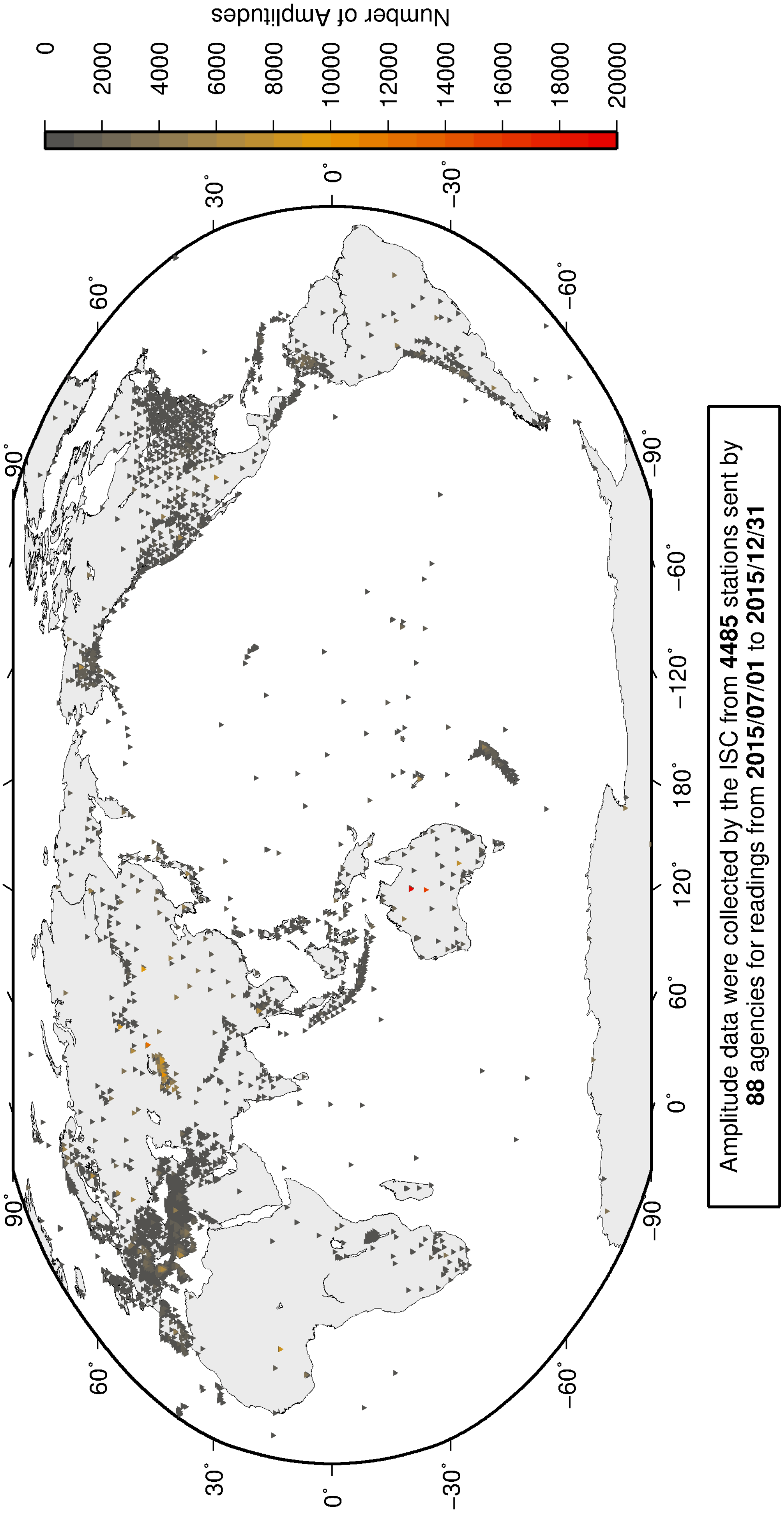

Figure 8.6: *Number of amplitude and period measurements for each station.*

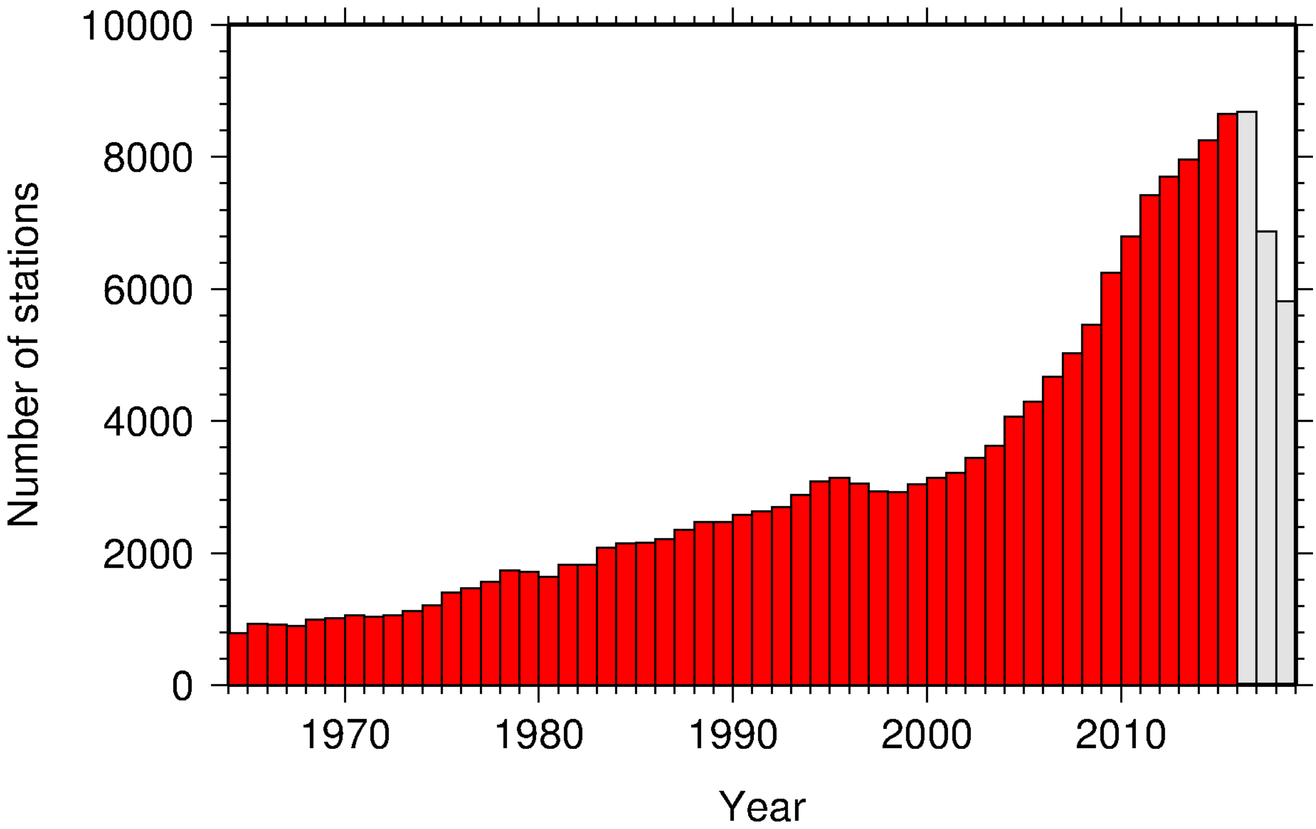

Figure 8.7: *Histogram showing the number of stations reporting to the ISC each year since 1964. The data in grey covers the current period where station information is still being collected before the ISC review of events takes place and is accurate at the time of publication.*

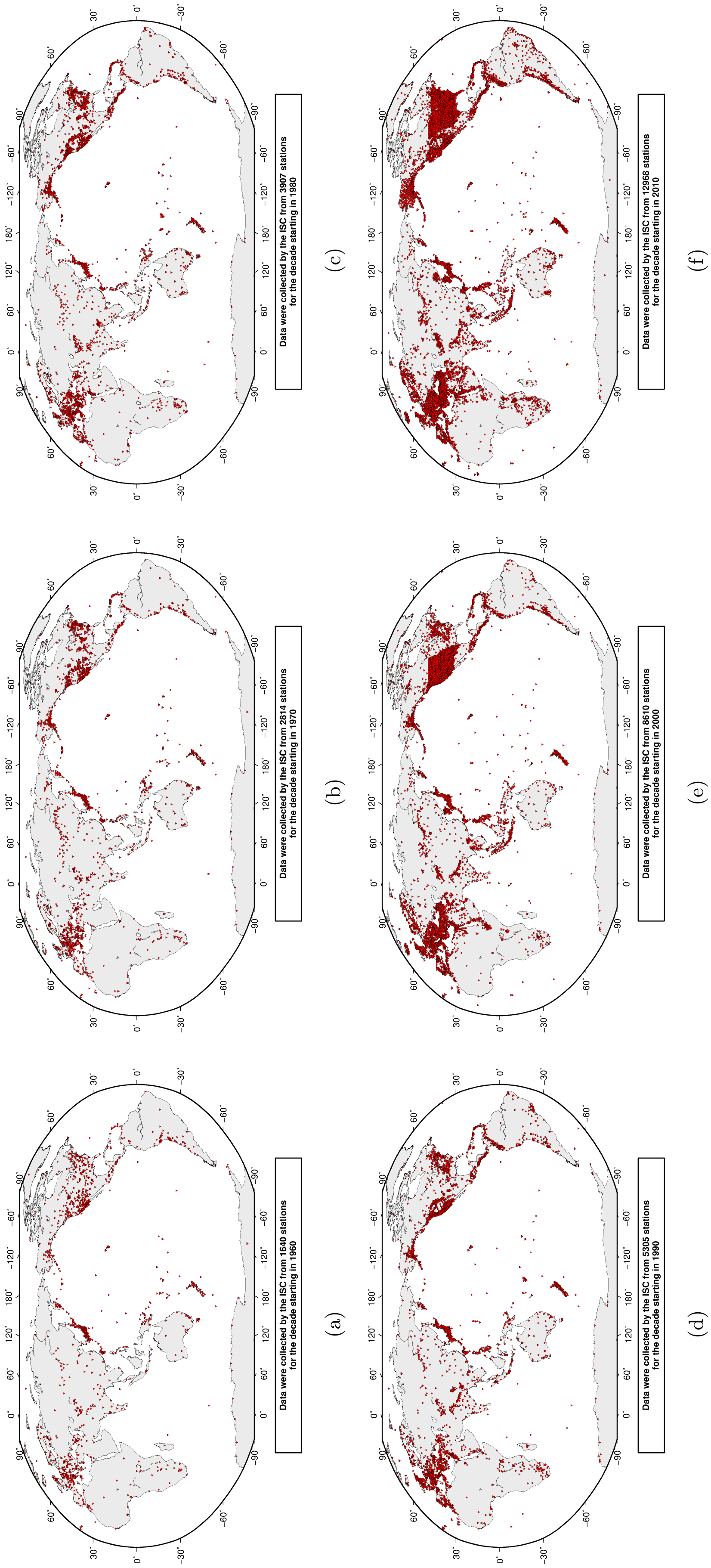

Figure 8.8: *Maps showing the stations reported to the ISC for each decade since 1960. Note that the last map covers a shorter time period.*

8.4 Hypocentres Collected

The ISC Bulletin groups multiple estimates of hypocentres into individual events, with an appropriate prime hypocentre solution selected. The collection of these hypocentre estimates are described in this section.

The reports containing hypocentres are summarised in Table 8.4. The number of hypocentres collected by the ISC has also increased significantly since 1964, as shown in Figure 8.9. A map of all hypocentres reported to the ISC for this summary period is shown in Figure 8.10. Where a network magnitude was reported with the hypocentre, this is also shown on the map, with preference given to reported values, first of M_W followed by M_S, m_b and M_L respectively (where more than one network magnitude was reported).

Table 8.4: *Summary of the reports containing hypocentres.*

Reports with hypocentres	3802
Reports of hypocentres only (no phase readings)	136
Total hypocentres received	327109
Number of duplicate hypocentres	10805 (3.3%)
Agencies determining hypocentres	168

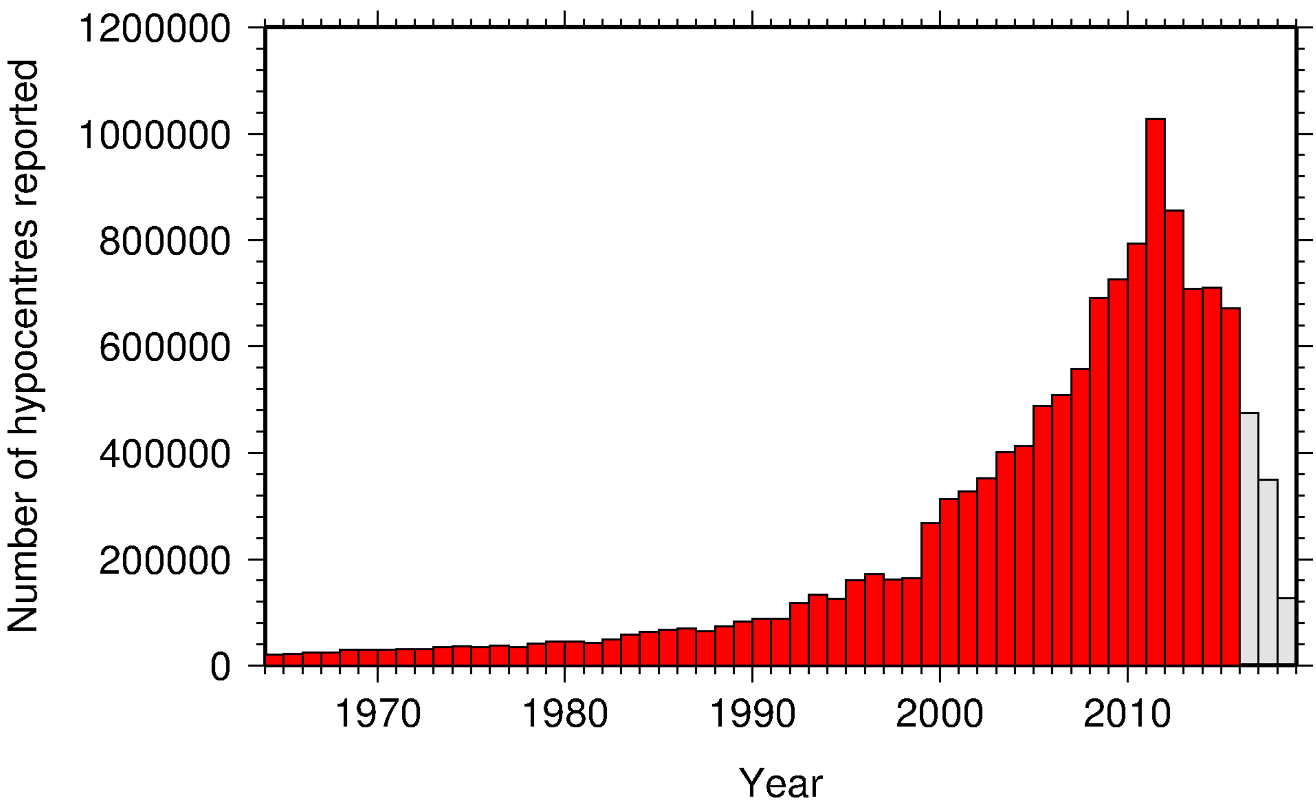

Figure 8.9: *Histogram showing the number of hypocentres collected by the ISC for events each year since 1964. For each event, multiple hypocentres may be reported.*

All the hypocentres that are reported to the ISC are automatically grouped into events, which form the basis of the ISC Bulletin. For this summary period 346029 hypocentres (including ISC) were grouped into 218811 events, the largest of these having 55 hypocentres in one event. The total number of events

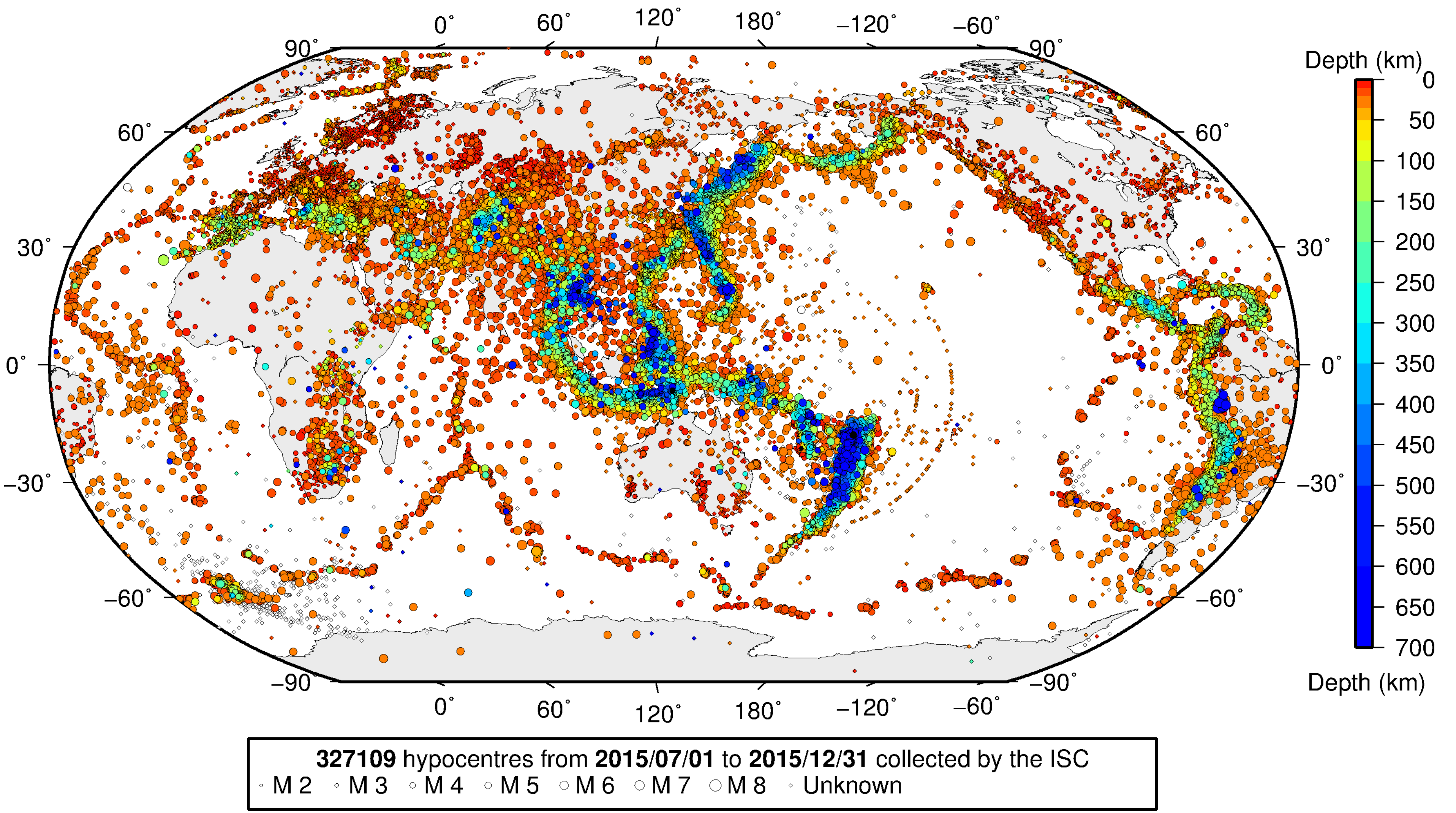

Figure 8.10: *Map of all hypocentres collected by the ISC. The scatter shows the large variation of the multiple hypocentres that are reported for each event. The magnitude corresponds with the reported network magnitude. If more than one network magnitude type was reported, preference was given to values of M_W, M_S, m_b and M_L respectively. Compare with Figure 9.2*

shown here is the result of an automatic grouping algorithm, and will differ from the total events in the published ISC Bulletin, where both the number of events and the number of hypocentre estimates will have changed due to further analysis. The process of grouping is detailed in Section 11.1.3 of issue I of the 2015 Bulletin Summary. Figure 9.2 on page 87 shows a map of all prime hypocentres.

8.5 Collection of Network Magnitude Data

Data contributing agencies normally report earthquake hypocentre solutions along with magnitude estimates. For each seismic event, each agency may report one or more magnitudes of the same or different types. This stems from variability in observational practices at regional, national and global level in computing magnitudes based on a multitude of wave types. Differences in the amplitude measurement algorithm, seismogram component(s) used, frequency range, station distance range as well as the instrument type contribute to the diversity of magnitude types. Table 8.5 provides an overview of the complexity of reported network magnitudes reported for seismic events during the summary period.

Table 8.5: *Statistics of magnitude reports to the ISC; M – average magnitude of estimates reported for each event.*

	$M<3.0$	$3.0\leq M<5.0$	$M\geq 5.0$
Number of seismic events	158829	38219	447
Average number of magnitude estimates per event	1.3	4.7	24.4
Average number of magnitudes (by the same agency) per event	1.2	2.6	3.4
Average number of magnitude types per event	1.2	3.9	12.6
Number of magnitude types	26	37	32

Table 8.6 gives the basic description, main features and scientific paper references for the most commonly reported magnitude types.

Table 8.6: *Description of the most common magnitude types reported to the ISC.*

Magnitude type	Description	References	Comments
M	Unspecified		Often used in real or near-real time magnitude estimations
mB	Medium-period and Broad-band body-wave magnitude	*Gutenberg* (1945a); *Gutenberg* (1945b); *IASPEI* (2005); *IASPEI* (2013); *Bormann et al.* (2009); *Bormann and Dewey* (2012)	
mb	Short-period body-wave magnitude	*IASPEI* (2005); *IASPEI* (2013); *Bormann et al.* (2009); *Bormann and Dewey* (2012)	Classical mb based on stations between 21°-100° distance

Table 8.6: *continued*

Magnitude type	Description	References	Comments
mb1	Short-period body-wave magnitude	*IDC* (1999) and references therein	Reported only by the IDC; also includes stations at distances less than 21°
mb1mx	Maximum likelihood short-period body-wave magnitude	*Ringdal* (1976); *IDC* (1999) and references therein	Reported only by the IDC
mbtmp	short-period body-wave magnitude with depth fixed at the surface	*IDC* (1999) and references therein	Reported only by the IDC
mbLg	Lg-wave magnitude	*Nuttli* (1973); *IASPEI* (2005); *IASPEI* (2013); *Bormann and Dewey* (2012)	Also reported as MN
Mc	Coda magnitude		
MD (Md)	Duration magnitude	*Bisztricsany* (1958); *Lee et al.* (1972)	
ME (Me)	Energy magnitude	*Choy and Boatwright* (1995)	Reported only by NEIC
MJMA	JMA magnitude	*Tsuboi* (1954)	Reported only by JMA
ML (Ml)	Local (Richter) magnitude	*Richter* (1935); *Hutton and Boore* (1987); *IASPEI* (2005); *IASPEI* (2013)	
MLSn	Local magnitude calculated for Sn phases	*Balfour et al.* (2008)	Reported by PGC only for earthquakes west of the Cascadia subduction zone
MLv	Local (Richter) magnitude computed from the vertical component		Reported only by DJA and BKK
MN (Mn)	Lg-wave magnitude	*Nuttli* (1973); *IASPEI* (2005)	Also reported as mbLg
MS (Ms)	Surface-wave magnitude	*Gutenberg* (1945c); *Vaněk et al.* (1962); *IASPEI* (2005)	Classical surface-wave magnitude computed from station between 20°-160° distance
Ms1	Surface-wave magnitude	*IDC* (1999) and references therein	Reported only by the IDC; also includes stations at distances less than 20°
ms1mx	Maximum likelihood surface-wave magnitude	*Ringdal* (1976); *IDC* (1999) and references therein	Reported only by the IDC

Table 8.6: *continued*

Magnitude type	Description	References	Comments
Ms7	Surface-wave magnitude	*Bormann et al.* (2007)	Reported only by BJI and computed from records of a Chinese-made long-period seismograph in the distance range 3°-177°
MW (Mw)	Moment magnitude	*Kanamori* (1977); *Dziewonski et al.* (1981)	Computed according to the *IASPEI* (2005) and *IASPEI* (2013) standard formula
Mw(mB)	Proxy Mw based on mB	*Bormann and Saul* (2008)	Reported only by DJA and BKK
Mwp	Moment magnitude from P-waves	*Tsuboi et al.* (1995)	Reported only by DJA and BKK and used in rapid response
mbh	Unknown		
mbv	Unknown		
MG	Unspecified type		Contact contributor
Mm	Unknown		
msh	Unknown		
MSV	Unknown		

Table 8.7 lists all magnitude types reported, the corresponding number of events in the ISC Bulletin and the agency codes along with the number of earthquakes.

Table 8.7: *Summary of magnitude types in the ISC Bulletin for this summary period. The number of events with values for each magnitude type is listed. The agencies reporting these magnitude types are listed, together with the total number of values reported.*

Magnitude type	Events	Agencies reporting magnitude type (number of values)
M	5713	WEL (5507), RSPR (143), KRSZO (25), PRU (25), FDF (10), ROM (3)
MB	2	IPEC (2)
mB	2013	BJI (1260), DJA (737), WEL (272), NOU (16), STR (5)
mb	29017	IDC (17303), NEIC (7945), KRNET (5398), NNC (4775), VIE (1658), MAN (1648), MOS (1545), DJA (1251), BJI (1239), VAO (658), BGR (293), NOU (285), MDD (162), SIGU (82), OMAN (45), CFUSG (43), NDI (36), STR (22), DSN (16), PGC (8), GII (7), DNK (6), DMN (4), PDG (2), BGS (1), WEL (1), ROM (1)
mb1	18016	IDC (18016)
mb1mx	18016	IDC (18016)
mB_BB	27	BGR (27)
mb_Lg	1480	NEIC (1456), TEH (22), MDD (1), OTT (1), BDF (1)
mbLg	2198	MDD (2198)
mbR	165	VAO (165)

Table 8.7: Continued.

Magnitude type	Events	Agencies reporting magnitude type (number of values)
mbtmp	18016	IDC (18016)
Mc	31	DNK (17), OSPL (13), BER (2), JSO (1), RSNC (1)
MD	12570	MEX (3644), LDG (1898), TRN (1770), RSPR (1766), ROM (669), ECX (442), EAF (362), GRAL (307), GCG (296), TIR (252), SOF (206), HLW (177), SSNC (174), GII (143), BUL (139), INMG (117), PNSN (94), PDG (83), SNET (79), SJA (78), JSN (74), SLM (51), CFUSG (50), TUN (46), NDI (43), LSZ (28), UPA (26), INET (26), BUG (14), SEA (12), UCR (7), NIC (7), BUT (5), HVO (5), DDA (5), NCEDC (4), AAE (3), UUSS (2), LDO (1), IGQ (1)
MJMA	54674	JMA (54674)
Mjma	3	JSO (2), WEL (1)
ML	113341	TAP (24272), ISK (10940), ATH (10855), IDC (10309), DDA (9608), HEL (7330), ROM (6774), RSNC (5567), GUC (5071), WEL (5044), THE (4663), UPP (3401), VIE (2372), AEIC (2179), LDG (2146), BER (2133), NEIC (1760), CNRM (1709), MAN (1669), ANF (1428), LJU (1381), BEO (1304), TUL (1289), SNET (1240), PGC (1137), DNK (1133), INMG (1104), BUC (956), RHSSO (714), NIC (696), KRSC (593), OSPL (583), GEN (562), NOU (540), PRE (535), MRB (535), SJA (528), TEH (514), NAO (479), INET (476), IGIL (456), IPEC (425), ECX (422), THR (372), BJI (261), ECGS (260), TIR (257), PDG (253), REN (252), ISN (251), LVSN (249), CRAAG (248), KRSZO (239), KNET (212), UCR (200), KISR (186), KOLA (186), SSNC (177), SFS (175), NDI (165), BGS (160), OMAN (154), DSN (154), HVO (135), MIRAS (131), BGR (127), SEA (126), HLW (124), OTT (72), ARE (67), PPT (64), DRS (61), UPA (60), UCC (60), BUT (46), AZER (46), NCEDC (38), WBNET (35), PAS (34), SCB (34), DMN (28), BNS (25), LSZ (24), CUPWA (18), UUSS (17), SGS (15), BUG (14), PLV (12), RISSC (8), MOS (4), LDO (4), EAF (3), CSEM (3), FIA0 (3), AUST (2), CLL (2), VAO (2), ZAG (2), HYB (1), SSN (1), AAE (1), SSS (1), JSO (1), ALG (1), SKO (1), LER (1)
MLh	440	ZUR (417), ASRS (26)
MLSn	535	PGC (535)
MLv	10051	WEL (5517), DJA (3008), STR (867), NOU (775), KRSZO (18), JSO (4), ASRS (2)
Mm	239	GII (239)
MN	288	OTT (288)
mpv	5051	NNC (5051)
MPVA	230	NORS (176), MOS (176)
MS	9798	IDC (8201), MAN (1672), BJI (977), MOS (438), BGR (129), SOME (71), NSSP (61), VIE (21), OMAN (12), DNK (3), IPEC (2), NDI (1), JSO (1), DSN (1)
Ms1	8201	IDC (8201)
ms1mx	8201	IDC (8201)
Ms7	968	BJI (968)

Table 8.7: *Continued.*

Magnitude type	Events	Agencies reporting magnitude type (number of values)
Ms_20	211	NEIC (211)
MW	5374	GCMT (1091), INET (1076), NIED (750), PGC (571), UPA (454), RSNC (429), FUNV (344), SJA (330), DDA (238), UCR (201), SSNC (155), GUC (98), MED_RCMT (69), BER (53), ASIES (51), WEL (37), ROM (18), UPSL (13), DJA (11), IEC (5), DNK (4), SNET (3), GFZ (1), SCB (1), THE (1)
Mw(mB)	277	WEL (272), STR (5)
Mwb	227	NEIC (227)
Mwc	216	GCMT (212), NEIC (31)
Mwp	104	DJA (95), OMAN (8), NEIC (1)
Mwr	633	NEIC (511), GUC (58), SLM (31), CAR (31), NCEDC (19), OTT (13), PAS (7), ROM (2), RSNC (1), TEH (1), GFZ (1)
Mww	285	NEIC (285)

The most commonly reported magnitude types are short-period body-wave, surface-wave, local (or Richter), moment, duration and JMA magnitude type. For a given earthquake, the number and type of reported magnitudes greatly vary depending on its size and location. The large earthquake of October 25, 2010 gives an example of the multitude of reported magnitude types for large earthquakes (Listing 8.1). Different magnitude estimates come from global monitoring agencies such as the IDC, NEIC and GCMT, a local agency (GUC) and other agencies, such as MOS and BJI, providing estimates based on the analysis of their networks. The same agency may report different magnitude types as well as several estimates of the same magnitude type, such as NEIC estimates of Mw obtained from W-phase, centroid and body-wave inversions.

Listing 8.1: *Example of reported magnitudes for a large event*

```
Event   15264887 Southern Sumatera
   Date        Time        Err   RMS Latitude Longitude  Smaj  Smin  Az Depth   Err Ndef Nsta Gap  mdist  Mdist Qual   Author      OrigID
2010/10/25 14:42:22.18   0.27 1.813  -3.5248  100.1042 4.045 3.327  54  20.0  1.37 2102 2149  23   0.76 176.43 m i de ISC       01346132
 (#PRIME)

Magnitude  Err Nsta Author      OrigID
mb      6.1        61 BJI       15548963
mB      6.9        68 BJI       15548963
Ms      7.7        85 BJI       15548963
Ms7     7.5        86 BJI       15548963
mb      5.3 0.1    48 IDC       16686694
mb1     5.3 0.1    51 IDC       16686694
mb1mx   5.3 0.0    52 IDC       16686694
mbtmp   5.3 0.1    51 IDC       16686694
ML      5.1 0.2     2 IDC       16686694
MS      7.1 0.0    31 IDC       16686694
Ms1     7.1 0.0    31 IDC       16686694
ms1mx   6.9 0.1    44 IDC       16686694
mb      6.1       243 ISCJB     01677901
MS      7.3       228 ISCJB     01677901
M       7.1       117 DJA       01268475
mb      6.1 0.2   115 DJA       01268475
mB      7.1 0.1   117 DJA       01268475
MLv     7.0 0.2    26 DJA       01268475
        7.1 0.4   117 DJA       01268475
Mwp     6.9 0.2   102 DJA       01268475
mb      6.4        49 MOS       16742129
MS      7.2        70 MOS       16742129
mb      6.5       110 NEIC      01288303
ME      7.3           NEIC      01288303
MS      7.3       143 NEIC      01288303
MW      7.7           NEIC      01288303
MW      7.8       130 GCMT      00125427
mb      5.9           KLM       00255772
ML      6.7           KLM       00255772
MS      7.6           KLM       00255772
mb      6.4        20 BGR       16815854
Ms      7.2         2 BGR       16815854
mb      6.3 0.3   250 ISC       01346132
MS      7.3 0.1   237 ISC       01346132
```

An example of a relatively small earthquake that occurred in northern Italy for which we received magnitude reports of mostly local and duration type from six agencies in Italy, France and Austria is given in Listing 8.2.

Listing 8.2: *Example of reported magnitudes for a small event*

```
Event 15089710 Northern Italy
   Date       Time        Err   RMS Latitude Longitude  Smaj  Smin  Az Depth   Err Ndef Nsta Gap  mdist  Mdist Qual   Author      OrigID
2010/08/08 15:20:46.22   0.94 0.778  45.4846    8.3212 2.900 2.539 110  28.6  9.22  172  110  82   0.41   5.35 m i ke ISC       01249414
 (#PRIME)

Magnitude  Err Nsta Author      OrigID
ML      2.4       10 ZUR       15925566
Md      2.6 0.2   19 ROM       16861451
Ml      2.2 0.2    9 ROM       16861451
ML      2.5          GEN       00554757
ML      2.6 0.3   28 CSEM      00554756
Md      2.3 0.0    3 LDG       14797570
Ml      2.6 0.3   32 LDG       14797570
```

Figure 8.11 shows a distribution of the number of agencies reporting magnitude estimates to the ISC according to the magnitude value. The peak of the distribution corresponds to small earthquakes where many local agencies report local and/or duration magnitudes. The number of contributing agencies rapidly decreases for earthquakes of approximately magnitude 5.5 and above, where magnitudes are mostly given by global monitoring agencies.

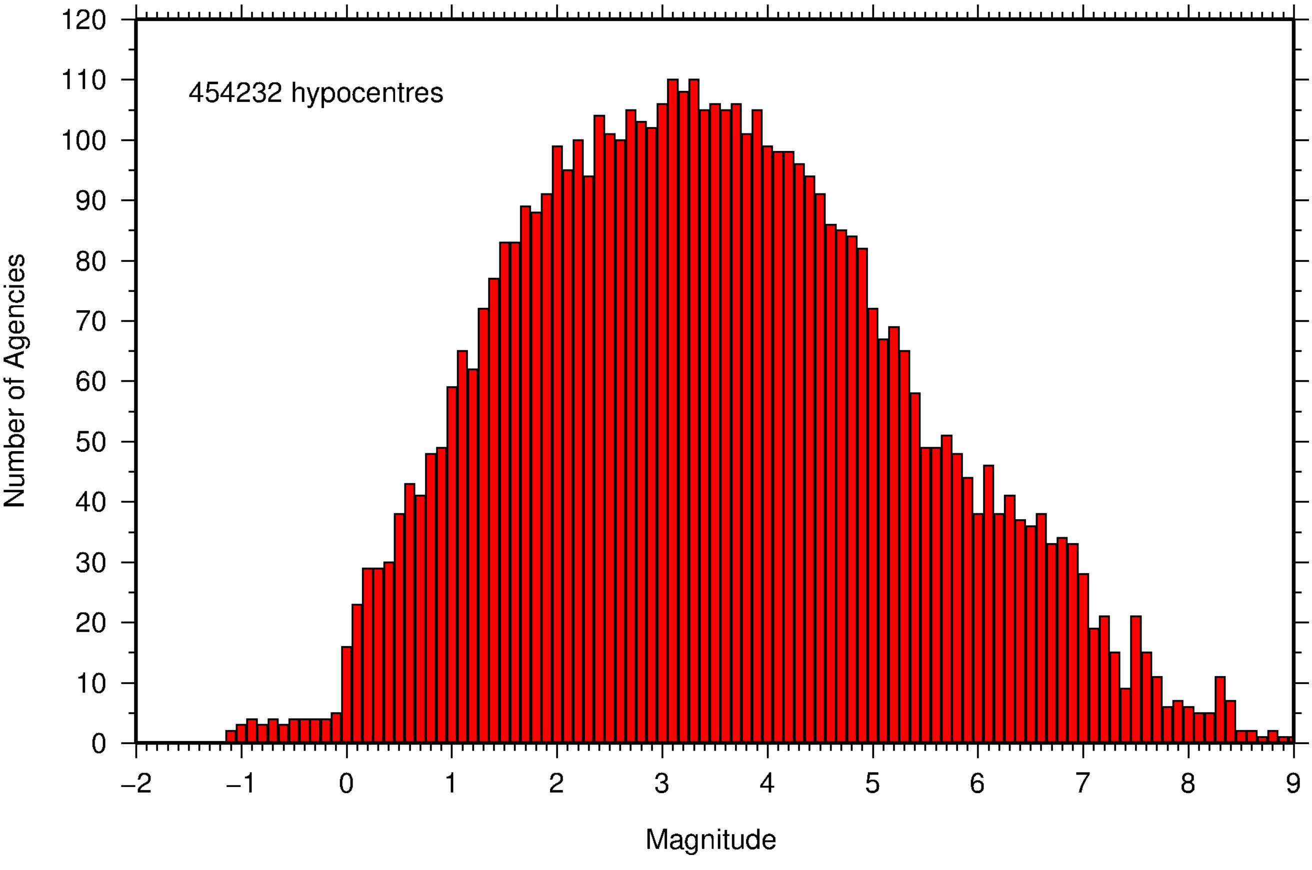

Figure 8.11: *Histogram showing the number of agencies that reported network magnitude values. All magnitude types are included.*

8.6 Moment Tensor Solutions

The ISC Bulletin publishes moment tensor solutions, which are reported to the ISC by other agencies. The collection of moment tensor solutions is summarised in Table 8.8. A histogram showing all moment tensor solutions collected throughout the ISC history is shown in Figure 8.12. Several moment tensor solutions from different authors and different moment tensor solutions calculated by different methods from the same agency may be present for the same event.

Table 8.8: *Summary of reports containing moment tensor solutions.*

Reports with Moment Tensors	60
Total moment tensors received	7127
Agencies reporting moment tensors	7

The number of moment tensors for this summary period, reported by each agency, is shown in Table 8.9. The moment tensor solutions are plotted in Figure 8.13.

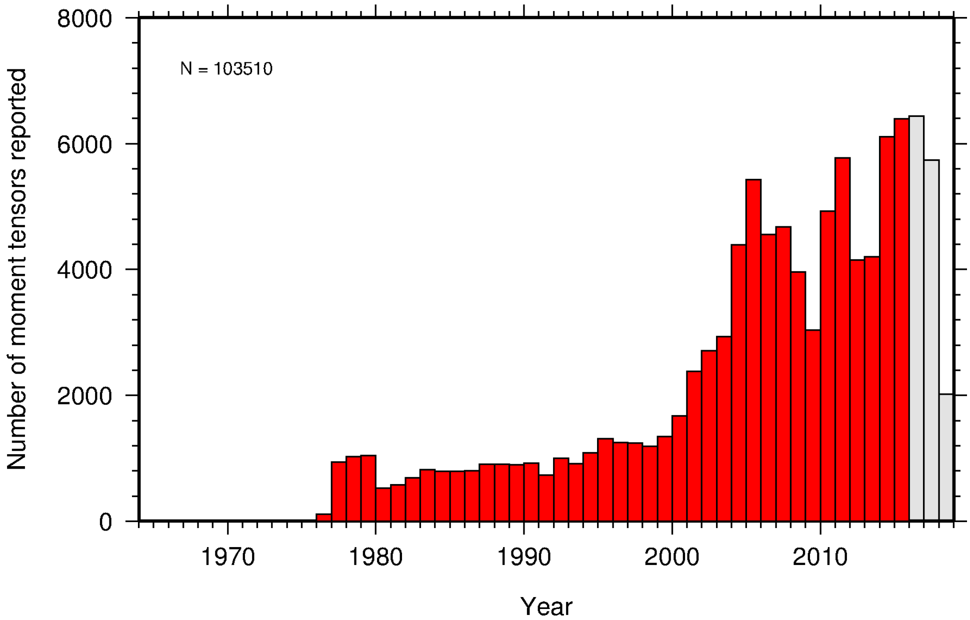

Figure 8.12: *Histogram showing the number of moment tensors reported to the ISC since 1964. The regions in grey represent data that are still being actively collected.*

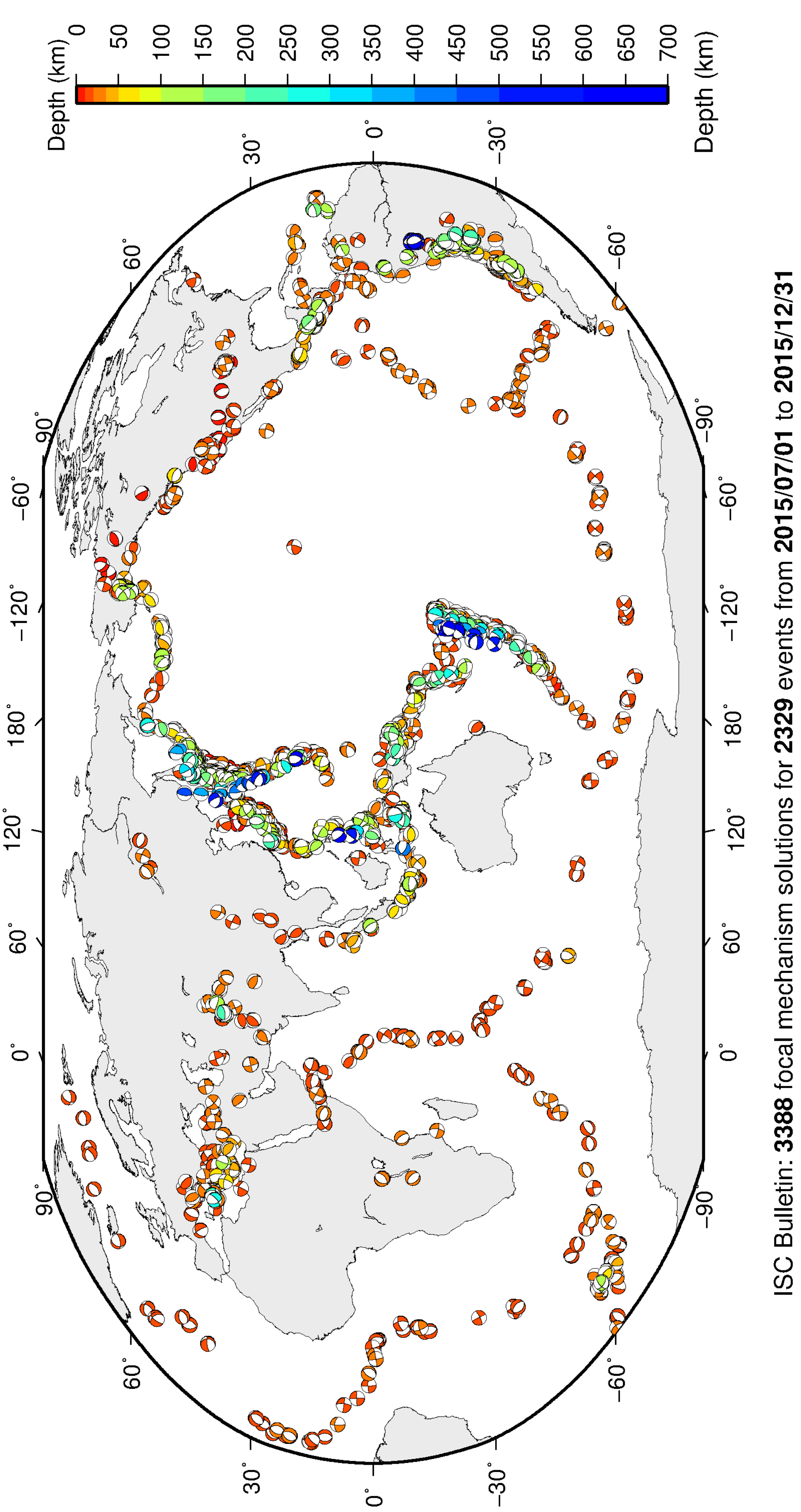

Figure 8.13: *Map of all moment tensor solutions in the ISC Bulletin for this summary period.*

Table 8.9: *Summary of moment tensor solutions in the ISC Bulletin reported by each agency.*

Agency	Number of moment tensor solutions
NEIC	1413
GCMT	1091
NIED	750
JMA	430
ISC	410
RSNC	190
PNSN	94
MED_RCMT	69
WEL	37
MOS	20
ECX	18
ROM	15
OSPL	13
UPSL	13
UCR	11
IEC	10
UPA	9
SNET	7
BER	3
THE	2

8.7 Timing of Data Collection

Here we present the timing of reports to the ISC. Please note, this does not include provisional alerts, which are replaced at a later stage. Instead, it reflects the final data sent to the ISC. The absolute timing of all hypocentre reports, regardless of magnitude, is shown in Figure 8.14. In Figure 8.15 the reports are grouped into one of six categories - from within three days of an event origin time, to over one year. The histogram shows the distribution with magnitude (for hypocentres where a network magnitude was reported) for each category, whilst the map shows the geographic distribution of the reported hypocentres.

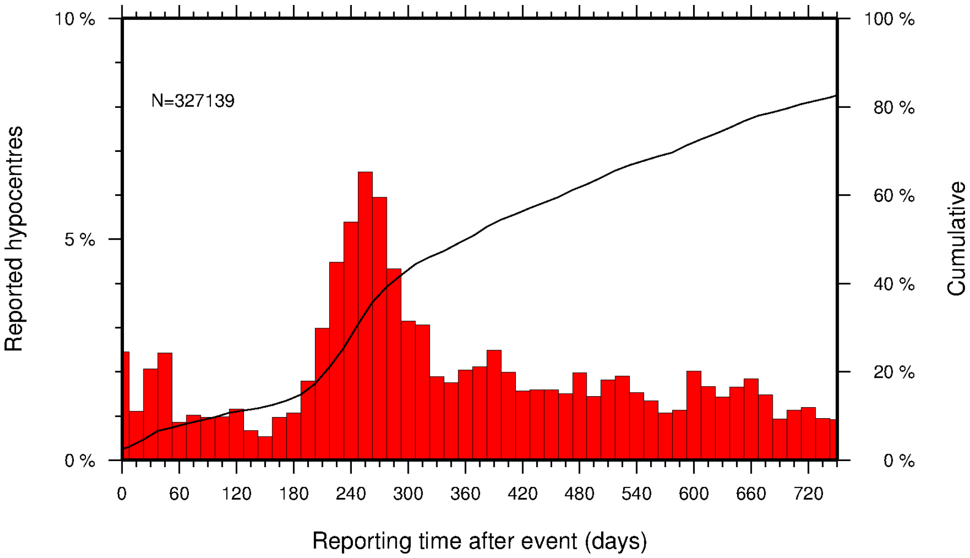

Figure 8.14: *Histogram showing the timing of final reports of the hypocentres (total of N) to the ISC. The cumulative frequency is shown by the solid line.*

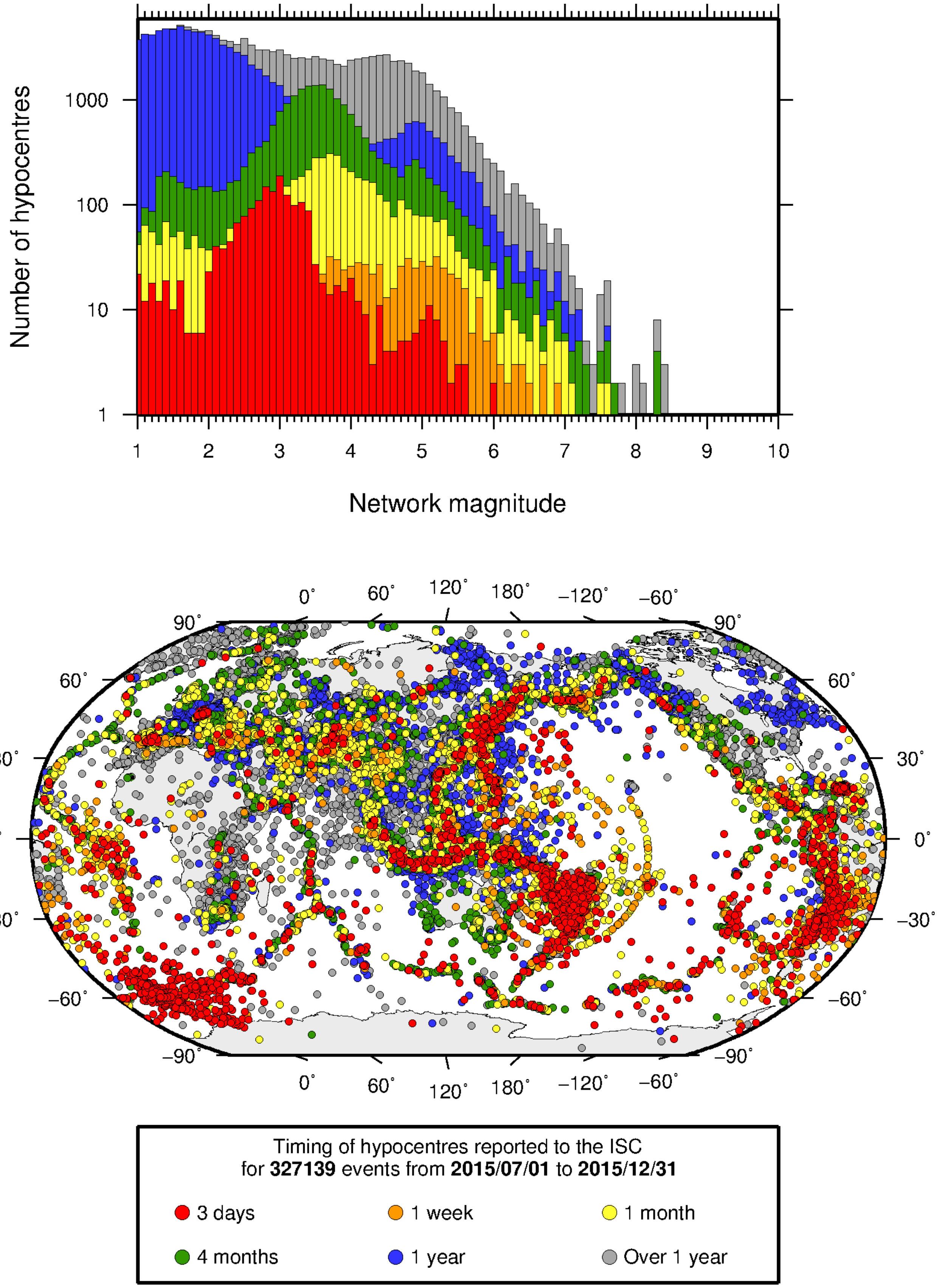

Figure 8.15: *Timing of hypocentres reported to the ISC. The colours show the time after the origin time that the corresponding hypocentre was reported. The histogram shows the distribution with magnitude. If more than one network magnitude was reported, preference was given to a value of M_W followed by M_S, m_b and M_L respectively; all reported hypocentres are included on the map. Note: early reported hypocentres are plotted over later reported hypocentres, on both the map and histogram.*

9

Overview of the ISC Bulletin

This chapter provides an overview of the seismic event data in the ISC Bulletin. We indicate the differences between all ISC events and those ISC events that are reviewed or located. We describe the wealth of phase arrivals and phase amplitudes and periods observed at seismic stations worldwide, reported in the ISC Bulletin and often used in the ISC location and magnitude determination. Finally, we make some comparisons of the ISC magnitudes with those reported by other agencies, and discuss magnitude completeness of the ISC Bulletin.

9.1 Events

The ISC Bulletin had 209163 reported events in the summary period between July and December 2015. Some 91% (190581) of the events were identified as earthquakes, the rest (18582) were of anthropogenic origin (including mining and other chemical explosions, rockbursts and induced events) or of unknown origin. As discussed in Section 11.1.3 of issue I of the 2015 Bulletin Summary, typically about 15% of the events are selected for ISC review, and about half of the events selected for review are located by the ISC. In this summary period 13% of the events were reviewed and 9% of the events were located by the ISC. For events that are not located by the ISC, the prime hypocentre is identified according to the rules described in Section 11.1.3 of issue I of the 2015 Bulletin Summary.

Of the 7999827 reported phase observations, 39% are associated to ISC-reviewed events, and 36% are associated to events selected for ISC location. Note that all large events are reviewed and located by the ISC. Since large events are globally recorded and thus reported by stations worldwide, they will provide the bulk of observations. This explains why only about one-fifth of the events in any given month is reviewed although the number of phases associated to reviewed events has increased nearly exponentially in the past decades.

Figure 9.1 shows the daily number of events throughout the summary period. Figure 9.2 shows the locations of the events in the ISC Bulletin; the locations of ISC-reviewed and ISC-located events are shown in Figures 9.3 and 9.4, respectively.

Figure 9.5 shows the hypocentral depth distributions of events in the ISC Bulletin for the summary period. The vast majority of events occur in the Earth's crust. Note that the peaks at 0, 10, 35 km, and at every 50 km intervals deeper than 100 km are artifacts of analyst practices of fixing the depth to a nominal value when the depth cannot be reliably resolved.

Figure 9.6 shows the depth distribution of free-depth solutions in the ISC Bulletin. The depth of a hypocentre reported to the ISC is assumed to be determined as a free parameter, unless it is explicitly labelled as a fixed-depth solution. On the other hand, as described in Section 11.1.4 of issue I of the

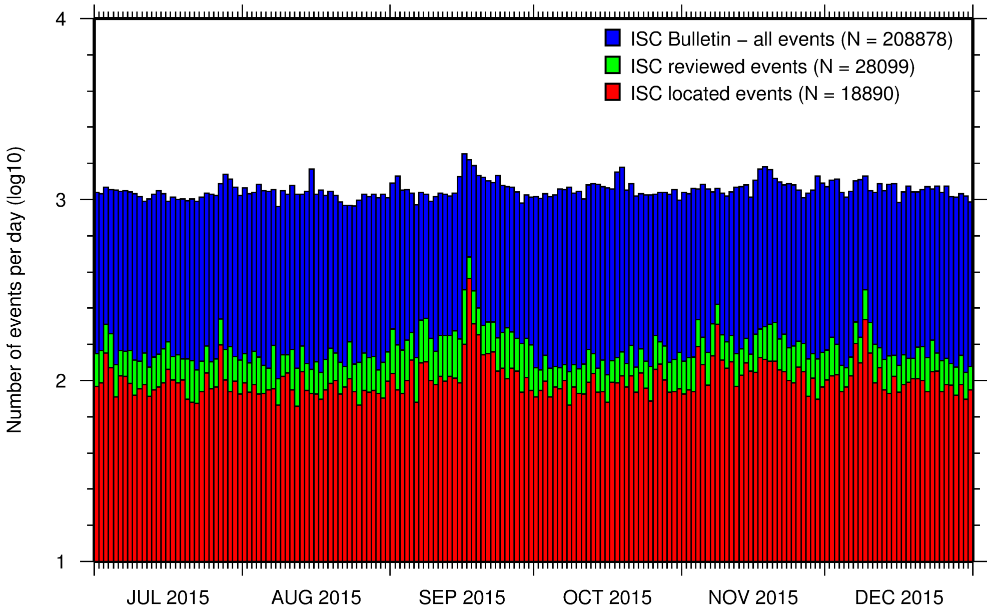

Figure 9.1: *Histogram showing the number of events in the ISC Bulletin for the current summary period. The vertical scale is logarithmic.*

2015 Bulletin Summary, the ISC locator attempts to get a free-depth solution if, and only if, there is resolution for the depth in the data, i.e. if there is a local network and/or sufficient depth-sensitive phases are reported.

Figure 9.7 shows the depth distribution of fixed-depth solutions in the ISC Bulletin. Except for a fraction of events whose depth is fixed to a shallow depth, this set comprises mostly ISC-located events. If there is no resolution for depth in the data, the ISC locator fixes the depth to a value obtained from the ISC default depth grid file, or if no default depth exists for that location, to a nominal default depth assigned to each Flinn-Engdahl region (see details in Section 11.1.4 of issue I of the 2015 Bulletin Summary). During the ISC review editors are inclined to accept the depth obtained from the default depth grid, but they typically change the depth of those solutions that have a nominal (10 or 35 km) depth. When doing so, they usually fix the depth to a round number, preferably divisible by 50.

For events selected for ISC location, the number of stations typically increases as arrival data reported by several agencies are grouped together and associated to the prime hypocentre. Consequently, the network geometry, characterised by the secondary azimuthal gap (the largest azimuthal gap a single station closes), is typically improved. Figure 9.8 illustrates that the secondary azimuthal gap is indeed generally smaller for ISC-located events than that for all events in the ISC Bulletin. Figure 9.9 shows the distribution of the number of associated stations. For large events the number of associated stations is usually larger for ISC-located events than for any of the reported event bulletins. On the other hand, events with just a few reporting stations are rarely selected for ISC location. The same is true for the number of defining stations (stations with at least one defining phase that were used in the location). Figure 9.10 indicates that because the reported observations from multiple agencies are associated to the prime, large ISC-located events typically have a larger number of defining stations than any of the reported event bulletins.

The formal uncertainty estimates are also typically smaller for ISC-located events. Figure 9.11 shows the

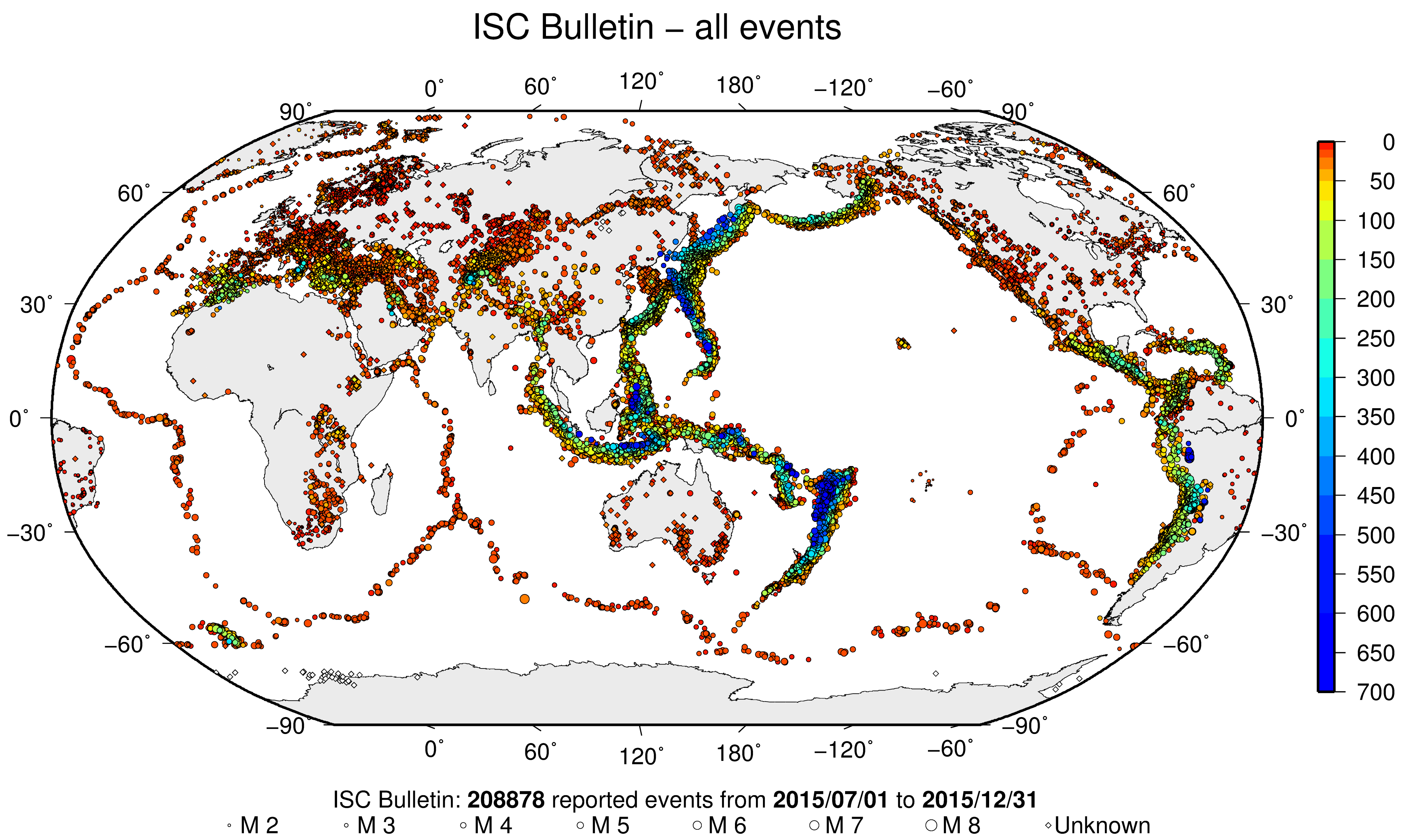

Figure 9.2: *Map of all events in the ISC Bulletin. Prime hypocentre locations are shown. Compare with Figure 8.10.*

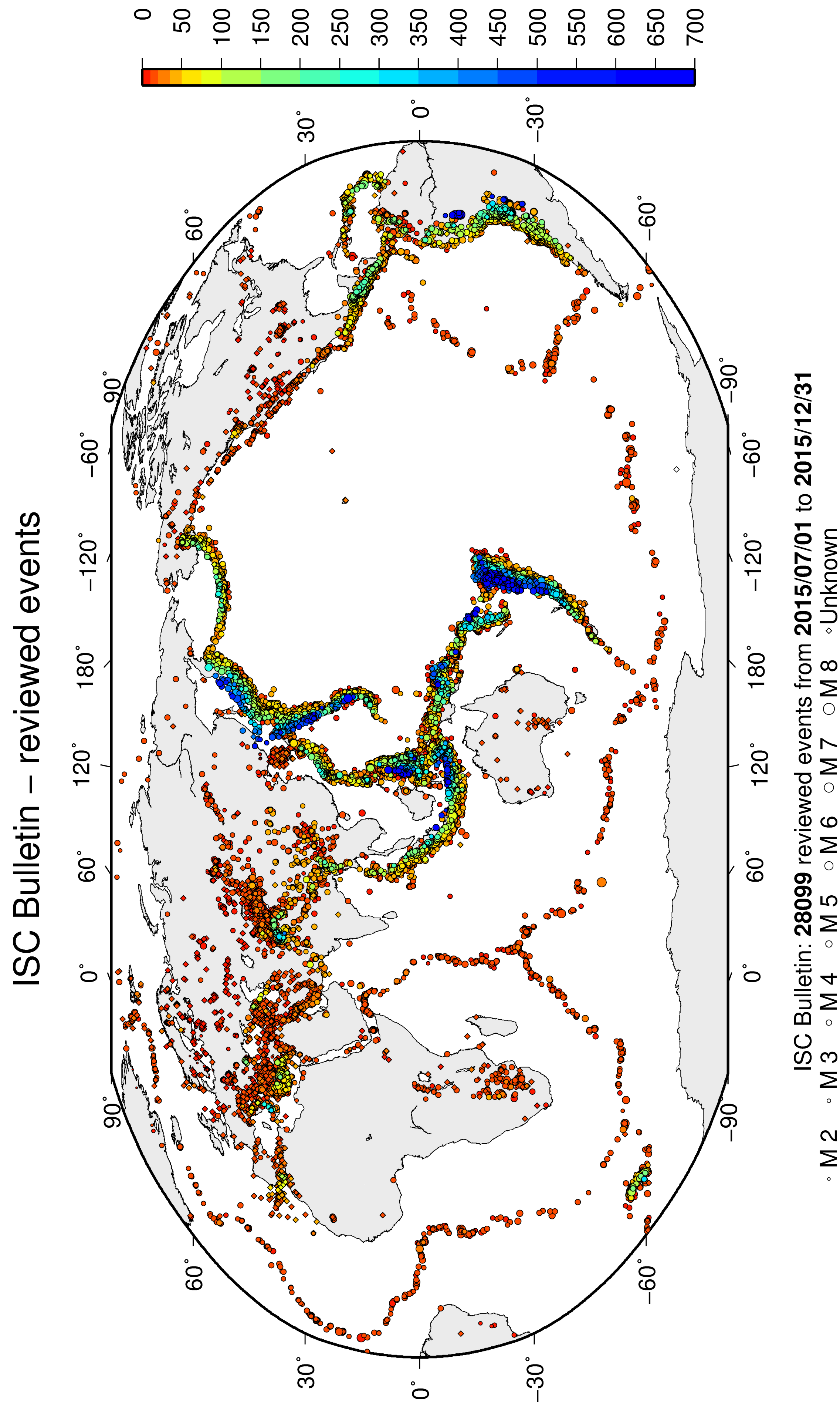

Figure 9.3: *Map of all events reviewed by the ISC for this time period. Prime hypocentre locations are shown.*

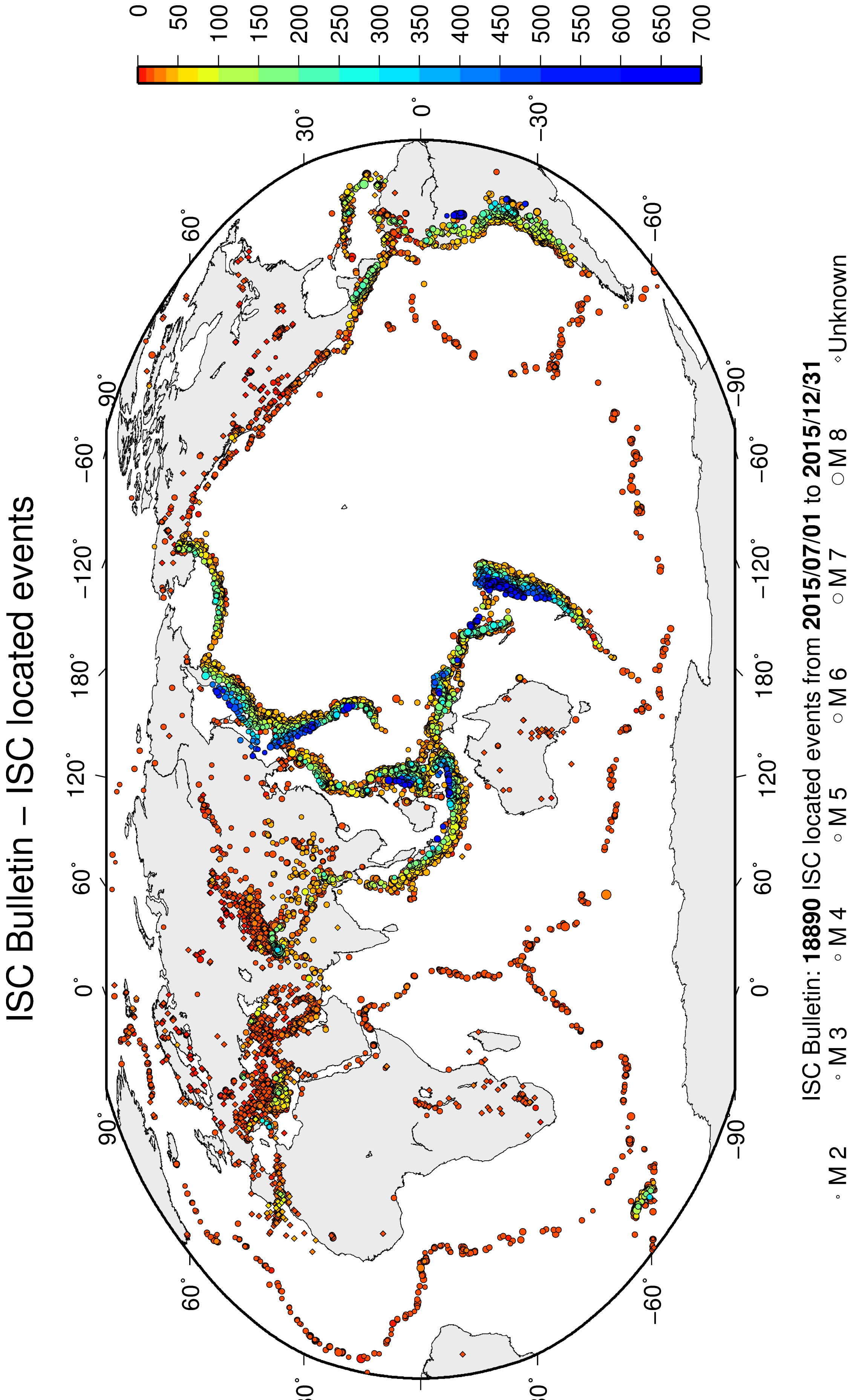

Figure 9.4: *Map of all events located by the ISC for this time period. ISC determined hypocentre locations are shown.*

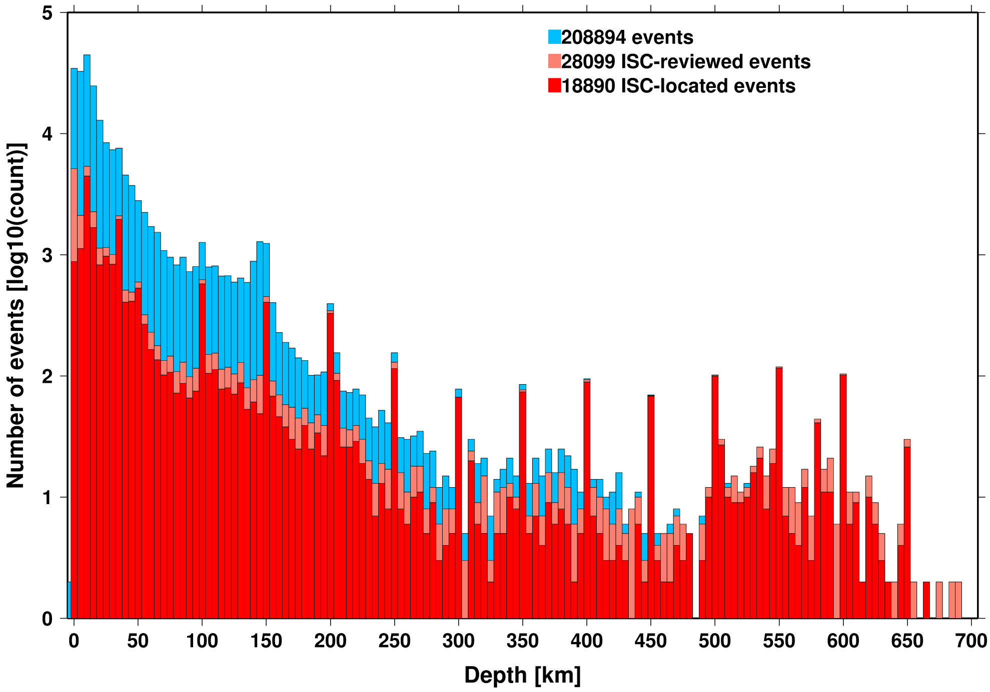

Figure 9.5: *Distribution of event depths in the ISC Bulletin (blue) and for the ISC-reviewed (pink) and the ISC-located (red) events during the summary period. All ISC-located events are reviewed, but not all reviewed events are located by the ISC. The vertical scale is logarithmic.*

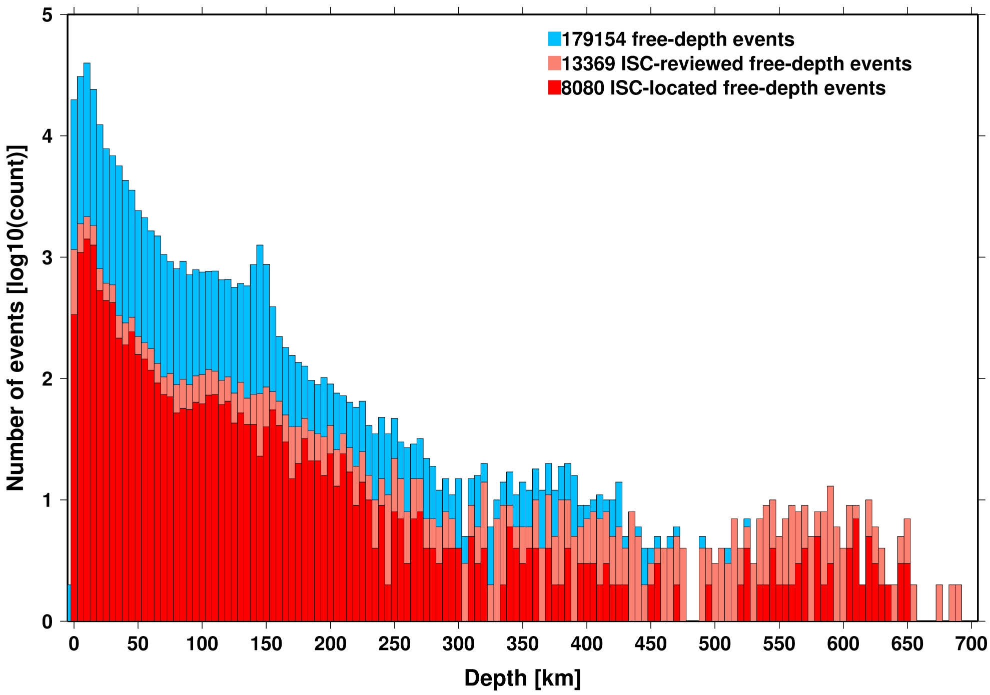

Figure 9.6: *Hypocentral depth distribution of events where the prime hypocentres are reported/located with a free-depth solution in the ISC Bulletin. The vertical scale is logarithmic.*

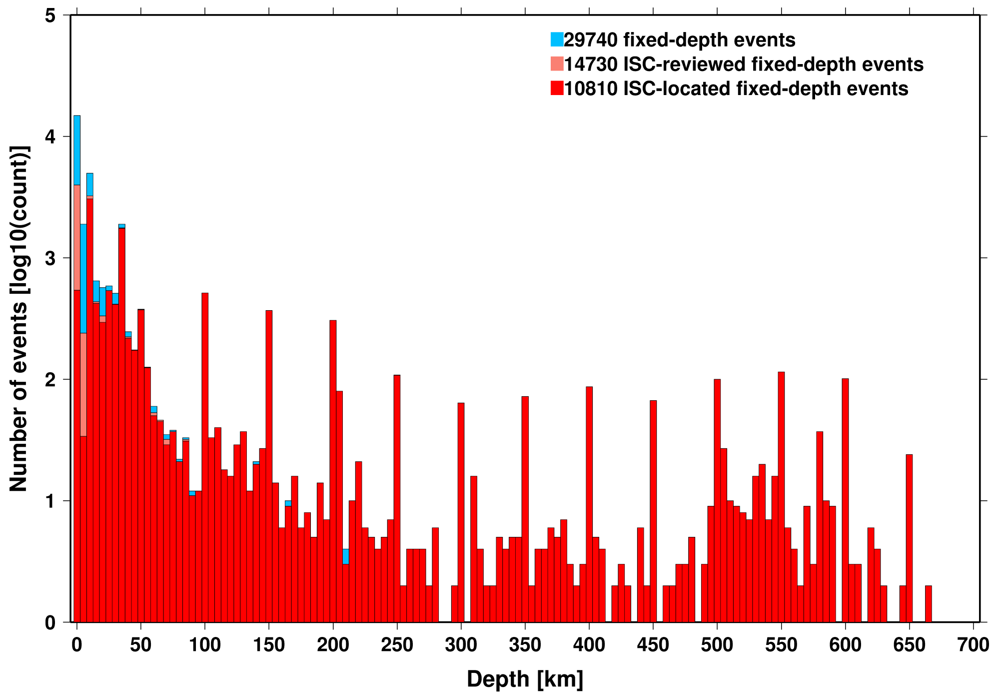

Figure 9.7: *Hypocentral depth distribution of events where the prime hypocentres are reported/located with a fixed-depth solution in the ISC Bulletin. The vertical scale is logarithmic.*

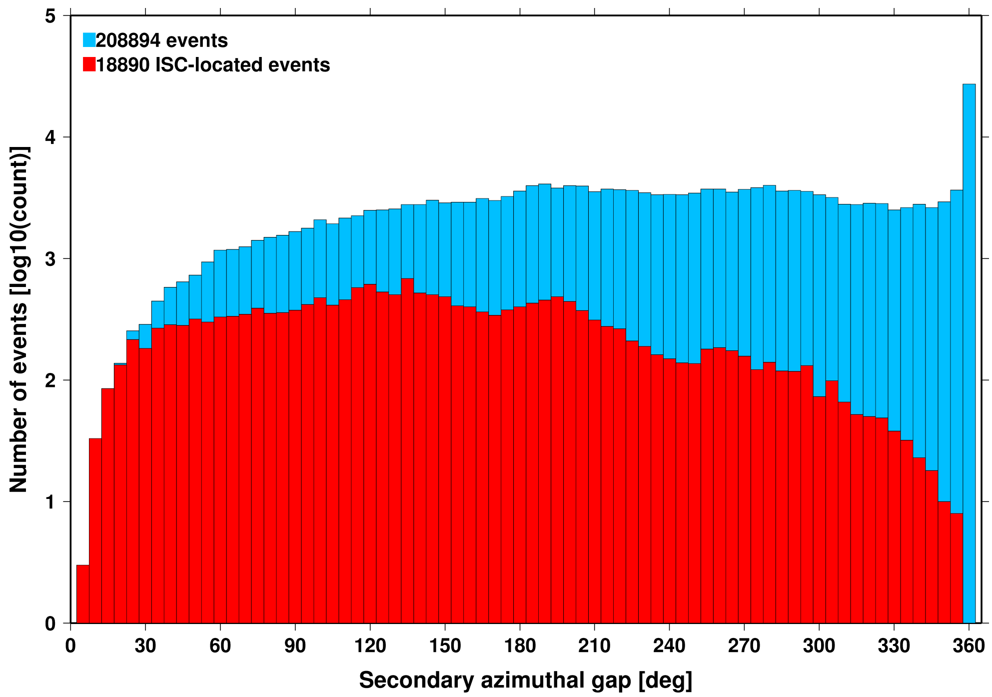

Figure 9.8: *Distribution of secondary azimuthal gap for events in the ISC Bulletin (blue) and those selected for ISC location (red). The vertical scale is logarithmic.*

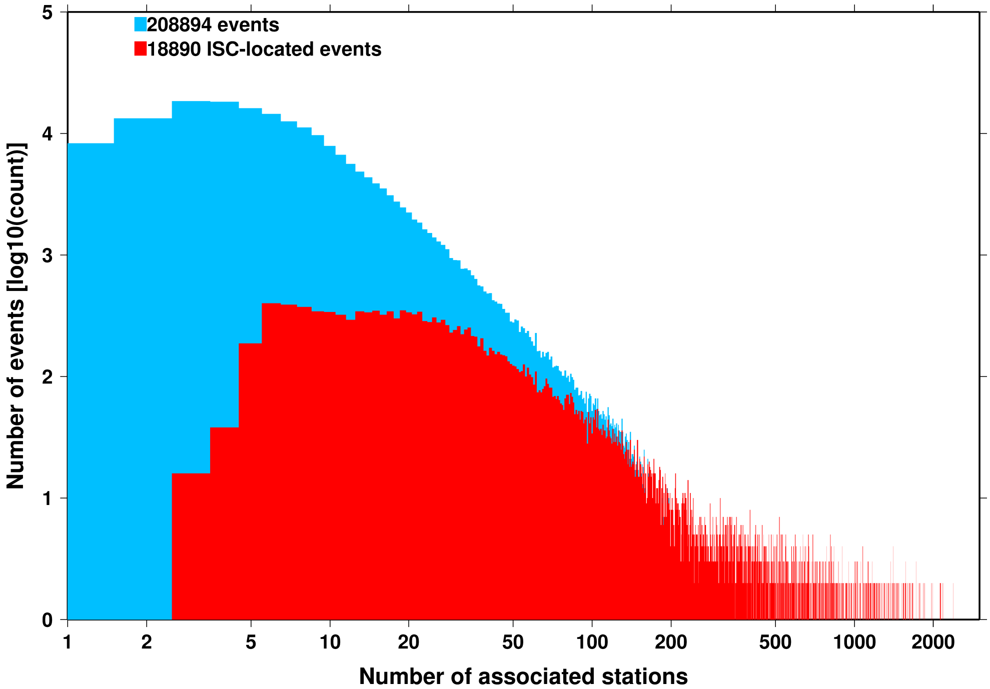

Figure 9.9: *Distribution of the number of associated stations for events in the ISC Bulletin (blue) and those selected for ISC location (red). The vertical scale is logarithmic.*

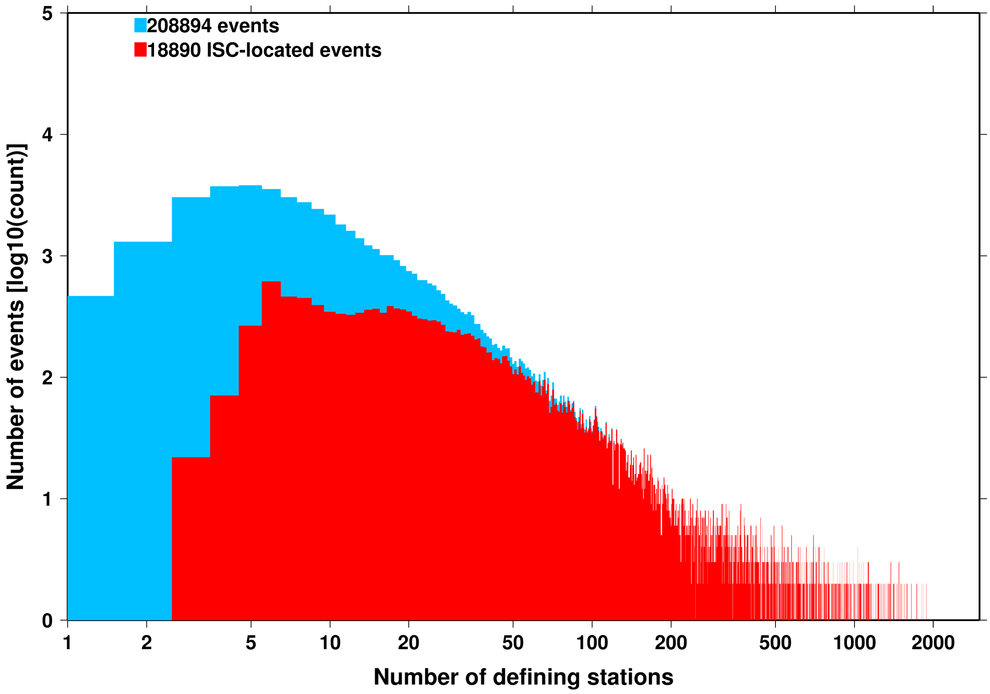

Figure 9.10: *Distribution of the number of defining stations for events in the ISC Bulletin (blue) and those selected for ISC location (red). The vertical scale is logarithmic.*

distribution of the area of the 90% confidence error ellipse for ISC-located events during the summary period. The distribution suffers from a long tail indicating a few poorly constrained event locations. Nevertheless, half of the events are characterised by an error ellipse with an area less than 206 km^2, 90% of the events have an error ellipse area less than 1320 km^2, and 95% of the events have an error ellipse area less than 2273 km^2.

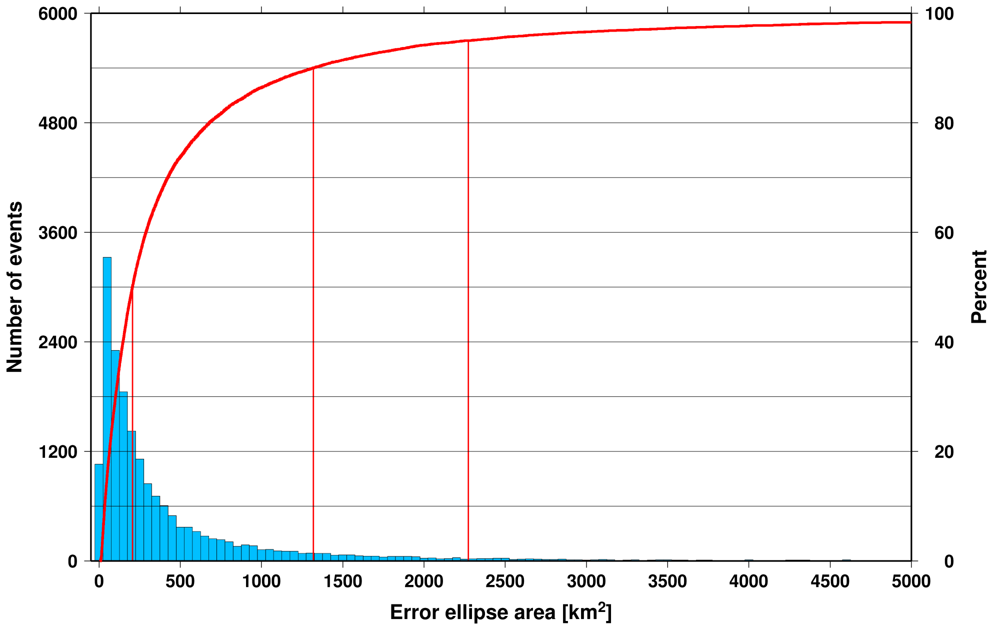

Figure 9.11: *Distribution of the area of the 90% confidence error ellipse of the ISC-located events. Vertical red lines indicate the 50th, 90th and 95th percentile values.*

Figure 9.12 shows one of the major characteristic features of the ISC location algorithm (Bondár and Storchak, 2011). Because the ISC locator accounts for correlated travel-time prediction errors due to unmodelled velocity heterogeneities along similar ray paths, the area of the 90% confidence error ellipse does not decrease indefinitely with increasing number of stations, but levels off once the information carried by the network geometry is exhausted, thus providing more realistic uncertainty estimates.

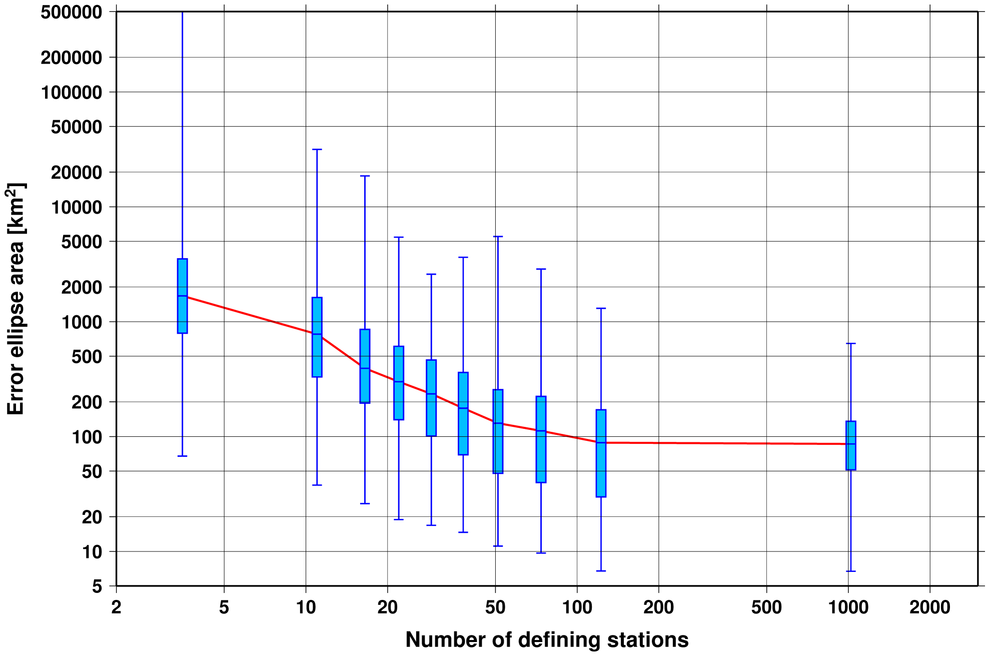

Figure 9.12: *Box-and-whisker plot of the area of the 90% confidence error ellipse of the ISC-located events as a function of the number of defining stations. Each box represents one-tenth-worth of the total number of data. The red line indicates the median 90% confidence error ellipse area.*

9.2 Seismic Phases and Travel-Time Residuals

The number of phases that are associated to events over the summary period in the ISC Bulletin is shown in Figure 9.13. Phase types and their total number in the ISC Bulletin is shown in the Appendix, Table 11.2. A summary of phase types is indicated in Figure 9.14.

In computing ISC locations, the current (for events since 2009) ISC location algorithm (*Bondár and Storchak*, 2011) uses all *ak135* phases where possible. Within the Bulletin, the phases that contribute to an ISC location are labelled as *time defining*. In this section, we summarise these time defining phases.

In Figure 9.15, the number of defining phases is shown in a histogram over the summary period. Each defining phase is listed in Table 9.1, which also provides a summary of the number of defining phases per event. A pie chart showing the proportion of defining phases is shown in Figure 9.16. Figure 9.17 shows travel times of seismic waves. The distribution of residuals for these defining phases is shown for the top five phases in Figures 9.18 through 9.22.

Table 9.1: *Numbers of 'time defining' phases (N) within the ISC Bulletin for 18890 ISC located events.*

Phase	Number of 'defining' phases	Number of events	Max per event	Median per event
P	916439	14178	2390	14
Pn	571851	17447	670	18
Sn	164228	14663	207	5
Pb	87277	7615	122	6
Pg	65387	6042	178	6
PKPdf	61095	4526	561	2
Sb	55232	7286	91	5
Sg	52631	5757	123	5
S	41016	3375	463	3
PKiKP	37201	3840	393	2
PKPbc	25234	3948	282	2
PKPab	18897	2958	355	2

Table 9.1: *(continued)*

Phase	Number of 'defining' phases	Number of events	Max per event	Median per event
PcP	11686	3363	103	2
Pdif	9604	865	462	2
pP	8551	1282	263	2
PP	8188	1285	156	2
SS	3801	1044	47	2
ScP	3568	1048	101	2
sP	2748	825	108	2
SKSac	2226	407	66	2
PKKPbc	2051	444	91	2
pwP	1429	447	37	2
pPKPdf	971	420	21	1
SKPbc	847	267	92	2
SnSn	835	470	12	1
ScS	748	334	15	1
PnPn	701	396	14	1
sS	636	314	47	1
SKiKP	584	258	20	1
PKKPab	546	219	25	1
PS	521	241	16	1
pPKPab	512	217	39	1
P'P'df	471	153	37	2
PKKPdf	465	196	30	1
sPKPdf	464	244	25	1
pPKPbc	458	273	17	1
sPKPab	328	90	135	1
SKSdf	317	217	8	1
SKPab	243	107	26	1
sPKPbc	225	141	23	1
SP	186	74	31	1
PcS	181	140	5	1
SKKSac	176	103	24	1
PKSdf	130	111	4	1
PnS	120	96	4	1
SKKSdf	106	96	2	1
SKKPbc	102	28	19	2
Sdif	100	53	9	1
pPdif	90	30	29	1
SKPdf	83	51	12	1
sPdif	57	20	20	1
PbPb	57	39	4	1
pS	54	47	3	1
pPKiKP	33	18	8	1
SKKPab	28	8	15	1
SbSb	25	20	4	1
PgPg	14	13	2	1
SPn	14	14	1	1
P'P'ab	13	7	7	1
P'P'bc	11	8	2	1
SKKPdf	10	7	4	1
sPKiKP	5	4	2	1
PKSbc	3	3	1	1
pPn	3	1	3	3
SgSg	3	3	1	1
S'S'ac	2	2	1	1
pSKSac	1	1	1	1
sSdif	1	1	1	1
sSKSdf	1	1	1	1
PKSab	1	1	1	1
sSn	1	1	1	1

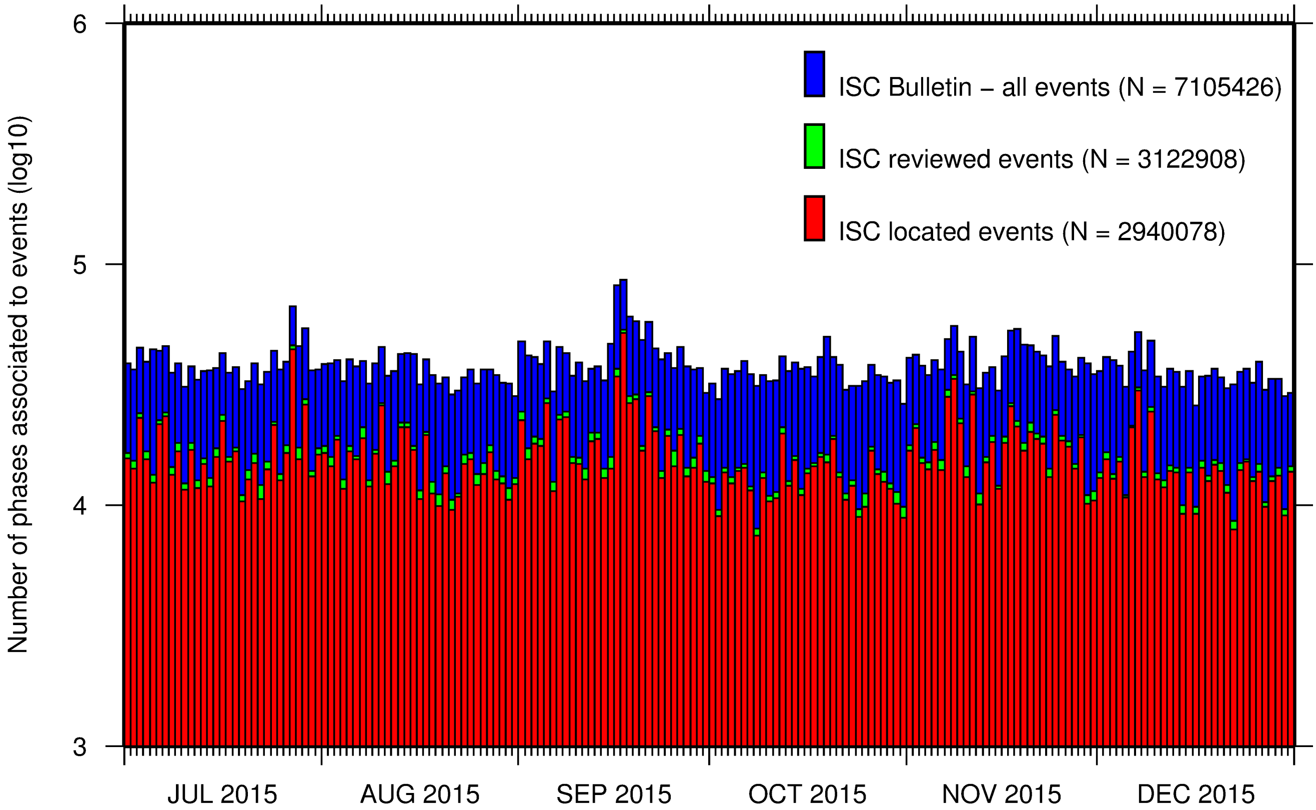

Figure 9.13: *Histogram showing the number of phases (N) that the ISC has associated to events within the ISC Bulletin for the current summary period.*

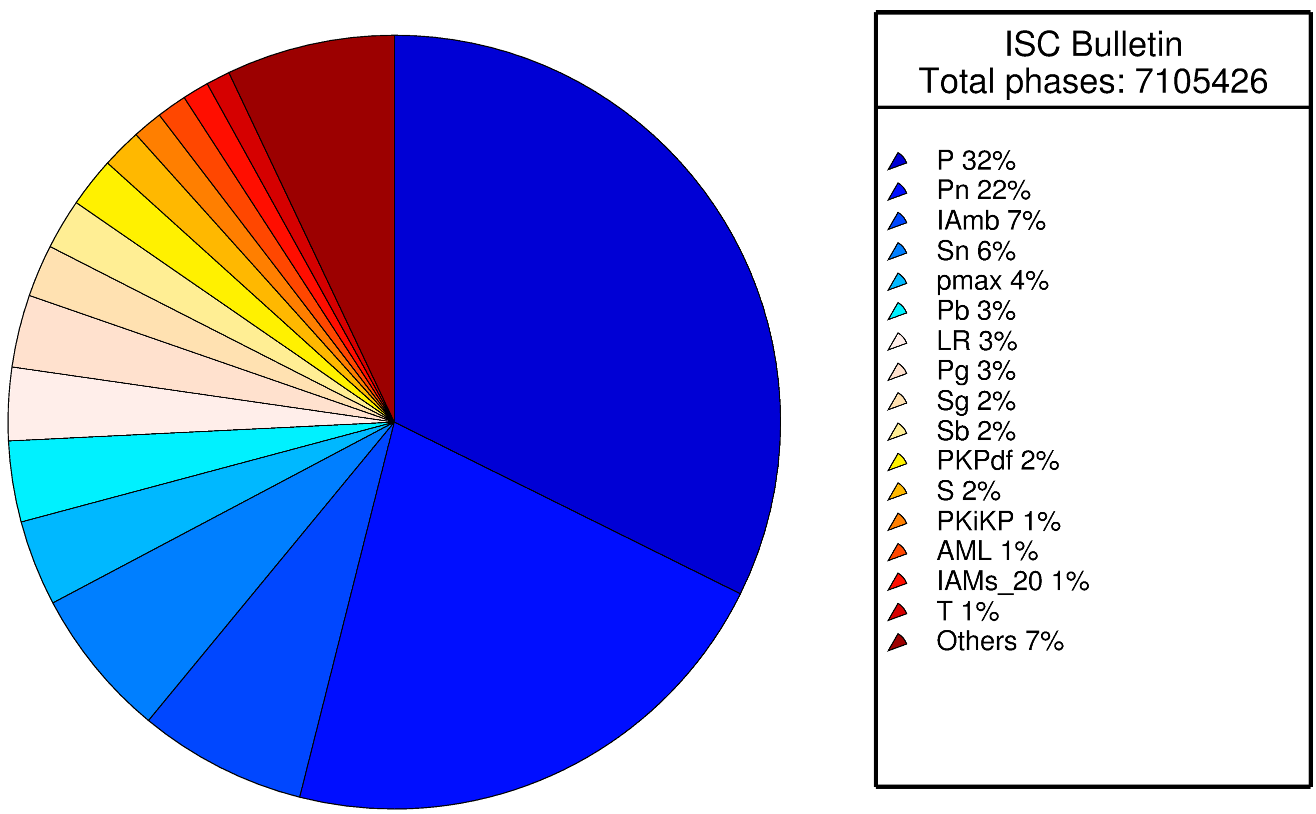

Figure 9.14: *Pie chart showing the fraction of various phase types in the ISC Bulletin for this summary period.*

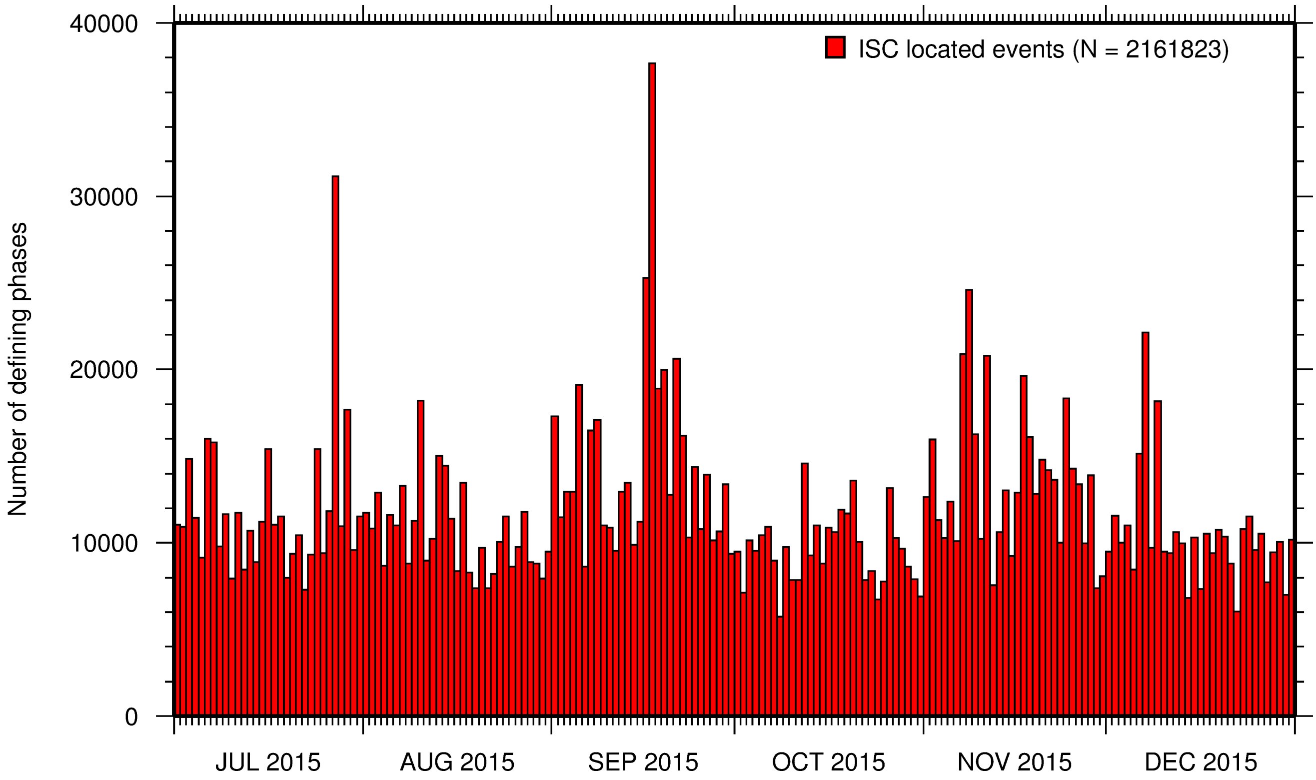

Figure 9.15: *Histogram showing the number of defining phases in the ISC Bulletin, for events located by the ISC.*

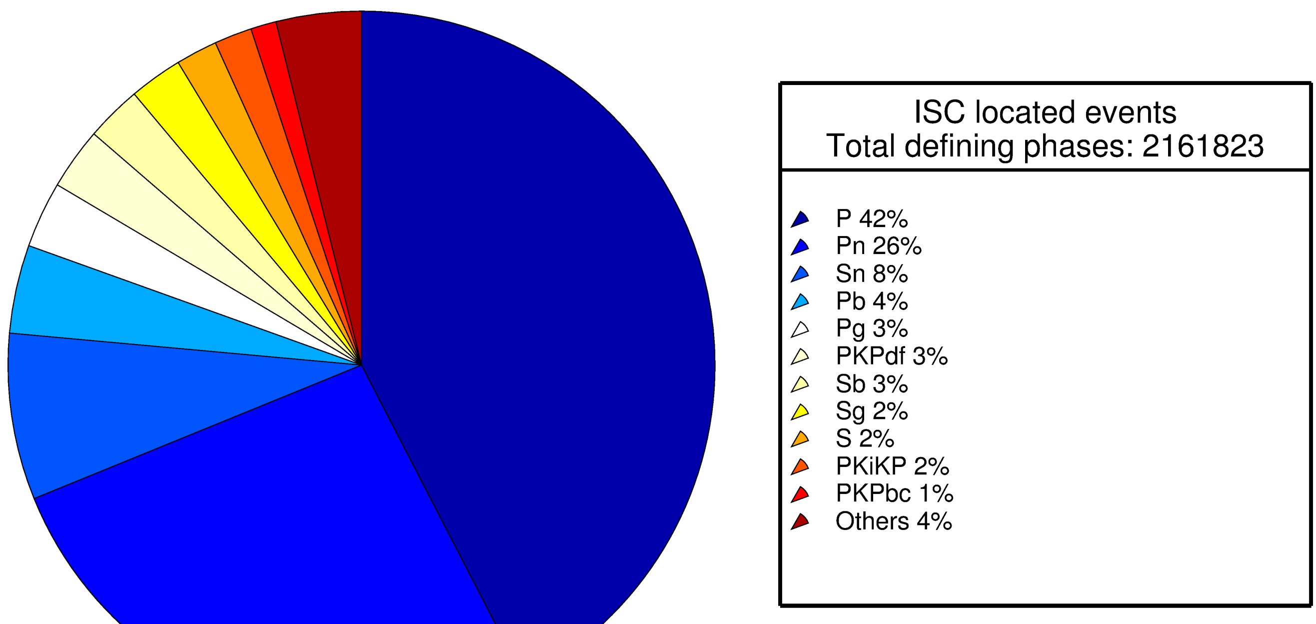

Figure 9.16: *Pie chart showing the defining phases in the ISC Bulletin, for events located by the ISC. A complete list of defining phases is shown in Table 9.1.*

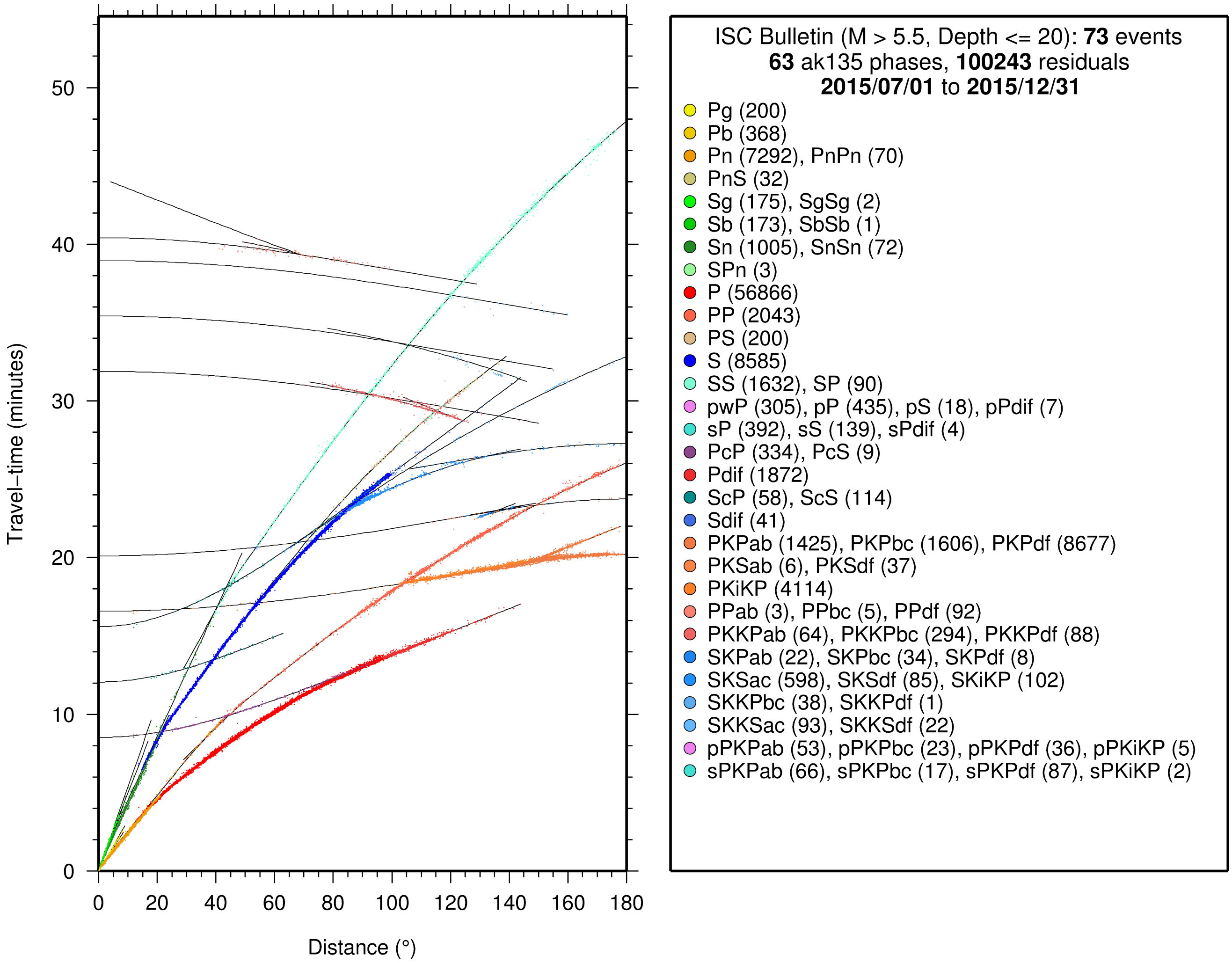

Figure 9.17: *Distribution of travel-time observations in the ISC Bulletin for events with M > 5.5 and depth less than 20 km. The travel-time observations are shown relative to a 0 km source and compared with the theoretical ak135 travel-time curves (solid lines). The legend lists the number of each phase plotted.*

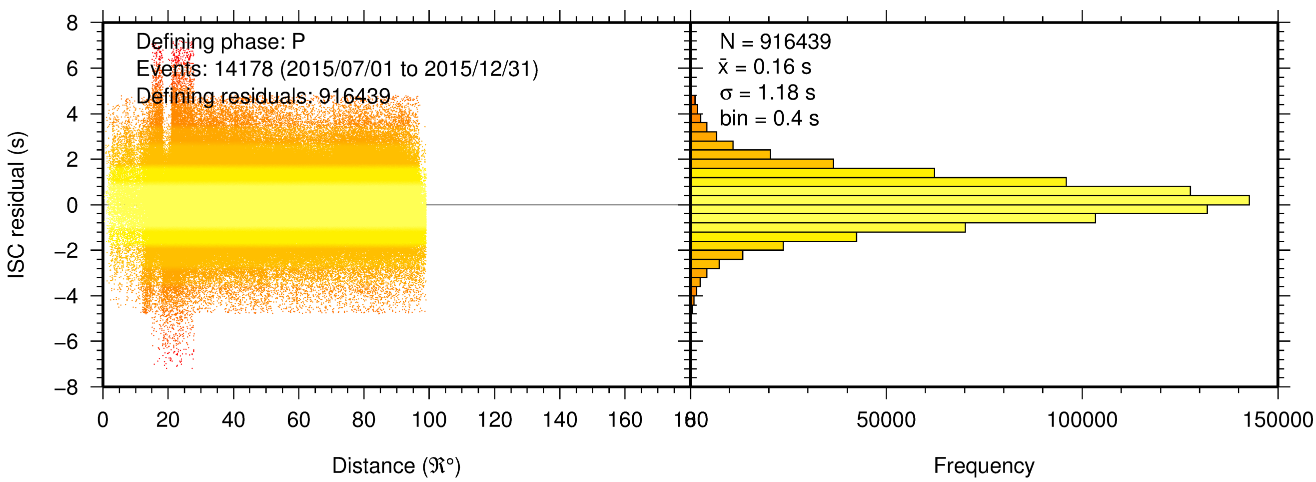

Figure 9.18: *Distribution of travel-time residuals for the defining P phases used in the computation of ISC located events in the Bulletin.*

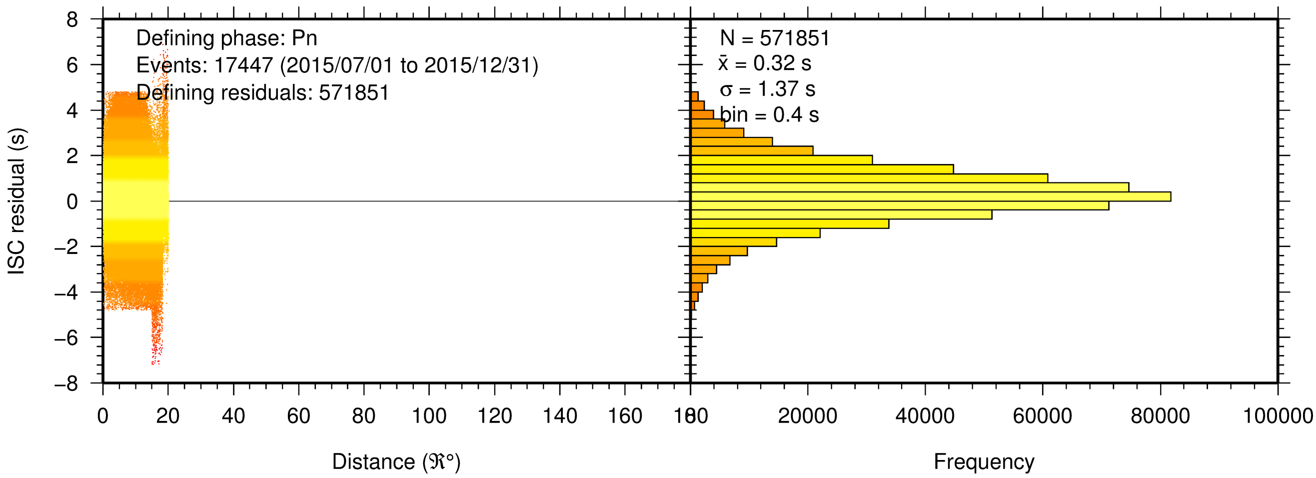

Figure 9.19: *Distribution of travel-time residuals for the defining Pn phases used in the computation of ISC located events in the Bulletin.*

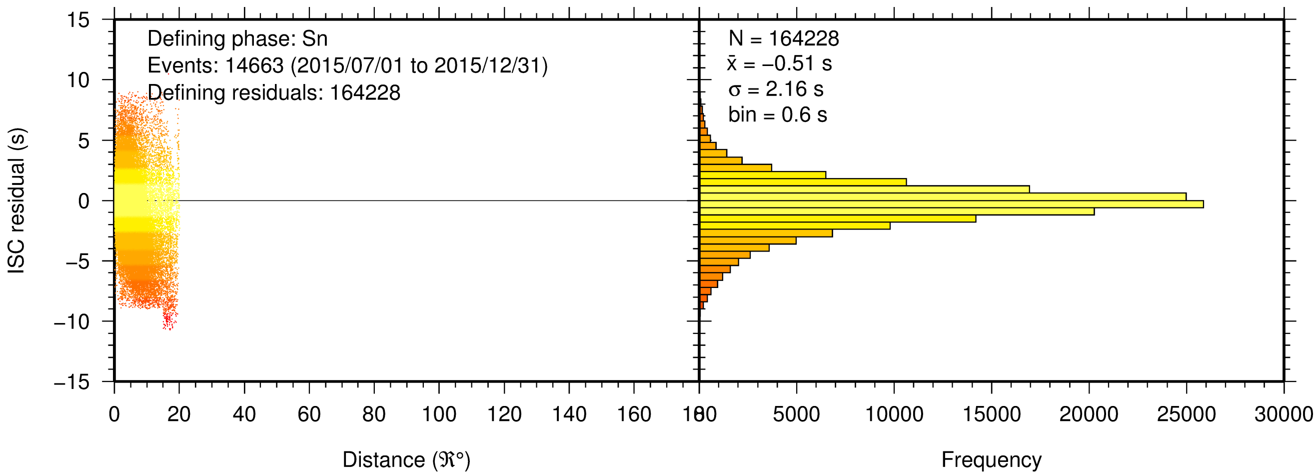

Figure 9.20: *Distribution of travel-time residuals for the defining Sn phases used in the computation of ISC located events in the Bulletin.*

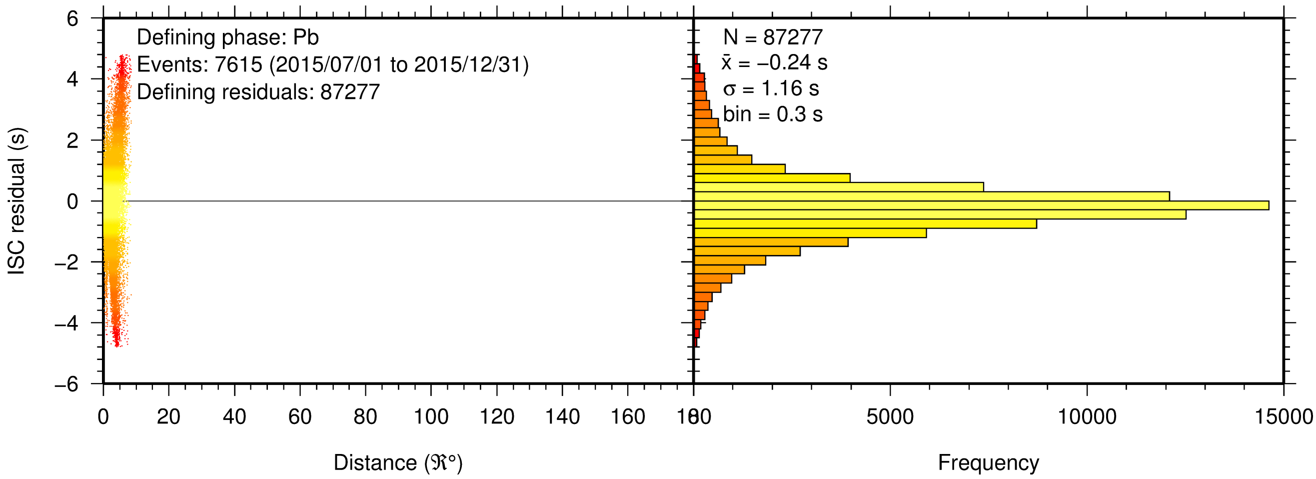

Figure 9.21: *Distribution of travel-time residuals for the defining Pb phases used in the computation of ISC located events in the Bulletin.*

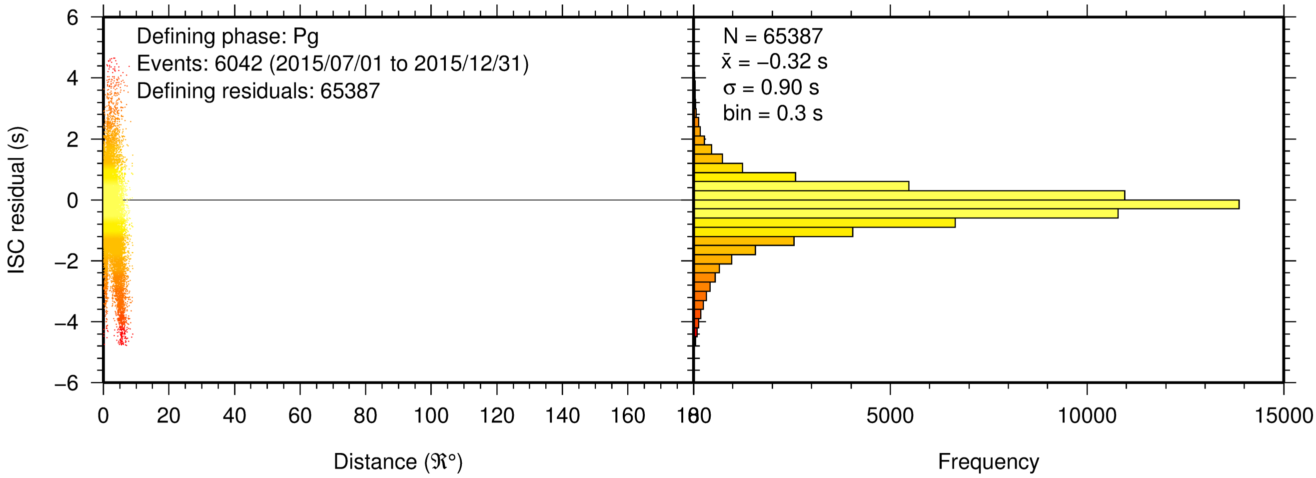

Figure 9.22: *Distribution of travel-time residuals for the defining Pg phases used in the computation of ISC located events in the Bulletin.*

9.3 Seismic Wave Amplitudes and Periods

The ISC Bulletin contains a variety of seismic wave amplitudes and periods measured by reporting agencies. For this Bulletin Summary, the total of collected amplitudes and periods is 545,785 (see Section 8.3). For the determination of the ISC magnitudes MS and mb, only a fraction of such data can be used. Indeed, the ISC network magnitudes are computed only for ISC located events. Here we recall the main features of the ISC procedure for MS and mb computation (see detailed description in Section 11.1.3 of issue I of the 2015 Bulletin Summary). For each amplitude-period pair in a reading the ISC algorithm computes the magnitude (a reading can include several amplitude-period measurements) and the reading magnitude is assigned to the maximum A/T in the reading. If more than one reading magnitude is available for a station, the station magnitude is the median of the reading magnitudes. The network magnitude is computed then as the 20% alpha-trimmed median of the station magnitudes (at least three required). MS is computed for shallow earthquakes (depth $\leq$ 60 km) only and using amplitudes and periods on all three components (when available) if the period is within 10-60 s and the epicentral distance is between 20° and 160°. mb is computed also for deep earthquakes (depth down to 700 km) but only with amplitudes on the vertical component measured at periods $\leq$ 3 s in the distance range 21°-100°.

Table 9.2 is a summary of the amplitude and period data that contributed to the computation of station and ISC MS and mb network magnitudes for this Bulletin Summary.

Table 9.2: *Summary of the amplitude-period data used by the ISC Locator to compute MS and mb.*

	MS	mb
Number of amplitude-period data	104799	440986
Number of readings	91129	436576
Percentage of readings in the ISC located events with qualifying data for magnitude computation	11.4	45.4
Number of station magnitudes	87542	392040
Number of network magnitudes	3191	12246

A small percentage of the readings with qualifying data for MS and mb calculation have more than one amplitude-period pair. Notably, only 11% of the readings for the ISC located (shallow) events included qualifying data for MS computation, whereas for mb the percentage is much higher at 45%. This is due to the seismological practice of reporting agencies. Agencies contributing systematic reports of amplitude and period data are listed in Appendix Table 11.3. Obviously the ISC Bulletin would benefit if more agencies included surface wave amplitude-period data in their reports.

Figure 9.23 shows the distribution of the number of station magnitudes versus distance. For mb there is a significant increase in the distance range 70°-90°, whereas for MS most of the contributing stations are below 100°. The increase in number of station magnitude between 70°-90° for mb is partly due to the very dense distribution of seismic stations in North America and Europe with respect to earthquake occurring in various subduction zones around the Pacific Ocean.

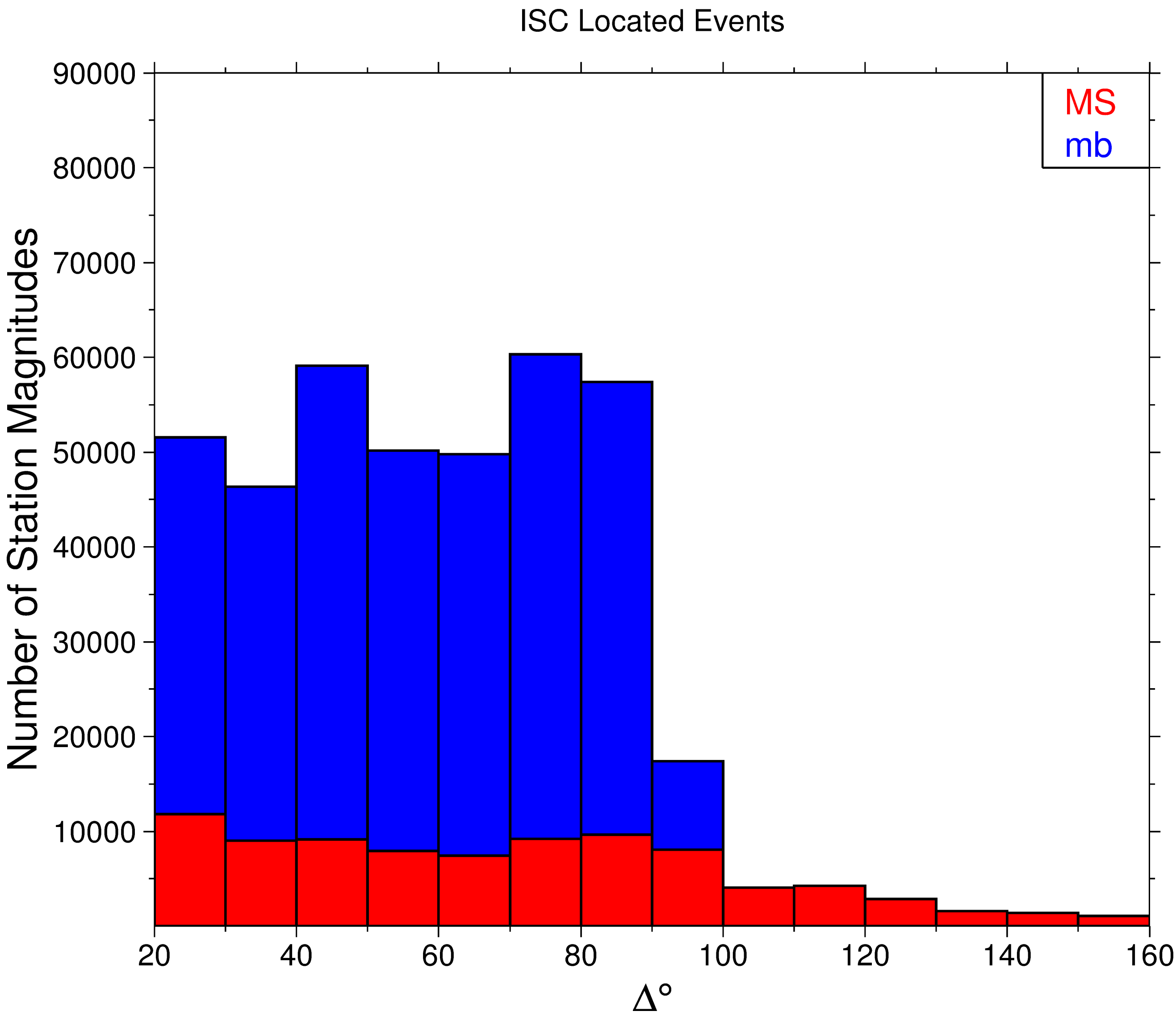

Figure 9.23: Distribution of the number of station magnitudes computed by the ISC Locator for mb (blue) and MS (red) versus distance.

Finally, Figure 9.24 shows the distribution of network MS and mb as well as the median number of stations for magnitude bins of 0.2. Clearly with increasing magnitude the number of events is smaller but with a general tendency of having more stations contributing to the network magnitude.

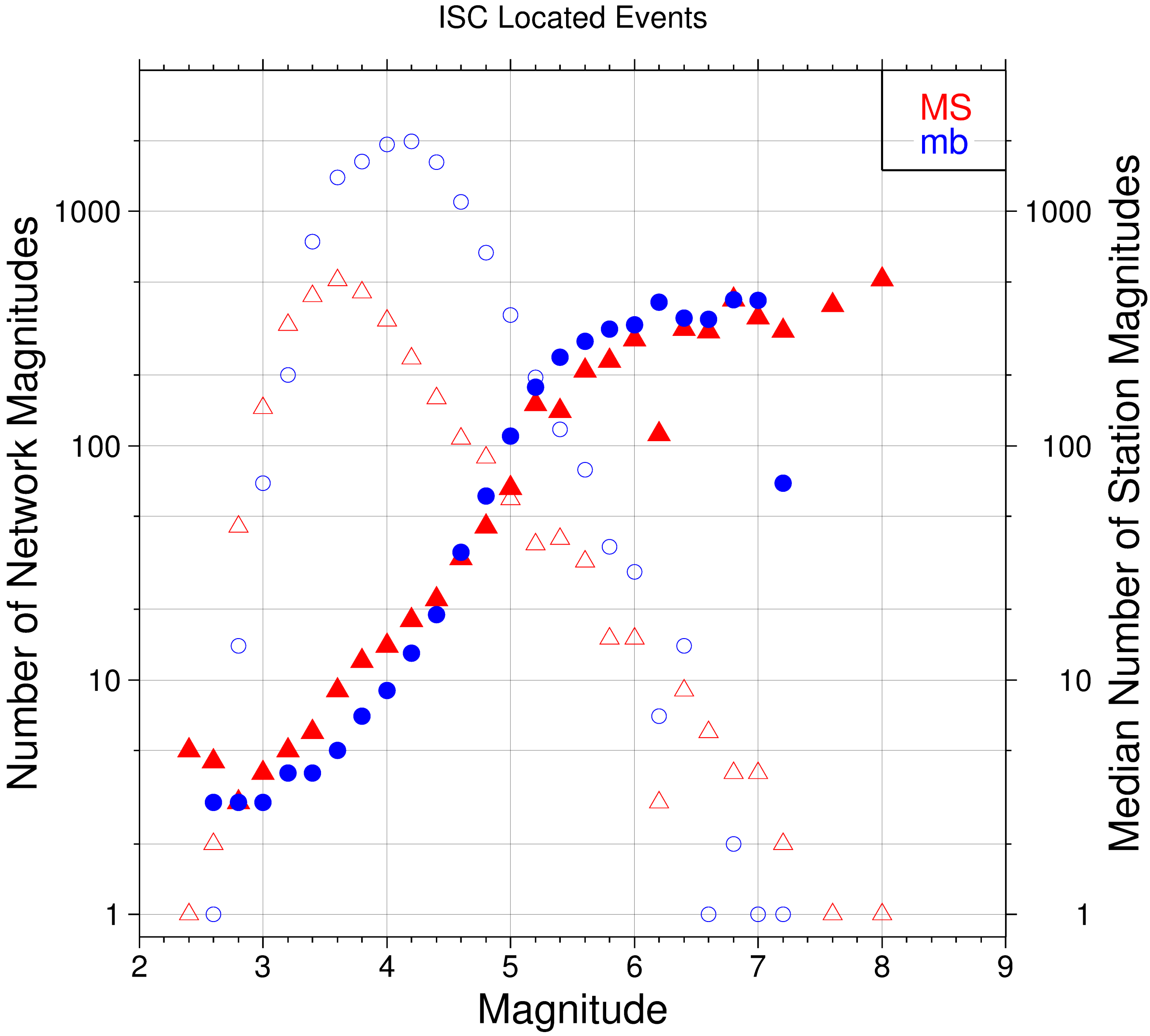

Figure 9.24: *Number of network magnitudes (open symbols) and median number of stations magnitudes (filled symbols). Blue circles refer to mb and red triangles to MS. The width of the magnitude interval δM is 0.2, and each symbol includes data with magnitude in $M \pm \delta M/2$.*

9.4 Completeness of the ISC Bulletin

The completeness of the ISC Bulletin can be expressed as a magnitude value, above which we expect the Bulletin to contain 100% of events. This magnitude of completeness, M_C can be measured as the point where the seismicity no longer follows the Gutenberg-Richter relationship. We compute an estimate of M_C using the maximum curvature technique of *Woessner and Wiemer* (2005).

The completeness of the ISC Bulletin for this summary period is shown in Figure 9.25. A history of completeness for the ISC Bulletin is shown in Figure 9.26. The step change in 1996 corresponds with the inclusion of the Prototype IDC (EIDC) Bulletin, followed by the Reviewed Event Bulletin (REB) of the IDC.

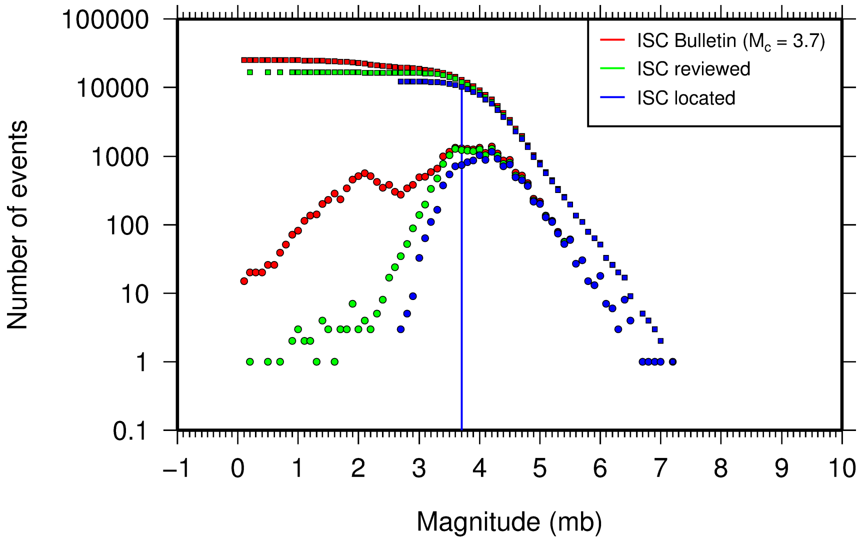

Figure 9.25: *Frequency and cumulative frequency magnitude distribution for all events in the ISC Bulletin, ISC reviewed events and events located by the ISC. The magnitude of completeness (M_C) is shown for the ISC Bulletin. Note: only events with values of mb are represented in the figure.*

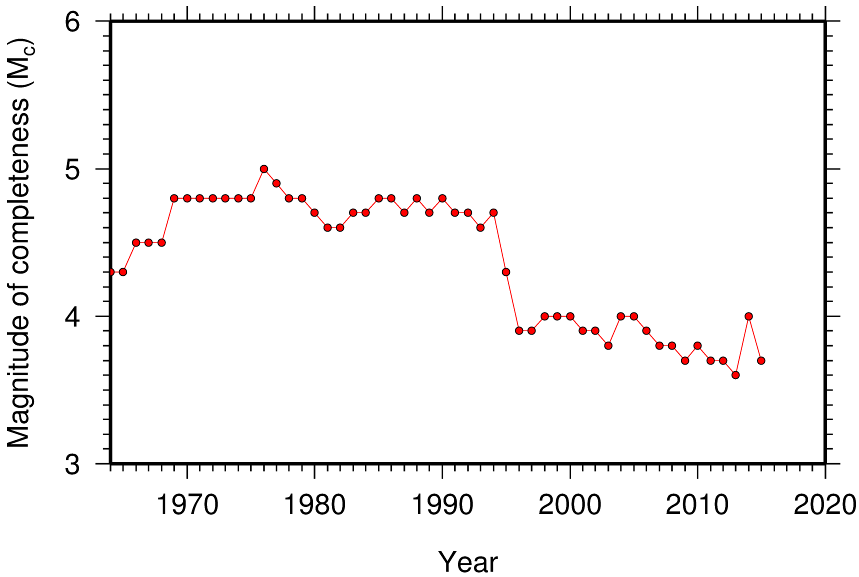

Figure 9.26: *Variation of magnitude of completeness (M_C) for each year in the ISC Bulletin. Note: M_C is calculated only using those events with values of mb.*

9.5 Magnitude Comparisons

The ISC Bulletin publishes network magnitudes reported by multiple agencies to the ISC. For events that have been located by the ISC, where enough amplitude data has been collected, the MS and mb magnitudes are calculated by the ISC (MS is computed only for depths $\leq$ 60 km). In this section, ISC magnitudes and some other reported magnitudes in the ISC Bulletin are compared.

The comparison between MS and mb computed by the ISC locator for events in this summary period is shown in Figure 9.27, where the large number of data pairs allows a colour coding of the data density.

The scatter in the data reflects the fundamental differences between these magnitude scales.

Similar plots are shown in Figure 9.28 and 9.29, respectively, for comparisons of ISC mb and ISC MS with M_W from the GCMT catalogue. Since M_W is not often available below magnitude 5, these distributions are mostly for larger, global events. Not surprisingly, the scatter between mb and M_W is larger than the scatter between MS and M_W. Also, the saturation effect of mb is clearly visible for earthquakes with $M_W > 6.5$. In contrast, MS scales well with $M_W > 6$, whereas for smaller magnitudes MS appears to be systematically smaller than M_W.

In Figure 9.30 ISC values of mb are compared with all reported values of mb, values of mb reported by NEIC and values of mb reported by IDC. Similarly in Figure 9.31, ISC values of MS are compared with all reported values of MS, values of MS reported by NEIC and values of MS reported by IDC. There is a large scatter between the ISC magnitudes and the mb and MS reported by all other agencies.

The scatter decreases both for mb and MS when ISC magnitudes are compared just with NEIC and IDC magnitudes. This is not surprising as the latter two agencies provide most of the amplitudes and periods used by the ISC locator to compute MS and mb. However, ISC mb appears to be smaller than NEIC mb for $mb < 4$ and larger than IDC mb for $mb > 4$. Since NEIC does not include IDC amplitudes, it seems these features originate from observations at the high-gain, low-noise sites reported by the IDC. For the MS comparisons between ISC and NEIC a similar but smaller effect is observed for $MS < 4.5$, whereas a good scaling is generally observed for the MS comparisons between ISC and IDC.

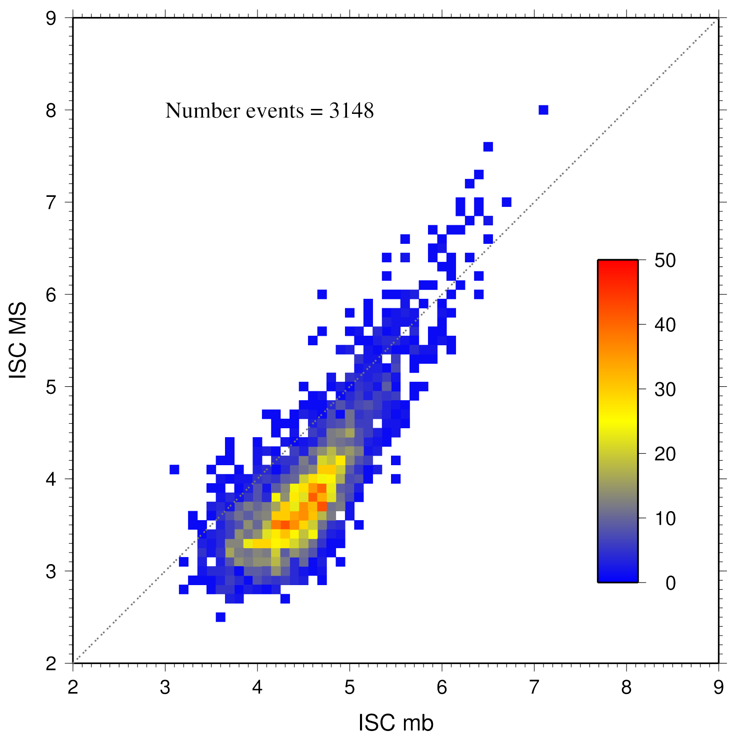

Figure 9.27: *Comparison of ISC values of MS with mb for common event pairs.*

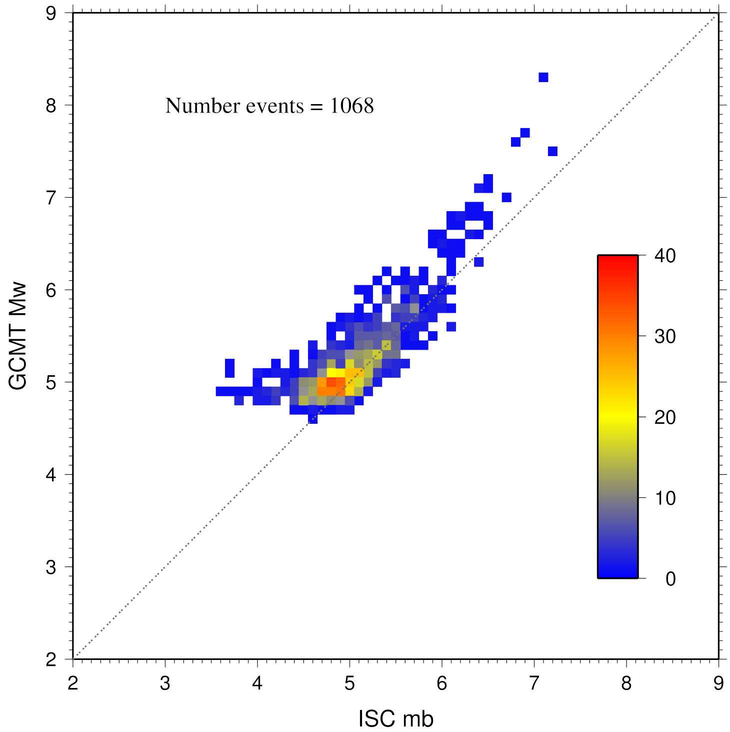

Figure 9.28: *Comparison of ISC values of mb with GCMT M_W for common event pairs.*

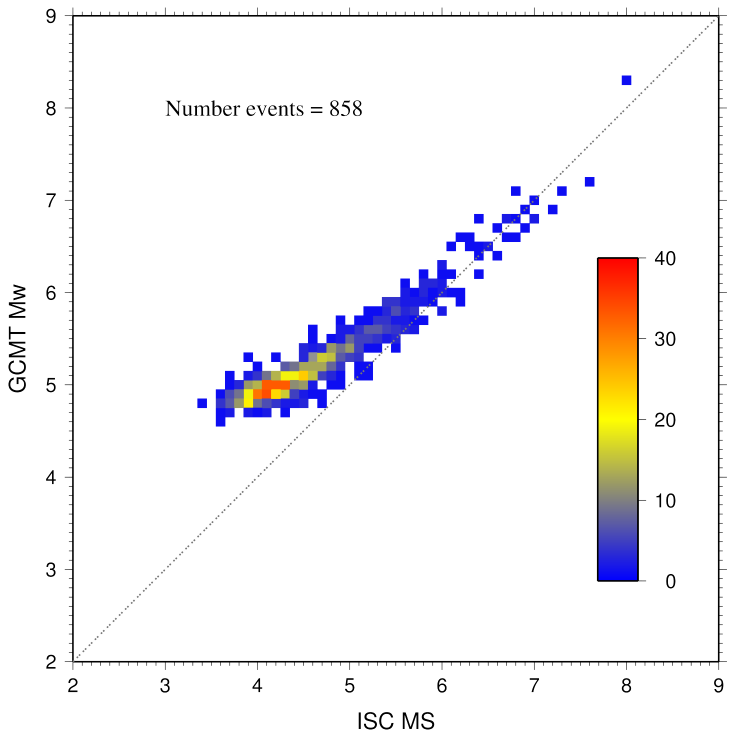

Figure 9.29: *Comparison of ISC values of MS with GCMT M_W for common event pairs.*

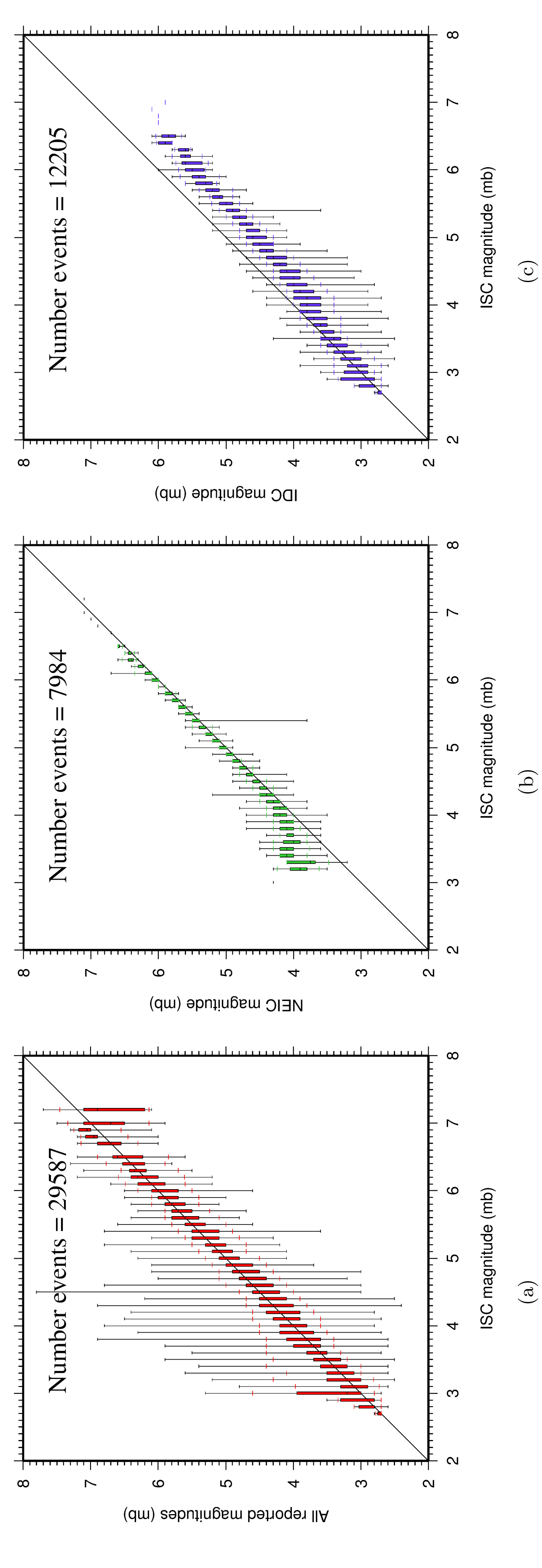

Figure 9.30: *Comparison of ISC magnitude data (mb) with additional agency magnitudes (mb). The statistical summary is shown in box-and-whisker plots where the 10th and 90th percentiles are shown in addition to the max and min values. (a): All reported magnitudes; (b): NEIC magnitudes; (c): IDC magnitudes.*

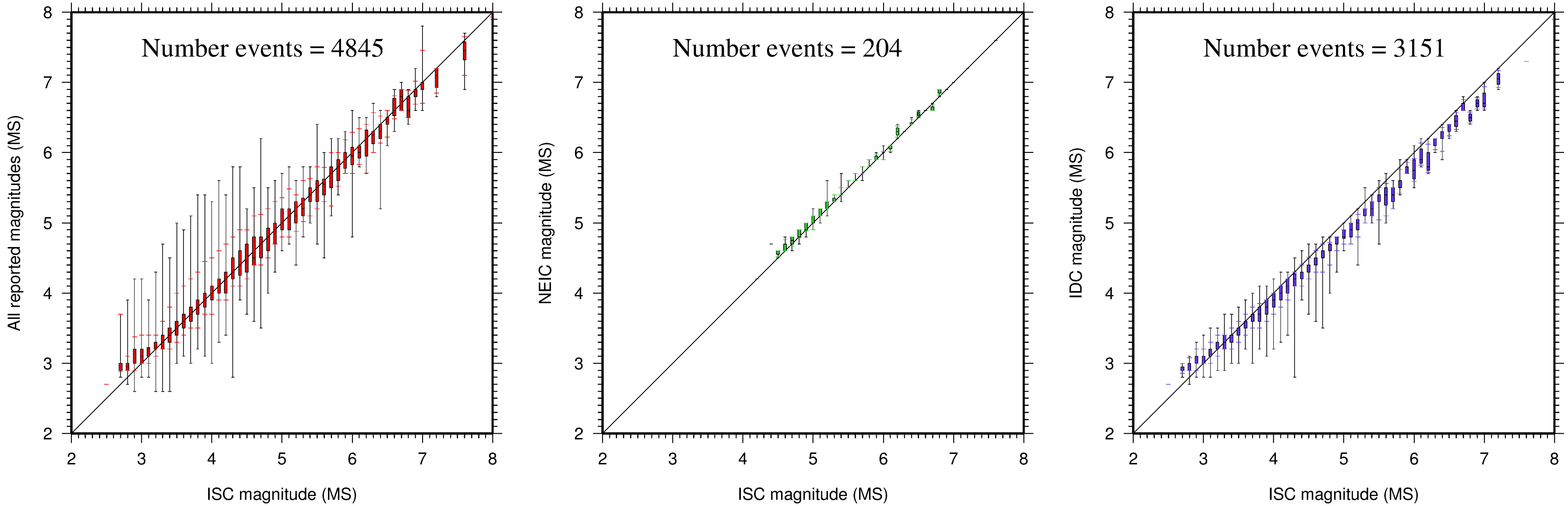

(a) (b) (c)

Figure 9.31: *Comparison of ISC magnitude data (MS) with additional agency magnitudes (MS). The statistical summary is shown in the box-and-whisker plots where the 10th and 90th percentiles are shown in addition to the max and min values. (a): All magnitudes reported; (b): NEIC magnitudes; (c): IDC magnitudes.*

10

The Leading Data Contributors

For the current six-month period, 150 agencies reported related bulletin data. Although we are grateful for every report, we nevertheless would like to acknowledge those agencies that made the most useful or distinct contributions to the contents of the ISC Bulletin. Here we note those agencies that:

- provided a comparatively large volume of parametric data (see Section 10.1),
- reported data that helped quite considerably to improve the quality of the ISC locations or magnitude determinations (see Section 10.2),
- helped the ISC by consistently reporting data in one of the standard recognised formats and in-line with the ISC data collection schedule (see Section 10.3).

We do not aim to discourage those numerous small networks who provide comparatively smaller yet still most essential volumes of regional data regularly, consistently and accurately. Without these reports the ISC Bulletin would not be as comprehensive and complete as it is today.

10.1 The Largest Data Contributors

We acknowledge the contribution of IDC, NEIC, MOS, BJI, BKK, AWI, CLL and a few others (Figure 10.1) that reported the majority of moderate to large events recorded at teleseismic distances. The contributions of NEIC, IDC, MEX, GUC and several others are also acknowledged with respect to smaller seismic events. The contributions of JMA, NEIC, IDC, TAP, ATH, ISK, DDA and a number of others are also acknowledged with respect to small seismic events. Note that the NEIC bulletin accumulates a contribution of all regional networks in the USA. Several agencies monitoring highly seismic regions routinely report large volumes of small to moderate magnitude events, such as those in Japan, Chinese Taipei, Turkey, Italy, Greece, New Zealand, Mexico and Columbia. Contributions of small magnitude events by agencies in regions of low seismicity, such as Finland are also gratefully received.

We also would like to acknowledge contributions of those agencies that report a large portion of arrival time and amplitude data (Figure 10.2). For small magnitude events, these are local agencies in charge of monitoring local and regional seismicity. For moderate to large events, contributions of IDC, USArray, NEIC, MOS are especially acknowledged. Notably, three agencies (IDC, NEIC and MOS) together reported over 75% of all amplitude measurements made for teleseismically recorded events. We hope that other agencies would also be able to update their monitoring routines in the future to include the amplitude reports for teleseismic events compliant with the IASPEI standards.

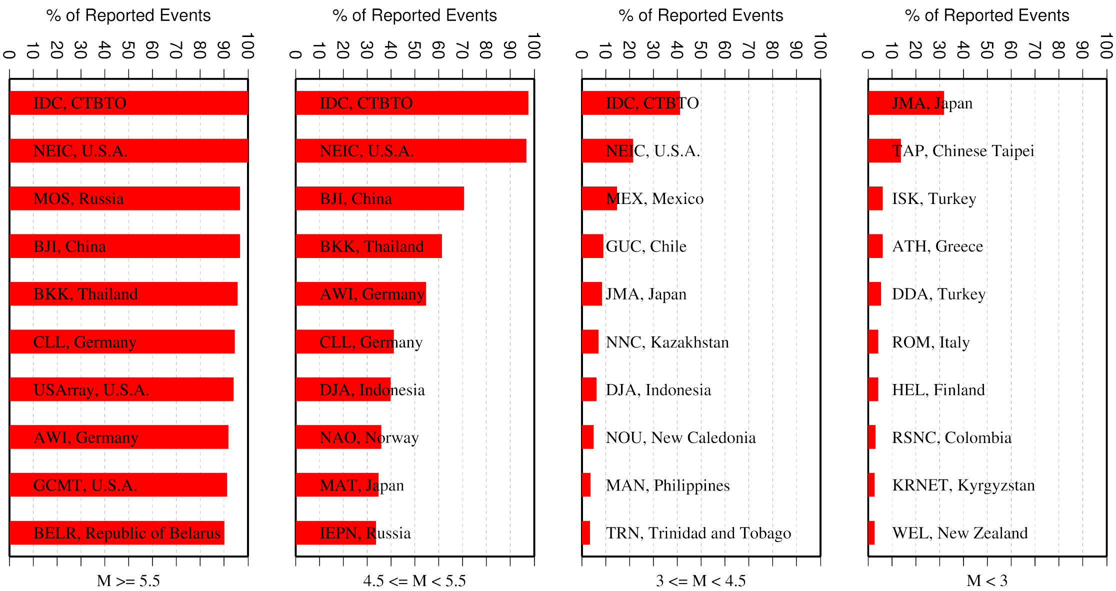

Figure 10.1: *Frequency of events in the ISC Bulletin for which an agency reported at least one item of data: a moment tensor, a hypocentre, a station arrival time or an amplitude. The top ten agencies are shown for four magnitude intervals.*

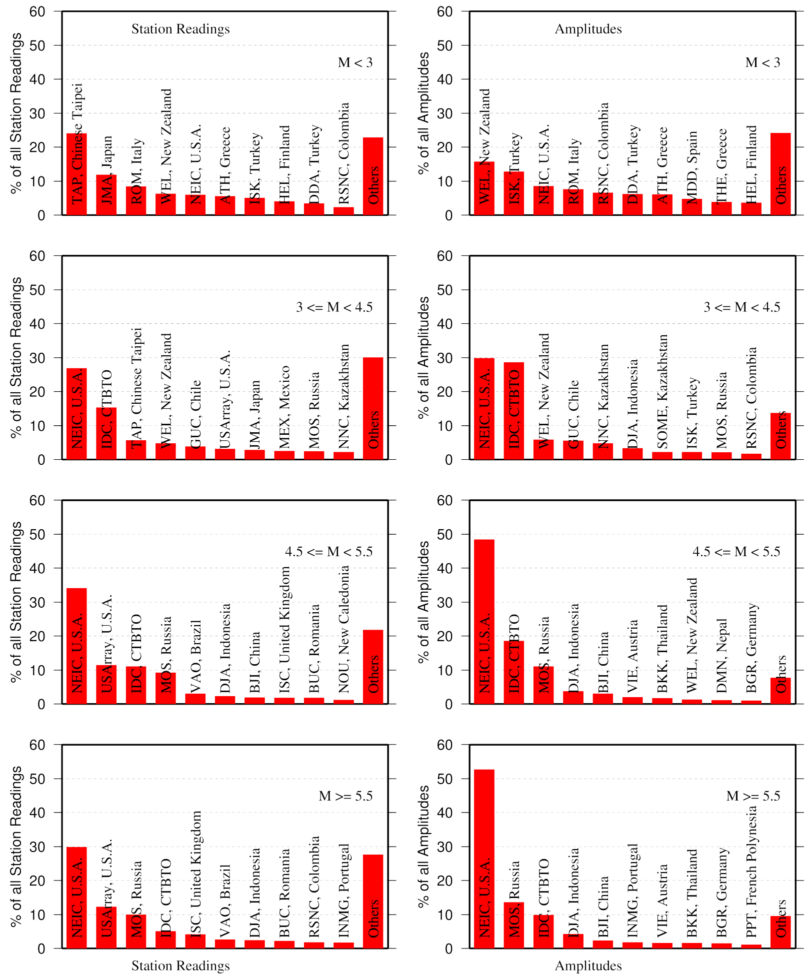

Figure 10.2: *Contributions of station arrival time readings (left) and amplitudes (right) of agencies to the ISC Bulletin. Top ten agencies are shown for four magnitude intervals.*

10.2 Contributors Reporting the Most Valuable Parameters

One of the main ISC duties is to re-calculate hypocentre estimates for those seismic events where a collective wealth of all station reports received from all agencies is likely to improve either the event location or depth compared to the hypocentre solution from each single agency. For areas with a sparse local seismic network or an unfavourable station configuration, readings made by other networks at teleseismic distances are very important. All events near mid-oceanic ridges as well as those in the majority of subduction zones around the world fall into this category. Hence we greatly appreciate the effort made by many agencies that report data for remote earthquakes (Figure 10.3). For some agencies, such as the IDC and the NEIC, it is part of their mission. For instance, the IDC reports almost every seismic event that is large enough to be recorded at teleseismic distance (20 degrees and beyond). This is largely because the International Monitoring System of primary arrays and broadband instruments is distributed at quiet sites around the world in order to be able to detect possible violations of the Comprehensive Nuclear-Test-Ban Treaty. The NEIC reported over 47% of those events as their mission requires them to report events above magnitude 4.5 outside the United States of America. For other agencies reporting distant events it is an extra effort that they undertake to notify their governments and relief agencies as well as to help the ISC and academic research in general. Hence these agencies usually report on the larger magnitude events. BJI, AWI, NAO, CLL, MOS, PRU, IEPN and PPT each reported individual station arrivals for several percent of all relevant events. We encourage other agencies to report distant events to us.

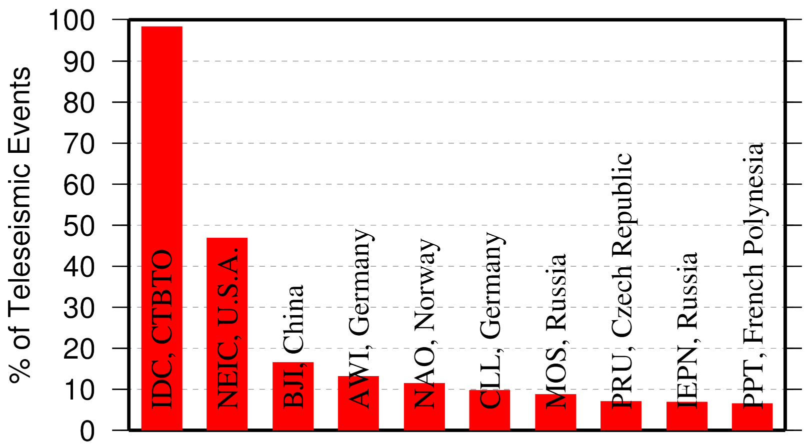

Figure 10.3: *Top ten agencies that reported teleseismic phase arrivals for a large portion of ISC events.*

In addition to the first arriving phase we encourage reporters to contribute observations of secondary seismic phases that help constrain the event location and depth: S, Sn, Sg and pP, sP, PcP (Figure 10.4). We expect though that these observations are actually made from waveforms, rather than just predicted by standard velocity models and modern software programs. It is especially important that these arrivals are manually reviewed by an operator (as we know takes place at the IDC and NEIC), as opposed to some lesser attempts to provide automatic phase readings that are later rejected by the ISC due to a generally poor quality of unreviewed picking.

Another important long-term task that the ISC performs is to compute the most definitive values of MS and mb network magnitudes that are considered reliable due to removal of outliers and consequent averaging (using alpha-trimmed median) across the largest network of stations, generally not feasible

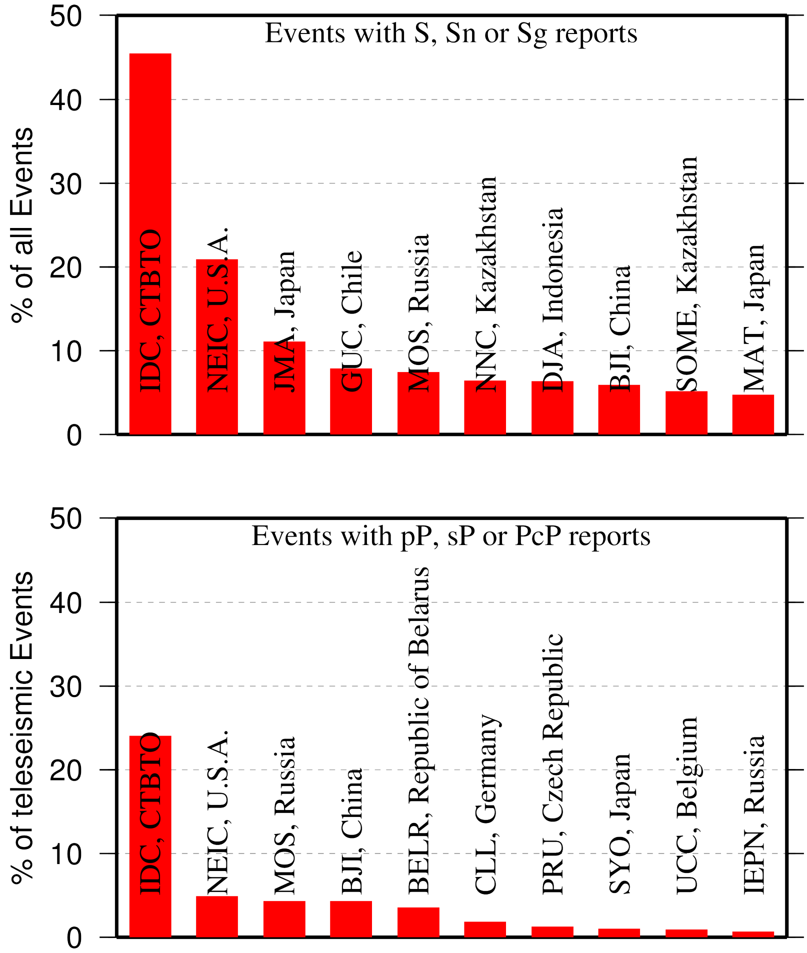

Figure 10.4: *Top ten agencies that reported secondary phases important for an accurate epicentre location (top) and focal depth determination (bottom).*

for a single agency. Despite concern over the bias at the lower end of mb introduced by the body wave amplitude data from the IDC, other agencies are also known to bias the results. This topic is further discussed in Section 9.5.

Notably, the IDC reports almost 100% of all events for which MS and mb are estimated. This is due to the standard routine that requires determination of body and surface wave magnitudes useful for discrimination purposes. NEIC, BJI, MOS, PPT, NAO, BELR and a few other agencies (Figure 10.5) are also responsible for the majority of the amplitude and period reports that contribute towards the ISC magnitudes.

Since the ISC does not routinely process waveforms, we rely on other agencies to report moment magnitudes as well as moment tensor determinations (Figure 10.6).

Among other event parameters the ISC Bulletin also contains information on event type. We cannot independently verify the type of each event in the Bulletin and thus rely on other agencies to report the event type to us. Practices of reporting non-tectonic events vary greatly from country to country. Many agencies do not include anthropogenic events in their reports. Suppression of such events from reports to the ISC may lead to a situation where a neighbouring agency reports the anthropogenic event as an earthquake for which expected data are missing. This in turn is detrimental to ISC Bulletin users studying natural seismic hazard. Hence we encourage all agencies to join the agencies listed on Figure

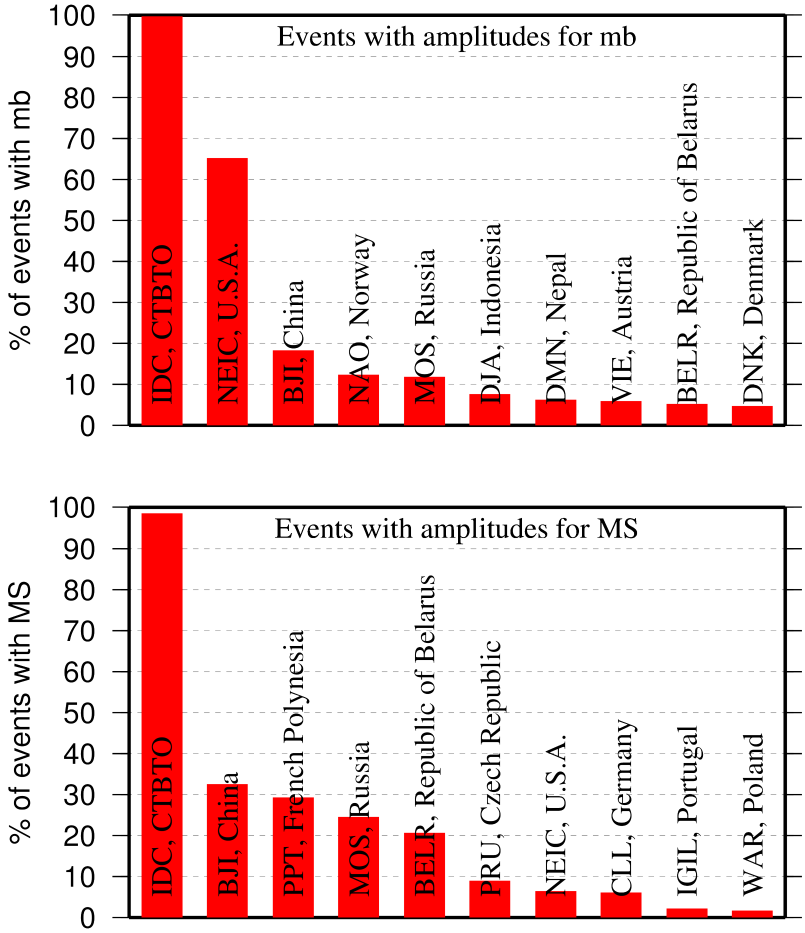

Figure 10.5: *Agencies that report defining body (top) and surface (bottom) wave amplitudes and periods for the largest fraction of those ISC Bulletin events with MS/mb determinations.*

10.7 and several others in reporting both natural and anthropogenic events to the ISC.

The ISC Bulletin also contains felt and damaging information when local agencies have reported it to us. Agencies listed on Figure 10.8 provide such information for the majority of all felt or damaging events in the ISC Bulletin.

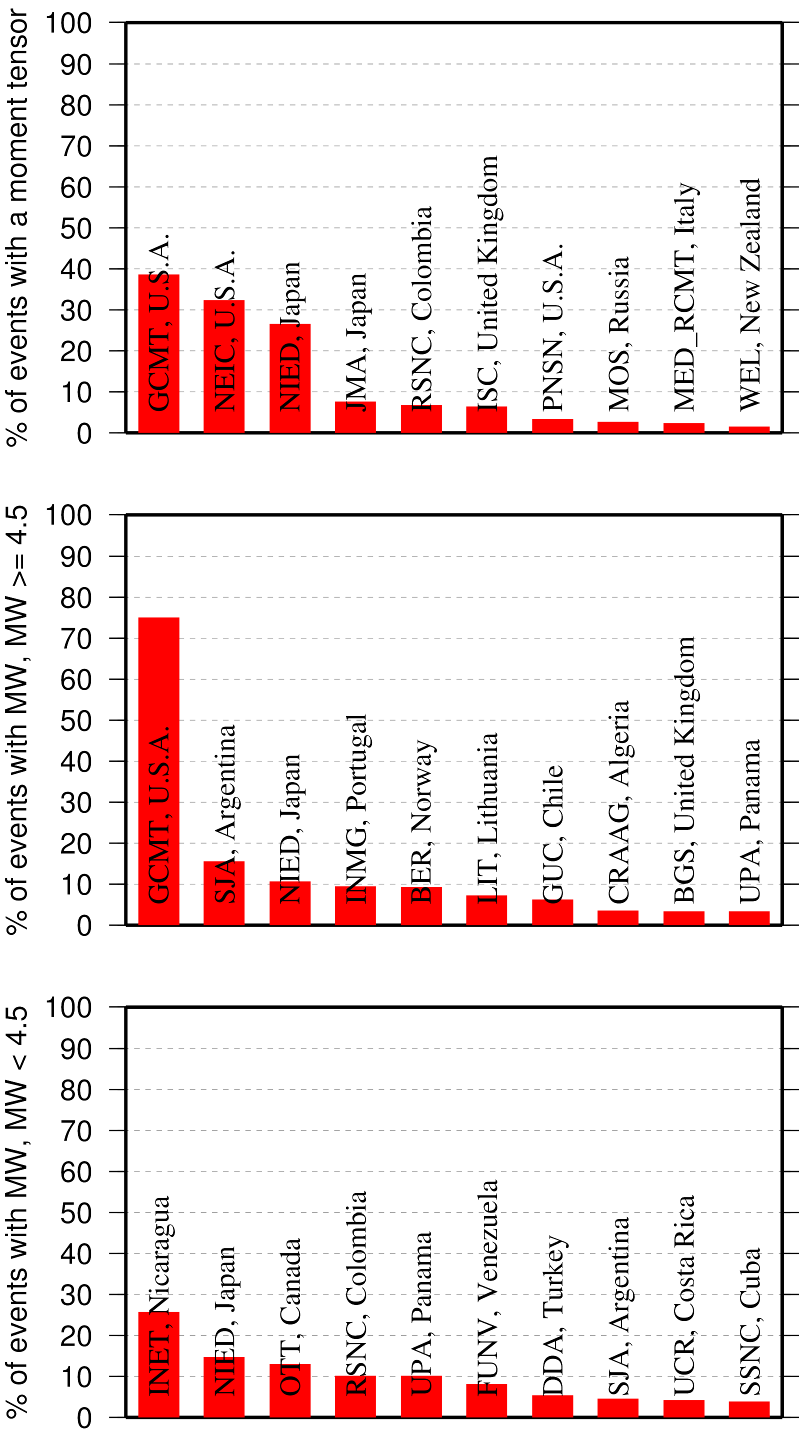

Figure 10.6: *Top ten agencies that most frequently report determinations of seismic moment tensor (top) and moment magnitude (middle/bottom for M greater/smaller than 4.5).*

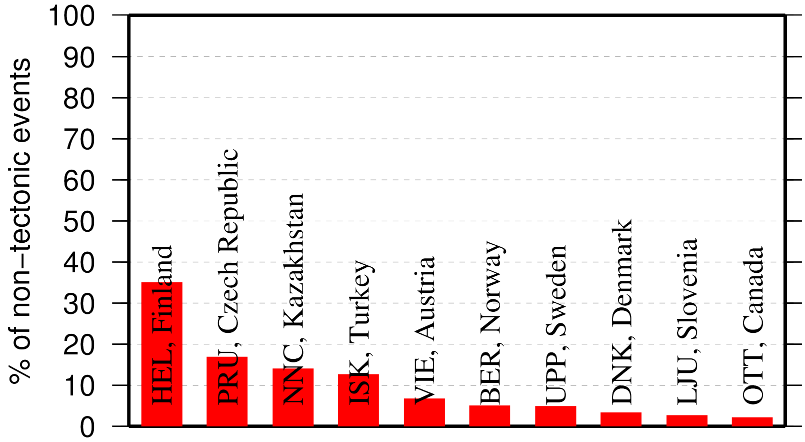

Figure 10.7: *Top ten agencies that most frequently report non-tectonic seismic events to the ISC.*

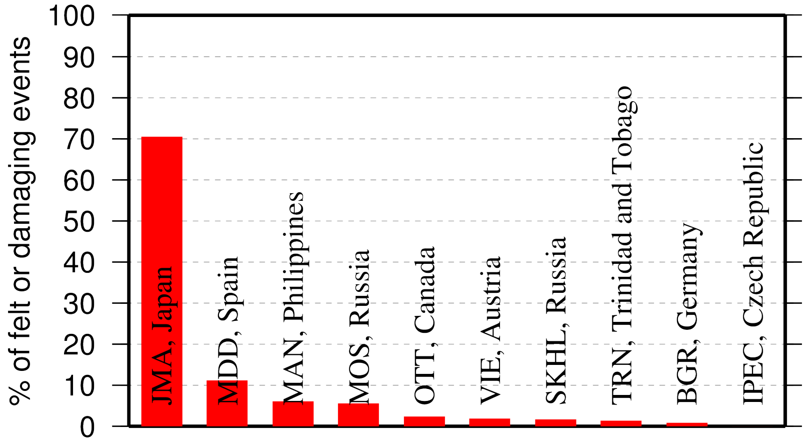

Figure 10.8: *Top ten agencies that most frequently report macroseismic information to the ISC.*

10.3 The Most Consistent and Punctual Contributors

During this six-month period, 43 agencies reported their bulletin data in one of the standard seismic formats (ISF, IMS, GSE, Nordic or QuakeML) and within the current 12-month deadline. Here we must reiterate that the ISC accepts reviewed bulletin data after a final analysis as soon as they are ready. These data, even if they arrive before the deadline, are immediately parsed into the ISC database, grouped with other data and become available to the ISC users on-line as part of the preliminary ISC Bulletin. There is no reason to wait until the deadline to send the data to the ISC. Table 10.1 lists all agencies that have been helpful to the ISC in this respect during the six-month period.

Table 10.1: *Agencies that contributed reviewed bulletin data to the ISC in one of the standard international formats before the submission deadline.*

Agency Code	Country	Average Delay from real time (days)
ZUR	Switzerland	13
PPT	French Polynesia	22
LIC	Ivory Coast	30
IGIL	Portugal	32
NAO	Norway	32
ATH	Greece	36
ECX	Mexico	38
NAM	Namibia	40
BUC	Romania	42
PRE	South Africa	43
ISN	Iraq	43
IDC	Austria	60
TIR	Albania	63
INMG	Portugal	67
SVSA	Portugal	74
ISK	Turkey	83
AUST	Australia	103
BEO	Serbia	117
BJI	China	127
VIE	Austria	133
KRSC	Russia	144
INET	Nicaragua	173
THE	Greece	213
KNET	Kyrgyzstan	226
STR	France	233
NERS	Russia	245
BGS	United Kingdom	247
UCR	Costa Rica	247
DSN	United Arab Emirates	254
SNET	El Salvador	258
THR	Iran	258
DDA	Turkey	259
MIRAS	Russia	275
DMN	Nepal	285
ASRS	Russia	290
YARS	Russia	298
SSNC	Cuba	303
BYKL	Russia	304
RHSSO	Bosnia and Herzegovina	316
LIT	Lithuania	328
IPEC	Czech Republic	332
UPA	Panama	336
SOME	Kazakhstan	356

11

Appendix

Table 11.1: *Listing of all 375 agencies that have directly reported to the ISC. The 150 agencies highlighted in bold have reported data to the ISC Bulletin for the period of this Bulletin Summary.*

Agency Code	Agency Name
AAA	Alma-ata, Kazakhstan
AAE	**University of Addis Ababa, Ethiopia**
AAM	University of Michigan, USA
ADE	Primary Industries and Resources SA, Australia
ADH	Observatorio Afonso Chaves, Portugal
AEIC	Alaska Earthquake Information Center, USA
AFAR	The Afar Depression: Interpretation of the 1960-2000 Earthquakes, Israel
AFUA	University of Alabama, USA
ALG	Algiers University, Algeria
ANDRE	USSR
ANF	USArray Array Network Facility, USA
ANT	Antofagasta, Chile
ARE	Instituto Geofisico del Peru, Peru
ARO	Observatoire Géophysique d'Arta, Djibouti
ASIES	**Institute of Earth Sciences, Academia Sinica, Chinese Taipei**
ASL	Albuquerque Seismological Laboratory, USA
ASM	University of Asmara, Eritrea
ASRS	**Altai-Sayan Seismological Centre, GS SB RAS, Russia**
ATA	The Earthquake Research Center Ataturk University, Turkey
ATH	**National Observatory of Athens, Greece**
AUST	**Geoscience Australia, Australia**
AVETI	USSR
AWI	**Alfred Wegener Institute for Polar and Marine Research, Germany**
AZER	**Republic Center of Seismic Survey, Azerbaijan**
BCIS	Bureau Central International de Sismologie, France
BDF	Observatório Sismológico da Universidade de Brasília, Brazil
BELR	**Centre of Geophysical Monitoring of the National Academy of Sciences of Belarus, Republic of Belarus**
BEO	**Seismological Survey of Serbia, Serbia**
BER	**University of Bergen, Norway**
BERK	Berkheimer H, Germany
BGR	**Bundesanstalt für Geowissenschaften und Rohstoffe, Germany**
BGS	**British Geological Survey, United Kingdom**
BGSI	Botswana Geoscience Institute, Botswana
BHUJ2	Study of Aftershocks of the Bhuj Earthquake by Japanese Research Team, Japan
BIAK	Biak earthquake aftershocks (17-Feb-1996), USA

Table 11.1: Continued.

Agency Code	Agency Name
BJI	**China Earthquake Networks Center, China**
BKK	**Thai Meteorological Department, Thailand**
BNS	Erdbebenstation, Geologisches Institut der Universität, Köl, Germany
BOG	Universidad Javeriana, Colombia
BRA	**Geophysical Institute, Slovak Academy of Sciences, Slovakia**
BRG	**Seismological Observatory Berggießhübel, TU Bergakademie Freiberg, Germany**
BRK	Berkeley Seismological Laboratory, USA
BRS	Brisbane Seismograph Station, Australia
BUC	**National Institute for Earth Physics, Romania**
BUD	**Geodetic and Geophysical Research Institute, Hungary**
BUEE	Earth & Environment, USA
BUG	Institute of Geology, Mineralogy & Geophysics, Germany
BUL	**Goetz Observatory, Zimbabwe**
BUT	Montana Bureau of Mines and Geology, USA
BYKL	**Baykal Regional Seismological Centre, GS SB RAS, Russia**
CADCG	Central America Data Centre, Costa Rica
CAN	Australian National University, Australia
CANSK	Canadian and Scandinavian Networks, Sweden
CAR	Instituto Sismologico de Caracas, Venezuela
CASC	Central American Seismic Center, Costa Rica
CENT	Centennial Earthquake Catalog, USA
CERI	Center for Earthquake Research and Information, USA
CFUSG	**Inst. of Seismology and Geodynamics, V.I. Vernadsky Crimean Federal University, Republic of Crimea**
CLL	**Geophysikalisches Observatorium Collm, Germany**
CMWS	Laboratory of Seismic Monitoring of Caucasus Mineral Water Region, GSRAS, Russia
CNG	Seismographic Station Changalane, Mozambique
CNRM	**Centre National de Recherche, Morocco**
COSMOS	Consortium of Organizations for Strong Motion Observations, USA
CRAAG	**Centre de Recherche en Astronomie, Astrophysique et Géophysique, Algeria**
CSC	University of South Carolina, USA
CSEM	Centre Sismologique Euro-Méditerranéen (CSEM/EMSC), France
CUPWA	**Curtin University, Australia**
DASA	Defense Atomic Support Agency, USA
DBN	Koninklijk Nederlands Meteorologisch Instituut, Netherlands
DDA	**Disaster and Emergency Management Presidency, Turkey**
DHMR	Yemen National Seismological Center, Yemen
DIAS	Dublin Institute for Advanced Studies, Ireland
DJA	**Badan Meteorologi, Klimatologi dan Geofisika, Indonesia**
DMN	**National Seismological Centre, Nepal, Nepal**
DNAG	, USA
DNK	**Geological Survey of Denmark and Greenland, Denmark**
DRS	Dagestan Branch, Geophysical Survey, Russian Academy of Sciences, Russia

Table 11.1: Continued.

Agency Code	Agency Name
DSN	**Dubai Seismic Network, United Arab Emirates**
DUSS	Damascus University, Syria, Syria
EAF	**East African Network, Unknown**
EAGLE	Ethiopia-Afar Geoscientific Lithospheric Experiment, Unknown
EBR	Observatori de l'Ebre, Spain
EBSE	Ethiopian Broadband Seismic Experiment, Unknown
ECGS	**European Center for Geodynamics and Seismology, Luxembourg**
ECX	**Centro de Investigación Científica y de Educación Superior de Ensenada, Mexico**
EFATE	OBS Experiment near Efate, Vanuatu, USA
EHB	Engdahl, van der Hilst and Buland, USA
EIDC	Experimental (GSETT3) International Data Center, USA
EKA	Eskdalemuir Array Station, United Kingdom
ENT	Geological Survey and Mines Department, Uganda
EPSI	Reference events computed by the ISC for EPSI project, United Kingdom
ERDA	Energy Research and Development Administration, USA
EST	Geological Survey of Estonia, Estonia
EVBIB	Data from publications listed in the ISC Event Bibliography, Unknown
FBR	Fabra Observatory, Spain
FDF	Fort de France, Martinique
FIA0	Finessa Array, Finland
FOR	Unknown Historical Agency, Unknown - historical agency
FUBES	Earth Science Dept., Geophysics Section, Germany
FUNV	**Fundación Venezolana de Investigaciones Sismológicas, Venezuela**
FUR	Geophysikalisches Observatorium der Universität München, Germany
GBZT	Marmara Research Center, Turkey
GCG	**INSIVUMEH, Guatemala**
GCMT	**The Global CMT Project, USA**
GDNRW	Geologischer Dienst Nordrhein-Westfalen, Germany
GEN	**Dipartimento per lo Studio del Territorio e delle sue Risorse (RSNI), Italy**
GEOMR	GEOMAR, Germany
GFZ	Helmholtz Centre Potsdam GFZ German Research Centre For Geosciences, Germany
GII	**The Geophysical Institute of Israel, Israel**
GOM	Observatoire Volcanologique de Goma, Democratic Republic of the Congo
GRAL	**National Council for Scientific Research, Lebanon**
GSDM	**Geological Survey Department Malawi, Malawi**
GTFE	German Task Force for Earthquakes, Germany
GUC	**Centro Sismológico Nacional, Universidad de Chile, Chile**
HAN	Hannover, Germany
HDC	Observatorio Vulcanológico y Sismológico de Costa Rica, Costa Rica
HEL	**Institute of Seismology, University of Helsinki, Finland**
HFS	Hagfors Observatory, Sweden

Table 11.1: *Continued.*

Agency Code	Agency Name
HFS1	Hagfors Observatory, Sweden
HFS2	Hagfors Observatory, Sweden
HIMNT	Himalayan Nepal Tibet Experiment, USA
HKC	**Hong Kong Observatory, Hong Kong**
HLUG	Hessisches Landesamt für Umwelt und Geologie, Germany
HLW	**National Research Institute of Astronomy and Geophysics, Egypt**
HNR	**Ministry of Mines, Energy and Rural Electrification, Solomon Islands**
HON	Pacific Tsunami Warning Center - NOAA, USA
HRVD	Harvard University, USA
HRVD_LR	Department of Geological Sciences, Harvard University, USA
HVO	Hawaiian Volcano Observatory, USA
HYB	**National Geophysical Research Institute, India**
HYD	National Geophysical Research Institute, India
IAG	Instituto Andaluz de Geofisica, Spain
IASBS	Institute for Advanced Studies in Basic Sciences, Iran
IASPEI	IASPEI Working Group on Reference Events, USA
ICE	Instituto Costarricense de Electricidad, Costa Rica
IDC	**International Data Centre, CTBTO, Austria**
IDG	Institute of Dynamics of Geosphere, Russian Academy of Sciences, Russia
IEC	Institute of the Earth Crust, SB RAS, Russia
IEPN	**Institute of Environmental Problems of the North, Russian Academy of Sciences, Russia**
IGGSL	Seismology Lab, Institute of Geology & Geophysics, Chinese Academy of Sciences, China
IGIL	**Instituto Geofisico do Infante Dom Luiz, Portugal**
IGQ	**Servicio Nacional de Sismología y Vulcanología, Ecuador**
IGS	Institute of Geological Sciences, United Kingdom
INDEPTH3	International Deep Profiling of Tibet and the Himalayas, USA
INET	**Instituto Nicaraguense de Estudios Territoriales - INETER, Nicaragua**
INMG	**Instituto Português do Mar e da Atmosfera, I.P., Portugal**
INMGC	Instituto Nacional de Meteorologia e Geofísica, Cape Verde
IPEC	**The Institute of Physics of the Earth (IPEC), Czech Republic**
IPER	Institute of Physics of the Earth, Academy of Sciences, Moscow, Russia
IPGP	Institut de Physique du Globe de Paris, France
IPRG	Institute for Petroleum Research and Geophysics, Israel
IRIS	**IRIS Data Management Center, USA**
IRSM	Institute of Rock Structure and Mechanics, Czech Republic
ISK	**Kandilli Observatory and Research Institute, Turkey**
ISN	**Iraqi Meteorological and Seismology Organisation, Iraq**
ISS	International Seismological Summary, United Kingdom
IST	Institute of Physics of the Earth, Technical University of Istanbul, Turkey
ISU	**Institute of Seismology, Academy of Sciences, Republic of Uzbekistan, Uzbekistan**

Table 11.1: Continued.

Agency Code	Agency Name
ITU	Faculty of Mines, Department of Geophysical Engineering, Turkey
JEN	Geodynamisches Observatorium Moxa, Germany
JMA	**Japan Meteorological Agency**, **Japan**
JOH	Bernard Price Institute of Geophysics, South Africa
JSN	**Jamaica Seismic Network**, **Jamaica**
JSO	**Jordan Seismological Observatory**, **Jordan**
KBC	Institut de Recherches Géologiques et Minières, Cameroon
KEA	Korea Earthquake Administration, Democratic People's Republic of Korea
KEW	Kew Observatory, United Kingdom
KHC	Geofysikalni Ustav, Ceske Akademie Ved, Czech Republic
KISR	**Kuwait Institute for Scientific Research**, **Kuwait**
KLM	**Malaysian Meteorological Service**, **Malaysia**
KMA	**Korea Meteorological Administration**, **Republic of Korea**
KNET	**Kyrgyz Seismic Network**, **Kyrgyzstan**
KOLA	**Kola Regional Seismic Centre, GS RAS**, **Russia**
KRAR	Krasnoyarsk Scientific Research Inst. of Geology and Mineral Resources, Russia, Russia
KRL	Geodätisches Institut der Universität Karlsruhe, Germany
KRNET	**Institute of Seismology, Academy of Sciences of Kyrgyz Republic**, **Kyrgyzstan**
KRSC	**Kamchatkan Experimental and Methodical Seismological Department, GS RAS**, **Russia**
KRSZO	**Geodetic and Geophysical Reasearch Institute, Hungarian Academy of Sciences**, **Hungary**
KSA	Observatoire de Ksara, Lebanon
KUK	Geological Survey Department of Ghana, Ghana
LAO	Large Aperture Seismic Array, USA
LDG	**Laboratoire de Détection et de Géophysique/CEA**, **France**
LDN	University of Western Ontario, Canada
LDO	Lamont-Doherty Earth Observatory, USA
LED	Landeserdbebendienst Baden-Württemberg, Germany
LEDBW	Landeserdbebendienst Baden-Württemberg, Germany
LER	Besucherbergwerk Binweide Station, Germany
LIB	Tripoli, Libya
LIC	**Station Géophysique de Lamto**, **Ivory Coast**
LIM	Lima, Peru
LIS	Instituto de Meteorologia, Portugal
LIT	**Geological Survey of Lithuania**, **Lithuania**
LJU	**Slovenian Environment Agency**, **Slovenia**
LPA	**Universidad Nacional de La Plata**, **Argentina**
LPZ	Observatorio San Calixto, Bolivia
LRSM	Long Range Seismic Measurements Project, Unknown
LSZ	**Geological Survey Department of Zambia**, **Zambia**
LVSN	**Latvian Seismic Network**, **Latvia**
MAN	**Philippine Institute of Volcanology and Seismology**, **Philippines**
MAT	**The Matsushiro Seismological Observatory**, **Japan**

***Table 11.1:** Continued.*

Agency Code	Agency Name
MATSS	USSR
MCO	**Macao Meteorological and Geophysical Bureau**, **Macao, China**
MCSM	Main Centre for Special Monitoring, Ukraine
MDD	**Instituto Geográfico Nacional**, **Spain**
MED_RCMT	**MedNet Regional Centroid - Moment Tensors**, **Italy**
MERI	Maharashta Engineering Research Institute, India
MES	Messina Seismological Observatory, Italy
MEX	**Instituto de Geofísica de la UNAM**, **Mexico**
MIRAS	**Mining Institute of the Ural Branch of the Russian Academy of Sciences**, **Russia**
MNH	Institut für Angewandte Geophysik der Universitat Munchen, Germany
MOLD	**Institute of Geophysics and Geology**, **Moldova**
MOS	**Geophysical Survey of Russian Academy of Sciences**, **Russia**
MOZ	Direccao Nacional de Geologia, Mozambique
MOZAR	, Mozambique
MRB	**Institut Cartogràfic i Geològic de Catalunya**, **Spain**
MSI	Messina Seismological Observatory, Italy
MSSP	**Micro Seismic Studies Programme, PINSTECH**, **Pakistan**
MSUGS	Michigan State University, Department of Geological Sciences, USA
MUN	Mundaring Observatory, Australia
NAI	University of Nairobi, Kenya
NAM	**The Geological Survey of Namibia**, **Namibia**
NAO	**Stiftelsen NORSAR**, **Norway**
NCEDC	Northern California Earthquake Data Center, USA
NDI	**National Centre for Seismology of the Ministry of Earth Sciences of India**, **India**
NEIC	**National Earthquake Information Center**, **USA**
NEIS	National Earthquake Information Service, USA
NERS	**North Eastern Regional Seismological Centre, GS RAS**, **Russia**
NIC	**Cyprus Geological Survey Department**, **Cyprus**
NIED	**National Research Institute for Earth Science and Disaster Prevention**, **Japan**
NKSZ	USSR
NNC	**National Nuclear Center**, **Kazakhstan**
NORS	North Ossetia (Alania) Branch, Geophysical Survey, Russian Academy of Sciences, Russia
NOU	**IRD Centre de Nouméa**, **New Caledonia**
NSSC	National Syrian Seismological Center, Syria
NSSP	**National Survey of Seismic Protection**, **Armenia**
OBM	Research Centre of Astronomy and Geophysics, Mongolia
OGAUC	Centro de Investigação da Terra e do Espaço da Universidade de Coimbra, Portugal
OGSO	Ohio Geological Survey, USA
OMAN	**Sultan Qaboos University**, **Oman**
ORF	Orfeus Data Center, Netherlands
OSPL	**Observatorio Sismologico Politecnico Loyola**, **Dominican Republic**

Table 11.1: Continued.

Agency Code	Agency Name
OSUB	Osservatorio Sismologico Universita di Bari, Italy
OTT	**Canadian Hazards Information Service, Natural Resources Canada**, **Canada**
PAL	Palisades, USA
PAS	California Institute of Technology, USA
PDA	Universidade dos Açores, Portugal
PDG	**Seismological Institute of Montenegro**, **Montenegro**
PEK	Peking, China
PGC	Pacific Geoscience Centre, Canada
PLV	**National Center for Scientific Research**, **Vietnam**
PMEL	Pacific seismicity from hydrophones, USA
PMR	Alaska Tsunami Warning Center,, USA
PNNL	Pacific Northwest National Laboratory, USA
PNSN	**Pacific Northwest Seismic Network**, **USA**
PPT	**Laboratoire de Géophysique/CEA**, **French Polynesia**
PRE	**Council for Geoscience**, **South Africa**
PRU	**Geophysical Institute, Academy of Sciences of the Czech Republic**, **Czech Republic**
PTO	Instituto Geofísico da Universidade do Porto, Portugal
PTWC	Pacific Tsunami Warning Center, USA
QCP	Manila Observatory, Philippines
QUE	Pakistan Meteorological Department, Pakistan
QUI	Escuela Politécnica Nacional, Ecuador
RAB	Rabaul Volcanological Observatory, Papua New Guinea
RBA	Université Mohammed V, Morocco
REN	MacKay School of Mines, USA
REY	**Icelandic Meteorological Office**, **Iceland**
RHSSO	**Republic Hydrometeorological Service, Seismological Observatory, Banja Luka**, **Bosnia and Herzegovina**
RISSC	**Laboratory of Research on Experimental and Computational Seimology**, **Italy**
RMIT	Royal Melbourne Institute of Technology, Australia
ROC	Odenbach Seismic Observatory, USA
ROM	**Istituto Nazionale di Geofisica e Vulcanologia**, **Italy**
RRLJ	Regional Research Laboratory Jorhat, India
RSMAC	Red Sísmica Mexicana de Apertura Continental, Mexico
RSNC	**Red Sismológica Nacional de Colombia**, **Colombia**
RSPR	**Red Sísmica de Puerto Rico**, **USA**
RYD	King Saud University, Saudi Arabia
SAPSE	Southern Alps Passive Seismic Experiment, New Zealand
SAR	Sarajevo Seismological Station, Bosnia and Herzegovina
SBDV	USSR
SCB	**Observatorio San Calixto**, **Bolivia**
SCEDC	Southern California Earthquake Data Center, USA
SCSIO	Key Laboratory of Ocean and Marginal Sea Geology, South China Sea, China
SDD	Universidad Autonoma de Santo Domingo, Dominican Republic

Table 11.1: Continued.

Agency Code	Agency Name
SEA	Geophysics Program AK-50, USA
SET	Setif Observatory, Algeria
SFS	**Real Instituto y Observatorio de la Armada**, **Spain**
SGS	**Saudi Geological Survey**, **Saudi Arabia**
SHL	Central Seismological Observatory, India
SIGU	**Subbotin Institute of Geophysics, National Academy of Sciences**, **Ukraine**
SIK	Seismic Institute of Kosovo, Unknown
SIO	Scripps Institution of Oceanography, USA
SJA	**Instituto Nacional de Prevención Sísmica**, **Argentina**
SJS	Instituto Costarricense de Electricidad, Costa Rica
SKHL	**Sakhalin Experimental and Methodological Seismological Expedition, GS RAS**, **Russia**
SKL	Sakhalin Complex Scientific Research Institute, Russia
SKO	**Seismological Observatory Skopje**, **FYR Macedonia**
SLC	Salt Lake City, USA
SLM	Saint Louis University, USA
SNET	**Servicio Nacional de Estudios Territoriales**, **El Salvador**
SNM	New Mexico Institute of Mining and Technology, USA
SNSN	Saudi National Seismic Network, Saudi Arabia
SOF	**Geophysical Institute, Bulgarian Academy of Sciences**, **Bulgaria**
SOMC	**Seismological Observatory of Mount Cameroon**, **Cameroon**
SOME	**Seismological Experimental Methodological Expedition**, **Kazakhstan**
SPA	USGS - South Pole, Antarctica
SPGM	Service de Physique du Globe, Morocco
SPITAK	, Armenia
SRI	Stanford Research Institute, USA
SSN	**Sudan Seismic Network**, **Sudan**
SSNC	**Servicio Sismológico Nacional Cubano**, **Cuba**
SSS	Centro de Estudios y Investigaciones Geotecnicas del San Salvador, El Salvador
STK	Stockholm Seismological Station, Sweden
STR	**EOST / RéNaSS**, **France**
STU	Stuttgart Seismological Station, Germany
SVSA	**Sistema de Vigilância Sismológica dos Açores**, **Portugal**
SYO	**National Institute of Polar Research**, **Japan**
SZGRF	Seismologisches Zentralobservatorium Gräfenberg, Germany
TAC	Estación Central de Tacubaya, Mexico
TAN	**Antananarivo**, **Madagascar**
TANZANIA	Tanzania Broadband Seismic Experiment, USA
TAP	**CWB**, **Chinese Taipei**
TAU	University of Tasmania, Australia
TEH	**Tehran University**, **Iran**
TEIC	Center for Earthquake Research and Information, USA
THE	**Department of Geophysics, Aristotle University of Thessaloniki**, **Greece**

Table 11.1: Continued.

Agency Code	Agency Name
THR	**International Institute of Earthquake Engineering and Seismology (IIEES), Iran**
TIF	**Institute of Earth Sciences/ National Seismic Monitoring Center, Georgia**
TIR	**The Institute of Seismology, Academy of Sciences of Albania, Albania**
TRI	**Istituto Nazionale di Oceanografia e di Geofisica Sperimentale (OGS), Italy**
TRN	**The Seismic Research Centre, Trinidad and Tobago**
TTG	Titograd Seismological Station, Montenegro
TUL	Oklahoma Geological Survey, USA
TUN	**Institut National de la Météorologie, Tunisia**
TVA	Tennessee Valley Authority, USA
TZN	University of Dar Es Salaam, Tanzania
UAF	Department of Geosciences, USA
UAV	Red Sismológica de Los Andes Venezolanos, Venezuela
UCB	University of Colorado, Boulder, USA
UCC	**Royal Observatory of Belgium, Belgium**
UCDES	Department of Earth Sciences, United Kingdom
UCR	**Sección de Sismología, Vulcanología y Exploración Geofísica, Costa Rica**
UCSC	Earth & Planetary Sciences, USA
UESG	School of Geosciences, United Kingdom
UGN	Institute of Geonics AS CR, Czech Republic
ULE	University of Leeds, United Kingdom
UNAH	Universidad Nacional Autonoma de Honduras, Honduras
UPA	**Universidad de Panama, Panama**
UPIES	Institute of Earth- and Environmental Science, Germany
UPP	**University of Uppsala, Sweden**
UPSL	**University of Patras, Department of Geology, Greece**
UREES	Department of Earth and Environmental Science, USA
USAEC	United States Atomic Energy Commission, USA
USCGS	United States Coast and Geodetic Survey, USA
USGS	United States Geological Survey, USA
UTEP	Department of Geological Sciences, USA
UUSS	The University of Utah Seismograph Stations, USA
UVC	Universidad del Valle, Colombia
UWMDG	University of Wisconsin-Madison, Department of Geoscience, USA
VAO	**Instituto Astronomico e Geofísico, Brazil**
VIE	**Zentralanstalt für Meteorologie und Geodynamik (ZAMG), Austria**
VKMS	Lab. of Seismic Monitoring, Voronezh region, GSRAS & Voronezh State University, Russia
VLA	Vladivostok Seismological Station, Russia
VSI	University of Athens, Greece
VUW	Victoria University of Wellington, New Zealand
WAR	**Institute of Geophysics, Polish Academy of Sciences, Poland**

Table 11.1: Continued.

Agency Code	Agency Name
WASN	, USA
WBNET	**West Bohemia Seismic Network**, **Czech Republic**
WEL	**Institute of Geological and Nuclear Sciences**, **New Zealand**
WES	Weston Observatory, USA
WUSTL	Washington University Earth and Planentary Sciences, USA
YARS	**Yakutiya Regional Seismological Center, GS SB RAS**, **Russia**
ZAG	**Seismological Survey of the Republic of Croatia**, **Croatia**
ZEMSU	USSR
ZUR	**Swiss Seismological Service (SED)**, **Switzerland**
ZUR_RMT	Zurich Moment Tensors, Switzerland

Table 11.2: *Phases reported to the ISC. These include phases that could not be matched to an appropriate* ak135 *phases. Those agencies that reported at least 10% of a particular phase are also shown.*

Reported Phase	Total	Agencies reporting
P	3320717	TAP (15%), NEIC (11%)
S	1535313	TAP (30%), JMA (14%)
AML	421410	ROM (77%), ATH (20%)
IAmb	414067	NEIC (98%)
NULL	339073	NEIC (40%), AEIC (20%), RSNC (15%)
IAML	273807	NEIC (44%), DDA (25%), GUC (14%)
Pn	250790	NEIC (48%)
Pg	178296	NNC (13%)
Sg	133752	ZAG (13%), NEIC (13%), LDG (11%)
PG	114476	ISK (57%), HEL (19%), PRU (11%)
pmax	110157	MOS (77%), BJI (23%)
LR	94467	IDC (61%), BJI (31%)
SG	89064	ISK (38%), HEL (26%), PRU (19%)
PN	77547	ISK (67%), MOS (13%)
Sn	74660	IDC (14%), LDG (11%), ZAG (11%)
IAMs_20	66716	NEIC (98%)
IAmb_Lg	63661	NEIC (100%)
Lg	60260	NNC (48%), MDD (35%)
PKP	30732	IDC (51%)
T	30292	IDC (94%)
MSG	22409	HEL (99%)
SN	19783	HEL (59%), ISK (19%)
PKPbc	19715	IDC (63%), NEIC (14%), BGR (11%)
A	17417	INMG (48%), SVSA (29%), SKHL (24%)
PKIKP	17082	MOS (96%)
MLR	16102	MOS (100%)
pP	15420	BJI (42%), IDC (23%)
PKPdf	14316	NEIC (62%)
PP	11018	IDC (21%), BJI (20%), BELR (18%)
PcP	10767	IDC (66%), NEIC (13%)
SB	10018	HEL (100%)
PB	9468	HEL (100%)
SS	8700	MOS (34%), BELR (23%), BJI (20%)
PKPab	8582	IDC (42%), NEIC (23%), BGR (11%)
smax	7149	MOS (77%), BJI (23%)
sP	6457	BJI (79%)
Sb	5126	IRIS (79%), BELR (17%)
PKiKP	4637	IRIS (44%), IDC (29%)
AMS	4138	PRU (88%), SKHL (12%)
Amp	4103	BRG (100%)
AMB	4021	SKHL (79%), BJI (21%)
PPP	3682	BELR (48%), MOS (45%)
Pb	3421	IRIS (61%), BELR (27%)
PKP2	3339	MOS (93%)
ScP	3329	IDC (80%)
LRM	3292	BELR (98%)
LQ	3278	BELR (45%), INMG (25%), PPT (19%)
SSS	3212	BELR (56%), MOS (32%)
END	3141	ROM (100%)
Trac	3013	OTT (100%)
x	2964	PRU (39%), NDI (37%), UCC (20%)
Pdiff	2712	IRIS (63%), IDC (17%)
AMP	2598	IEPN (53%), TIR (31%)
*PP	2519	MOS (100%)
LG	2423	BRA (81%), OTT (19%)
Smax	2280	BYKL (100%)
PKKPbc	2224	IDC (94%)
Pmax	1781	BYKL (98%)
sS	1766	BJI (74%), BELR (18%)
PS	1594	MOS (37%), BELR (32%)
PKhKP	1483	IDC (100%)
pPKP	1464	IDC (42%), BJI (36%)
SKS	1351	BELR (41%), BJI (35%), PRU (13%)
L	1219	BGR (59%), WAR (26%), BRA (11%)
Pdif	1058	BER (42%), NEIC (26%), UCC (11%)

Table 11.2: (continued)

Reported Phase	Total	Agencies reporting
X	1051	JMA (78%), SYO (16%)
SKPbc	999	IDC (89%)
SP	845	BER (39%), MOS (16%), PRU (13%)
max	807	BYKL (100%)
Sm	805	SIGU (70%), CFUSG (30%)
PKHKP	751	MOS (100%)
pPKPbc	748	IDC (64%), BGR (26%)
SKKS	741	BELR (50%), BJI (43%)
PKPPKP	731	IDC (94%)
IVMs_BB	705	BER (91%)
ScS	704	BJI (57%), BELR (19%), IDC (16%)
Pm	684	SIGU (81%), CFUSG (19%)
PKPDF	674	PRU (90%)
PKPAB	671	PRU (100%)
SKSac	614	BER (37%), INMG (22%), CLL (11%)
*SP	603	MOS (100%)
PKP1	571	LIC (97%)
sPKP	567	BJI (78%), BELR (13%)
m	540	SIGU (100%)
PDIFF	510	PRU (46%), BRA (36%), IPEC (17%)
Lm	509	CLL (100%)
SKP	509	IDC (39%), BELR (37%)
PKKP	463	IDC (74%), PRU (14%)
IVmB_BB	428	BER (95%)
*SS	417	MOS (100%)
E	380	ZAG (99%)
PKKPab	359	IDC (80%)
pPKPdf	347	NEIC (21%), AWI (20%), BER (19%), CLL (11%)
pPKPab	342	NEIC (50%), IDC (18%), CLL (16%)
PKS	272	BELR (69%), BJI (20%)
p	267	ROM (99%)
s	264	ROM (100%)
Sgmax	260	NERS (100%)
PPS	259	CLL (66%), MOS (17%), BELR (15%)
PKP2bc	234	IDC (100%)
LmV	227	CLL (100%)
Rg	202	NAO (41%), IDC (26%), NNC (23%)
PcS	198	BJI (87%)
SKKPbc	197	IDC (94%)
P3KPbc	165	IDC (100%)
LmH	159	CLL (100%)
SSSS	156	CLL (100%)
PKPpre	126	NEIC (71%), PRU (25%)
pPcP	124	IDC (93%)
PCP	117	LPA (58%), PRU (32%)
SKKSac	113	BGR (48%), CLL (40%)
SKPdf	107	BGR (25%), CLL (24%), BER (21%), NEIC (18%), AWI (11%)
pPP	93	LPA (57%), CLL (41%)
P4KPbc	92	IDC (100%)
IVmBBB	87	BER (99%)
pPKiKP	86	UCC (47%), CLL (28%)
Pgmax	85	NERS (99%)
PmP	76	BGR (68%), ZUR (32%)
MSN	74	HEL (68%), BER (24%)
SKIKS	73	LPA (100%)
SKIKP	73	LPA (100%)
SmS	67	BGR (93%)
Lmax	66	CLL (100%)
sPP	66	CLL (52%), BGR (47%)
PnPn	61	UCC (92%)
RG	61	IPEC (98%)
pPdiff	60	SYO (90%)
Sdif	59	CLL (81%)
PKIKS	58	LPA (100%)
SCS	57	LPA (93%)
SKPab	56	IDC (95%)
SgSg	51	BYKL (100%)

Table 11.2: (continued)

Reported Phase	Total	Agencies reporting
PgPg	51	BYKL (94%)
PKP2ab	49	IDC (100%)
Sgm	47	CFUSG (100%)
(P)	46	CLL (98%)
PKKPdf	45	AWI (64%), CLL (22%), NEIC (13%)
r	43	BRG (100%)
SKKP	41	IDC (54%), BELR (24%), PRU (12%)
PSKS	40	CLL (100%)
P3KP	36	IDC (100%)
SPP	35	BELR (74%), CLL (11%)
PKPf	35	BRG (100%)
ASPG	34	OSPL (88%), BER (12%)
ASSG	34	OSPL (88%), BER (12%)
ATPG	34	OSPL (88%), BER (12%)
ATSG	33	OSPL (88%), BER (12%)
P*	32	BGR (62%), MOS (25%), BJI (12%)
pwP	32	NEIC (100%)
(sP)	30	CLL (100%)
PPPP	30	CLL (100%)
AMd	27	NIC (100%)
PKPdiff	26	CLL (100%)
sPKPab	26	INMG (58%), CLL (23%), AWI (12%)
PKSdf	25	BER (52%), CLL (40%)
H	24	IDC (100%)
SDIFF	24	IPEC (50%), LPA (42%)
MPN	23	HEL (61%), BER (39%)
Pgm	23	CFUSG (100%)
Pif	23	BRG (100%)
(SSS)	23	CLL (100%)
(SS)	22	CLL (100%)
sPKPdf	22	CLL (50%), AWI (27%), SYO (23%)
(SSSS)	21	CLL (100%)
PbPb	21	UCC (100%)
del	20	AUST (90%)
SKSdf	19	BER (79%), CLL (16%)
PDIF	19	PRU (63%), IPEC (37%)
sSS	19	CLL (100%)
sPKiKP	19	UCC (42%), CLL (37%), AWI (16%)
Lq	18	MOLD (100%)
PKPdif	18	NEIC (83%), LJU (11%)
(PP)	18	CLL (100%)
Sdiff	17	IDC (59%), LJU (41%)
pPn	17	UCC (71%), SYO (18%), OMAN (12%)
Sif	17	BRG (100%)
sPKPbc	16	BGR (50%), UCC (25%), IDC (19%)
rx	16	SKHL (100%)
(PKPdf)	16	CLL (100%)
Snm	16	CFUSG (100%)
(PcP)	14	CLL (100%)
PPlp	14	CLL (100%)
pS	13	BELR (62%), IPEC (23%), IEPN (15%)
SKKSa	13	BRG (100%)
SKKSdf	12	CLL (100%)
(pP)	12	CLL (100%)
PKPPKPdf	11	CLL (100%)
SKSp	11	BRA (100%)
pScP	11	IDC (100%)
S*	11	BGR (73%), BJI (27%)
SKiKP	11	IDC (100%)
PSP	11	LPA (100%)
PKPpB	11	BUD (100%)
Plp	10	CLL (100%)
PSS	10	CLL (100%)
pPdif	10	CLL (70%), NEIC (20%)
LMZ	10	WAR (100%)
sSKS	9	BELR (89%), HYB (11%)
(Pg)	9	CLL (89%), BRG (11%)

Table 11.2: *(continued)*

Reported Phase	Total	Agencies reporting
PKKS	9	BELR (56%), IEPN (44%)
sPdiff	9	SYO (100%)
SnSn	9	UCC (100%)
SKKPdf	8	CLL (100%)
IVMsBB	8	BER (88%), DNK (12%)
(PKiKP)	8	CLL (100%)
(PKPab)	8	CLL (100%)
SH	7	SYO (100%)
(S)	7	CLL (100%)
sSKSac	7	CLL (100%)
AMSG	7	BER (86%), AAE (14%)
AMPG	7	BER (86%), SSNC (14%)
sPPS	7	CLL (100%)
sPdif	7	CLL (86%), INMG (14%)
sPS	7	CLL (100%)
SKSP	7	CLL (100%)
Cod	6	SFS (100%)
PSPS	6	CLL (100%)
Pnm	6	CFUSG (100%)
PPPrev	6	CLL (100%)
(PS)	6	CLL (100%)
(PPS)	6	CLL (100%)
PKPlp	5	CLL (100%)
SKPDF	5	BRA (100%)
(pPKiKP)	5	CLL (100%)
LQM	5	MOLD (100%)
SKSSKSac	5	CLL (100%)
PPmax	5	CLL (100%)
sSSSS	5	CLL (100%)
LV	5	CLL (100%)
SDIF	5	PRU (100%)
(Pdif)	5	CLL (100%)
PKPBC	5	PRU (100%)
sPPP	4	CLL (100%)
Pd0	4	ATH (100%)
AMb	4	LVSN (75%), ISN (25%)
(PKPbc)	4	CLL (100%)
SKPPKPdf	4	CLL (100%)
pPKIKP	4	IPEC (100%)
PPP(2)	4	LPA (75%), CLL (25%)
sSdiff	4	CLL (100%)
(Sn)	4	CLL (100%)
sSP	4	CLL (100%)
(SKSP)	4	CLL (100%)
Sglp	4	CLL (100%)
P(2)	4	CLL (100%)
SCP	4	IPEC (100%)
PPPPrev	4	CLL (100%)
sPDIFF	4	IPEC (100%)
PKSbc	4	CLL (100%)
PKPb	4	BRG (100%)
M	4	MOLD (100%)
(SKKSac)	4	CLL (100%)
pSKKSac	4	CLL (100%)
(SP)	4	CLL (100%)
sPcP	3	CLL (100%)
pPKKPbc	3	CLL (67%), BGR (33%)
SSP	3	HYB (67%), CLL (33%)
pPKP2	3	BJI (100%)
pPKKPab	3	CLL (100%)
sPKP2	3	BJI (100%)
(Pn)	3	CLL (67%), BRG (33%)
pPS	3	CLL (100%)
sSSS	3	CLL (100%)
sPKIKP	3	IPEC (100%)
(pPKPab)	3	CLL (100%)
pSKSac	3	CLL (100%)

Table 11.2: *(continued)*

Reported Phase	Total	Agencies reporting
P9	3	EAF (100%)
SKPa	3	NAO (67%), BER (33%)
PKPab(2)	3	CLL (100%)
Sx	3	YARS (100%)
pPPS	3	CLL (100%)
PSSrev	3	CLL (100%)
sPSKS	2	CLL (100%)
pPPPP	2	CLL (100%)
PKKSdf	2	CLL (100%)
pPPPrev	2	CLL (100%)
sPg	2	OMAN (50%), UCC (50%)
AnL	2	INMG (100%)
(sPP)	2	CLL (100%)
sPKKPab	2	CLL (100%)
(sPKPab)	2	CLL (100%)
SKKPab	2	CLL (50%), IDC (50%)
PM	2	MOLD (100%)
AP	2	MOS (100%)
(SKPbc)	2	CLL (100%)
-ML	2	INMG (100%)
PKPac	2	BER (100%)
sSKKPbc	2	CLL (100%)
P4KP	2	IDC (100%)
SS(2)	2	LPA (100%)
ws	2	SKO (100%)
sSn	2	UCC (100%)
O	2	SYO (50%), SFS (50%)
(SKPdf)	2	CLL (100%)
sSKSP	2	CLL (100%)
(sPdif)	2	CLL (100%)
PKKSbc	2	IEPN (100%)
3PKPdf	2	CLL (100%)
(PKKPbc)	2	CLL (100%)
XS	2	PRU (100%)
sPn	2	SYO (100%)
APKP	2	MOS (100%)
XSKS	2	PRU (100%)
SM	2	MOLD (100%)
PKPdiff2	2	CLL (100%)
KIKS	2	LPA (100%)
PP(2)	2	CLL (100%)
PGN	2	HEL (100%)
SKKSf	2	BRG (100%)
(PSKS)	2	CLL (100%)
sPmax	2	CLL (100%)
(PSPS)	2	CLL (100%)
pPSKS	2	CLL (100%)
SKSf	2	BRG (100%)
Li	2	MOLD (100%)
(pPdif)	2	CLL (100%)
SSmax	2	CLL (100%)
(SKKSdf)	2	CLL (100%)
(Sdif)	2	CLL (100%)
PKPPKP’	2	BRG (100%)
pn	1	ISN (100%)
PSKSrev	1	CLL (100%)
PPSmax	1	CLL (100%)
SKSmax	1	CLL (100%)
P4	1	UPA (100%)
PpP	1	INMG (100%)
PPrev	1	CLL (100%)
pSKS	1	BELR (100%)
PKPbc(2)	1	CLL (100%)
(sPPP)	1	CLL (100%)
(SKSdf)	1	CLL (100%)
sPSPS	1	CLL (100%)
sSKPdf	1	CLL (100%)

Table 11.2: (continued)

Reported Phase	Total	Agencies reporting
pP(2)	1	CLL (100%)
PSPSrev	1	CLL (100%)
pSKKPdf	1	CLL (100%)
Pma	1	BRG (100%)
PKPbcmax	1	CLL (100%)
PKPPKPab	1	CLL (100%)
PPk	1	CLL (100%)
(pPP)	1	CLL (100%)
SKKSacr	1	CLL (100%)
(sSdiff)	1	CLL (100%)
sPSS	1	CLL (100%)
(SKSac)	1	CLL (100%)
(ScS)	1	CLL (100%)
AMPN	1	OSPL (100%)
pSKPbc	1	CLL (100%)
KIKP	1	LPA (100%)
Pcp	1	SYO (100%)
SSS(2)	1	LPA (100%)
(pPKSdf)	1	CLL (100%)
pPmax	1	CLL (100%)
(PKSdf)	1	CLL (100%)
(pPcP)	1	CLL (100%)
pPif	1	BRG (100%)
Pd1	1	ATH (100%)
(sSSS)	1	CLL (100%)
HZ	1	SJA (100%)
(PkP)	1	CLL (100%)
(PKP)	1	CLL (100%)
EH	1	SJA (100%)
PKPdfmax	1	CLL (100%)
SMsm	1	MOLD (100%)
19	1	SJA (100%)
PxPxdf	1	BGR (100%)
Pnmax	1	CLL (100%)
IAMP	1	DNK (100%)
Piff	1	BRG (100%)
SbSb	1	UCC (100%)
L(360	1	CLL (100%)
pPKKPdf	1	CLL (100%)
sPKSdf	1	CLL (100%)
-Mb	1	INMG (100%)
pPPP	1	CLL (100%)
pg	1	ISN (100%)
XM	1	MOLD (100%)
PSmax	1	CLL (100%)
SSKS	1	LPA (100%)
PKPdf(2)	1	CLL (100%)
PsP	1	MOLD (100%)
Lm(360	1	CLL (100%)
sPPPP	1	CLL (100%)
(sPKPbc)	1	CLL (100%)
R	1	MOLD (100%)
PKPM	1	MOLD (100%)
pSKP	1	LPA (100%)
sPKKPdf	1	CLL (100%)
SKPPKP	1	BRG (100%)
tx	1	IEPN (100%)
ScSScS	1	CLL (100%)
(sPKiKP)	1	CLL (100%)
PKK	1	INMG (100%)
1	1	SJA (100%)
PO	1	SFS (100%)
Pdiffmax	1	CLL (100%)
(pPKPbc)	1	CLL (100%)
SSrev	1	CLL (100%)
sSKSdf	1	CLL (100%)
SKPd	1	BER (100%)

Table 11.2: *(continued)*

Reported Phase	Total	Agencies reporting
PKPPKPbc	1	CLL (100%)
sPPmax	1	CLL (100%)
PXPXdf	1	BGR (100%)
(pPKPdf)	1	CLL (100%)
Pn(2)	1	CLL (100%)
(PPPP)	1	CLL (100%)
[	1	ECX (100%)
Sd2	1	ATH (100%)
sSKKSac	1	CLL (100%)
(PPP)	1	CLL (100%)

Table 11.3: Reporters of amplitude data

Agency	Number of reported amplitudes	Number of amplitudes in ISC located events	Number used for ISC mb	Number used for ISC MS
NEIC	657336	272306	181856	30725
IDC	326794	308044	126846	35072
ROM	325690	12908	0	0
WEL	223688	31470	3	0
MOS	108680	105420	51194	10820
NNC	94792	34659	47	0
ISK	90484	12302	0	0
ATH	86064	11500	0	0
DJA	83293	58597	12229	0
DDA	68559	7868	0	0
SOME	63769	21370	1684	0
BKK	58838	17646	7853	0
BJI	57162	54277	13786	16179
MDD	55739	9993	0	0
RSNC	50965	4875	1	0
GUC	38018	12834	2	0
VIE	37395	20717	8071	0
THE	29050	5668	0	0
HEL	22273	521	0	0
LDG	19780	3104	0	0
INMG	13174	7022	3513	0
PRU	12624	4724	0	2632
BER	12451	2406	0	0
DNK	10537	4479	2967	283
PPT	9962	8317	927	2642
DMN	9574	9145	5996	0
NIC	8691	3207	0	0
BELR	7849	6100	651	1736
SKHL	7775	5792	0	0
BGR	7062	6930	5394	0
LJU	6584	387	51	0
ZUR	6299	403	0	0
BUC	6218	1457	0	0
MAN	5745	1500	0	0
SVSA	5578	706	479	0
MRB	5088	159	0	0
BYKL	4904	1622	0	0
YARS	4813	153	0	0
NOU	4764	3998	2688	0
SNET	4650	1414	0	0
SJA	4498	4449	0	0
TEH	4405	2807	0	0
BRG	4103	2182	0	0
BGS	3533	1952	1044	444

Table 11.3: *Continued.*

Agency	Number of reported amplitudes	Number of amplitudes in ISC located events	Number used for ISC mb	Number used for ISC MS
PDG	3272	2147	0	0
PRE	3236	393	34	0
OTT	3011	361	0	0
NDI	2871	2702	818	9
CLL	2832	2496	446	371
KNET	2759	1232	0	0
SIGU	2128	717	0	0
NAO	2102	2064	1515	0
SKO	2055	273	0	0
LVSN	2023	48	0	0
LIC	1979	1755	1120	0
OSPL	1895	409	0	0
IEPN	1600	1447	17	0
KRSZO	1551	631	0	0
IPEC	1351	259	0	0
SSNC	1293	338	0	0
THR	1240	891	0	0
UCC	1226	1140	966	0
ECX	1186	129	0	0
IGIL	1090	531	139	169
UCR	1029	971	0	0
TIR	806	434	0	0
WBNET	657	0	0	0
ISN	606	238	0	0
CFUSG	545	496	0	0
MOLD	516	361	39	0
MIRAS	475	56	0	0
KISR	458	112	7	0
NERS	347	69	0	0
WAR	322	308	0	221
ASRS	314	163	0	0
ISC	295	249	41	0
LIT	202	131	5	0
SCB	201	185	0	0
HYB	109	99	69	0
JSO	101	101	0	0
PLV	74	30	0	0
UPA	74	6	0	0
EAF	36	13	0	0
LSZ	34	11	0	0
SSN	14	1	0	0
AAE	4	4	0	0
BUL	3	3	0	0

12

Glossary of ISC Terminology

- Agency/ISC data contributor

  An academic or government institute, seismological organisation or company, geological/meteorological survey, station operator or author that reports or contributed data in the past to the ISC or one of its predecessors. Agencies may contribute data to the ISC directly, or indirectly through other ISC data contributors.

- Agency code

  A unique, maximum eight-character code for a data reporting agency (e.g. NEIC, GFZ, BUD) or author (e.g. ISC, EHB, IASPEI). Often the agency code is the commonly used acronym of the reporting institute.

- Arrival

  A phase pick at a station is characterised by a phase name and an arrival time.

- Associated phase

  Associated phase arrival or amplitude measurements represent a collection of observations belonging to (i.e. generated by) an event. The complete set of observations are associated to the prime hypocentre.

- Azimuthal gap/Secondary azimuthal gap

  The azimuthal gap for an event is defined as the largest angle between two stations with defining phases when the stations are ordered by their event-to-station azimuths. The secondary azimuthal gap is the largest azimuthal gap a single station closes.

- BAAS

  Seismological bulletins published by the British Association for the Advancement of Science (1913-1917) under the leadership of H.H. Turner. These bulletins are the predecessors of the ISS Bulletins and include reports from stations distributed worldwide.

- Bulletin

  An ordered list of event hypocentres, uncertainties, focal mechanisms, network magnitudes, as well as phase arrival and amplitude observations associated to each event. An event bulletin may list all the reported hypocentres for an event. The convention in the ISC Bulletin is that the preferred (prime) hypocentre appears last in the list of reported hypocentres for an event.

- Catalogue

  An ordered list of event hypocentres, uncertainties and magnitudes. An event catalogue typically lists only the preferred (prime) hypocentres and network magnitudes.

- CoSOI/IASPEI

  Commission on Seismological Observation and Interpretation, a commission of IASPEI that prepares and discusses international standards and procedures in seismological observation and interpretation.

- Defining/Non-defining phase

  A defining phase is used in the location of the event (time-defining) or in the calculation of the network magnitude (magnitude-defining). Non-defining phases are not used in the calculations because they suffer from large residuals or could not be identified.

- Direct/Indirect report

  A data report sent (e-mailed) directly to the ISC, or indirectly through another ISC data contributor.

- Duplicates

  Nearly identical phase arrival time data reported by one or more agencies for the same station. Duplicates may be created by agencies reporting observations from other agencies, or several agencies independently analysing the waveforms from the same station.

- Event

  A natural (e.g. earthquake, landslide, asteroid impact) or anthropogenic (e.g. explosion) phenomenon that generates seismic waves and its source can be identified by an event location algorithm.

- Grouping

  The ISC algorithm that organises reported hypocentres into groups of events. Phases associated to any of the reported hypocentres will also be associated to the preferred (prime) hypocentre. The grouping algorithm also attempts to associate phases that were reported without an accompanying hypocentre to events.

- Ground Truth

  An event with a hypocentre known to certain accuracy at a high confidence level. For instance, GT0 stands for events with exactly known location, depth and origin time (typically explosions); GT5 stands for events with their epicentre known to 5 km accuracy at the 95% confidence level, while their depth and origin time may be known with less accuracy.

- Ground Truth database

  On behalf of IASPEI, the ISC hosts and maintains the IASPEI Reference Event List, a bulletin of ground truth events.

- IASPEI

  International Association of Seismology and Physics of the Earth Interior, www.iaspei.org.

- International Registry of Seismograph Stations (IR)

  Registry of seismographic stations, jointly run by the ISC and the World Data Center for Seismology, Denver (NEIC). The registry provides and maintains unique five-letter codes for stations participating in the international parametric and waveform data exchange.

- ISC Bulletin

  The comprehensive bulletin of the seismicity of the Earth stored in the ISC database and accessible through the ISC website. The bulletin contains both natural and anthropogenic events. Currently the ISC Bulletin spans more than 50 years (1960-to date) and it is constantly extended by adding both recent and past data. Eventually the ISC Bulletin will contain all instrumentally recorded events since 1900.

- ISC Governing Council

  According to the ISC Working Statutes the Governing Council is the governing body of the ISC, comprising one representative for each ISC Member.

- ISC-located events

  A subset of the events selected for ISC review are located by the ISC. The rules for selecting an event for location are described in Section 11.1.3 of issue I of the 2015 Bulletin Summary; ISC-located events are denoted by the author ISC.

- ISC Member

  An academic or government institute, seismological organisation or company, geological/meteorological survey, station operator, national/international scientific organisation that contribute to the ISC budget by paying membership fees. ISC members have voting rights in the ISC Governing Council.

- ISC-reviewed events

  A subset of the events reported to the ISC are selected for ISC analyst review. These events may or may not be located by the ISC. The rules for selecting an event for review are described in Section 11.1.3 of issue I of the 2015 Bulletin Summary. Non-reviewed events are explicitly marked in the ISC Bulletin by the comment following the prime hypocentre "Event not reviewed by the ISC".

- ISF

  International Seismic Format (www.isc.ac.uk/standards/isf). A standard bulletin format approved by IASPEI. The ISC Bulletin is presented in this format at the ISC website.

- ISS

  International Seismological Summary (1918-1963). These bulletins are the predecessors of the ISC Bulletin and represent the major source of instrumental seismological data before the digital era. The ISS contains regionally and teleseismically recorded events from several hundreds of globally distributed stations.

- Network magnitude

  The event magnitude reported by an agency or computed by the ISC locator. An agency can report several network magnitudes for the same event and also several values for the same magnitude type. The network magnitude obtained with the ISC locator is defined as the median of station magnitudes of the same magnitude type.

- Phase

  A maximum eight-character code for a seismic, infrasonic, or hydroacoustic phase. During the ISC processing, reported phases are mapped to standard IASPEI phase names. Amplitude measurements are identified by specific phase names to facilitate the computation of body-wave and surface-wave magnitudes.

- Prime hypocentre

  The preferred hypocentre solution for an event from a list of hypocentres reported by various agencies or calculated by the ISC.

- Reading

  Parametric data that are associated to a single event and reported by a single agency from a single station. A reading typically includes one or more phase names, arrival time and/or amplitude/period measurements.

- Report/Data report

  All data that are reported to the ISC are parsed and stored in the ISC database. These may include event bulletins, focal mechanisms, moment tensor solutions, macroseismic descriptions and other event comments, as well as phase arrival data that are not associated to events. Every single report sent to the ISC can be traced back in the ISC database via its unique report identifier.

- Shide Circulars

  Collections of station reports for large earthquakes occurring in the period 1899-1912. These reports were compiled through the efforts of J. Milne. The reports are mainly for stations of the British Empire equipped with Milne seismographs. After Milne's death, the Shide Circulars were replaced by the Seismological Bulletins of the BAAS.

- Station code

  A unique, maximum six-character code for a station. The ISC Bulletin contains data exclusively from stations registered in the International Registry of Seismograph Stations.

13

Acknowledgements

We thank our colleagues at BGR in Hanover, Germany, for kindly accepting our invitation and submitting the article on the current status of the German Regional Seismic Network and processing of its data at the central seismological observatory at BGR.

We also thank our colleagues at the Mining Institute of the Ural Branch of the Russian Academy of Sciences in Perm for submitting an updated English version of the article (previously published in Russian, with permission from the original publisher) on a notable rare earthquake in their area of responsibility.

We are also grateful to the developers of the Generic Mapping Tools (GMT) suite of software (Wessel and Smith, 1998) that was used extensively for producing the graphical figures.

Finally, we thank the ISC Member Institutions, Data Contributors, Funding Agencies (including NSF Award EAR-1417970 and USGS Award G15AC00202) and Sponsors for supporting the long-term operation of the ISC.

References

Balfour, N., R. Baldwin, and A. Bird (2008), Magnitude calculations in Antelope 4.10, *Analysis Group Note of Geological Survey of Canada*, pp. 1–13.

Bisztricsany, E. A. (1958), A new method for the determination of the magnitude of earthquakes, *Geofiz. Kozl*, pp. 69–76.

Bondár, I., and D. Storchak (2011), Improved location procedures at the International Seismological Centre, *Geophysical Journal International*, *186*, 1220–1244.

Bormann, P., and J. W. Dewey (2012), The new iaspei standards for determining magnitudes from digital data and their relation to classical magnitudes, is 3.3, *New Manual of Seismological Observatory Practice 2 (NMSOP-2), P. Bormann (Ed.)*, pp. 1–44, doi:10.2312/GFZ.NMSOP-2_IS_3.3,10.2312/GFZ.NMSOP-2, `http://nmsop.gfz-postsdam.de`.

Bormann, P., and J. Saul (2008), The new IASPEI standard broadband magnitude mB, *Seism. Res. Lett*, *79*(5), 698–705.

Bormann, P., R. Liu, X. Ren, R. Gutdeutsch, D. Kaiser, and S. Castellaro (2007), Chinese national network magnitudes, their relation to NEIC magnitudes and recommendations for new IASPEI magnitude standards, *Bulletin of the Seismological Society of America*, *97*(1B), 114–127, doi:10.1785/012006007835.

Bormann, P., R. Liu, Z. Xu, R. Ren, and S. Wendt (2009), First application of the new IASPEI teleseismic magnitude standards to data of the China National Seismographic Network, *Bulletin of the Seismological Society of America*, *99*, 1868–1891, doi:10.1785/0120080010.

Choy, G. L., and J. L. Boatwright (1995), Global patterns of readiated seismic energy and apparent stress, *J. Geophys. Res.*, *100*(B9), 18,205–18,228.

Dziewonski, A. M., T.-A. Chou, and J. H. Woodhouse (1981), Determination of earthquake source parameters from waveform data for studies of global and regional seismicity, *J. Geophys. Res.*, *86*, 2825–2852.

Engdahl, E. R., and A. Villaseñor (2002), Global seismicity: 1900-1999, *International Handbook of Earthquake Engineering and Seismology, International Geophysics series*, *81A*, 665–690.

Engdahl, E. R., R. van der Hilst, and R. Buland (1998), Global teleseismic earthquake relocation with improved travel times and procedures for depth determination, *Bulletin of the Seismological Society of America*, *88*, 722–743.

Gutenberg, B. (1945a), Amplitudes of P, PP and S and magnitude of shallow earthquakes, *Bulletin of the Seismological Society of America*, *35*, 57–69.

Gutenberg, B. (1945b), Magnitude determination of deep-focus earthquakes, *Bulletin of the Seismological Society of America*, *35*, 117–130.

Gutenberg, B. (1945c), Amplitudes of surface waves and magnitudes of shallow earthquakes, *Bulletin of the Seismological Society of America*, *35*, 3–12.

Hutton, L. K., and D. M. Boore (1987), The ML scale in southern California, *Bulletin of the Seismological Society of America*, *77*, 2074–2094.

IASPEI (2005), Summary of magnitude working group recommendations on standard procedures for determining earthquake magnitudes from digital data, `http://www.iaspei.org/commissions/CSOI.html#wgmm,http://www.iaspei.org/commissions/CSOI/summary_of_WG_recommendations_2005.pdf`.

IASPEI (2013), Summary of magnitude working group recommendations on standard procedures for determining earthquake magnitudes from digital data, `http://www.iaspei.org/commissions/CSOI/Summary_of_WG_recommendations_20130327.pdf`.

IDC (1999), IDC processing of seismic, hydroacoustic and infrasonic data, *IDC Documentation*.

Kanamori, H. (1977), The energy release in great earthquakes, *J. Geophys. Res.*, *82*, 2981–2987.

Lee, W. H. K., R. Bennet, and K. Meagher (1972), A method of estimating magnitude of local earthquakes from signal duration, *U.S. Geol. Surv.*, Open-File Rep.

Nuttli, O. W. (1973), Seismic wave attenuation and magnitude relations for eastern North America, *J. Geophys. Res.*, *78*, 876–885.

Richter, C. F. (1935), An instrumental earthquake magnitude scale, *Bulletin of the Seismological Society of America*, *25*, 1–32.

Ringdal, F. (1976), Maximum-likelihood estimation of seismic magnitude, *Bulletin of the Seismological Society of America*, *66*(3), 789–802.

Tsuboi, C. (1954), Determination of the Gutenberg-Richter's magnitude of earthquakes occurring in and near Japan, *Zisin (J. Seism. Soc. Japan)*, *Ser. II*(7), 185–193.

Tsuboi, S., K. Abe, K. Takano, and Y. Yamanaka (1995), Rapid determination of Mw from broadband P waveforms, *Bulletin of the Seismological Society of America*, *85*(2), 606–613.

Vaněk, J., A. Zapotek, V. Karnik, N. V. Kondorskaya, Y. V. Riznichenko, E. F. Savarensky, S. L. Solov'yov, and N. V. Shebalin (1962), Standardization of magnitude scales, *Izvestiya Akad. SSSR.*, *Ser. Geofiz.*(2), 153–158, pages 108–111 in the English translation.

Woessner, J., and S. Wiemer (2005), Assessing the quality of earthquake catalogues: estimating the magnitude of completeness and its uncertainty, *Bulletin of the Seismological Society of America*, *95*(2), doi:10/1785/012040,007.

AQUARIUS

Get near real-time seismic data from the ocean floor... ...without cables.

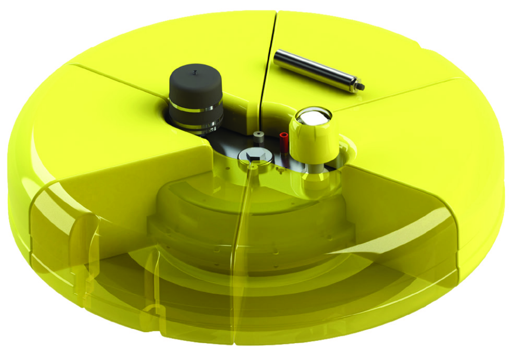

The Aquarius from Güralp is a compact freefall ocean bottom seismometer (OBS) with optional features for earthquake or tsunami early warning applications.

The Aquarius uses acoustic telemetry capability to deliver near real-time seismic data from the ocean floor to the surface without cables.

The Aquarius sensor is a digital feedback, triaxial, broadband seismometer with a flat response between 120 s and 100 Hz and is operational at any angle.

An additional sensor such as a hydrophone or a pressure sensor can also be incorporated.

AQUARIUS RESEARCH OPTION:

> Receive 'State of Health' parameters and noise performance data direct from the seabed following deployment, for confident seismic recording projects lasting up to 18 months

> Fo when data transfer is needed only at the installation and at the recovery of the OBS

> The OBS is equipped with an omni-directional transducer

> The battery can be sized to record seismic data from 3 to 18 months

AQUARIUS+ RESEARCH AND ALERT OPTION:

> Receive triggered (STA/LTA) event notifications to the surface in near real time with options to receive more detailed data for further analysis selected by time frame or by event

> Bi-directional communication and controls between the underwater system and the ocean surface infrastructure

> The battery is sized to transfer 10-15 MB of data per month for a deployment lasting 12 months.

güralp

Want to find out more?

www.guralp.com/aquarius

If It Moves, You'll Know It. Immediately.

For over 40 years REF TEK®, a Trimble brand, has been the trusted partner for seismologists around the globe. If it shakes, sinks or shifts our reliable sensors and recorders will know about it instantaneously. And you will too, anytime, as sophisticated application software informs you immediately. Always on the job, offering some peace of mind in an unstable world.

REF TEK 130S-01 High Resolution Seismic Recorder

A compact and lightweight seismic recorder, with IP Communications, ultra-low latency data transmission and removeable data storage. Meets the requirements for earthquake early warning (EEW) systems.

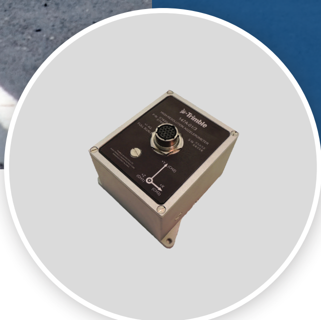

REF TEK 147A Strong Motion Accelerometer

With high sensitivity, large linear range, high resolution and dynamic range the 147A is suitable for free field applications such as microzonation, site response, earthquake monitoring and more.

REF TEK 151B-120 Observer, High Performance Broadband Seismometer

The low self-noise performance makes the Observer an ideal seismometer for seismicity studies in different installation configurations, including observatory and portable, surface and posthole applications.

For more information visit
www.reftek.com

REF TEK®
A TRIMBLE BRAND

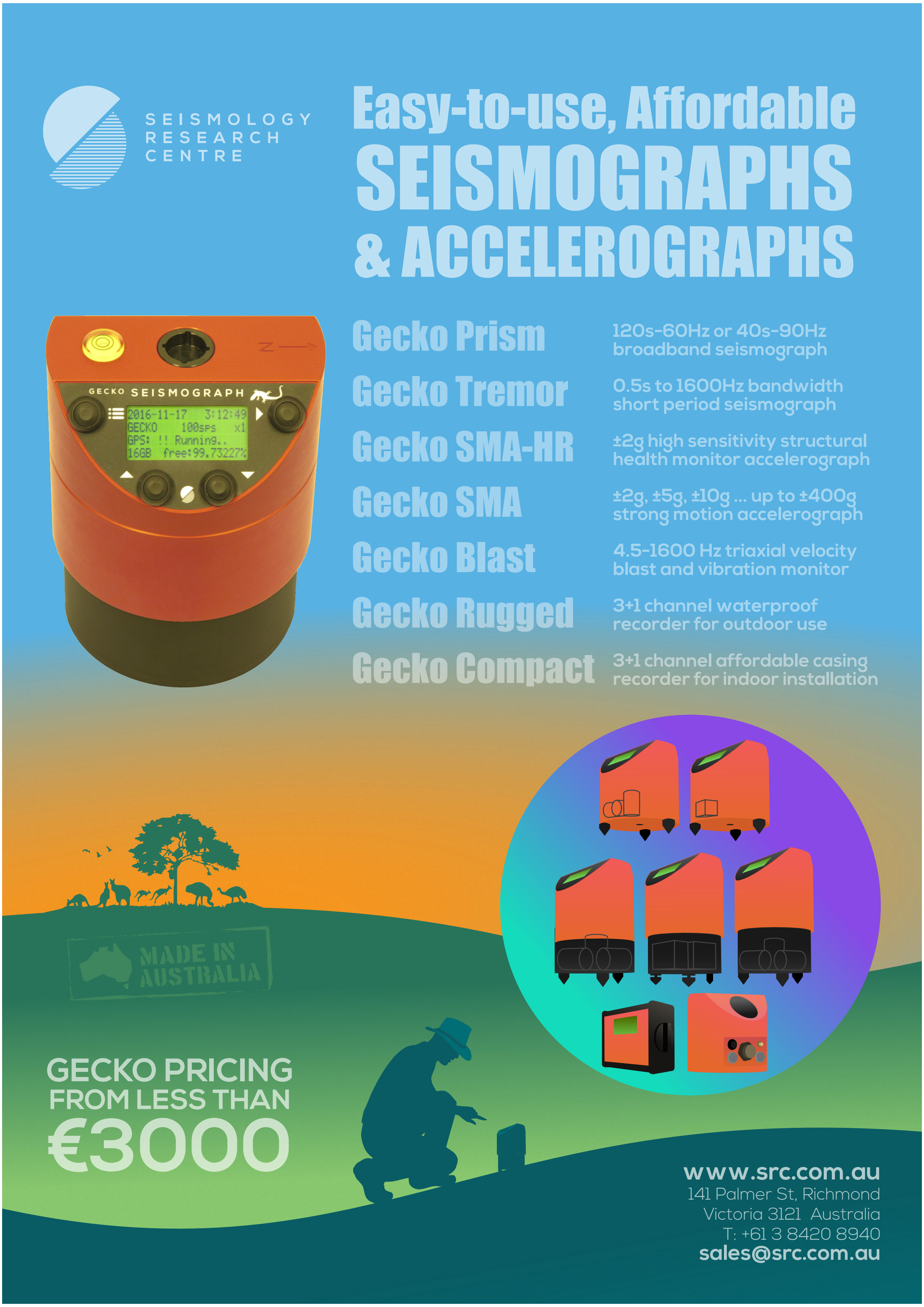
SEISMOLOGY RESEARCH CENTRE
Easy-to-use, Affordable
SEISMOGRAPHS
& ACCELEROGRAPHS
Gecko Prism
120s-60Hz or 40s-90Hz broadband seismograph
Gecko Tremor
0.5s to 1600Hz bandwidth short period seismograph
Gecko SMA-HR
±2g high sensitivity structural health monitor accelerograph
Gecko SMA
±2g, ±5g, ±10g ... up to ±400g strong motion accelerograph
Gecko Blast
4.5-1600 Hz triaxial velocity blast and vibration monitor
Gecko Rugged
3+1 channel waterproof recorder for outdoor use
Gecko Compact
3+1 channel affordable casing recorder for indoor installation
GECKO SEISMOGRAPH
MADE IN AUSTRALIA
GECKO PRICING
FROM LESS THAN
€3000
www.src.com.au
141 Palmer St, Richmond
Victoria 3121 Australia
T: +61 3 8420 8940
sales@src.com.au

#THANKYOU
Earthquake science is about knowing;
earthquake engineering is about doing.
Together you are saving lives.
This is a worthy mission!
GeoSIG
swiss made to measure

2 minutes

is all it takes to answer our survey about seismic instruments
and be entered into our prize draw. It's that simple.

One lucky winner will receive an APPLE Watch!

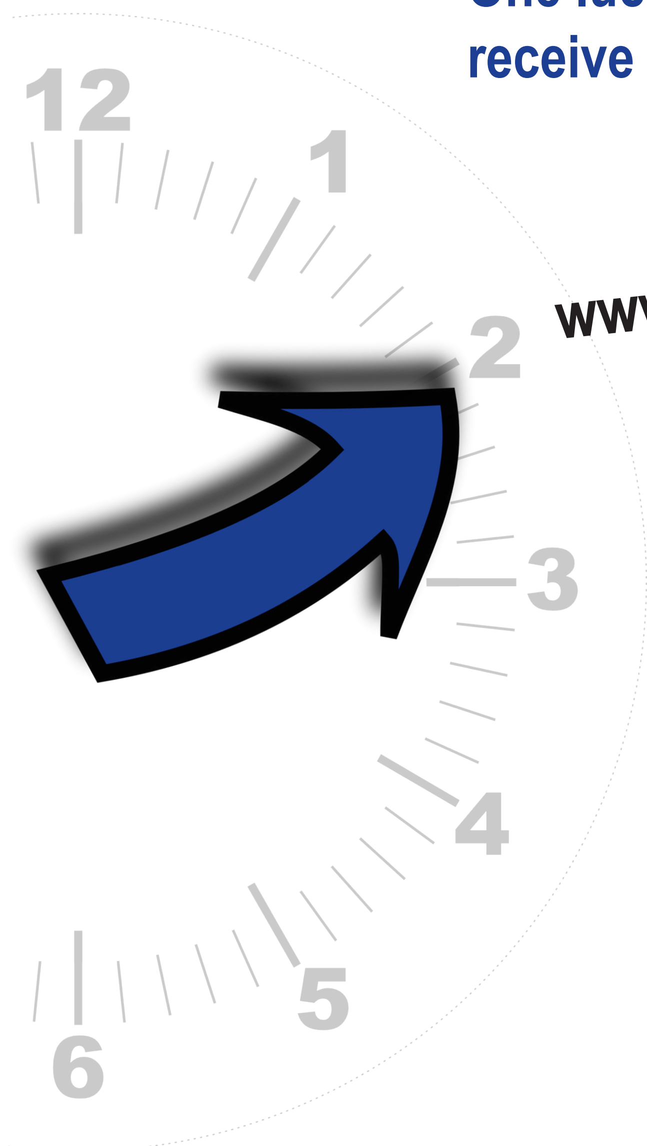

www.geosig.com/draw

GeoSIG
swiss made to measure